Intracelluar mediators of axonal sprouting *in vivo*

Milan Makwana

A thesis submitted to

University College London, University of London

for the degree of

Doctor of Philosophy

2008

ProQuest LLC
789 East Eisenhower Parkway
P.O. Box 1346
Ann Arbor, MI 48106-1346

Declaration

I, Milan Makwana, confirm that the work presented in this thesis is my own. Where information has been derived from other sources, I confirm that this has been indicated in the thesis.

ABSTRACT

Generation of new axonal sprouts and the process of axonal elongation play a vital role in neural regeneration and repair. The facial nerve axotomy model is a well-established, prototypical experimental paradigm for the systematic study of nerve regeneration and degeneration, providing insights into molecular signals that determine axonal regeneration and neuronal cell death. Interestingly, this model of peripheral injury induces a delayed appearance of galanin+ and calcitonin gene-related peptide+ (CGRP) neuropeptide-immunoreactive growth cones in the facial nucleus which peak at 14 days following axotomy and surprisingly, increase in number if recut within this time window. Furthermore, application of the retrograde tracer mini-ruby to the distal portion of the cut nerve demonstrates the motoneuron origin of these sprouting neurites.

To gain an insight into the molecular mechanisms inducing the sprouting response we examined how neuronal cell death and the inflammatory response of various transgenics affected sprouting and regeneration. Deletion of the α7 integrin, which demonstrated a moderate reduction in regeneration, showed enhanced sprouting; neural c-jun blocked regeneration, abolished regeneration-associated neuronal proteins and neuronal cell death, also completely eliminated central axonal sprouting. Absence of TNFR1&2 which displayed reduced neuronal cell death and inflammation, showed a tendency toward enhanced sprouting; TGFβ1 deletion, which showed an elevated inflammatory response and a 4-fold increase in neuronal cell death, resulted in decreased central sprouting. Similarly, enhanced neural inflammation following systemic injection of E.coli lipopolysaccharide (LPS) also reduced central sprouting. Finally, neuronally expressed constitutively active Ras (Ras+), dominant-negative MEK1 (MEK1dn) and Ras+xMEK1dn double mutant (DM) all demonstrated reduced neuronal cell death as well as substantially enhanced central sprouting, particularly in the MEK1dn mutant, suggesting that the sprouting response in these mutants may be beneficial for improving regeneration in the CNS.

Sprouting and regeneration studies in Ras+ and MEK1dn mutants were therefore extended to the injured corticospinal tract (CST) and rubrospinal tract. These mutants showed extensive collateral sprouting of corticospinal tract (CST) axons, in the grey and white matter on the ipsilateral side in Ras+,

MEK1dn and DM animals compared with wild-type (WT) controls when the injury spared the dorsolateral CST. enhanced green fluorescent protein (EGFP) labelled rubrospinal axons showed increased sprouting below the site of injury following a C4 injury in Ras+, MEK1dn and DM mice but this was not statistically significant compared with wild-type controls. To determine functional recovery rearing and grid-walk tests over 28 days following a unilateral left dorsal hemisection (DH) at C4 were used. Ras+, MEK1dn and DM groups performed significantly better in left forepaw use than WT in the rearing test at day 28 (25.0%±3.0%; 32%±1%; 50.0%±9.0%) compared with WT (13.0%±5.0%). Similarly, Ras, MEK1dn and DM animals showed significantly less footslips on the left forepaw compared with WT at day 28 (11.0%±2.0%; 10.0%±1.0%+/-; 12.0%±1.0%; 19.0%±2.0%; respectively).

Overall, data from facial nucleus studies suggest central axonal sprouting is an injury but not a reinnervation-driven response that it is not directly connected to neuronal cell death, that excessive inflammation is detrimental, and that jun-, Ras-, and MEK1-mediated changes in regeneration-associated gene and protein expression play a vital part in shaping the growth cone response. Following spinal injury, expression of MEK1dn enhanced CST sprouting below the injury site. Furthermore, the combination with Ras+ also enhanced functional recovery following C4 DH. These data suggest that neuronal expression of active Ras and MEK1dn might serve as a promising biochemical strategy for regrowth in the injured spinal cord.

TABLE OF CONTENTS

INDEX OF FIGURES

INDEX OF TABLES

ACKNOWLEDGEMENTS

I would like to thank those who made the completion of this degree possible.

First, Gennadij Raivich for accepting me into his lab and providing support, encouragement and expertise. Patrick Anderson for teaching me how to perform spinal cord injuries and tract tracing, for critically reading large parts of my thesis and providing useful comments.

I am sincerely grateful to: Mariya Hristova for making time for me, regardless of the pressures of her own work; Marion Bohatschek and Daniel Cuthill for topical conversation, helping me to maintain a social life and providing advice during stressful and demoralising periods in the lab; Kismet Hossain-Ibrahim for helping me with surgical techniques; Matt Mason for numerous valuable discussions about regeneration research; and, Adam Wallace for much encouragement during my final year and for reviving my love for tea. Ahad Rahim for kindly providing the EGFP used in rubrospinal injections, Gemma Holding for helping me to maintain some sanity during the final year and Julia Winterbottom for protocols and help with histological techniques during the first year. Also, Axel Behrens and everyone in the laboratory at Cancer Research.

Thanks to BSc students Melissa Campbell, Daniel Gordon, Anna Gilchrist, Holly Thompson and Alejandro Acosta-Saltos for motivating me as much as I hope I motivated them.

I would like to thank my parents, Arvinda and Navin for tirelessly encouraging my academic endeavours and for teaching me the value of education. Thanks also to my sister Ameeta and John and Diane Dane.

My greatest thanks to Alan, for getting me through it with love and moral support.

This degree was funded by a generous Nathalie Rose-Barr PhD Studentship from International Spinal Research Trust and GlaxoSmithKline, for both of which I am most grateful.

CHAPTER 1

General Introduction

Injury to peripheral nerves results in a sequence of molecular and cellular responses that are associated with, and that may play an important role in, the mounting of a successful regenerative response, and the ensuing recovery of function. In the injured neuron, the rapid arrival of signals from the injured axon is followed by the induction of transcription factors (and possibly microRNAs), adhesion molecules, growth–associated proteins and structural components needed for axonal elongation. These changes are accompanied by immense shifts in cellular organization: the appearance of growth cones at the proximal tip of the lesioned axons, the swelling of the neuronal cell body associated with a strong increase in cellular metabolism and protein synthesis, and the increase and regional dispersion of areas of rough endoplasmic reticulum or Nissl substance in neuronal cytoplasm.

This neuronal response is also associated with the expression of growth factors, cytokines, neuropeptides and other secreted molecules involved in cell-to-cell communication, which may be involved in the activation of neighbouring non-neuronal cells around the cell body of the injured neuron and along the injured axon. The result of all these changes is vigorous regeneration. Conversely, axons injured inside the central nervous system (CNS), normally fail to regenerate, regardless of whether their cell bodies are located inside the CNS and generally show a meagre cell body response to axotomy. This introductory chapter aims to provide a background to the processes involved in the cellular response to axonal injury both in the PNS and CNS and describe an overview of the current knowledge of the processes involved in the neuron being able to mount a successful regenerative response.

The response of the neuron to injury

The neuronal response to axotomy (also termed retrograde reaction) can present with various changes ranging from swelling of the cell body through atrophy of the cell body all the way through to cell death (Tetzlaff et al., 1991; Lieberman, 1971). The mode of cellular death as a result of axotomy can be either apoptotic, necrotic, or can have characteristics of both of these processes

(de Bilbao and Dubois-Dauphin, 1996; Pettmann and Henderson, 1998). Regenerative responses begin within hours of axotomy but degenerative changes can occur quickly or over a period of many weeks or months. The molecular mechanisms associated with the varied response to injury are not fully understood and much work over the last few decades has focussed on identifying the processes that underlie axon regeneration and cell death.

Numerous studies have identified that while, on the whole, neurons respond to axotomy in the same way, different types of neurons such as motoneurons, or retinal ganglion neurons have characteristically different responses from one another (Goldberg and Barres, 2000). For example, 60% of motoneurons in the facial nucleus survive and regenerate (Raivich et al., 1999) after facial nerve transection, whereas, Purkinje cells survive but do not regenerate their axons (Rossi et al., 1995) and the majority of retinal ganglion cells die after optic nerve injury (Bray et al., 1991). Indeed these differences are likely to be due to intrinsic properties of neurons such as the availability of certain proteins or transcription factors which, either execute or delay cell death or illicit a dual response (Goldberg and Barres, 2000).

At least two factors have been demonstrated to contribute to whether a neuron survives or dies after axotomy: firstly, the regenerative environment of the axon. For example, neurons that send their axons into peripheral nerves are better at surviving axotomy, which is probably because the environment of the peripheral nerve is hospitable to axonal regeneration (Lieberman, 1971). In contrast however, intrinsic CNS neurons often die following axotomy probably due to the inability of the axon to regenerate in the CNS environment, resulting in the inability of the neuron to re-establish target connections and thus sustain itself. Studies by both Berry et al. (1988a) and Bray and colleagues (1991) support these observations since survival of axotomised retinal ganglion cells improves if they are allowed to regenerate axons into a peripheral nerve graft. Other examples of cell death of intrinsic CNS neurons following axotomy include Clarke's column neurons which die after spinal cord white matter lesions (McBride et al., 1988), and septal cholinergic neurons, 90% of which die following transection of the fimbria/fornix (Tuszynski et al., 1990). However, this is not always the case. Both corticospinal (Merline and Kalil, 1990) and

rubrospinal (Prendergast and Stelzner, 1976; Tetzlaff et al., 1991) neurons do not die following injury to their axons within the spinal cord.

Some evidence points to the fact that neuronal survival following axotomy depends heavily on the remaining collaterals proximal to the site of injury, so that axons will die back to the collateral branch point which may sustain the fibre. Alternatively, if axons die back to the neuronal cell body, neuronal cell death occurs (Ramon y Cajal, 1928; Fry and Cowan, 1972).

The survival of axotomised neurons, both intrinsic CNS neurons and those projecting into peripheral nerves depends on the distance between the injury site and the cell body. So, Sievers et al. (1987) show that 90% of retinal ganglion cells die following intraorbital axotomy, however, after intracranial axotomy, the initial survival rate seems to be significantly higher (Misantone et al., 1984), although the regeneration potential is markedly reduced (Richardson et al., 1982). Similarly, in Clarke's column, axotomy at L1 induces 30% of neurons to die, whereas about 15% of neurons die following axotomy at C5 (Loewy and Schader, 1977). Finally, death rates of septal cholinergic neurons following fimbria/fornix lesions varies with distance both in the caudo-rostral and dorso-ventral directions (Sofroniew and Isacson, 1988). This evidence suggests that in these neuronal systems, proximal axotomy results in less neuronal cell death.

Morphological and chemical changes

The acute phase of the chromatolytic response following axotomy is characterised by the dispersal of Nissl bodies, cellular swelling, displacement of the nucleus to the periphery of the cell and retraction of synaptic terminals (Lieberman, 1971). This initial reaction remains common to all PNS neurons and many CNS neurons and, may be related to the ability of cells to regenerate axons (Anderson et al., 1998). When neurons regenerate their axons, the cell bodies remain swollen throughout the period of regrowth, and the cell body is generally littered with vast numbers of intracellular organelles such as ribosomes and mitochondria, associated with increased metabolism and protein synthesis (Lieberman et al, 1971). When neurons are unable to regenerate, for

example those with axons in central white matter, the neuronal cell bodies begin to atrophy both in cell volume and in the number of dendrites, and may persist in this atrophied state for an indefinite period of time (Lieberman, 1971; Tetzlaff, 1991). The significance of the cell body response for axonal regeneration is shown by two series of experiments. When PNS grafts are implanted into the CNS, the neurons which regenerate axons into the grafts are usually those with the greatest cell body response to axotomy. Secondly, axonal regeneration in dorsal roots of spinal neurons is generally poor and this has been correlated with a feeble cell body response of DRG neurons to axotomy of their central processes. Furthermore, a peripheral conditioning lesion both produces a massive cell body response in the DRG neurons and also increases the regeneration potential of the central processes within the dorsal root (Richardson and Verge, 1987; Chong et al., 1996; Zeng et al., 1995).

Parallel to the morphological changes occurring to the neuron following axotomy, there are a number of biochemical changes that also occur, which vary in different neuronal groups. Microarray studies show changes in expression of hundreds of genes in DRG or autonomic ganglia after peripheral nerve injury (Costigan et al., 2002). In regenerating motoneurons, there is an increase in the expression of growth associated proteins such as GAP-43, CAP-23, SCG10, the adhesion molecules L1 and CHL1 and microtubule associated proteins (Mason et al., 2002; Zhang et al., 2000; Tetzlaff et al., 1991). There is also a change in the expression of some neuropeptides such as galanin and VIP which begin to be expressed in sensory, sympathetic and motoneurons, whereas the normal expression of substance P and neuropeptide Y in sensory and sympathetic neurons decreases (Zigmond et al., 1996).

Cell death signals.

A number of studies point to presence of several cell surface molecules that mediate neuronal cell death following neonatal and adult axonal injury, including fas and tumour necrosis factor receptors (TNFR) 1 and 2 (Terrado et al., 2000; Raivich et al., 2002; Ugolini et al., 2003). With the exception of TNFR2, these cell surface receptors carry a cytoplasmic death domain that exerts a pro-apoptotic signal through FADD. Furthermore, expression of dominant negative

form of Fas associated death domain (FADD) has been shown to block the axotomy-induced cell death signal due to fas and TNFR (Ugolini et al., 2003). Associated downstream cytoplasmic cell death signals play a key role in promoting neuronal cell death in neonatal and immature animals that are sensitive to axonal injury. Deletion of bax or inhibition of caspase 3, or the whole family of caspases has been shown to prevent cell death (Sun and Oppenheim, 2003; Chan et al., 2003), but with an enhanced and more persistent effect for broad spectrum caspase inhibitors rather than those that affect caspase 3 alone (Chan et al., 2003). In both cases, bax and caspases appear to act downstream of jun phosphorylation, suggesting a sequence of events beginning with jun-P, leading to atrophy, activation of bax and ending with the initiation of the caspase cascade. Unlike neonates, the effects of caspases in adult neurons are still poorly understood. For example, the global deletion of caspase 1, the interleukin-1 β-converting enzyme, increases the extent of motoneuron cell death by 40%, compared with wild type controls (de Bilbao et al., 2000). Overall, the effects studied so far seem to be centred around neuronal survival, and the number of axons proximal to the injury site, although there was some indirect evidence for an enhancing effect of bax deletion on regeneration (Sun and Oppenheim, 2003).

The response of the peripheral axon to injury – an overview

Axonal responses distal to the lesion site

Following peripheral nerve injury, the distal portion of the nerve undergoes a process called Wallerian degeneration (Waller, 1850) involving several concomitant events. Firstly, there is a rapid breakdown of the axoplasm resulting in a granular disintegration of the axonal cytoskeleton (Bignami et al., 1981) as well as the disassembly of microtubules and neurofilament proteins (Trojanowski et al., 1984). The process is usually complete within 3-10 days post injury, although for neurofilament proteins this can vary between 3 and 21 days (Trojanowski et al., 1984). Secondly, the myelin sheath also swells, eventually becoming fragmented and breaking down into fatty material that is deposited around the axon (Lassmann et al., 1978). Thirdly, as early as 1-3 days post injury, macrophages invade the area, phagocytosing the myelin and

axonal breakdown products (Perry and Brown, 1992). In addition, Schwann cells are also crucial to this early process since they aid in phagocytosis (Liu et al., 1995). In all, the process of clearing debris takes about 2 weeks.

Axonal responses proximal to the lesion site

Whilst true Wallerian degeneration does not occur on the proximal side of the injured nerve, several similar events do take place. For example, like the distal portion of the nerve, there is myelin breakdown up to several nodes of Ranvier proximal to the lesion. There is also early invasion of macrophages which engulf the remains of damaged axons (Lieberman, 1971; Grafstein, 1975). The proximal end of the cut axon seals and depending on the regenerative potential of the neuron, the axon forms a bulbous swelling at the tip due in part to the arrival of new axoplasm including cytoskeletal components such as neurofilament and microtubules, and mitochondria (Meller, 1987; Vallee and Bloom, 1991). Eventually what forms are club-like structures described in detail by Ramon y Cajal (1928) which give rise to growth cones that may sustain axonal regeneration to the target.

The environment of the injured peripheral axon allows for axonal regeneration

Following crush injury to the peripheral nerve, axonal regeneration is typically successful even though axons need to regrow and remyelinate over long distances. This successful regeneration depends largely on the anatomical organisation of the peripheral nerve. Axons within the PNS are divided into distinct bundles contained within three types of connective tissue: the epineurium which surrounds the entire nerve and protects from injury and stretch; perineurium, which divides the nerves into multiple units that project to various related targets; and finally the neurilemmal sheath, consisting of basal lamina which encloses a Schwann cell and its ensheathed axon (Crossman and Neary, 1998).

Peripheral nerve injury results in the distal segment of the nerve degenerating, leaving hollow tubes of basal lamina containing Schwann cells. Schwann cells

proliferate and align themselves into columns known as Bands of Büngner (Büngner, 1891; reviewed in Ide, 1996). Regenerating axons are typically guided along these Schwann cell basal lamina tubes, eventually reaching target tissues. The Schwann cells eventually remyelinate the adjacent regenerated axon (Ide, 1996). Schwann cells appear to perform an important secondary function in addition to mechanical guidance and myelination. Schwann cells secrete neurotrophic factors including NGF (Funakoshi et al., 1993; Lindholm et al., 1987), BDNF (Meyer et al., 1992), NT-4 and GDNF (Hammarberg et al., 1996). These neurotrophins may aid growth and guidance along Bands of Büngner (Ide, 1996). The effect of neurotrophins on peripheral regeneration is discussed later in the Introduction

In addition to neurotrophins, Schwann cells secrete other molecules capable of influencing axonal growth including collagen, laminin and fibronectin (Fawcett and Keynes, 1990) and express L1, CHL1 and NCAM (Martini and Schachner, 1988; Zhang et al., 2000) which are believed to play important roles in axonal regeneration on Schwann cell surfaces (Raivich and Makwana, 2007). Both Schwann cells and resident macrophages in the peripheral nerve also assist in the rapid and efficient removal of degenerated axons and myelin debris from the site of injury allowing regeneration to proceed (Avellino et al., 1995; Reichert et al., 1994; Liu et al., 1995). However, the importance of macrophage proliferation for myelin clearance and axonal regeneration has been questioned (Perry et al., 1995).

Signals inducing a regenerative response

The molecular signals from the injured nerve contributing to the cell body response to axotomy remain debatable. There is evidence that the signals from the injured nerve to the cell bodies of neurons, which initiate the cell body response, are both positive (signals from the injured axon or from non-neuronal cells at the injury site) and negative (loss of retrograde transport of neurotrophic factors such as NGF and FGF2).

The tip of the injured axon is exposed to an environment that is different to that of the intact nerve and very complex, including early on factors released from

neighbouring damaged axons and Schwann cells (Sendtner et al., 1997; Kirsch et al., 2003), and later to the extracellular environment of the inflamed neural tissue (Lindholm et al., 1987). Furthermore, a rapid entry of extracellular ions such as calcium and sodium through the transiently opened plasma membrane, before it is resealed (Yoo et al., 2003), results in depolarisation and a sequence of injury-induced action potentials (Berdan et al., 1993). The calcium influx and bystander activation of intra-axonal proteases and cytoskeleton remodelling underlie growth cone formation (Spira et al., 2001), and may also be involved in changing intra-axonal protein synthesis (Zheng et al., 2001). At later stages, axonal injury also leads to the recruitment of leukocytes, the production of inflammatory cytokines and attendant changes in neighbouring non-neuronal cells with the synthesis of neurotrophins, chemokines, extracellular matrix molecules and proteolytic enzymes (for reviews, see Perry et al., 1992; Kreutzberg and Raivich, 2000) changing the extracellular milieu of the lesioned axons.

Although these signals at the site of injury can act in complementary and possibly synergistic ways (Ambron and Walters, 1996), it remains speculative which of the three, or whether all three, are involved in the post-traumatic generation and/or activation of axoplasmic proteins with the nuclear localization signal (NLS) sequences. These axoplasmic NLS proteins perform an important function as positive injury signals (Ambron et al., 1996, Hanz et al., 2003).
Nerve injury interferes with the retrograde flow of signals from the normal innervation target, which may lead to the emergence of a negative, denervation signal, following the disconnection. Data on nerve growth factor (NGF), a neurotrophin that is retrogradely transported from periphery to the cell bodies of sympathetic and some sensory neurons are particularly informative. Analysis of its retrograde transport in the injured sciatic nerve shows a drastic, almost 10-fold decrease immediately following axotomy (Raivich et al., 1991) and although this strong decrease is only short-lived, for approximately 48 hours, a 3-fold reduction continues until the onset of regeneration. The evidence concerning motor neurons is that p75 upregulation in sciatic motoneurons following axotomy is under the influence of positive signals from the injury site but ChAT downregulation is the result of the loss of retrograde signals (Bussman and Sofroniew, 1999).

The rate of nerve regeneration and target reinnervation

Regeneration of crushed axons typically proceeds at a rate of 1-2mm per day (Gutmann et al., 1942). However, the rate of regeneration can be accelerated by the effect of a prior, conditioning lesion (McQuarrie et al., 1977; McQuarrie and Grafstein, 1973). Electrical stimulation of the proximal stump of severed peripheral nerves also reduces the time taken for functional recovery, but does so by reducing the delay before regeneration begins in some motor axons (Al Majed et al., 2000; Brushart et al., 2002). In addition to the robust outgrowth of crushed peripheral axons, they have also been shown to accurately reconnect to their original peripheral targets (Nguyen et al., 2002). In contrast to crush injuries, following transection of a peripheral nerve, robust regeneration does occur, but functional recovery is much delayed, depending on a number of factors. Firstly, if the distance of the two cut ends is more than 1cm, regeneration will fail (Lundborg, 2005) resulting in a dense tangles of abortively sprouted nerve terminals (neuromas). Secondly, re-anastomosing the nerve ends aids successful regeneration (Forman et al., 1979). Although target reinnervation is evident, it is somewhat misguided and inaccurate (Valero-Cabre et al., 2004; Nguyen et al., 2002; Galtrey et al., 2007; Smith et al., 2007). These studies suggest that successful peripheral regeneration depends on the correct alignment of cut axons or allowing a sufficient degree of plasticity for axons to innervate appropriate targets.

The response of the central axon to injury – an overview

There are major differences in injury-induced responses of CNS tissue compared with peripheral nerves. While in the PNS, there is an efficient mechanism for the removal of the products of Wallerian degeneration, such as axonal and myelin debris by Schwann cells and macrophages, the response in the CNS is considerably slower (George and Griffin, 1994).

Wallerian degeneration was compared in sensory axons of the PNS and CNS by transecting the dorsal roots at L1-4. The initial rate at which sensory axons degenerate in both compartments is virtually the same. However, whilst peripheral nerve roots are almost completely clear of myelin debris at 30 days

post lesion, myelin debris and neurofilamentous accumulations in degenerating axons were still visible in the spinal cord 90 days after injury (George and Griffin, 1994). In other injury models such as the lesioned optic nerve, Wallerian degeneration was extended by up to 4 weeks compared with lesioned peripheral nerve (Ludwin and Bisby, 1992).

The delay in clearance of axonal and myelin debris in the CNS may be due to oligodendrocytes lacking phagocytic properties (Bignami and Ralston, 1969), although microglia are numerous in the CNS. Moreover, macrophages are rapidly recruited to sites of Wallerian degeneration in peripheral but not central nervous tissue (Perry et al., 1987), although they do appear rapidly at lesions in both. In the periphery macrophages are recruited to the degenerating nerves, are characteristically rounded in morphology and engulf damaged cellular debris (Bohatschek et al., 2001). They are observed within 2-4 days of peripheral nerve injury. In the CNS, circulating macrophages are not recruited into sites of Wallerian degeneration although they do appear at lesion sites. Instead, resident microglial cells take on the phagocytic phenotype among the degenerating axons (Popovich et al., 2002), the transformation of which usually takes place within 1-2 days post injury (Bohatschek et al., 2001).

The glial cells in the CNS behave very differently from Schwann cells following injury. In the injured CNS there is extensive glial cell death in the days following injury resulting in a lesion site largely devoid of astrocytes and oligodendroglia. In contrast Schwann cells proliferate extensively in injured nerves and repopulate lesions sites rapidly. The anatomical arrangement of the CNS differs markedly from the PNS. Unlike peripheral nerve, axons in the CNS are not structurally separated by perineurial or neurilemmal sheaths, but are organised into tracts of related function without distinct physical barriers separating them. Oligodendrocytes typically myelinate several axons and cannot provide guidance for regenerating axons. Hence, following injury, there are no biomechanical guidance cues in the CNS that can be compared with the bands of Büngner in peripheral nerves.

The ability of central axons to regenerate

For a long time the belief was held that axonal regeneration in the CNS was not possible. This was despite observations by Tello (reported in Ramon y Cajal, 1928) that CNS axons could grow into pieces of peripheral nerve implanted into the brain. Le Gros Clark (1943) had made similar observations of regenerating axons in nerve grafts implanted into the brain but was unable to convince himself that the axons were derived from CNS neuron. He suggested that CNS axons had no intrinsic capacity for regrowth following injury. Ramon y Cajal (1928) demonstrated that injured CNS axons could undergo limited sprouting but were unable to cross the lesion barrier. It was not until 1958 when Liu and Chambers demonstrated, using the spared root preparation, that axons in the spinal cord were capable of sprouting collaterals, i.e. that limited axonal growth could occur in the hostile CNS environment. Furthermore, limited growth on the proximal side of a spinal cord injury was evident in axons of hibernating squirrels (Guth et al., 1981). The prevailing view on CNS axonal regeneration was changed dramatically by observations on the growth of axons from transplanted neurons in the adult mammalian CNS and by observations on the regeneration of axons into peripheral nerve grafts in the brain and spinal cord. It was first demonstrated that fetal monoaminergic neurons and embryonic forebrain neurons could grow long axons when transplanted into the adult CNS (Bjorklund and Stenevi, 1984; Bjorklund and Stenevi, 1979; Nornes et al., 1983; Stenevi et al., 1976). Peripheral nerve grafts to the brain or spinal cord were used to test the hypothesis that CNS axons could regenerate if given a suitable environment through which to extend. These studies used the same techniques as Tello and Le Gros Clarke but took advantage of the newly developed technology for the retrograde labelling of neurons from their axons. In landmark experiments, Aguayo and colleagues convincingly demonstrated that CNS neurons would grow axons into a peripheral nerve graft implant (Richardson et al., 1980; David and Aguayo, 1981) by applying a retrograde tracer to the distal end of the graft and identifying labelled neurons in the spinal cord and brainstem. Numerous later studies demonstrated that most parts of the CNS contain neurons that will extend axons into peripheral nerves For example, retinal ganglion cells regenerated axons into peripheral nerve grafts on the retina (So and Aguayo, 1985). The thalamus and cerebellum also contain neurons that regenerate (Benfey et al., 1985; Morrow et al., 1993; Chaisuksunt

et al., 2000). However, there still remained the possibility that the growing axons originated from collaterals of intact axons. It was not until Berry and colleagues (1988a) demonstrated that axons from severed optic nerve would grow into an anastomised peripheral nerve graft that it was demonstrated conclusively that injured CNS axons could regenerate into permissive environments. Although peripheral nerve grafts showed great initial promise for repair of the CNS it was soon found that regenerating axons were reluctant to leave the environment of the nerve (Oudega et al., 1994). While CNS axons enjoy the hospitable environment of the peripheral nerve, they do not grow or regenerate axons into nerve grafts where Schwann cells have been killed by freezing (Berry et al., 1988b). This shows the critical importance of living peripheral glia for regeneration.

In contrast to PNS neurons, most CNS neurons show an attenuated cell body response to axotomy, and do not regenerate axons. Retinal ganglion neurons show a marked cell body response to axotomy and represent an example of the few CNS neurons that are able to spontaneously regenerate (very few) axons across and beyond a lesion site within the CNS (Campbell et al., 1999). The expression of growth associated genes by neurons has profound effects on their ability to regenerate axons. Studies of axonal regeneration following injury to the dorsal roots of spinal nerves have shown that there is an insignificant cell body response, which, can be correlated with the inadequate regeneration of the injured axons, particularly those which are myelinated (Chong et al., 1996). However, regeneration of dorsal root axons can be markedly stimulated by a conditioning peripheral nerve lesion. For example, DRG axons are more likely to grow into peripheral grafts in the spinal cord if given a prior lesion to the sciatic nerve (Richardson and Issa, 1984). This was later identified as being due to a strong cell body response (Richardson and Verge, 1986; Chong et al., 1996).

Indeed some neurons that can grow into peripheral nerve grafts will only do so with a prior injury such as a crush or axotomy. Moreover, ascending sensory fibres in the dorsal columns do not normally regenerate following dorsal column lesion, however, with a sciatic nerve crush performed up to 7 days prior to the spinal lesion, axonal regeneration is greatly enhanced, although it is important

to note that the regeneration of these axons does not extend significant distances rostral to the lesion (Bavetta et al., 1999; Neumann and Woolf, 1999). This suggests that while the cell body regenerative response of neurons is required for vigorous axonal regeneration, it is insufficient without a supportive environment for growing axons.

The non-permissive nature of the environment of the CNS was further demonstrated by studies of the PNS/CNS interface at the dorsal root entry zone (DREZ). Cell bodies of the sensory dorsal root ganglion neurons are situated in the PNS and extend bipolar axons into the periphery and into the spinal cord, providing a unique model to study regeneration in the two environments. Here, crush injury of the peripheral branch of the axon leads to successful regeneration into the PNS. However, although injuring the central branch elicits a regenerative response, axons stop at the border of the spinal cord (Golding et al., 1999). These data suggest that while DRG central axons do regenerate, it is the CNS environment that is repulsive to growth.

In rat neonatal pups (P0-P7), regenerating dorsal root axons are capable of re-entering the CNS (Carlstedt et al., 1987) demonstrating that the interface of PNS and CNS is more permeable at a young age or that when young, neurons are intrinsically more capable of regenerating. For example, embryonic neuronal precursor cells transplanted into myelinated tracts, without injury, survive and extend axons (Li and Raisman, 1993; Davies et al., 1993; Davies et al., 1994). Furthermore, embryonic medullary and mesencephalic raphé cells (Foster et al., 1985), human forebrain neuroblasts (Wictorin et al., 1990) and grafts of human embryonic spinal cord (Wictorin and Bjorklund, 1992) transplanted in the injured CNS environment do grow, suggesting that these neurons have an intrinsic vigour for growth or, that they lack the receptors or cell surface mediators that respond to the inhibitory nature of the CNS environment. Moreover, it seems that damaging the CNS creates an inhospitable environment (Berry, 1982) since robust regeneration of adult DRG neurons up to 6-7mm was evident when transplanted with minimal trauma to central white matter tracts (Davies et al., 1997)

The inhibitory environment in the CNS

The two dominant hypotheses concerning the failure of axonal regeneration in the CNS are that it is prevented by inhibitory molecules or that it is the result of an unsatisfactory cell body response to axotomy. The inhibitory molecule hypothesis was boosted by the results of peripheral nerve grafting to the CNS, which clearly emphasised the importance of the environment around the injured axons. Subsequently, the identification in the CNS of many molecules capable of blocking neurite outgrowth in vitro greatly substantiated this hypothesis.

Inhibitors at the lesion site

A large variety of potentially inhibitory molecules are found in CNS lesion sites, including chondroitin sulphate proteoglycans (CSPGs) (Tang et al., 2003; Carulli et al., 2005), tenascins (Zhang et al., 1997), semaphorins (Pasterkamp et al., 2001) and ephrins (Goldshmit et al., 2004). The evidence that any individual molecule in this region plays a significant role in blocking axonal regeneration is weak but the evidence that the scar is a profoundly inhibitory region is strong. Tenascin C knockout mice have been available for many years, but although some spinal injury experiments have been performed (Steindler et al., 1995), no reports of an effect on axonal regeneration have been published. The molecules for which there is the best evidence that they play a significant role in inhibiting axonal regeneration within the spinal cord are CSPGs, semaphorins and ephrins.

CSPGs

CSPGs are proteoglycans comprising a core protein with variable numbers of glycosaminoglycan (GAG) side chains. Aggrecan, versican, neurocan, brevican, neuroglycan D, NG2, the receptor-type protein tyrosine phosphatase PTPb and its splice variant phosphacan are among the CSPGs found in the CNS of mammals (Hartmann and Maurer, 2001; reviewed by Carulli et al., 2005).

There have been many reports that CSPGs cause growth-cone collapse, inhibit neurite outgrowth and are a non-conducive substrate for neural cell adhesion (Hynds and Snow, 1999; Snow et al., 1990; McKeon et al., 1995) although not all CSPGs have these effects (Davies et al., 2004) and some have neurotrophic

activity (Junghans et al., 1995). The action of CSPGs has been reported to be a function of the GAG sidechains (Yamada et al., 1997; Talts et al., 2000), the core proteins (Dou and Levine, 1994; Schmalfeldt et al., 2000) or both (Ughrin et al., 2003), depending on the CSPG studied and the type of investigation. The pattern of sulphation of the GAGs is also a factor in inhibitory activity (Gilbert et al., 2005).

CSPGs are not evenly distributed at lesion sites in the CNS and individual CSPGs have characteristic patterns of expression. Neurocan and NG2 are rapidly upregulated in and around spinal injury sites and phosphacan and brevican are more slowly upregulated. Phosphacan, NG2 and tenascin C are strongly expressed in the lesion by invading meningeal cells whereas neurocan is strongly expressed by glia at the lesion margins. NG2 glia accumulate around lesions and become rounded; it is difficult to be certain whether rounded NG2 positive cells inside the lesion site are of glial or other origin. In contrast to the main myelin associated inhibitors of axonal regeneration, little is known about signal transduction following CSPG exposure although there is now evidence that activation of Rho-A through a mechanism involving EGFR and intracellular calcium is involved (Koprivica et al., 2005). The evidence that CSPGs play a role in inhibiting axonal regeneration in the spinal cord comes from two sources: first they are most strongly expressed, unlike Nogo isoforms, in and around lesion sites where axons fail to regenerate and, second, treatment with chondroitinase ABC to remove GAGs, is reported to enhance axonal regeneration in CNS tissue.

In vivo numerous studies has shown promising results for regenerative growth after enzymatic cleavage of GAG side chains with the administration of Chondroitinase ABC (ChABC). For example, ChABC infusion into the brain allowed lesioned nigrostriatal axons to regenerate back to their targets (Moon et al., 2001); and intrathecal administration of ChABC enhanced corticospinal axon regeneration caudal to a dorsal column crush lesion (Bradbury et al., 2002). A study by Houle et al. (2006) sought to enhance the extension of regenerated axons from the distal end of a peripheral nerve graft back into the C5 spinal cord, having bypassed a hemisection lesion at C3. Here they showed that applying ChABC to a cervical level 5 (C5) dorsal quadrant lesion of the adult rat spinal cord to degrade the local accumulation of inhibitory chondroitin

sulfate proteoglycan allowed many more axons to extended for much longer distances into the cord after ChABC treatment and bridge insertion, with concomitant functional improvement, compared with the control groups, in which axons regenerated into the PN graft but growth back into the spinal cord was extremely limited.

More recently, using the gfap promotor to express a CSPG-degrading enzyme chondroitinase ABC (ChABC) in astrocytes. Corticospinal axons were shown to extend within the lesion site, but not caudal to it, after dorsal hemisection in the transgenic mice, although the functional outcome was insignificant. In contrast, however, the same study demonstrated, functionally significant sensory axon regeneration after dorsal rhizotomy (Cafferty et al., 2007). In an attempt to explain why CST axons do not leave the lesion site into which they have grown, the authors suggest that this is probably due to the myelin inhibitory nature of the caudal cord (Cafferty et al., 2007). Both studies by Houle et al. (2006) and Cafferty et al. (2007) highlight the need for a combinatorial approach to enhance regeneration with several mediators disinhibiting the environment of regenerating axons as well as numerous factors boosting the intrinsic capability of the injured neuron (see sections below).

Ephrins in the adult mammalian nervous system

Expression of ephrins is downregulated postnatally in most tissues, however, substantial expression of ephrins and receptor ephs remains in adult brain and spinal cord of humans (Hafner et al., 2004; Sobel, 2005), other primates (Xiao et al., 2006) and rodents (Liebl et al., 2003). EphrinB3 plays an important role in limiting axonal regeneration in the mammalian spinal cord. It is a midline guidance marker for growing EphA4-positive corticospinal tract axons (Kullander et al., 2001), but is also strongly expressed in adult myelin (Benson et al., 2005). Myelin ephrinB3 is potent: the contribution of this molecule in CNS myelin to the repulsion/retraction response of cortical neurites was similar to that of Nogo, MAG and OMgp combined (Benson et al., 2005). Ephs are expressed on various classes of neuron in adult mammals and have been shown to be upregulated following contusion or compression injuries of the thoracic spinal cord (Miranda et al., 1999; Willson et al., 2002). Of particular

interest is prominent accumulation of EphA4 in lesioned corticospinal axons (Fabes et al., 2006) which may make these fibres sensitive to most ephrins. Some mammalian DRG neurons express EphA4 during development, are appears to be involved in in the control of sprouting following skin lesions (Moss et al., 2005), however, it is unclear whether expression in DRGs includes those neurons that contribute to the ascending dorsal columns or whether expression is retained into adulthood. Eph expression by astrocytes (Miranda et al., 1999) has been implicated in gliosis and scar formation. Bundesen et al. (2003) showed that, following partial spinal cord transection injuries in mice, reactive astrocytes upregulated ephrinB2 and meningeal cells upregulated EphA4. Furthermore, they also suggested that signalling between astrocytes and meningeal cells may initiate the development of the glia limitans at the injured surface of the cord. The presence of ephrinB2 in the astrocytic scar would also present a further barrier to regeneration of Eph-positive axonal tracts.

Synthesis of cytoskeletal components required for axonal growth

As noted earlier, synthesis and transport of cytoskeletal components down the axon to support the formation and extension of growth cones occurs after injury. This has become a major field of research interest and applies both to PNS and CNS regeneration. The synthesis and transport of numerous cytoskeletal components including actin, tubulin and neurofilament components are required for growth cone formation and extension during development (reviewed in Gordon-Weeks, 2004). In the adult, following injury there are changes in these cytoskeletal components which occur to aid a regenerative response. For example, following facial nerve axotomy, the facial nucleus increases synthesis of both actin and tubulin but decreases in neurofilament (Tetzlaff et al., 1988). Moreover, following lesions to the internal capsule, thalamic neurons also upregulate β-tubulin (Geisert and Frankfurter, 1989). In addition increases in tubulin are also observed in the facial nerve following injury (Gloster et al., 1994) and these increases are associated with target denervation (Wu et al., 1997). The decrease in neurofilament synthesis may serve to allow more essential components of the cytoskeleton such as actin and tubulin to initiate regrowth of the axon (Tetzlaff et al., 1988).

In contrast to the PNS, although tubulin expression is significantly less robust in non-regenerating axotomised CNS neurons such as corticospinal (Kost and Oblinger, 1993) and rubrospinal (Tetzlaff et al., 1991) neurons, there is a sustained increase in a specific tubulin isoform – α1 in rubrospinal neurons (Tetzlaff et al., 1991). As mentioned earlier, Tubulin α1 is expressed during development and following peripheral nerve injury (Gloster et al., 1994). In corticospinal neurons, tubulin α1 synthesis is reduced two days post injury which may contribute to the ineffective regenerative response of these long-tract CNS neurons (Mikucki and Oblinger, 1991). This suggests that the lack of cytoskeletal synthesis correlates with regeneration failure. However, it is unlikely that this is the primary reason for regenerative failure and is more a contribution to the overall decreased response of these neurons to regeneration.

Scar and cavity formation in the injured mammalian CNS

Cavity formation

Cavitation often occurs following compression and contusion injuries to the spinal cord, resulting in increased volume of damaged tissue, surrounded by scar tissue, contributing to regenerative failure (Schwab and Bartholdi, 1996). These large fluid-filled cavities are largely thought to be due to necrosis and apoptosis of cells at the centre of the lesion (Beattie et al., 2000). Cavities are filled with ependymal cells, macrophages, Schwann cell and astrocytes (Wallace et al., 1987).

Moreover, Fitch and colleagues (1999) hypothesised that secondary damage is the result of inflammation. To test this, zymosan, a non-toxic particulate yeast wall preparation which is used as a macrophage/microglia activator in tissue culture experiments was injected into the corpus callosum of adult rats via a single microinjection that minimised cellular injury and did not break the BBB. Here, a persistant inflammatory reaction mediated by activated macrophages and microglia generated a cavity which was free from GFAP and vimentin positive astrocytes, but were filled with activated macrophages and microglia (Fitch et al., 1999).

It is important to note however, that there are considerable species differences in whether cavitation occurs after injury. In rats, cavitation is prominent whereas in mice, rather than displaying progressive necrosis and cavitation at the injury site, the lesion site fills with connective tissue, which then undergoes a remodelling in which it contracts, drawing the two ends of the injured spinal cord closer together (Inman and Steward, 2003)

The astrocyte reaction and the glial scar

Astrocytes are the principal neuroglial cell in the CNS, providing both physical and metabolic support to surrounding neurons. The astrocyte response to injury proceeds through several stages and depends on the extent of trauma. Following injury to the facial nerve, local protoplasmic astrocytes in the facial nucleus upregulate synthesis of glial fibrillary acidic protein (GFAP) at transcriptional and translational levels, as well as other astrocytic markers such as CD44 (Tetzlaff et al., 1988; Raivich et al., 1999; Ridet et al., 1997). This early molecular response is followed by a second phase associated with an enlargement of astrocyte processes as the cells reorganize cytoskeleton-associated molecules, such as GFAP to the perinuclear cytoplasm, and transform into reactive, fibrous astrocytes (Graeber and Kreutzberg, 1986). Cytokines play a crucial role in this transformation, especially interleukin (IL)-6 and transforming growth factor β-1 (TGFβ1). The absence of IL-6 in genetically deficient mice leads to a reduction in the number of GFAP-positive fibrous astrocytes, indicating a stimulatory role for IL-6, whilst absence of TGFβ1 leads to an increase in both GFAP synthesis and an increase in the number of protoplasmic astrocytes (Klein et al., 1997; Raivich et al., 1999) indicating a generalized inhibitory effect. One function of the reactive astrocytes in the facial nucleus following nerve injury may be to divide damaged from healthy tissue (i.e. injured and dyiing neurons from intact cells). This increased synthesis of GFAP and vimentin also appears to contribute to tissue rigidity and the stability of newly formed vessels (Pekny et al., 1999). Astrocytes form thin sheet-like lamellar processes, which eventually displace microglia and surround regenerating neuronal cell bodies, isolating them from their synaptic input and eventually forming a small glial scar (Graeber and Kreutzberg, 1988).

The astrocyte response to facial nerve injury is relatively mild compared with that of direct insults to the CNS. Direct physical trauma, for example spinal cord injury, or ischemia will lead to a much stronger response, with astrocyte proliferation and the formation of massive scars (reviewed in Fawcett and Asher, 1999). It is widely believed that the glial scar forms one of the main barriers for regenerating axons in the mammalian CNS. Whereas injured optic nerve axons are able to penetrate dense glial scars in Xenopus (Reier, 1979) they regrow much more slowly and for shorter distances in mammals (Campbell et al., 1999). At the border of lesions in the mammalian CNS, axons stop growing and become dystrophic and were thought to be quiescent (Ramon y Cajal, 1928). However, a recent in vitro study demonstrated that despite their highly abnormal appearance and stalled forward progress, dystrophic endings near spinal lesions are extremely dynamic, being involved in endocytosis and the continuous protrusion of processes (Tom et al., 2004).

The glial scar is composed of a dense network of cells consisting mainly of reactive hypertrophic astrocytes with thick interdigitating processes associated with an inhibitory extracellular matrix. They inhibit neurite outgrowth, a phenomenon attributed both to the molecules on the cell surface of reactive astrocytes and components of the extracellular matrix, including CSPGs, ephrins and semaphorins. Other cells also form this part of the scar and include oligodendrocytes, NG2+ glia and microglia which surround a fibrotic scar that consists of meningeal cells, vascular endothelial cells, OPC's and macrophages. Both layers are separated by the glia limitans, a structure which is formed at the interface of astrocytes and meningeal cells but is also present in the uninjured CNS where it forms a barrier between the pia mater and CNS tissue (Fawcett and Asher, 1999; Shearer et al., 2003)

Like in the facial nucleus, the role of reactive hypertrophied astrocytes is to form a barrier to prevent further injury to uninjured areas (Reier and Houle, 1988). This was aptly demonstrated by Bush and colleagues (1999) where reactive astrocytes adjacent to a forebrain stab injury were selectively ablated in adult mice expressing herpes simplex virus thymidine kinase (HSV-TK) from the GFAP promoter by treatment with ganciclovir. Later Faulkner et al. (2004)

showed that small stab injuries in transgenic mice given ganciclovir to ablate reactive astrocytes caused failure of blood-brain barrier repair, leukocyte infiltration, local tissue disruption, severe demyelination, neuronal and oligodendrocyte death, and pronounced motor deficits, while small stab injuries in control mice caused little tissue disruption, little demyelination, no neuronal death, and mild functional impairments. This implies that GFAP+ astrocytes have a protective role, sealing the site of injury from unharmed tissue.

In GFAP null mice, post-traumatic reactive gliosis proceeds normally suggesting that GAP protein is not essential for this process (Pekny et al., 1995). However, there is some overlap of the function of GFAP with a similar protein vimentin. Vimentin appears to compensate for deficiencies in GFAP since scar formation appeared normal after spinal cord or brain lesions in GFAP-/- or vimentin-/- mice. However, gliosis was severely impaired in GFAP and vimentin double KO mice developed less dense scars frequently accompanied by bleeding (Pekny et al., 1999).

The inhibitory nature of the glial scar was demonstrated in vitro using three-dimensional astrocyte cultures which showed that postnatal DRG and RGC cultures were unable to penetrate the scar (Fawcett et al., 1989). One of the best in vivo models for the study of reactive astrocytes is following a dorsal root injury (rhizotomy) where primary sensory neurons can be studied as they reach the dorsal root entry zone (DREZ).

Following dorsal root rhizotomy, astrocytes in the spinal cord hypertrophy and extend processes, up to 700μm into the basal lamina tubes of the connected dorsal roots (Zhang et al., 2001). Regenerating sensory axons stop upon contacting these astrocytes and form either end bulbs (Liuzzi and Lasek, 1987) or turn around and extend toward the somata (Zhang et al., 2001). However, application of neurotrophins has shown to be beneficial for aiding axons to grow across the DREZ and this is discussed later.

Overcoming glial inhibition and regeneration of corticospinal axon regrowth following contusion lesion has also been achieved using X-irradiation with both low (Kalderon and Fuks, 1996; Ridet et al., 2000) and high doses (Zeman et al., 2001). And, while astrocytes were not completely eliminated, there was a marked improvement in functional outcome.

Myelin-associated inhibitors of axonal regeneration

Most myelinated tracts in the CNS fail to re-grow after injury although there is at least one exception, namely the olfactory sensory projections in the olfactory bulb where neuronal recovery and reconnection persists well into old age (Morrison and Costanzo, 1995). Whilst the ability of the glial scar to impede axonal growth has already been discussed, another, perhaps more severe hurdle is the problem of myelin associated inhibitors of regeneration (reviewed Anderson et al., 2007). The idea that myelin derived molecules could be inhibitory to axonal growth in the CNS first stemmed from the work of Berry (1982). He hypothesised that while axons regenerated following chemical ablation which did not damage adjacent axons, mechanical damage nearly always elicited myelin damage and resulted in reduced regeneration.

A number of myelin associated proteins have been identified that exert inhibitory action on axonal growth. Schwab and Caroni, (1988) demonstrated that CNS myelin inhibited neurite growth in vitro and that two components of this myelin had most of the inhibitory activity (Caroni and Schwab, 1988a). The generation of a function blocking antibody, IN-1, against one of these proteins (Caroni and Schwab, 1988b) lead to a landmark paper demonstrating that blocking myelin inhibitory components with IN-1 lead to massive sprouting and regeneration of injured corticospinal axons (Schnell and Schwab, 1990). The IN-1 antibody lead to the cloning of the Nogo gene (Chen et al., 2000; GrandPre et al., 2000; Prinjha et al., 2000). The Nogo gene locus gives rise to three transcripts, Nogo-A and B which are alternatively spliced and Nogo-C which is transcribed from an alternative promoter (Oertle et al., 2003). Furthermore, two other major myelin associated inhibitors have been identified; oligodendrocyte myelin associated glycoprotein (OMGP) (Wang et al., 2002a) and myelin associated glycoprotein (MAG) (McKerracher et al., 1994). All three related proteins signal through a common receptor, Nogo-receptor (NgR) (Fournier et al., 2001) which appears to interact with p75 neurotrophin receptor (NTR) (Wang et al., 2002b) eventually activating the RhoA signalling pathway (Yamashita et al., 2002). Song et al. (2004) suppressed p75NTR in mice, and showed that regenerative ability in the CNS did not improve significantly,

postulating that other co-receptors existed which associate with NgR. Recently, Lingo-1 and TAJ/TROY, two new partners known to interact with NgR have been identified and may form a complex through which NgR might function (Mi et al., 2004; Shao et al., 2005; Anderson et al., 2007).

Null mutants for the variants of the Nogo protein however, have yielded mixed results (Kim et al., 2003; Simonen et al., 2003; Zheng et al., 2003) and while there has been some attempt at clarification, these studies still remain somewhat controversial (Steward et al., 2007; Cafferty et al., 2007). Furthermore, blocking NgR by intrathecal administration of Nogo-66(1 40) antagonist peptide (NEP1 40) results in significant axon growth of the corticospinal tract, and improves functional recovery following mid-thoracic spinal cord hemisection (GrandPre et al., 2002). However, somewhat surprisingly, NgR deficient mice did not show enhanced regeneration of corticospinal tract axons in comparison with wild-type controls after spinal dorsal hemisection (Zheng et al., 2005).

Interestingly treatment of rats with Nogo antibody following a unilateral pyramidotomy elicits both intact and lesioned tracts to sprout and allow full recovery in motor and sensory tests compared with untreated controls (Thallmair et al., 1998). Furthermore, crossing of non-injured CST axons into the red nucleus (Z'Graggen et al., 1998) as well as increased sprouting of rubrospinal projections into the ventral horn after a bilateral pyramidotomy (Raineteau et al., 2002) following application of Nogo antibody has been demonstrated. Thus, Nogo antibody induced collateral sprouting of denervated axons onto uninjured or spared fibres could be beneficial in partial spinal cord lesions, although sprouting of uninjured CST axons into aberrant locations has been demonstrated (Bareyre et al., 2002) which could have adverse physiological effects.

Inflammatory Changes

Axonal injury causes acute inflammatory changes at the lesion site, in the distal part of the nerve and around the cell body of injured neurons. In peripheral nerves, these changes are characterised by an influx of leukocytes that assist

Schwann cells in clearing dysfunctional myelin debris, around the cell body. These local inflammatory cells are rapidly activated and move into direct contact with the cell body to interact with T-cells that patrol injured neural tissue (Kloss et al., 1999).

In spite of these effects there appears to be little or moderate obvious correlation between the inflammatory changes described here and the speed of axonal regeneration. Hence, deficiency for the macrophage colony-stimulating factor (MCSF) causes a severe reduction in microglial proliferation as well as early lymphocyte recruitment but does not affect the speed of axonal regeneration (Raivich et al., 1994; Kalla et al., 2001). Similarly, a lack of effect on regeneration has also been observed in mutant mice with enhanced inflammatory response to axonal injury, following deletion of the common neurotrophin receptor p75NTR (Gschwendtner et al., 2003) or the protein tyrosine phosphatase shp1 (Horvat et al., 2001). Nevertheless, some studies do show a mild positive correlation. Gene deletion of IL-6 reduces inflammatory changes significantly around axotomised motoneurons (Klein et al., 1997), but also causes a moderate decrease in the speed of axonal regeneration (Zhong et al., 1999; Galiano et al., 2001). Inflammatory responses are more pronounced in the CNS, particularly with respect to the microglial response and this is discussed further later.

Inflammatory Response Following Nerve Injury

Inflammatory responses to injury serve two functions. Firstly to allow repair and regeneration with the aim of restoring normal function, and secondly, to provide protection against infectious pathogens (Raivich et al., 1999). Although fundamentally similar, there are key differences in the inflammatory response to injury in the PNS and CNS. These differences are at least partially responsible for the difference in regenerative capacity of the two tissues.

In the peripheral nerve, initial activation following injury results in local synthesis of signalling molecules important in shaping the cellular response to trauma including; immediate early genes (IEG), cytokines, neurotrophic factors, mitogen receptors and chemokines. This induction of cell signalling molecules results in recruitment of neutrophils, granulocytes and macrophages. Schwann cells initiate phagocytosis of myelin debris, but hematogenous macrophages

are required to complete the process. They break down and remove myelin at the lesion site and release cytokines and mitogens, which act on schwann cells and fibroblasts. The mitogenic action on fibroblasts causes the formation of a scar in the nerve (Raivich and Kreutzberg, 2001; Fenrich and Gordon, 2004).
In central nerve tracts, the oligodendrocytes show little activation, and myelin detachment is slow. Recruitment of the myelin-removing hematogenous macrophages is restricted to the site of injury and so the process of myelin removal falls on microglia, which are inefficient at removing myelin despite being functionally related to macrophages. As a result, myelin breakdown is poor, and much of the debris remains. Another key difference is the CNS astrocytes, which undergo hypertrophy and form scars that block axonal regeneration (Raivich and Kreutzberg, 2001; George and Griffin, 1994). The inability of CNS neurons to regenerate was long considered a protective mechanism, as misdirected sprouting axons could compromise the intricate CNS connections. It has recently been suggested however, that the predominant function is to prevent the spread of infectious disease, as demonstrated in the graded neuroglial response resulting in insulation of the injured tissue (Raivich et al., 1999).

The Microglial Response

Molecular characterisation of microglial activation has been intensively studied in the facial nucleus model. Resting microglia are thought to play a role in immune surveillance of the cellular environment of the uninjured nervous system (Raivich, 2005). Microglia activation proceeds though several stages, accompanied by changes in production of cytokines (Raivich et al., 1999). The state of alert (Stage 1) is the first stage of activation, and occurs within the first 24 h (Raivich et al., 1999). There is an increase in molecules with an immune function including integrin subunits αM and β2 (Kloss et al., 1999). There is also an increase in the leukocyte adhesion molecule intercellular cell adhesion molecule-1 (ICAM-1), which shows an increase 1-2 days post-facial nerve transection in mice. ICAM-1 plays an important role in leukocyte extravasation and in the interaction of lymphocytes with antigen-presenting cells (Werner et al., 1998). The homing stage (Stage 2) involves changes which increase microglial mobility for homing and adhesion to the damaged structures (Raivich

et al., 1999). αM, β2 and ICAM-1, the molecules induced during stage 1 decline whilst others such as α5, α6, and β1 are upregulated around 4 days post-injury (Kloss et al., 1999, Werner et al., 1998). The microglia also begin to proliferate in response to an increase in receptors for the mitogens macrophage-colony stimulating factor (MCSF) and granulocyte-macrophage colony-stimulating factor (GMCSF) (Raivich et al., 1991). It is during the homing stage that microglia engage in the process of synaptic stripping, whereby they actively displace synaptic inputs from the cell body of the regenerating neuron, which are subsequently wrapped by astrocytic cell processes. Synaptic stripping is a likely explanation for the failure to regain complex motor movements following facial nerve injury (Graeber et al., 1993).

Transition to Stage 3 occurs in the presence of neuronal cell death and is characterized by the transformation of the microglia into phagocytes (Streit et al., 1988). There is a massive induction of molecules present during the first 2 stages, including integrins, ICAM-1, and a number of new cell adhesion molecules which may play a part in the binding and internalizing of injury-associated debris (Werner et al., 1998, Kloss et al., 1999, Raivich et al., 1999). There is also an induction of molecules needed for antigen presentation including major histocompatability complex molecules (MHC), proteases and proinflammatory cytokines, accompanied by an induction in costimulatory molecules, ICAM-1, B7.2 and the αXβ2-integrin (Werner et al., 1998; Kloss et al., 1999; Raivich et al., 1999). Phagocytosis also causes the activation of adjacent microglia, in a process known as bystander activation. The activated microglia show slight differences in expression of costimulatory factors and integrins and as a result induce energy in lymphocytes. It is suggested that this is designed to direct invading lymphocytes only against antigens processed by the phagocytic microglia (Raivich et al.,1999).

Activation of microglial cells is closely related with the local synthesis of inflammation-associated cytokines, which is a highly graded response, forming a cytokine pyramid (Raivich et al., 1999). MCSF and TGFβ1 are already present in the normal brain, however, slight or indirect injury leads to increased synthesis of TGFβ1, and the induction of IL-6 and the receptor for MCSF. Neuronal cell death is associated with high levels of two additional cytokines, IL-

1β and TNFα (Raivich et al., 1999). Studies utilising mice with cytokine deficiencies have begun to reveal the molecular cascades involved in microglial activation (Raivich et al., 1999). The early cytokines, MCSF, IL-6 and TGFβ1 play a key role in the early phases of microglial activation (stages 1, 2); TNF and TNF receptor type 1 are involved in the bystander activation (Bohatschek et al., 2004) and IFNγ for the immune-mediated response (Deckert-Schluter et al., 1996). Interestingly, constitutive levels of TGFβ1 are needed to maintain normal microglial biology even in the normal, uninjured brain (Makwana et al., 2007 and Chapter 6). These cytokine-activated microglia appear to exert trophic or toxic effects on the surrounding injured neurons, depending on the CNS region and the stage of microglial activation. Only microglia and macrophages express the specific MCSF receptors in the injured nervous system (Raivich et al., 1998), suggesting a microglia-mediated, neuroprotective effect of the early cytokines, at least in the case of MCSF (Raivich et al., 1999).

Leukocyte Recruitment

Leukocyte recruitment, as with microglial and astrocyte activation, is one of the processes that occurs in response to neuronal injury and varies according to the severity of the injury. Like the microglial response, leukocyte infiltration is a graded response conferring to a number of stages as assessed by both indirect trauma like in the facial nerve axotomy model or direct trauma to the brain or spinal cord (reviewed in Raivich et al., 1999).

In the facial axotomy model (indirect trauma), entry of leukocytes (grade 1) is restricted to the facial motor nucleus of the injured neuron (Raivich et al., 1998). Extensive posttraumatic cell death leads to T-cell recruitment (grade 2). Other leukocyte cell types are recruited following more direct trauma. Lesions to the brain and spinal cord elicit the entry of both granulocytes and macrophages (grade 3) in addition to the leukocytes and T-cells (Raivich et al., 1999), although the number of recruited macrophages and granulocytes seems to be much higher following injury to the cerebral cortex than spinal cord (Schnell et al., 1999).

These grade 3 leukocytes have a number of cytotoxic effects and result in considerable secondary injury contributing to axonal degeneration and tissue loss (Popovich et al., 1999). Depletion of circulating infiltrating macrophages

using liposome-encapsulated clodronate enhances hindlimb usage during over-ground locomotion as well as significant preservation of myelinated axons, decreased cavitation in the rostrocaudal axis of the spinal cord, and enhanced sprouting and/or regeneration of axons at the site of injury (Popovich et al., 1999).

There are also differential temporal expression patterns to leukocyte influx. For example, infiltrating lymphocytes generally avoid the injury zone, accumulating instead at the periphery and peaking between day 1 and 4. In contrast, blood-borne macrophages seem to restrict their activity to immediate site of the lesion, peaking between day 4 and 7; whilst granulocytes have an intermediate distribution pattern and tend to peak as early as 24h after injury (Raivich et al., 1999; Schnell et al., 1999).

Examining the role of adhesion molecules has begun to increase our understanding of the mechanism involved in leukocyte recruitment. For instance, indirect trauma associated with neuronal cell death and strong, selective recruitment of lymphocytes (grade 2) that aggregate around phagocytic microglia, express high levels of MHC, B7.2 and αXβ2. It also leads to an upregulation of the endothelial α5β1 and α6β1 integrins (Kloss et al., 1999) but leave the levels of ICAM-1 and VCAM-1 unchanged (Werner et al., 1998). Pro-inflammatory cytokines expressed by microglia and macrophages, including IL-1, IL-6 and TNFα which appear to have an important role leukocyte recruitment (Raivich et al., 1998; Raivich et al., 1999). In more direct trauma, there are increases in levels of ICAM1 and VCAM1 as well as P- and E-selectin which could increase axonal pathology since these adhesion molecules are involved in leukocyte recruitment. Certainly genetic deletion of ICAM-1 inhibits neutrophil extravasation (Bohatschek et al., 2001). Interestingly, a recent study has demonstrated that macrophages can have a positive effect following injury. Yin et al. (2006) show that macrophages secrete a novel growth factor, oncomodulin which promotes the regrowth of axons in the injured adult optic nerve and sensory neurons in vitro by enhancing intracellular cAMP. Harnessing this effect may prove to be a useful strategy in promoting axonal regrowth.

Neurotrophins

Neurotrophins are localised to, and exert their effects, in the nervous system. Members of this family of proteins include nerve growth factor (NGF), brain derived neurotrophic factor (BDNF), neurotrophin-3 (NT-3), neurotrophin-4/5 (NT-4/5), neurotrophin-6 (NT-6) and neurotrophin-7 (NT-7) (Barde et al., 1987; Leibrock et al., 1989; Maisonpierre et al., 1990; Hallbook et al., 1991; Gotz et al., 1994; Lai et al., 1998; for review see Reichardt, 2006). They share common structural features, including a tertiary fold and cysteine knot (Robinson et al., 1995; Butte et al., 1998) that are also present in several other growth factors including TGF-β and platelet derived growth factor. Neurotrophins have an important role in developmental neurobiology where they control cell survival and neuronal differentiation (Reichardt, 2006).

The neurotrophic factor hypothesis is based around the first neurotrophin to be characterised – NGF and suggests that these target derived molecules undergo retrograde transport as internalised receptor-ligand complexes in neurotrophin dependent CNS and PNS neurons (Thoenen et al., 1988), travel up to the cell body and initiate a response upon arrival (Kaplan and Miller, 2000). In recent years, however, it has become evident that BDNF and NT-3 are also anterogradely transported. Studies by von Bartheld et al. (1996) in retinal ganglion cells suggest that these neurotrophins are stored within vesicles in axon terminals and can be released in an activity dependent manner.

Nerve growth factor (NGF)

The prototypic neurotrophic factor NGF was the first identified neurotrophin, isolated from mouse sarcoma tissue over five decades ago (Levi-montalcini and Hamburger, 1951). Not long after its discovery it was shown to be crucial for the survival and maintenance of peripheral sympathetic neurons in neonatal rodents (Cohen, 1960), and that administration of anti-NGF to the developing embryo results in loss of developing primary sensory neurons of the dorsal root ganglia (Johnson, Jr. et al., 1983). During development large numbers of primary sensory neurons are present in the nervous system. Those that manage to form connections survive, since the target tissues excrete neurotrophins such as NGF which retrogradely transport to the cell body

maintaining the survival of the cell (Jones and Reichardt, 1990). Sensitivity to NGF remains throughout their lifetime, and while it is not required for survival of adult cells, it does stimulates neurite outgrowth (Lindsay, 1988). Expression of NGF in the adult rodent nervous system is variable. For example, strong expression of NGF transcripts and protein are detectable in the intact hippocampus and neocortex as well as the cholinergic neurons of the basal forebrain (Large et al., 1986). While dorsal root ganglia and the adjacent spinal nerves contained NGF, no NGF was detectable in dorsal roots and spinal cord, reinforcing the fact that sensory neurons are supplied with NGF exclusively from their peripheral and not from their central field of projection (Korsching and Thoenen, 1985). However, following mechanical injury, there is upregulation of NGF in meningeal cells adjacent to the lesion as well as marked increases in nerve roots and Schwann cells (Widenfalk et al., 2001).

Brain Derived Neurotrophic Factor (BDNF)

BDNF was the second neurotrophin to be identified and was isolated in 1982 from pooled extracts of porcine brain (Barde et al., 1982). BDNF is involved in a number of processes in the developing as well as the mature nervous system including, neuroprotection (Jones and Reichardt, 1990), chemotaxis (Ming et al., 2002) and neurotransmission (for review see Huang and Reichardt, 2001). Like NGF, expression of BDNF is variable in the nervous system and includes high levels in neurons of CA2, CA3, and the hilar region of the dentate gyrus; in the external and internal pyramidal layers of the cerebral cortex, with lower levels in CA1 and in the granular layer of the hippocampus (Ernfors et al., 1990). In the spinal cord, it is found only in some neurons of lamina VII of the dorsal horn, where it modulates some aspects of pain transmission (Pezet and McMahon, 2006). In addition a subpopulation of adult dorsal root ganglion neurons strongly expresses BDNF (Ernfors et al., 1990), and these appear to be of varying size. Unlike NGF, BDNF dependent neurons are continuously reliant on this molecule for survival and secrete it in an autocrine manner (Acheson et al., 1995)

Neurotrophin-3 (NT-3)

NT-3 discovered in 1990 (Hohn et al., 1990; Maisonpierre et al., 1990a; Rosenthal et al., 1990) is by far the most highly expressed in immature regions of the CNS in which proliferation, migration, and differentiation of neuronal precursors is ongoing. NT-3 expression dramatically decreases with maturation of these regions (Maisonpierre et al., 1990b). In the adult, NT-3 transcripts are primarily detected in the CA1 and CA2 neurons of the hippocampus (Ernfors et al., 1990). NT-3 mRNA is not detectable in the adult spinal cord, either before or after compression or complete transection of the thoracic spinal cord (Widenfalk et al., 2001).

Interestingly, myelin formation is inhibited in the absence of NT-3, acting as an inhibitory modulator through the TrkC receptor (Cosgaya et al., 2002). Absence of NT-3 causes severe neurological dysfunction, severe defects of the limbs, substantial portions of peripheral sensory and sympathetic neurons are missing, although motoneurons are not affected (Ernfors et al., 1994; Tessarollo et al., 1994). The most notable gene deletion study for NT-3 displayed high perinatal mortality. Here Donovan et al. (1996) reported that NT-3 is essential for the normal development of atria, ventricles, and cardiac outflow tracts since mutant mice showed severe cardiovascular abnormalities including atrial and ventricular septal defects, and tetralogy of Fallot, resembling some of the most common congenital malformations in humans.

Neurotrophin receptors

Most effects of neurotrophins on neurons appear to be mediated by tyrosine kinase (Trk) receptors. There are a number of biological responses mediated by Trk receptors including neuronal survival, neuronal differentiation, axon outgrowth, synaptic plasticity and neurotransmitter expression.

Three forms of the Trk receptor have been characterised and are designated TrkA (Kaplan et al., 1991; Cordon-Cardo et al., 1991; Klein et al., 1991), TrkB (Squinto et al., 1991), and TrkC (Lamballe et al., 1991). Each Trk receptor possesses specific ligands: NGF binds to TrkA, BDNF and NT4/5 binds to TrkB and NT-3 binds primarily to TrkC. In addition the low affinity neurotrophin

receptor (NTR), p75NTR also binds most of these neurotrophins. Trk receptors are transmembrane glycoproteins with intracellular tyrosine kinase elements. Binding of a neurotrophin induces dimerisation of its Trk receptor, thereby activating the tyrosine kinase and inducing autophosphorylation of specific Trk residues which then bind and activate other messenger systems (for review see Bothwell, 1995)

Intracellular Signalling in the Injured Neuron

In the injured neurons, the prompt arrival of signals for cellular injury and stress is followed by the induction of transcription factors, adhesion molecules, growth–associated proteins and structural components required for axonal elongation. Accompanying this is the activation of intracellular signaling molecules, particularly molecules that control cell cycle and differentiation, synthesis of axonal transport molecules and cytoskeleton components, secreted growth factors and cytokines, and a general increase in energy, amino acid and lipid metabolism (Livesey et al., 1997; Su et al., 1997; Klein et al., 1997; Schmitt et al., 2003; Vogelaar et al., 2003; Fujitani et al., 2004). Moreover, the introduction of gene chip array technology has lead to a dramatic increase in the number of identified genes regulated in the injured and regenerating neurons (Bonilla et al., 2002; Kubo et al., 2002; Boeshore et al., 2004; Kury et al., 2004) as well as the surrounding glia (Cameron et al., 2003; Moran et al., 2004). One of the earliest biochemical changes following axonal injury is the transient upregulation of polyamine-producing enzymes (ornithine decarboxylase, transglutaminase). This has been linked to an increase in mRNA metabolism and protein synthesis (Schwartz et al., 1981; Tetzlaff et al., 1988) resulting in polyamines such as putrescine, spermine and spermidine which show a strong enhancing effect on neurite outgrowth both in vitro and in vivo (Sebille et al., 1980; Schreiber et al., 2004; Oble et al., 2004).

Intracellular signalling mediated by neurotrophin binding to Trk receptors

Genetic studies in invertebrates together with biochemical studies in mammalian systems have established that a conserved linear signalling pathway exists between receptor tyrosine kinases on the cell surface to

intracellular MAP kinases (Olson and Marais, 2000). In mammals the Ras protein family is comprised of H-Ras, N-Ras and K-Ras (Kolch, 2000) and are small (Mw ~ 21000 Da) membrane localised guanine-nucleotide binding proteins which are regulated by a GDP/GTP cycle being inactive when bound to GDP and active when bound to GTP. Several members of the Ras superfamily are activated by neurotrophins binding to Trk receptors including H-, K- and N-Ras (reviewed in Kolch, 2000). As well as, Rit and Rin (Spencer et al., 2002a; Spencer et al., 2002b). The various members of this family suggest that they perform some distinctive roles with respect to the extracellular signals. While the three closely related family members H-, K- and N-Ras, are 85% identical and execute similar downstream signalling with respect to MAP kinase (Segal, 2003), mutations in K-Ras are lethal, but neither H-Ras or N-Ras are essential for growth and development (Reuther and Der, 2000; Umanoff et al., 1995). Biological differences in function between this otherwise highly homologous protein could be reflective of the cellular localisation of the various isoforms of Ras. For example, H-Ras is found in cholesterol-rich lipid rafts within the plasma membrane whereas K-Ras is localised predominantly in the disordered plasma membrane (Prior and Hancock, 2001).

Within activated Trk receptors the phosphotyrosines and surrounding amino acid residues serve as specific recognition sites for effector molecules such as Shc. Activation of Ras is mediated by the adaptor protein Shc. Trk mediated phosphorylation of Shc creates a phosphotyrosine site on Shc that allows the adaptor Grb2 to bind. Grb2 then associates with the nucleotide exchange factor son of sevenless (SOS). A Grb-SOS complex translocates to the plasma membrane, where SOS activates the small G protein Ras by replacing GDP with GTP (Segal and Greenberg, 1996; Reichardt, 2006). This classical mechanism of Ras activation has been extensively studied (Kolch, 2000). However, novel mediators of Ras activation are appearing to emerge, for example, the Ras G protein releasing factor-1 RasGRF1 (Robinson et al., 2005). Active Ras exerts its effects through two major pathways that are linked to neuronal survival and axonal growth - Raf-MEK-ERK, and PI3 kinase pathways (Kolch, 2000; Vanhaesebroeck et al., 2001), as well as indirect activation of pathways such as p38 MAP kinase and Ral GDP dissociation stimulator (RalGDS) (Xing et al., 1998).

Activation of extracellular signal-regulated kinase (ERK)1 and ERK2 is mediated via the protein kinase Raf. Raf in turn phosphorylates mitogen associated protein kinase kinase (MEK)1 and/or MEK2 which then phosphorylate ERK1 and ERK2 (English et al., 1999). These pathways also share common mediators which allow a certain degree of crosstalk and parallel activation. For example, p38 is activated by Ras mediated binding and activation of the exchange factor RalGDS, resulting in the activation of Ral and Src (Ouwens et al., 2002). In addition neurotrophin stimulation of the Ras-family G proteins Rin and Rit can also activate p38 MAP kinase (Shi and Andres, 2005). p38 MAP kinase also activates MAP kinase-activated protein kinase 2. Ras also triggers the proteins Wnk1, and MEK5 resulting in the activation of ERK5 (Watson et al., 2001). MEK5 can also be activated through the RalGDS-Ral-Src pathway (Scapoli et al., 2004). Importantly, the MAP kinase cascades feedback to attenuate and terminate responses. For example, both ERK and RSK mediate the phosphorylation of SOS resulting in the dissociation of SOS-Grb2 (Reichardt, 2006).

In addition to this intermediate complexity in cell signalling, MAP kinase cascades also have both distinct and overlapping targets in the cell (Pearson et al., 2001). For instance, ERK1/2 and ERK5 phosphorylate and activate RSK kinases. Moreover, RSKs and MAP kinase-activated protein kinase 2 both phosphorylate CREB which is essential for normal differentiation and survival of neurons (Reichardt, 2006). In contrast to these shared targets, ERK5 but not ERK1/2 has been shown to activate MEF2 required for neuronal survival (Heidenreich and Linseman, 2004) whilst ERK1/2 but not ERK5 activates ELK1, which has a range of functions ranging from neuronal differentiation to tumorigenesis (Barrett et al., 2006 ;Reichardt, 2006).

PI3-kinase is also activated by the binding of Shc to Grb2. Activation of Ras also initiates PI3-kinase signalling. Activation of PI3 kinase triggers the activation of two protein kinases, the serine threonine kinase, Akt and RAC-PK (Burgering and Coffer, 1995; Marte and Downward, 1997) as well as p70 ribosomal protein S6 kinase (Chung et al., 1994).

PI3-K is a key regulator of cell survival, morphology and growth cone extension in neural cells (Dudek et al., 1997). A mechanism by which PI3-K promotes the survival of neurons is via the activation of the serine/threonine Akt or protein kinase B (PKB) (Dudek et al., 1997). PKB inhibits apoptosis through the phosphorylation of cell death regulatory molecules such as BAD, caspase and forkhead transcription factors (Datta et al., 1997; Brunet et al., 1999; Cardone et al., 1998). Neurotrophin deprived cells in which PI3-K has been constitutively activated or cells in which Ras selectively activates PI3-K are resistant to apoptosis (Rodriguez-Viciana et al., 1996).

Hence, the Ras dependent cell survival required for axonal sprouting or indeed regeneration may be mediated by both the Ras-Raf-MEK-ERK and the PI3-K pathways. In primary neurons, the role of Ras in neurotrophin-regulated cell survival and differentiation varies depending on the cell type assayed. Ras activity is necessary and sufficient for the survival and neuritogenesis of rat and chick sensory but not sympathetic neurons (Klesse and Parada, 1998). Conversely, Ras activity is required for the survival but not neuritogenesis of rat sympathetic neurons (Markus et al., 1997). Understanding the mechanisms behind conflicting data like this remains to be determined.

Inhibition of Ras, Raf, MEK and the group of ERK1, ERK2 molecules that are up-regulated after axonal injury (Kiryu et al., 1995), have been shown to inhibit the survival and neurite outgrowth of embryonic neurons (Borasio et al., 1989; Ihara et al., 1997). Conversely, studies in adult neurons suggest a loss or reversal of this pro-survival/pro-neurite outgrowth role (Liu and Snyder, 2001; Wiklund et al., 2002), stressing the dissimilarity in the embryonic/neonatal and adult signalling.

Increased activity of the Ras⇒Raf⇒MEK⇒ERK pathway is complemented by a robust induction of phosphatidyl-inositol-3 kinase or PI3K gene expression (Ito et al., 1996), and the subsequent activation of protein kinase B or Akt (Owada et al., 1997; Murashov et al., 2001). Expression of active Akt also promotes axonal regeneration, verified using retrograde transport from peripheral target (Namikawa et al., 2000); this effect may be associated with enhanced Akt-mediated distal branching observed in vitro (Markus et al., 2002). Active Akt

also enhances postnatal but not adult motoneuron survival; these effects are reversed by the expression of the dominant negative form of Akt (Namikawa et al., 2000). Interestingly, the neuronal expression of constitutively activated, V12-substituted Ras enhances adult motoneuron survival, and does not result in the activation of Akt, but rather that of ERK1 and ERK2, the downstream targets of the Ras⇒Raf⇒MEK⇒ERK pathway (Heumann et al., 2000).

Neurotrophic factors involved in PNS regeneration

Numerous studies on injured peripheral neurons and neurotrophins have centred on the effects on post-traumatic neuronal survival, particularly in neonatal animals, where cell death is very pronounced (Miyata et al., 1986; Obouhova et al., 1994; Moran and Graeber, 2004; Schmalbruch et al., 1987). In most cases, these studies showed a protective effect (Sendtner et al., 1990; 1994; Yan et al., 1992; Koliatsos et al., 1993; Arenas and Persson, 1994). However, there were cases where externally applied neurotrophins reduced survival, particularly in the case of NGF; the toxic effect depended on the presence of the common neurotrophin receptor, the p75NTR (Wiese et al., 1999).

A similar, toxic effect of p75NTR was observed on axonal regeneration in the sciatic (Boyd and Gordon, 2002) but not in the facial motor nerve (Gschwendtner et al., 2003). Application of various neurotrophins, growth factors and cytokines has also been demonstrated to encourage axonal outgrowth across the space between the disconnected, proximal and distal part of the axotomised peripheral nerve (for reviews see Varon et al., 1983; Raivich and Kreutzberg, 1993; Terenghi, 1999; Boyd and Gordon, 2003). These neurotrophic factors may both stimulate the growth of injured axons and guide axons down Schwann cells aligned in bands of Büngner, perhaps by presenting growth factor receptors on their surface (Taniuchi et al., 1986). Indeed, evidence for both NGF secretion and binding to p75 receptors on the surface of Schwann cells has been demonstrated (Taniuchi et al., 1988).

Studies concentrating on the speed of axonal regeneration in the distal part of the nerve have thus far focussed on three groups of factors – the trophic factors IGF1, IGF2 and BDNF, the TGF β superfamily member GDNF, and the

neurokines LIF and IL-6. All three groups are implicated in the endogenous regulation of the repair process. Application of the closely related exogenous growth factors IGF-1 and IGF-2 enhanced and application of antibodies reduced the pinch test-determined speed of axonal regeneration (Kanje et al., 1989; Glazner et al., 1993). The combined overexpression of the neurokine IL-6 and its receptor resulted in improved nerve regeneration (Hirota et al., 1996), whereas, genetic deletion of IL-6 has been shown to lead to a 15% reduction in the morphometrically-determined speed of axonal regeneration in the crushed facial motor nerve (Galiano et al., 2001). Similarly, a moderate effect was also observed using a functional, walking test assessment following sciatic nerve crush (Inserra et al., 2000). In contrast to this consistent but mild IL-6-mediated action in the periphery, there is substantial controversy regarding its effects on the CNS. Thus, deletion of IL-6 has been shown to reduce glial scar formation and improve central axonal sprouting in the facial motor nucleus model (Galiano et al., 2001), enhance functional recovery after spinal cord injury (Okada et al, 2004), but eliminate the conditional injury-induced spinal axon regeneration (Cafferty et al., 2004).

While both BDNF and GDNF are robustly and reliably induced in the distal portion of the injured peripheral nerve, the expression of their receptors on axotomised neurons slowly decreases during chronic disconnection (Hammarberg et al., 2000). Application of BDNF or GDNF did not improve regeneration immediately following injury, however, it promoted axonal regeneration of motoneurons whose regenerative ability has decreased by chronic axotomy two months prior to nerve resuture (Boyd and Gordon, 2002; 2003a). These delayed activities totally reversed the harmful effects of late nerve repair, which could indicate insufficient BDNF/GDNF-mediated support following chronic axotomy. These findings are in keeping with the strong, 50% reduction in the enduring success of the reinnervation of peripheral muscle in trkB+/- mice, where gene dosage of the primary BDNF receptor is also reduced by 50% (Boyd and Gordon, 2001). Inhibition of endogenous BDNF (Streppel et al., 2002) and GDNF (Sun and Oppenheim, 2003) also decreases the post-axotomy collateral sprouting in the peripheral nerve.

Furthermore, NGF deprivation by neutralizing the endogenous activity with specific antibodies induces axotomy-like changes even in the intact, NGF-

sensitive sensory and sympathetic neurons, particularly with expression of transcription factors such as c-jun and numerous neuropeptides including galanin, VIP, substance P; CGRP and NPY (Shadiack et al., 2001). Aside from these profound biochemical changes, additional antibody-mediated deprivation does not affect the speed of axonal regeneration of NGF-sensitive neurons (Diamond et al., 1987) and certainly, although speculative, this could be due to a functionally stable state of NGF deprivation during the regeneration program, which coincides with a significant reduction in high affinity NGF receptors (Raivich and Kreutzberg, 1987; Verge et al., 1989).

Neurotrophins involved in CNS axonal sprouting and regeneration

There is numerous circumstantial evidence of the involvement of neurotrophins in central axonal sprouting, both in vitro and in vivo. For example in vitro, FGF, BDNF and NT-3 induce axonal, but not dendritic branching of dentate granule neurons (Patel and McNamara, 1995). In addition, cultured chick embryo DRGs sprout filopodia from axonal shafts when in contact with NGF coated polystyrene beads (Gallo and Letourneau, 1998). Furthermore, BDNF application to embryonic cultures of Xenopus spinal neurons induced collateral protrusions of lamellipodia along the neurite processes (Gibney and Zheng, 2003).

In vivo, the evidence is more complex. For example during development, administration of mouse NGF to dorsal root axons in the spinal cord enhances axonal sprouting into the dorsal funiculus and grey matter, with some dorsal root axons having twice the surface area of controls (Zhang et al., 1994). Conversely, in the same model, NT-3 inhibits branching or DRG's (Zhang et al., 1994). In the adult rat, application of NGF antiserum to sensory nerves blocks local sprouting into neighbouring denervated axons (Diamond et al., 1987). In addition, intraventricular administration of NGF antiserum prevented the collateral sprouting of septohippocampal cholinergic axons following unilateral lesions of the entorhinal cortex (Van der Zee et al., 1992). Moreover, intraventricular administration of NGF also increases mossy fibre sprouting in the CA3 region (Adams et al., 1997). However, whilst BDNF promotes the sprouting of mature, uninjured serotonergic axons and enhances the survival or

sprouting of 5-HT axons normally damaged by the serotonergic neurotoxin p-chloroamphetamine, both NT-3 and NGF fail to do so (Mamounas et al., 1995). Therefore, whilst differences exist in the efficacy of a particular neurotrophin to a region of the CNS, neurotrophins are able to enhance collateral sprouting of axons (Hagg, 2006).

Giehl and Tetzlaff (1996) demonstrated, using in situ hybridization, that corticospinal neurons express both TrkB and TrkC receptors. Hence several studies have explored the effect of BDNF and NT-3 on CST sprouting and regeneration (Hagg, 2006). For example, in adult rats, administration of NT3 enhanced axonal sprouting of lesioned corticospinal tract as well as long distance regeneration when accompanied with an IN-1 antibody to neutralise myelin associated growth inhibitors (Schnell et al., 1994). In addition, local, sustained expression of NT-3 supports axonal plasticity of intact CST axons after spinal cord lesion.

BDNF applied to the cell bodies of axotomised corticospinal neurons showed a significant increase in collateral sprouting of injured axons and an increase in the number of contacts with propriospinal interneurons (Vavrek et al., 2006). Moreover, injection of BDNF into the sensorimotor cortex following a pyramidotomy with concomitant delivery of NT-3 to the spinal cord enhanced CST sprouting (Zhou and Shine, 2003). While the effects of NT-3 in these studies spears to promote sprouting as well as axon outgrowth, BDNF has been shown to lack the ability to induce axon outgrowth (Ozdinler and Macklis, 2006). Collateral sprouting of lower motoneurons from the non-injured side to injured side can also be promoted with NT-3 (Zhou et al., 2003). Moreover, collateral sprouting of intact CST axons toward injured parallel RST axons can be induced through a combination of a lesion plus NT-3 application (Jeffery and Fitzgerald, 2001). Similarly, corticofugal plasticity can be enhanced using NT-3, both in the midbrain between corticospinal and rubrospinal neurons, as well as at the level of the spinal cord, resulting in enhanced functional recovery following spinal cord injury (Iarikov et al., 2007). Recently, a study by Hagg et al. (2005) does place some doubt on the effects of NT-3, since local application of NT-3 close to a pyramidotomy reduced the number sprouting collaterals by almost 40% compared with vehicle treated group and instead there was an

enhanced response of local CGRP positive fibres, suggesting that these local sensory axons might interfere with NT3 action on CST fibres (Hagg, 2006).

Many studies investigating the function of neurotrophins have utilised the unique model of dorsal root rhizotomy to assess regeneration of peripheral axons across the dorsal root entry zone (DREZ) into the CNS. For example, intraspinal injection of adeno-associated virus expressing neurotrophin-3 (NT3) or NGF resulting in strong expression of these factors in glial cells and motoneurons, promotes regeneration (Zhang et al., 1998; Romero et al., 2001). Moreover, intrathecal administration of NT3, NGF, or glial-cell-line-derived neurotrophic factor (GDNF), but not BDNF, resulted in selective regrowth of damaged axons across the dorsal root entry zone and into the spinal cord resulting in the reestablishment of functional recovery (Ramer et al., 2000). It has been reported that continuous infusion of NGF to the dorsal spinal cord can promote the ingrowth of up to 37% of central processes from primary sensory neurons after dorsal root crush, by two weeks post operation (Oudega and Hagg, 1996). It is important to note however, that these latter studies examined the effects of neurotrophin administration after rhizotomy by crush rather than transection which inevitably raises the possibility that some fibres may have been spared.

Studies utilising transplantation of autologous grafts modified to express neurotrophins have been successful to a degree. For example, transplantation of primary fibroblasts which have been modified to express high levels of NGF, into spinal cord, successfully entered these grafts but were not found to exit them. The authors of this study suggested that this arrested growth is perhaps due to the axons having arrived at the point where the concentration of growth factors is highest, and that a better strategy for spinal cord repair might be a system whereby the highest concentration of neurotrophin can be sequentially switched to sites downstream of the growing axons (Tuszynski et al., 1997; Jones et al., 2001).

Mechanisms of axonal sprouting

The mechanisms underlying axonal sprouting following injury are unclear. However, given that neurotrophins acting on Trk receptors contribute to axonal sprouting, one might consider that major pathways downstream of Trk receptor activation are involved (Hagg, 2006). One such pathway involves the common downstream mediator PI3K. PI-3 kinase has been shown to be involved in the transduction of NGF signals mediating nerve fibre growth (Rodriguez-Viciana et al., 1994; Jackson et al., 1996), retinal neurite outgrowth (Lavie et al., 1997) and in the signaling pathways of other growth factors (Chung et al., 1994). Gallo and Letourneau, (1998) showed that neurite outgrowth and collateral sprouting was reduced when using the PI3K inhibitors wortmannin and LY294002. Furthermore, neurite elongation in primary DRG neurons was decreased following application of wortmannin (Jones et al., 2003). Moreover, both phospholipase C-γ and PI3K have been shown to be crucial to TrkA induced growth cone guidance (Ming et al., 1999). Neurotrophin induced sprouting along the axon could be Trk mediated since there is evidence of these receptors along the extent of the axon. For example, Richardson and Riopelle (1984) demonstrated that radiolabelled NGF injected at the cervical cord is transported down to L4/5 DRG, suggesting that sensory axons have TrkA. Furthermore, recently Chang and Popov (1999) showed that focal exposure of a soma or a small axonal segment of Xenopus embryonic axons to NT-3, resulted in the spontaneous neurotransmitter secretion from the presynaptic nerve terminals located some distance away from the site of NT-3 application (Hagg, 2006).

The other major pathway activated downstream of Trk receptors is the Ras-Raf-MEK-ERK. Evidence of sprouting mechanisms are conflicting with respect to this pathway and given that the effects of Ras and MEK form a major part of this thesis, sprouting mechanisms relating to them are discussed further in Chapters 4, 5 and 7.

Axonal sprouting can also be induced by inhibiting myelin associated growth inhibitors. Inhibiting Nogo receptor with antagonists or antibodies induces much collateral sprouting rostral to the lesion (Schwab, 2004) suggesting that Nogo receptor is normally involved in preventing sprouting or branching of myelinated axons (Hagg, 2006). This implies that collateral sprouting may occur

predominantly at the nodes of Ranvier where there is a gap in the myelin sheath. Certainly, MAG and OMgp (Scherer et al, 1995) and CSPG's like versican (Oohashi et al., 2002) are present at the nodes of Ranvier making collateral sprouting from these regions, following inhibition of the inhibitors, a plausible theory (Hagg, 2006).

Intracellular signalling related to myelin inhibitors has been shown to induce growth cone collapse via a RhoA mechanism and reduce actin cytoskeletal dynamics (Hagg, 2006). Moreover, both myelin inhibitors of axon growth and CSPGs activate protein kinase C and blocking PKC activity pharmacologically and genetically attenuates the ability of CNS myelin and CSPGs to activate Rho and inhibit neurite outgrowth. Intrathecal infusion of a PKC inhibitor, G06976, into the site of dorsal hemisection promotes regeneration of dorsal column axons across and beyond the lesion site in adult rats (Sivasankaran et al., 2004).

Transcription factors.

Following activation of MAP kinase pathways, phosphorylation and nuclear localisation of a host of transcription factors including c-jun, junD, activating transcription factor (ATF)3, P311, Sox11 and Signal Transducer and Activator of Transcription 3 (STAT3), as well as decreased expression and activity of islet-1, ATF2 as well as NF kappa B (Herdegen et al., 1991; Jenkins and Hunt, 1991; Doyle et al., 1997; Povelones et al., 1997; Schwaiger et al., 2000; Mason et al., 2002; Tanabe et al., 2003; Fujitani et al., 2004) contribute to the change in gene expression of the injured neuron.

In many cases, complete deletions for these transcription factors are embryonically lethal, limiting studies in vivo, in the adult animal. Nevertheless, recent advances in cre/loxP technology has permitted cell type specific, neuronal deletion of the loxP site flanked or floxed genes have begun to provide insight into the specific roles of these transcription factors. Neuronal specific deletion of STAT3 increases neuronal cell death after injury (Schweizer et al., 2002), to a degree similar as that observed for CNTF and LIF (Sendtner et al., 1996), thus pointing to the role of STAT3 as an intracellular survival-promoting factor.

The effects of transcription factors on nerve regeneration are well characterized in the case of c-jun. A recent study using the facial axotomy model showed that neuronal deletion of c-jun hinders the expression of genes and proteins associated with axonal regeneration, reduces the speed of target reinnervation and functional recovery significantly and also completely blocks central axonal sprouting (Raivich et al., 2004). This is in keeping with previously demonstrated data (Ham et al., 1995; Xia et al., 1995; Palmada et al., 2002; Lindwall et al., 2004) where deletion of jun blocks post-traumatic neuronal cell death and leads to severe neuronal atrophy. It also inhibits the recruitment of lymphocytes, and the activation of neighbouring microglia. Some axonal regeneration still continues in the absence of c-jun highlighting the importance of alternative pathways and compensatory mechanisms, which may be shared during developmental axonal outgrowth. These compensatory molecules may incorporate additional transcription factors such as STAT3 and ATF3 (Pearson et al., 2003; Zhou et al., 2004); clarification of their role is needed to understand the signals regulating the gene expression switches occurring in the regenerating neuron.

Importantly, peripheral axons and non-neuronal cells contain numerous growth inducing and trophic molecules including the ciliary neurotrophic factor (CNTF), neurotrophin-3 (NT3) and fibroblast growth factors/FGFs (Eckenstein et al., 1991; Funakoshi et al., 1993; Sendtner et al., 1994), which are secreted following injury. Both CNTF and the nuclear transcription factor STAT3, the downstream target of activated CNTF receptor, have regulatory roles that are particularly informative. Neuronal deletion of STAT3 results in enhanced post-traumatic cell death, implicating a neurotrophic-like role for STAT3 (Schweizer et al., 2002). Deletion of CNTF, which is abundantly present in myelinated Schwann cells but not in or around the cell bodies of axotomized motoneurons (Rende et al., 1992; Dobrea et al., 1992) causes a delay in the appearance of the phosphorylated STAT3 and its nuclear translocation in neuronal cell bodies. Therefore in summary, this points to a signalling cascade beginning with local release of CNTF by damaged myelinated Schwann cells, its local action on adjacent axons, intraaxonal phosphorylation of STAT3 and its retrograde transport to the cell bodies of injured neurons.

Cell Adhesion Molecules

Functional studies in vivo have thus far centred on the role of laminin, its α7 β1 integrin receptor and galectin. Deletion of the gene encoding α7 integrin subunit results in a severe, approximately 40% reduction in the speed of motor axon regeneration following facial axotomy and a strong delay in the reinnervation of its peripheral target (Werner et al., 2000). Neuronal jun-deficient mice do not show an up-regulation of α7 after injury, which appears to contribute to the very poor regenerative response seen in these animals (Raivich et al., 2004). The absence of laminin, the primary ligand for the α7 β1 integrin, led to similar but more marked and lasting effects. Thus, cell type specific deletion of the gene for the gamma 1 laminin chain, an essential component of the laminin α β gamma trimer in peripheral Schwann cells, caused a large decrease in the number of axons crossing into the distal portion of the crushed sciatic nerve for up to 30 days (Chen and Strickland, 2003), in contrast to the more transient defect in α7-deficient animals (Werner et al., 2000). Interestingly, these α7-deficient mice show immense up-regulation of the β1 integrin following injury, which corresponds with a significant increase in central axonal sprouting (Werner et al., 1998) and may imply compensatory mechanisms involving other, closely related α subunits. Central axonal sprouting on injury-induced neuronal cell surface molecules such as L1 and the close homologue of L1 (CHL1) relies on β 1-integrin function (Buhusi et al., 2003; Chaisuksunt et al., 2003; Becker et al., 2004), and may be involved in the effects observed in α7-deficient mice.

Evidence suggests that there is a developmental decline in the activation state of CNS neuronal integrins. This decline may underlie some of the intrinsic loss of regenerative ability sustained by CNS neurons during development. For example, during late-embryonic mouse development, retinal neurons lose the ability to attach and extend neurites on laminin-1 in spite of retaining expression of laminin-1 (Ivins et al, 2000). Such a decrease in integrin affinity can be reversed by increasing the activation states of integrins, e.g. by increasing the concentration of Mn^{2+} cations. In these cases outgrowth was mediated by α6β1 and not α3β1, even though these neurons express α3β1 and use it for outgrowth on other laminin isoforms. Integrins α2, α3 and β1 have been detected in the developing mouse spinal cord, where they are implicated in axonal path-finding processes (Ohyama et al, 1997). Expression of these

integrins is virtually lost in the spinal cord at birth, suggesting that decreased integrin expression accompanies the decline in regenerative capacity of CNS cells. Embryonic CNS neurons have far greater regenerative capacity compared to adult CNS. Cultured adult neurons do not adapt to in vitro conditions that mimic the extracellular environment in injured adult CNS including low levels of growth-promoting molecules and the presence of inhibitory proteoglycans. Young neurons readily adapt to such conditions and this adaptation is accompanied by an increase in the expression of integrins (Condic, 2001). More interestingly, adult CNS neurons can be induced to exhibit the regenerative capacity of embryonic neurons by gene transfer-mediated expression of single α-integrin subunits, α1 and α5 (Condic, 2001; Lemons and Condic, 2007). It may be possible therefore; that by modulating integrin function in the injured adult brain we can revert damaged adult neurons to a "younger" state and induce regeneration (Lemons and Condic, 2007).

In keeping with their trimeric and multimodal structure, the various laminins can act as ligands for a plethora of different receptors, including the integrins, gicerin/CD146, the 67 kDa laminin-receptor, α-dystroglycan, and β 1,4-galactosyltransferase (Ekblom et al., 2003; Powell and Kleinman, 1997; Taira et al., 1994). Application of exogenous galectin-1 has been shown to increase neurite outgrowth, whereas the removal of endogenous galectin with antibody neutralisation or through gene deletion decrease it (Horie et al., 2000; Fukaya et al., 2003; McGraw et al., 2004). Galectin-1, in its oxidized form, also stimulates the migration of Schwann cells from the proximal and distal stumps, assisting in the formation of cellular bridges permitting axonal growth into the distal part of the injured nerve.

Cell Surface Interactions

Normally, successful axonal regeneration is accompanied by the appearance of numerous, functionally diverse families of molecules that regulate surface-cytoskeletelal interaction. The GMC family includes cytoplasmic proteins GAP43, MARCKS and CAP23 (Skene and Willard, 1981; Verhaagen et al., 1986; McNamara et al., 2000; Bomze et al., 2001), that co-distribute with the phosphoinositol-4,5-diphosphate, PI(4,5)P2, at the semi-crystalline, raft regions

of the cell membrane (Frey et al., 2000). These GMC molecules are functionally exchangeable, they bind exclusively to acidic phospholipids such as PI-(4,5)-P2, calcium/calmodulin, protein kinase C and actin filaments, and modify the raft-recruitment of signalling molecules such as src, regulate actin cytoskeleton polymerisation, organization and disassembly (Laux et al., 2000; Caroni et al., 2001), and have a formative role in the appearance of filopodia and microspikes, in addition to the process of neurite outgrowth (Bomze et al., 2001).

Interactions of calcium containing and non-containing forms of calmodulin with the GMC molecules (Gerendasy, 1999; Dunican and Doherty, 2000) offer an important connection for translating receptor-mediated calcium fluxes into signals guiding growth cone activity (Henley and Poo, 2004; Kulbatski et al., 2004). Inhibition of calcium influx in vivo with nimodipine clearly improves axonal regeneration (Angelov et al., 1996; Mattson et al., 2001).

Microtubule disassembly molecules such as SG10, stathmin and RB3, and associated counterparts – the collapsin response-mediated proteins, e.g. CRMP2, form second, microtubule-targeting group of axonal adaptor molecules up-regulated after nerve injury (Iwata et al., 2002; Mori and Morii, 2002; Mason et al., 2002; Suzuki et al., 2003). Neuronal overexpression of CRMP2 has been shown to improve axonal regeneration (Suzuki et al., 2003). These functions are supplemented by the microtubule associated protein 1b (MAP1B) that mediates the directionality of growth cone migration and axonal branching in the regeneration of sensory neurons (Bouqet et al., 2004).

The Rho GTPases, whose major members are RhoA, Rac, Cdc42 and TC10, form a third family of proteins that act as molecular switches which regulate cytoskeletal structure, dynamics, and cell adhesion (Etienne-Manneville and Hall, 2002). Activation of these GTPases is mediated by adaptor molecules connected with cell surface receptors such as the slit-robo GTPase-activating protein 2 (Madura et al., 2004). Axonal injury results in a small upregulation of rhoA, rac, cdc42, and a massive increase in TC10 (Tanabe et al., 2000). Inhibition of rhoA in vivo triggers a striking induction of the normally absent axonal regeneration inside the CNS (Ellezam et al., 2002; Fournier et al., 2003). Overexpression of the cyclin-dependent-kinase inhibitor p21 (Cip1/WAF1), which develops a complex with rho-kinase and inhibits its activity, also encourages regeneration and functional recovery in lesioned CNS (Tanaka et

al., 2004). Furthermore, molecules that stimulate the expression of p21, such as the nuclear localized protein p311, also promote regeneration in injured motor nerves, resulting in accelerated reinnervation of peripheral targets (Fujitani et al., 2004). Conversely, not every cyclin-dependent kinase inhibits regeneration. Certainly, pharmacological blockade of cyclin-dependent kinase 5 with roscovitine or oloumucine has demonstrated a reduction in the ability of regenerating axons to overcome the moderate barrier to axonal elongation presented by the lesion site of the crushed facial nerve (Namgung et al., 2004).

Aims of this study

Boosting the regenerative growth potential of axotomised axons using exogenously applied neurotrophins has proved to be a useful and moderately successful strategy to promote regeneration and functional recovery following peripheral and central nervous system lesions. One of the major downstream signalling pathways that neurotrophins activate is the Ras-Raf-MEK-ERK pathway. Therefore, this thesis aims to address the likely role of the intracellular signalling proteins Ras and MEK1 in mediating axonal sprouting and regeneration in vivo. The work was first undertaken in the facial nerve injury model, a simple, reliable and reproducible model of both peripheral nerve regeneration and central axonal sprouting. This enabled the assessment of the extent and nature of any possible regeneration or sprouting that may arise from altering these proteins in vivo

A first experiment was undertaken to assess the time course and molecular characterisation of the sprouting response in the facial motor nucleus following facial nerve axotomy. This was necessary to establish at what time point after axotomy central sprouting peaks and the distribution of sprouting axons in the facial nucleus; and to assess whether neuronal cell death, inflammation or target reinnervation of the peripheral nerve affected central sprouting.

Three different mutant groups of animals, constitutively active Ras (Ras+), dominant-negative MEK1 (MEK1dn) and TGFβ1KO were examined for the effects on neuronal cell death, axotomy induced inflammatory response, speed of axonal outgrowth following peripheral nerve crush, target reinnervation, whisker motor recovery and central axonal sprouting. TGFβ1 KO mice were examined since reports have shown that gliosis is reduced in mice given antibody for TGFβ1, suggesting that this may reduce glial inhibition.

Constitutively active Ras and dominant-negative MEK1 both showed a good propensity to sprout and were analysed further by means of a spinal cord injury an anterograde tracing of both the corticospinal and rubrospinal tracts to assess the sprouting and regenerative response induced in these mutants. In addition, both Ras+ and MEK1dn mutants were combined to form a double mutant (DM)

with both active transgenes to assess the spinal cord sprouting responses. Behavioural tests were also performed to analyse the extent of functional recovery 4-6 weeks following spinal cord injury.

CHAPTER 2

Materials and Methods

Animals

All animals were kept under standard conditions with a 12 hour light-dark cycle with constant temperature (21-23°C) and humidity (60%±5) and access to pelleted food and water *ad libitum*. All experiments were conducted in accordance with the UK Animals (Scientific Procedures) Act, 1986. All animal procedures were conducted with the approval of the Home Office and UK animal experimentation legislation.

Several lines of transgenic mice were used in this study. These were sourced from a number of different laboratories and are summarised in Table 1.

Table 1. Summary of Transgenic mice

Transgenic Mouse	Reference
Ras (constitutively active)	Heumann et al., 2000
MEK1 (dominant negative)	Mansour et al., 1994
TGFβ1 KO	Shull et al., 1992
α7 integrin KO	Mayer et al., 1997
c-Jun conditional KO	Raivich et al., 2004
TNFR1/2 KO	Raivich et al., 2002

Facial nerve injury

Mice were anaesthetised with 2.5% 2,2,2-tribromoethanol (Avertin) (Sigma-Aldrich, UK) dissolved in distilled water given in a dose of 10µl/g body weight and depth of anaesthesia determined using the paw withdrawal reflex. An incision was made below the right ear at the level of the mastoid process. Superficial muscles were bluntly dissected to expose the facial nerve. The main branch of the facial nerve was transected at the stylomastoid foramen and included the retro-auricular branch. For facial nerve crush; firstly, the retro-auricular branch was cut. The main branch of the facial nerve was crushed approximately 1mm distal from its exit from the stylomastoid foramen using fine

forceps (FST 5/90, UK) and which were held in place for 10 seconds before letting go. The skin was closed with wound clips (AutoClip, USA) and the animal was left to recover in a heated chamber (32°C).

Retrograde tracing of the facial nerve

Reinnervation of the whisker pad was assessed 28 days after facial nerve lesion. Mice were anaesthetised with 10µl/g body weight of 2.5% Avertin. A midline incision was made and a cavity created under both whisker pads. A 5x5 mm square piece of gelfoam (Johnson and Johnson, UK) previously soaked in 15µl of 4% Fluoro-Gold (Fluorochrome, Denver, USA) was placed in the cavity under both whisker pads for 30 minutes, after which the pad was removed, the skin sutured using 6-O prolene sutures (Johnson and Johnson, UK), and the animals left to recover in a heated chamber (32°C).

Perfusion fixation

Mice were terminally anaesthetised with Euthatal (200 mg/ml sodium pentobarbital). Sufficient depth of anaesthesia was determined using the paw withdrawal reflex. A midline incision was made below the xiphoid process and the peritoneal cavity exposed. The rib cage was lifted, and the exposed diaphragm was incised at its junction with the anterior abdominal wall. The incision was continued circumferentially until adequate exposure of the pleural cavity was achieved. Whilst holding the xiphiod process, a deep cut was made along both sides of the rib cage and the anterior section of the ribcage lifted upwards so as to allow access to the mediastinum. A small incision was made at the base of the apex of the heart and a needle, attached to a perfusion pump (Gilson, USA), was inserted. The mouse was perfused transcardially via the left ventricle. The inferior vena cava was then cut permitting exsanguination. The mouse was perfused at a rate of 0.02L/min for 5 minutes with cold (4°C) phosphate buffer with 0.9% saline (PBS: 10 mM Na_2HPO_4, 0.85% NaCl, pH 7.4) followed by cold (4°C) 4% paraformaldehyde in 10mM phosphate buffered saline solution (PFA/PBS) at the same flow rate (0.02L/min).

Histological Procedures

Cryostat sectioning.

Frozen brain or spinal cord was placed on a cryostat chuck The chuck was housed in the cryostat (Leica, Germany), and the chamber temperature was set at -20°C.

Brainstem specimens were cut at 20 or 25µm, taken through the level of the facial motor nucleus, to incorporate both ipsilateral and contralateral facial nuclei in their entirety. For immunohistochemistry, 20µm sections were taken, unless where otherwise stated. For tract-tracing studies, spinal cords were sectioned longitudinally dorsal to ventral at 40µm on a cryostat, spread in anatomical order on gelatinised glass slides and stored at -80°C.

Cresyl violet (Nissl) staining

Mounted sections at the level of the facial motor nucleus were fixed in 4% formaldehyde (BDH) overnight followed by 70% ethanol overnight. The slides were immersed in a 1% cresyl violet solution (BDH, UK) for 10 minutes. Excess cresyl violet was removed by washing in water, and the slides were then dehydrated by passing sequentially through an increasing concentration of ethanol (70%, 90%, 95%, 95% with glacial acetic acid (to de-stain), 100%, isopropanol, and three washes in xylene, each for 2 minutes) prior to being cover slipped using DePex (BDH, UK).

Standard light-microscopic immunohistochemistry

Frozen brain stems were cut at the level of the facial nucleus, 20 µm sections were collected on warm, 0.5% gelatin-coated slides (Merck, UK), refrozen on dry ice and stored at -80°C until further use. The sections were rethawed, pretreated for LM-IHC as described by Moller et al. (1996), rehydrated in bidistilled water, spread onto the slide, dried for 5 minutes and then incubated for 5 minutes in 4% PFA/PB, 2min each in 50% acetone/H_2O, 100% acetone, 50% acetone/ H_2O, twice in PB, in PB/0.1% bovine serum albumin (PB/BSA) (BSA; Sigma, UK) and then preincubated for 30 minutes in PB/5% goat or donkey non-immune serum, to match the source of the final, secondary or tertiary antibody (Vector, UK). These preincubated sections were incubated

overnight at 4°C with the primary antibody and then for 1 hours at room temperature with appropriate biotinylated secondary antibody. Source and dilution of all antibodies used are listed in Table 2. All incubations with primary, secondary, and where indicated, tertiary antibodies, were carried out in PB/BSA, and finished by washing in 3 changes of PB/BSA. Exposure to the biotinylated secondary antibody was followed 1 hour incubation with the Avidin-Biotinylated horse radish peroxidase Complex (1:100) (ABC, Vector, Wiesbaden, Germany) and visualized with diaminobenzidine (DAB; Sigma, UK) and hydrogen peroxide (H_2O_2). The reaction mixture consisted of 0.5 g/l DAB, 1:3000 dilution of 30% H_2O_2 in PBS, pH 7.4, and was allowed to react for 5 minutes at room temperature. Following the DAB reaction, the sections were washed in distilled water, dehydrated in graded alcohols and xylene and mounted with Depex (BDH, UK).

Quantification of light-microscopic Immunohistochemistry.

A Sony AVT-Horn 3CCD colour video camera was used to obtain 8-bit digital images based on a 0-255 (8-bit) scale of optical luminosity values. Images of both control and axotomized nuclei and for the glass were captured at x10 magnification on a light microscope with 0.06 Neutralfilter. Captured images were run against an algorithm to obtain mean and standard deviation values for optical luminosity. Standard deviation was subtracted from the mean for each image and the resulting values for axotomized and control sides were each subtracted from that of the mean optical luminosity values of the glass as described in previous study (Moller et al, 1996).

Table 2. Summary of antibodies				
Antigen	*Antibody*	*Dilution*	*Application*	*Source*
	primary			
α6 (α6β1)	RtM	1:3000	IHC, DIF	Camon, UK
αM (αMβ2)	5C6, RtM	1:6000	IHC, DIF	Camon, UK
αX̣ αXβ2)	HmM	1:100	IHC, DIF	Endogen, UK
VaChT	GtM	1:6000	DIF	Chemicon, UK
β1	RtM	1:3000	IHC, DIF	Chemicon, UK
CD3	RtM	1:1600	IHC	Pharmingen, UK
B7.2	RtM	1:3000	IHC, DIF	Pharmingen, UK
CGRP	α-CGRP, RbP	1:400	IHC, DIF	Penninsula, Belmont, USA
CD44	α-CD44, RtM	1:5000	IHC, DIF	Chemicon, UK
Galanin	RbP	1:400	IHC, DIF	Penninsula, Belmont, USA
GFAP	RbP	1:6000	IHC, DIF	Dako, UK
IBA1	α-IBA1, RbP	1:6000	IHC, DIF	Dr Imai, Dept Neurochem, Natl Inst Neurosci, Tokyo
ICAM1	α-ICAM1, RtM	1:3000	IHC, DIF	Camon, UK
MHC1	RtM	1:250	IHC, DIF	BMA Biomedicals, Switz.
TGFβ RII	RbP	1:2000	IHC	Santa Cruz Inc, USA
	secondary and tertiary			
Goat Ig	FITC-cj α-Gt Ig, DkP	1:100	DIF	Dianova, UK
Hamster Ig	FITC-cj α-Hm Ig, GtP	1:100	DIF	Dianova, UK
Rat Ig	Biot. α-Rt Ig, GtP	1:100	IHC	Vector, UK
Rat Ig	FITC-cj α-Rt Ig, GtP	1:100	DIF	Dianova, UK
Rabbit Ig	Biot α-Rb Ig, GtP	1:100	IHC	Vector, UK
Rabbit Ig	Biot α-Rb Ig, DkP	1:100	DIF	Dianova, UK

Abbreviations. Antigens: CGRP - Calcitonin Gene-Related Peptide, GFAP – Glial Fibrillary Acidic Protein, IBA1 - Ionized ca-Binding Adaptor protein 1, ICAM1 - intercellular adhesion molecule-1, Ig – Immunoglobulin, MHC1 – Major Histocompatibility Complex Class I, TGFβ RII – Transforming Growth Factor β Receptor type 2, VaChT – vesicular acetylcholine transporter. **Antibodies:** RtM - rat monoclonal, HmM - hamster monoclonal, RbP - rabbit polyclonal, DkP – donkey polyclonal. FITC-cj – fluorescein isothiocyanate conjugated. **Applications:** DIF - double immunofluorescence, IHC - immunohistochemistry (light microscopy).

Quantification of central axonal sprouting

Quantification of growth cones was performed on 5 sections per facial nucleus, with an interval of 200 µm between each section. Briefly, the sections were scanned on a TCS 4D confocal laser microscope (Leica, Nussloch, Germany) with a 10x objective using Cy5 settings (ex-wavelength: 647nm; LP665; pinhole 30). Fourteen consecutive, equidistant levels were recorded and condensed using the MaxIntense projection.

Small, strongly fluorescent growth cones were differentiated from the large neuronal cell bodies with the Sobel filter and a 3-step Growth Cone Detection (GCD) algorithm using the Optimas 6.2 software (Media Cybernetics, UK). In the first step, mean value of the overall luminosity (MEANcor) and the standard deviation (SDcor) of the corrected images (normal image) was recorded. This procedure was repeated following Sobel filter treatment (MEANsob, SDsob, sobel image), which calculates the direction-independent local intensity gradient in a 3 x 3 pixel kernel. The threshold for neuropeptide-immunofluorescent growth cones in the Sobel image was set with the formula:

Threshold = MEANsob + 11 x SDcor.

Areas at and above threshold were filtered with the "Object Classes" function using 2 additional criteria in the normal image:

A. Area size > 10 pixel,
B. MEANarea – SDarea > 1.4 x MEANcor,

with MEANarea the mean intensity, and SDarea the standard deviation for each individual area profile. The remaining areas matched with the profiles of the neuropeptide-immunofluorescent neuronal growth cones and served as a measure for their total area in the tissue section.

Neuronal cell counts

Motoneuron cell counts were determined in the axotomised facial nucleus and on the contralateral side 30 days after a right facial nerve cut. 20um thick paraformaldehyde-fixed brainstem sections were cut in the caudo-rostral

direction through the facial motor nucleus. The tissue was stained with toluidine blue and all neuronal profiles in every section of the facial nucleus were counted and corrected for cell size using the Abercrombie Correction coefficient (Abercrombie, 1946), according to the formula:

$N = n \times D/(D + d)$,

With N the corrected neuronal number, n the counted number of neurons, D the section thickness (20um) and d the mean neuronal diameter, calculated from the cell size. Neuronal cell size was determined from three tissue sections 100um apart. Digital images from the stained sections in a 24-bit RGB format were obtained using a Sony 3 CCD video camera (AVT-Horn, Aachen, Germany), neuronal cell profiles were detected with Optimas 6.2 using a mean – 1.5 x standard deviation (Mean – 1.5SD) threshold in the red channel, and the mean diameter (d) was calculated form the mean area (Area), assuming a near spherical form, with the formula:

$d = \text{root}(4 \times \text{Area}/\text{pi})$

Agarose gel electrophoresis

1% agarose-TAE gels were used in resolving DNA samples. 1% agarose was made up with 1x TAE buffer (0.4M Tris, 0.2M sodium acetate, 20mM EDTA, pH), boiled and left to cool to approximately 50°C before ethidium bromide was added to a final concentration of 0.2µg/ml. The solution was poured to an appropriate depth in a gel tray containing a comb, and left for 1 hour to set. PCR samples were mixed with loading buffer (1x TAE, 50% glycerol, 0.025% bromophenol blue) immediately prior to well loading. Samples were run against 5µl of a 1 kilobase DNA ladder (Promega, UK).

CHAPTER 3

Peripheral nerve axotomy in mice causes sprouting of motor axons into perineuronal central white matter: time course and molecular characterisation

Introduction

Generation of new axonal sprouts and the process of axonal elongation play a vital role in the neural repair programme following injury to the nervous system. In the classical case of axonal regeneration in the injured peripheral nerve, the tip of the proximal axon still connected to neuronal cell body is gradually transformed into a motile and sprouting growth cone that moves across the gap between the proximal and distal nerve stump, enters neural tube(s) in the distal part, and uses them as a scaffold on its way to the peripheral target (Witzel et al., 2005). Supernumerary axonal sprouts can also develop more proximally, at the nodes of Ranvier (Ramon y Cajal, 1928; Friede and Bischausen, 1980; Ide and Kato; 1990), from distal dendrites (Fenrich et al., 2007) and occasionally, even at the level of the injured neuronal cell body (Linda et al, 1985).

In addition to outright regeneration, nerve injury can also elicit sprouting from uninjured axons. This includes collateral sprouting from functionally appropriate or inappropriate, adjacent intact axons into the deafferented part of the central nervous system (Goldberger and Murray, 1974; Murray and Goldberger, 1974), or peripheral tissues including skin (Nurse et al., 1984), muscle (Nguyen et al., 2002) or nerve (Ide and Kato, 1990; Tanigawa et al., 2005). Peripheral axotomy can also induce the sprouting of central sensory processes of the affected dorsal root ganglia (DRG) neurons in the spinal cord (Woolf et al., 1992) as well as the appearance of perineuronal neurite baskets in the DRGs themselves (McLachlan et al., 1993; McLachlan and Hu, 1998; Li et al., 2001; Liu et al., 2005). Both processes have been implicated to contribute to posttraumatic neuropathic pain (Woolf et al., 1992; Liu et al., 2005). Despite the variability in origin, regulation and dynamics, in most cases these different forms of post-traumatic neurite outgrowth appear to start within the first few days after injury,

or to represent a very late response, that may be associated with frustrated regeneration.

Transection of the adult facial nerve is a well-established model system to study the axonal response and regeneration (Moran and Graeber, 2004). Moreover, experimental work in transgenic mice, overexpressing or deficient in various molecules have begun to provide insight into molecular signals – transcription factors, cell adhesion molecules, cytokines and neurotrophins - that determine axonal regeneration as well as post-traumatic neuronal survival and cell death, and different aspects of the neural inflammatory response (Werner et al., 2000; Kalla et al., 2001; Heumann et al., 2000; Raivich et al., 2004; for review see Raivich and Makwana, 2007). However, these studies also suggested a de novo appearance of neuropeptide-immunoreactive sprouts in and around the axotomized facial motor nucleus, during the midphase of axonal regeneration after facial nerve cut (Kloss et al., 1999; Werner et al., 2000; Galiano et al., 2001).

The aim of the current study was to determine the precise neuronal origin of these sprouting neurites, and define their time course, neuroanatomical distribution and molecular characteristics. It shows that these axons originate from injured and regenerating neurons, are capable of growing for up to 0.5mm into different white matter tracts surrounding the lesioned facial motor nucleus, and express high levels of cell adhesion molecules such as CD44 and the α 7 β1 integrin. Surprisingly, deletion of the α 7 integrin subunit led to a further increase in the number and extent of neuropeptide-immunoreactive neurite growth cones, suggesting an inhibitory role of α7 integrin in this form of post-traumatic central axonal sprouting.

Materials and Methods

Animals, Surgical Procedures and Tissue Treatment

Normal, wild type, C57Bl/6 mice were generated at our animal facilities at Max-Planck Institute of Neurobiology, Martinsried, and then at the Biological Services Unit, UCL. Transgenic, TNFR1&2-/- mice and wild-type controls (+/+) were obtained from BRL (Basle, Switzerland) and were on a mixed B6*129 background. c-jun animals were generated by crossing mice carrying a floxed *c-*

jun allele, *c-jun*^{f} (Behrens et al., 2002) with those expressing cre recombinase under the control of nestin promoter (Tronche et al., 1999) and then crossed again to generate the *c-jun*$^{f/f}$;nestin-cre+ mutant mice, in which both *c-jun* alleles are inactivated in cells derived from embryonic neuroepithelium (*c-jun*$^{\Delta n}$). Compound *c-jun*$^{\Delta n}$ mice were on a mixed 129Ola/C57BL6/FVBN genetic background. Sibling animals lacking the cre transgene, with functional, unrecombined homozygous *c-jun*^{f} (*c-jun*$^{f/f}$), served as controls. The homozygous α7-/- and littermate controls on the 129/Sv background used in this study were obtained from heterozygous crossing of α7+/- mice (Mayer et al., 1997).

To study the effects of enhanced neural inflammation, E. coli lipopolysaccharide (O55:B5 serotype, 1mg, Sigma, Deisenhofen, Germany) was dissolved in phosphate-buffered saline (PBS: 10mM Na2HPO4, 0.85% NaCl, pH 7.4), and injected intraperitoneally into C57 black 6 mice (8 weeks old, 25-30g weight; n=3 per group) 12 to 96 hours prior to 14 day time point.

All surgical techniques were performed under anaesthesia with 2,2,2-tribromethanol (Avertin®, Sigma, Deisenhofen, Germany), 0.4 mg/g body weight, on 3-6 month old mice. All animals belonging to the same experimental group (day 1 group, day 2 group, day 4 group, etc) were also operated on the same day, inside a narrow time window of 1-3 hours. Animal experiments and care protocols were approved Home Office (Scientific Procedures Act) in the UK. The right facial nerve (including the retro-auricular branch) was cut or crushed at its exit from the stylomastoid foramen. For the reaxotomy experiments, the cut was made 1mm distal to the original injury and the retro-auricular branch was not re-cut. Animals were sacrificed after survival time of 1-42 days, perfusion-fixed with 200 ml phosphate-buffered saline (PBS: 10 mM Na_2HPO_4, 0.85% NaCl, pH 7.4), followed by 200 ml of 4% paraformaldehyde in PBS (PFA/PBS) as described in Chapter 2 Materials and Methods. This was followed by a 2 hour immersion of the brainstem in 1% PFA/PBS at 4° C on a rotator (8 rpm), an overnight rotating immersion in a phosphate-buffered sucrose solution (PB: 10 mM Na_2HPO_4, pH 7.4, 4°C; 30% sucrose) and frozen on dry ice.

Immunofluorescence, Double-Labelling and Confocal Scanning Microscopy

Frozen brain stems were cut at the level of the facial nucleus, 20 µm sections were collected on warm, 0.5% gelatin-coated slides (VWR, UK), refrozen on dry ice and stored at -80°C until further use. For standard immunofluorescence the sections were thawed, rehydrated and spread in distilled water, fixed in 4% formaldehyde in 0.1M PB, defatted in acetone, and pretreated with 5% goat serum (Vector, Wiesbaden, Germany) in phosphate buffer/PB as described in Möller et al. (1996). Briefly, the sections were incubated overnight at 4°C with primary antibodies summarized in table 2, washed in PB, incubated with a biotinylated goat anti-rabbit antibody, -rat (1:100, Vector), Texas-Red streptavidin (Jackson laboratories, UK). The sections were covered with VectaShield (Vector) and stored in the dark at 4°C for confocal scanning and quantification. Omission of the primary antibody or replacement with non-specific immunoglobulin from the same species (rat, rabbit or hamster) at the same dilution led to the disappearance of specific labeling.

Axonal growth cones in and around the facial motor nuclei were quantified using immunofluorescence against CGRP or galanin, the neuropeptides expressed in axotomized facial motoneurons. A summary of primary, secondary and tertiary antibodies used to characterize the facial sprouts using double labelling with antibodies for galanin, CGRP or vesicular acetylcholine transporter (VAChT) 14 days after facial nerve cut are listed in Table 2. Fixed sections were preincubated as in bright field immunohistochemistry. Both primary antibodies were applied overnight at 4°C, washed, incubated with two appropriate secondary antibodies, biotin-conjugated donkey anti-rabbit Ig and FITC-conjugated goat anti-rat Ig (1:100; Dianova), washed again and then incubated with a tertiary FITC-conjugated donkey anti-goat antibody (1:100; Sigma) and Cy3-Avidin (1:1,000; Dianova). In the case of colocalization with the goat anti-VAChT, only the donkey anti-goat antibody was used.

Digital micrographs of FITC and Cy3 or Texas red fuorescence was taken using a Leica TCS confocal laser microscope with a 10X objective for quantification and a 100x objective for illustrations in 8-bit greyscale, 1024 X 1024 pixel format as described in previous studies (Raivich et al., 1998; Kloss et al., 1999). 12 consecutive equidistant levels with 30µm spacing with a 10x objective or 20

levels with 0.5 µm spacing at 100x objective were recorded and condensed onto a single bitmap using the MaxIntense algorithm.

Quantification of central axonal sprouting

Quantification of growth cones was performed on 5 sections per facial nucleus, with an interval of 200 µm between each section as described in Chapter 2 – Materials and Methods.

Immunohistochemistry for Light and Electron microscopy

Immunohistochemistry for light microscopy was performed using the same procedure as in immunofluorescence up to the secondary antibody, followed by incubation with the ABC-reagent (Vector), visualization with diaminobenzidine/H_2O_2 (DAB; Sigma, Deisenhofen, Germany), dehydration in alcohol and xylene and then mounted with Depex (BDH, Poole, England).

For electron microscopy, 80 micrometer thick vibratome sections were cut at the facial nucleus level were stained for α7 integrin subunit using a slightly modified protocol (Werner et al, 2000). Briefly, the vibratome sections were floated, treatment with acetone was omitted, pre-incubation with goat serum was extended to 4 hours at RT, the rabbit anti-mouse α7 antibody was applied at a concentration of 1:500 overnight, the biotinylated goat-anti-rabbit secondary antibody (Vector) applied for 8 hours (4°C) and the incubation with the ABC reagent performed overnight (4°C).

For the DAB staining, vibratome sections were first pre-incubated in DAB (without H_2O_2) for 20 minutes, followed by a 15 minute DAB/H_2O_2-reaction at RT, with Co/Ni enhancement (see above). The sections were then fixed for seven days in 2% glutaraldehyde in PBS, osmicated, dehydrated and embedded in araldite (Fluka, Basel, Switzerland). Semithin sections were counterstained with toluidine blue for light microscopy, and ultrathin, 100 nm sections, were counterstained with uranyl acetate and lead citrate and examined in a Zeiss EM 10 and EM 109 electron microscope (done at Cancer Research Laboratories).

Quantification of light microscopic Immunohistochemistry.

Sections stained for standard light microscopic immunohistochemistry were quantified as described in Chapter 2 – Materials and Methods.

Statistical analysis.

Statistical analysis for growth cone areas in two group comparisons was performed using a standard, 2-tailed Student's t-test, and with ANOVA followed by post-hoc Tukey in cases of more than 2 groups.

Results

Facial axotomy causes delayed central axonal sprouting

As shown in figure 3.1, facial axotomy following nerve transection at the stylomastoid foramen was associated with the appearance of sprout-like, galanin-immunoreactive (galanin+) neurites inside the brainstem in and around the lesioned facial motor nucleus (figure 3.1). High number of galanin+ sprouts with a 4-10 μm large terminal bulb were observed in the white matter surrounding the lesioned facial motor nucleus, in the ventral corticobasal tract, in the ascending part of the intracerebral portion of the facial motor nerve, and medial and lateral parts of the facial nucleus. Some neurites were located as far as 0.5-1.0 mm away from the border of the facial nucleus, with the stalk attached to a bulb usually pointing away from the nucleus. Sprouting neurites were also present inside the facial motor nucleus itself, but they were less dense in the horseshoe form of the facial nucleus grey matter, containing the axotomised motoneurons than in its white matter-like ventral cleavage. A similar distribution was also observed for the CGRP+ sprouts, but their density was considerably lower compared to that of the galanin+ fibres. No galanin+ or CGRP+ sprouts were observed in the contralateral facial nucleus or in other brainstem, cerebellar or cortical white matter tracts. CGRP and galanin immunoreactivities were also present in adjacent axotomized motoneurons, each labelling approx 40-45% of the total facial motoneuron pool (Moore, 1989; Raivich et al., 1995), but the intensity of the cell body labelling was weaker than that observed in the sprouts.

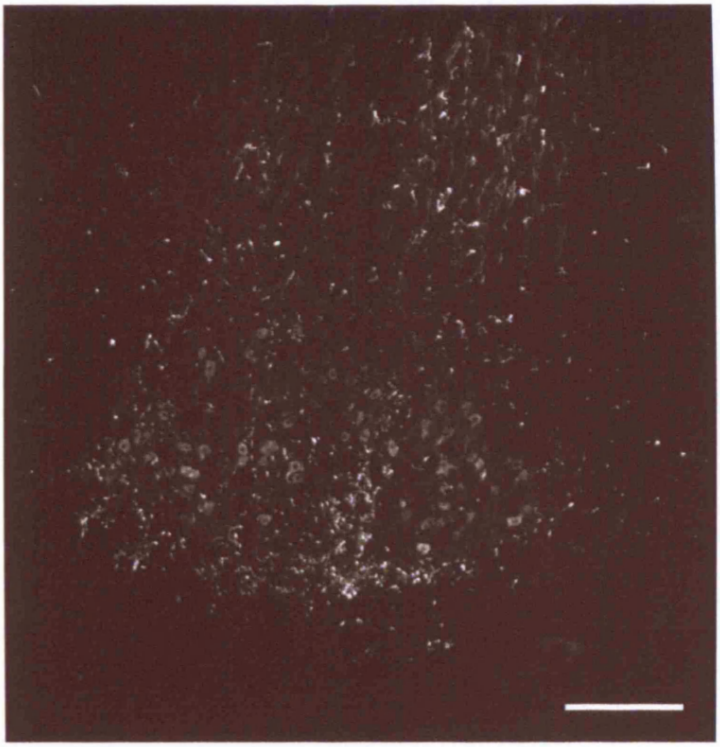

Figure 3.1. Localisation and distribution of galanin-immunoreactive sprouts in the facial motor nucleus, 14 days following facial nerve cut. A typical section through the facial motor nucleus stained for galanin. There are numerous immunoreactive sprouts in the white matter surrounding the lesioned facial motor nucleus, in the ventral corticobasal tract, in the ascending part of the intracerebral portion of the facial motor nerve, and medial and lateral parts of the facial nucleus. Neurites are located as far as 0.5-1.0 mm away from the border of the facial nucleus, with the stalk attached to a bulb usually pointing away from the nucleus. Sprouting neurites are also present inside the facial motor nucleus itself, but appear to be less common in the horseshoe form of the facial nucleus grey matter, containing the axotomised motoneurons, than in its white matter-like ventral cleavage. Scale bar: 250µm

Time course

Comparison of the galanin- and CGRP-immunostained, axotomised facial motor nuclei 1-42 days after facial nerve cut with unoperated controls (day 0), revealed a transient sprouting pattern shown in figure 3.2. No sprouts were observed in the unoperated facial nuclei, or 1-4 days after nerve cut. A moderate number of galanin+ and CGRP+ sprouting neurites were observed at day 7, the galanin+ ones became much more common at day 14, decreased in their number at day 21, and disappeared by 42 days after nerve injury and the ensuing regeneration. The CGRP+ neurites showed an elevated plateau between day 7 and 21.

Automatic quantification of the intensely neuropeptide-immunofluorescent end-bulbs in and around the facial motor nucleus using confocal scanning and the growth cone detection algorithm (see Materials & Methods) reproduced this time course for galanin, with a peak density at day 14, with 5.20 parts per thousand (ppt) or 0.52% of the total area of the 1mm*1mm region with the facial nucleus at its centre covered with galanin+ end-bulb structures (figure 3.2, bottom row). Quantification of the CGRP+ end-bulbs also revealed statistically significant elevation on days 7-21 compared to the contralateral side, but the overall levels (0.26-0.20 ppt) were much lower than with those observed with galanin immunoreactivity.

Molecular markers and ultrastructure

To define the molecular markers of axotomy-induced sprouts we next examined the presence of vesicular acetylcholine transporter (VAChT), the CD44 hyaluronic acid receptor and the α7 and β1 subunits of the β1 integrin family using double immunofluorescence with galanin, CGRP or VAChT.

Since many α7+ sprout end bulbs were particularly pronounced in the basal white matter located ventral to of the axotomized facial motor nuclei, we next explored their utrastructural morphology using transmission electron microscopy (EM), 14 days after facial nerve cut (figure 3.4A,B). Here, immunolabelling against the intracellular part of the α7 integrin subunit revealed strong cytoplasmic staining surrounding numerous mitochondria and vesicles and demarcating 2-5 μm large structures characteristic of growth cone morphology and associated 0.3-0.5μm thin axonal stalks, frequently directly in contact with neighbouring, α7-negative oligodendroglial surfaces (figure 3.4A). There was no α7 immunoreactivity on the associated myelin or myelinated axons (figure 3.4A), blood vessel endothelia or large perivascular cells (figure 3.4B). However, some submembraneous α7 immunoreactivity was also present on the small pericytes and the astrocytic processes contacting the perivascular basal laminae (figure 3.4B).

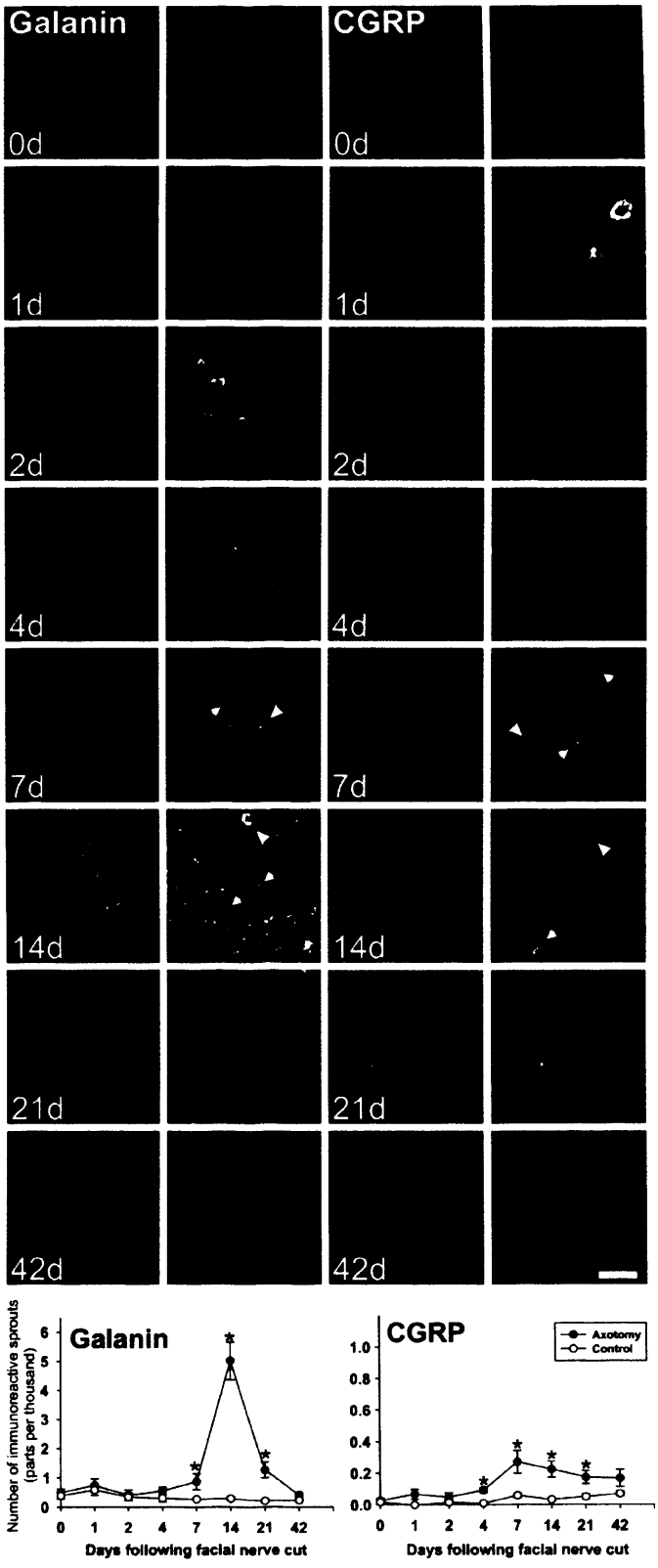

Figure 3.2. Time course, and quantification of galanin- and CGRP-immunoreactive sprouts in the facial motor nucleus. Central axonal sprouting in the facial motor nucleus 0, 1, 2, 4 7, 14, 21, and 42 days after facial nerve axotomy. The four columns show the immunofluorescence in uninjured and injured facial nucleus. Significant numbers of CGRP and galanin immunoreactive growth cones are present in and around the facial nucleus between 4 and 21 days following facial nerve cut, with a peak at day 7 for galanin and d14 for galanin compared with control. Quantification of galanin and

CGRP immunoreactive growth cones. Graphs show total area of immunoreactive sprouts (in parts per million). *p<0.05 in Student's t-test.
Scale bar = 250μm in the first and third columns, 67.5μm in the second column and 31μm in the last column.

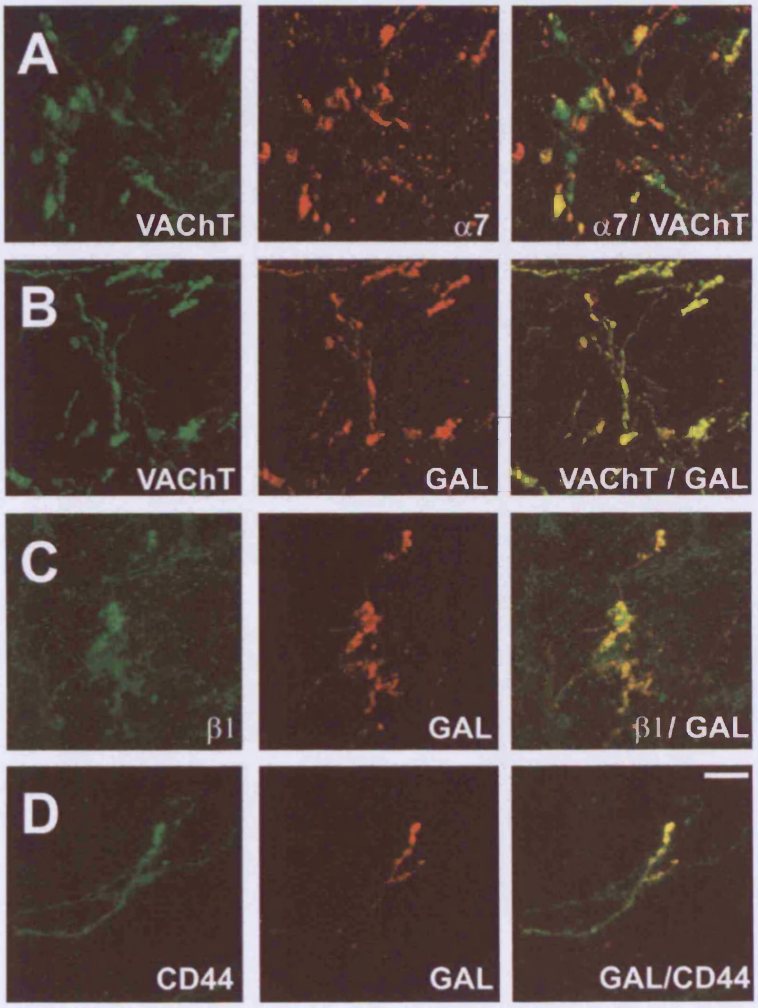

Figure 3.3. Molecular characterisation of growth cones in the facial nucleus 14 days following facial nerve cut. First two columns show the individual immunofluorescence, the third column shows the colocalisation. **A:** Colocalisation of VAChT (green) with the integrin α7 (red) or **B:** neuropeptide galanin (red) in growth cones of the facial nucleus. **C:** β1 integrin (green) colocalisation with galanin (red). **D:** CD44 (green) is present in galanin-immunoreactive growth cones (red). Scale bar = 20um

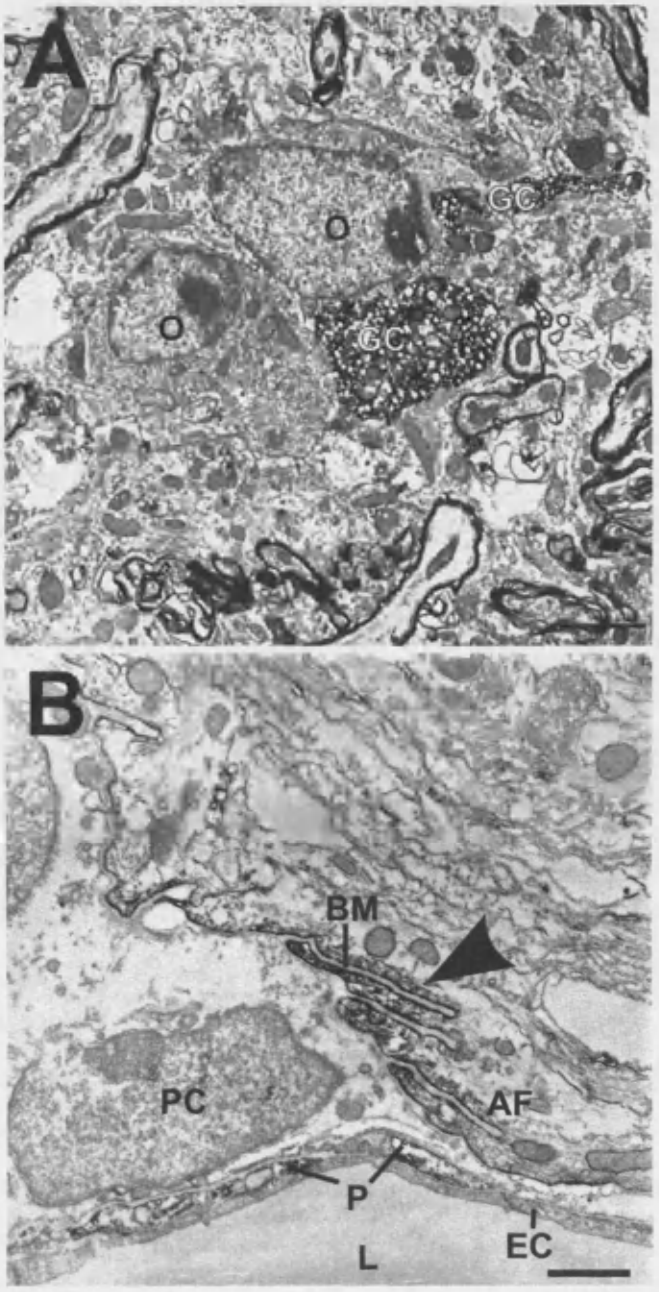

Figure 3.4. Electronmicrographs of α7 immunostaining in the white matter surrounding the facial motor nucleus, 14 days following facial nerve cut in WT animals. **A.** Growth cones intensely immunostained for α7 integrin and are littered with vesicles and mitochondria. Note the adherence of the growth cone to the adjacent oligodendrocyte. **B.** Immunoreactivity for α7 is seen in astrocytes. Here much of the immunoreactivity is particular intense where the astrocyte has closely associated with finger-like protrusions of the basal membrane. GC: growth cone, O: oligodendrocyte, B: basal membrane, PC: perivascular cell, P: perivasculum, AF, astrocyte fibrils. Scale bar: 2um

Posttraumatic Facial Sprouts: Origin and Dependance on Mode of Injury and Timing

To determine whether the bulb-carrying neurites originate from the lesioned motoneurons, axotomised neurons were retrogradely labelled with 1% Miniruby®. As shown in figure 3.5A, B, application of the retrograde tracer on the proximal nerve stump surface immediately after facial nerve cut led, 14 days later, to a successful labelling of the facial sprouts that also revealed strong galanin-immunofluorescence.

Since the time course of sprouting, with a peak at day 14, occurs at roughly the same time as the morphological reinnervation and functional recovery in the facial axotomy model (Gilad et al., 1996; Werner et al., 2000; Raivich et al., 2004), whether the appearance of sprouts is due to target reinnervation was next investigated. As reinnervation is known to occur earlier, more promptly and with less error after crush than after cut (Nguyen et al., 2002; Witzel et al., 2005), the differential effects of the facial nerve crush versus cut on galanin+ growth cone profiles at day 7, 10 and 14 was examined. As shown in figure 3.5C, facial nerve crush induced a delayed appearance of galanin+ sprouts that peaked at day 10, with 0.8ppt of the total area. Facial nerve transection produced a more robust sprouting response than nerve crush, with a slight but not significant increase at day 7 and 10, and an almost 10-fold increase at day 14 ($p<0.05$, Student's t-test).

To further determine whether the appearance of growth cones was due to the onset in the reinnervation of peripheral targets occurring 8-14 days after injury, the effects of single facial nerve cut versus a second transection were examined. The facial nerve was re-cut 1mm below the initial lesion ($n = 5$ animals per group) on day 8 with survival to day 14, or re-cut on day 14 and survival to day 22 and compared with normal animals 8, 14 and 22 days after facial nerve cut that served as controls (figure 3.5D). Surprisingly, the growth cones were not reduced in number, in fact the area under growth cone profiles was 1.5-2 fold greater than in control day 14 or day 22 post-cut brainstems ($p<2\%$, ANOVA). Preliminary studies using shorter recut times (1, 2 & 4 days) and total transection time of 14 days revealed that the growth cone profiles were more numerous than after a simple 14 cut, but the effects were less pronounced than in 8+6 vs 14, or 14+8 vs 22 (data not shown). Finally, retrograde tracing experiments using application of MiniRuby into the ipsilateral

whiskerpad after axotomy, the principal peripheral target of the facial nerve maxillary and zygomatic branches on day 12, showed some motoneuron cell body labelling but no labelling in the facial growth cones at day 14 (data not shown).

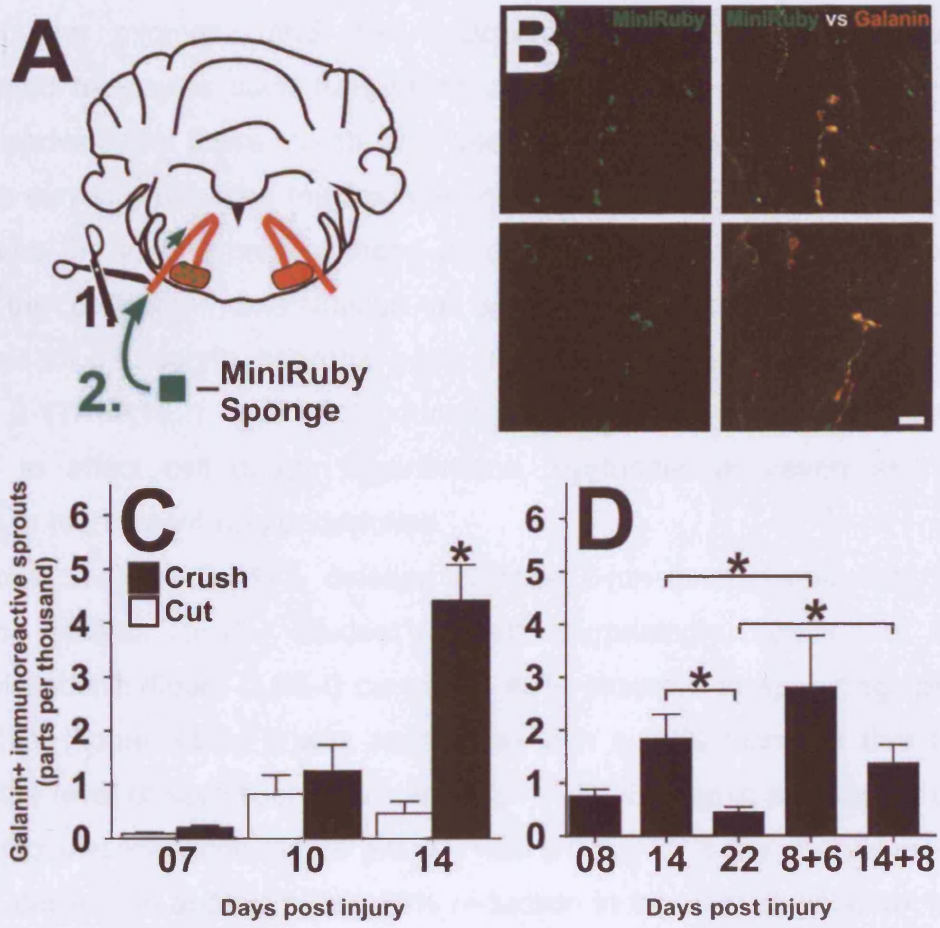

Figure 3.5. Neuronal origin of central sprouts in the facial motor nucleus. **A.** Neuronal retrograde tracer Mini-Ruby was applied to the proximal cut end of the facial nerve followed by a 14 day survival. **B.** Central axonal sprouts from cut motoneurons labelled with the retrograde tracer Mini-Ruby co-localise with galanin immunofluorescence confirming their motoneuron origin. **C.** Growth cone number is dependent on the mode of injury. Quantification of galanin immunoreactive sprouts (area in parts per million) at day 07, 10 or 14 following either crush or cut injury. *$p<0.05$ in Student t-test. **D.** Re-injury of the facial nerve exacerbates central axonal sprouting but only within a specified time window. Quantification of central axonal sprouting shows total area (parts per thousand) of galanin-immunoreactive sprouts at day 08, 14, 22 and day 14 with a reaxotomy at day 08 (8+6) and day 22 with a reaxotomy at day 14 (14+8). *$p<0.05$ in one-way ANOVA. Scale bar: 25um

Effects of LPS-induced inflammation and α7, brain c-jun and TNFR1&2 deletions

Previous studies using the facial axotomy model to examine neuronal cell death (Möller et al., 1996, Raivich et al., 2002), leukocyte influx (Raivich et al., 1998; Bohatschek et al., 2001), bystander-activation inflammatory changes in neighbouring microglia and the induction of late neuronal regeneration associated molecules such as galanin and β1 integrin subunit (Kloss et al., 1999), showed that these events also peak at day 14 after axotomy, coinciding with the currently detected maximum in intracerebral facial axonal sprouting. To determine the involvement of these processes in sprouting of facial neurons within the brainstem, examination of sprouting in mice with specific gene deletions for α7 integrin, neuronal c-jun and tumor necrosis factor receptor type 1 and 2 (TNFR1&2), and LPS-induced inflammation, which were previously shown to affect cell death, regeneration, bystander activation and neural leukocyte recruitment was undertaken.

As shown in figure 3.6A-C, deletion of brain c-jun caused complete loss of galanin+ sprouts ($p<1\%$, Student's t-test). Surprisingly, deletion of the α7 integrin subunit (figure 3.6G-I) caused a 40% increase in sprouting ($p<0.05$), TNFR1&2 (figure 3.6D-F), was associated with a 39% increase that did not reach the level of statistical significance ($p=0.15$). Systemic application of 1mg E.coli lipopolysaccharide (figure 3.6J-O) with a 0.5, 1 or 2 day interval preceding day 14 caused an approximately 50% reduction in the area of galanin+ sprouts ($p<0.02$, one way ANOVA followed by post hoc Tukey); the effect disappeared 96h after the administration of LPS.

Changes in β1 integrin levels.

Since the β1 integrin subunit is the obligate partner of α7 and shows a peak of expression in neurons 14 days following facial nerve cut (Kloss et al., 1999), the relationship between sprouting response and levels of this regeneration associated molecule was explored. As shown in figure 3.7A, absence of the α7 integrin, caused significantly elevated β1 integrin levels at day 14 compared with littermate controls (+34%, $p<0.05$, Student's t-test). Similarly, deletion of neuronal c-jun also showed a 68% decrease in β 1 integrin immunoreactivity at

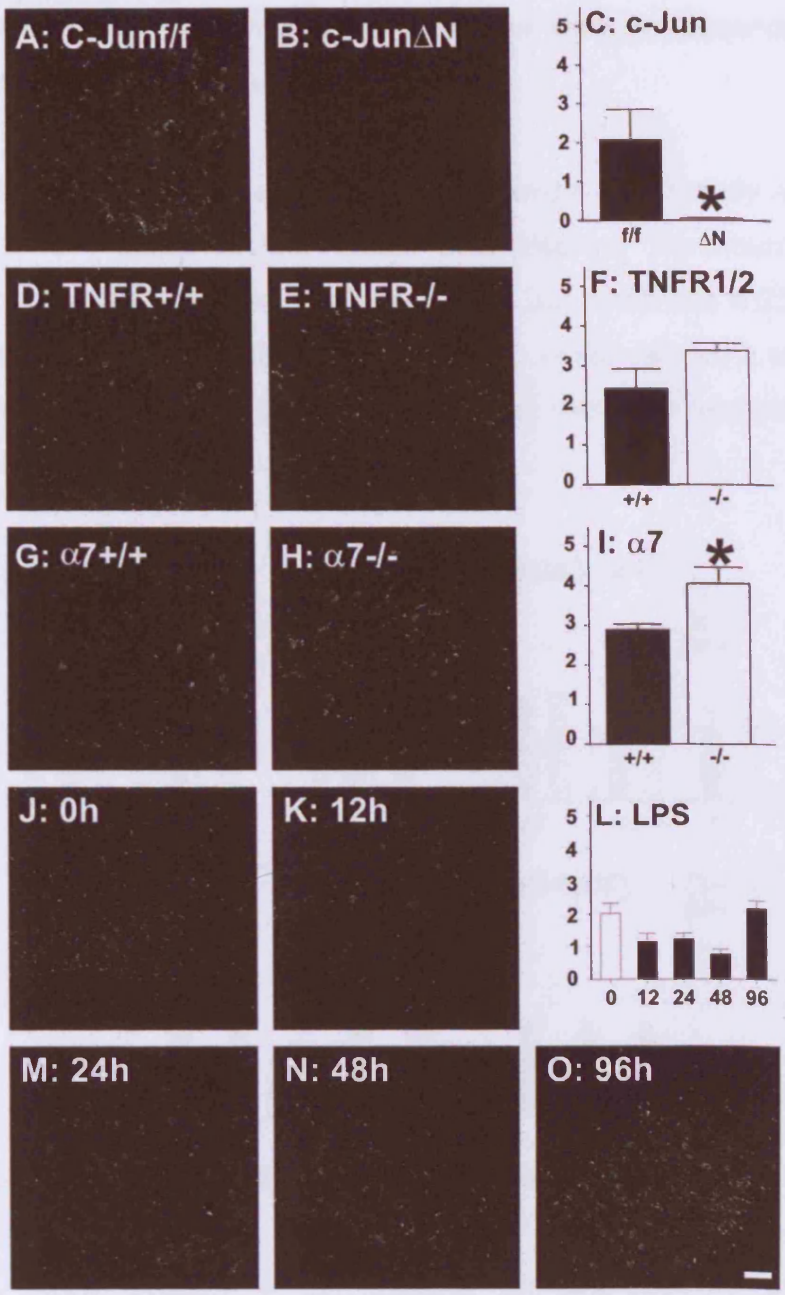

Figure 3.6. Quantification of immunofluorescent growth cones following facial nerve injury: the effects of α7, c-jun and TNFR1&2 gene deletions as well as enhanced inflammation on central axonal sprouting in the facial motor nucleus at day 14 following facial nerve cut. **A, D, G** shows the sprouting response in littermate controls of c-jundeltaN, TNFR1&2KO and α7KO, **B, E, H** shows the mutant response and **C, F, I**, the quantification of immunoreactive sprouts (in parts per thousand) respectively. Sprouting response was also measured following intraperitoneal administration of LPS. **K** shows the response at day 14 (control), **L** at 12, **N** at 24, **O** at 48 and **P** at 96 hours prior to day 14 endpoint. **M** shows the quantification (in parts per thousand). Scale bar = 125um. *$p<0.05$ in Student's t-test. Uninjured nucleus is not shown.

day 14 following facial axotomy ($p<0.05$), in line with the absence in central sprouting observed in these mutants.

Administration of LPS did not affect β1 integrin levels significantly at any of the time points (0.5-4 days) tested. There was also no significant difference between cut and crush injury at day 7 or day 14, but there was a 25% increase at day 10. Interestingly, re-injury paradigms (8+6, 14+8) caused a significant 26 and 27% decrease in β1 integrin levels, compared with their respective controls at day 14 and 22.

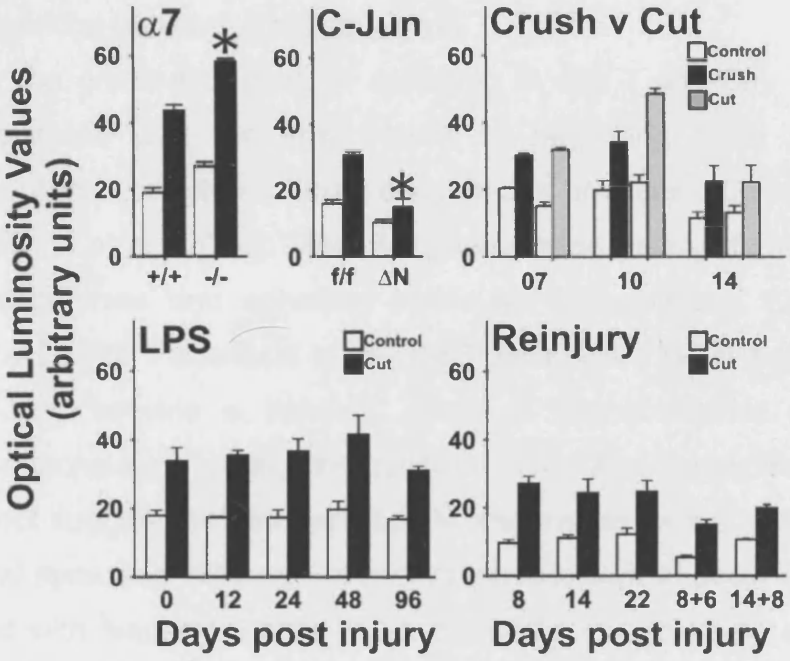

Figure 3.7. Quantification of β1 integrin immunoreactivity using optical luminosity values (OLV) in mutants lacking α7 or c-jun, 14 days after facial nerve cut; following administration of LPS; in crush versus cut injury; and, following reaxotomy of the facial nerve. *$p<0.05$ in Student's t-test

Discussion

Regenerative axonal sprouting is critical for the repair of the adult nervous system, but the specific signals involved in its induction are only beginning to be understood. The facial nerve axotomy model is a well-characterized paradigm to study molecular mechanisms involved in successful peripheral regeneration and functional recovery. As shown in the current study, transection of axons in the peripheral part of the facial motor nerve caused the delayed appearance of

sprouting, galanin+, and to a lesser extent CGRP+, neurites inside the central nervous system, in and and around the affected facial motor nucleus. These sprouts appeared to originate from axotomized facial motoneurons based on their selective appearance on the injured side, the presence of vesicular acetylcholine transporter as a marker of cholinergic phenotype, the presence of both galanin+ and CGRP+ subpopulations of facial motoneurons, and the colocalization with the bidirectional, retrograde and anterograde tracer Mini-Ruby first applied to the proximal stump of the cut facial nerve. In addition, sprouts located outside the nucleus and visualized with their stalk and bulb had their leading structure, the growth cone bulb typically pointing away from the nucleus, suggesting outward-directed growth.

Interestingly, the onset and peak of sprouting at day 7 and day 14 after cut appear to coincide with the time course of beginning facial motoneuron reinnervation of their peripheral target described in previous studies (Werner et al., 2000; Raivich et al., 2004). Moreover, denervated muscle fibres are a rich source of neutrophins and adhesion molecules (Covault and Sanes, 1985; Koliatsos et al., 1993; Funakoshi et al., 1993; Ishii et al., 1994; Springer et al., 1995) that could provide a transient surge in trophic signals available to axotomized motoneurons during the initial process of reconnection. However, the data do not suggest that reinnervation is responsible for the sudden burst in central axonal sprouting. Although reinnervation is known to occur earlier, more promptly and with less error after crush than after cut (Nguyen et al., 2002; Witzel et al., 2005), peak levels of sprouting after cut were more than 5-fold higher than after crush. Similarly, the reinterruption of axonal connections with a recut (8+6, 14+8) led to a significantly stronger sprouting response compared to that observed following single cut at day 14 and 22, respectively. This enhanced sprouting could be due to conditioning effect (Woolf et al 1992; Gilad et al 1996). However, the 14+8 sprouting was less than at day 14, suggesting that overall duration and presence of recut, rather than the conditioning effect, are the primary variables that define the extent of central sprouting.

Surprisingly, these facial axonal sprouts were particularly numerous in the white matter tissue that appears to inhibit the outgrowth of corticospinal, rubrospinal or peripheral sensory axons via a rapid growth cone collapse (Fouad et al., 2001; Li et al., 1996). At the ultrastructural level, the facial sprouts also showed close contact with neighbouring oligodendroglial cell bodies while maintaining

an active growth state. Understanding molecular signals associated with the formation of facial axonal sprouts could thus provide clues to improving regenerative response in the white matter of central nervous system.

Effects of neuronal cell death, peripheral regeneration and inflammation

Central axonal sprouting in the mouse facial axotomy model peaks at day 14 after facial nerve cut. This time point coincides with the maximum in substantial neuronal cell death, but also with inflammatory changes in microglia and astrocytes and leukocyte recruitment observed in this CNS injury and repair model. Previous evidence also shows those subtypes of neurons that are most likely to be programmed to launch a regenerative response after injury, for example retinal ganglion cells, also exhibit a high rate of cell death (Berkelaar et al., 1994) which is in line with observations where particular transcription factors such as c-jun that contribute to cell death are also required for regeneration (Raivich et al., 2004).

In the same vein, brain c-jun deficient animals with an absence of neuronal cell death following facial nerve cut (Raivich et al., 2004), show an abolished sprouting response in the mutant animals. However, this correlation is not maintained in other mutants with effects on cell death in the same model. TNFR1&2 null mice show a 4-fold reduction in cell death (Raivich et al., 2002) but a slight, though not significant tendency toward higher central sprouting. TGFβ1 null mice show greatly increased cell death together with a significantly reduced sprouting response (Makwana et al., 2007). Similar lack of linear correlation is also observed for peripheral regeneration, with enhanced sprouting in IL-6 null (Galiano et al., 2001) and α7 null (figure 3.6D-F), and reduced sprouting in the brain c-jun deficient animals (figure 3.6A-C); all 3 groups of mutant mice show a significant reduction in the speed of peripheral nerve outgrowth (Zhong et al., 1999; Werner et al., 2000; Galiano et al., 2001; Raivich et al., 2004).

Interestingly, current data do show a relatively straightforward correlation between neural inflammation and reduced central axonal sprouting in the facial axotomy model. Systemic application of 1mg E.coli endotoxin causing severe neural inflammation and granulocyte recruitment (Bohatschek et al., 2001) resulted in a 50% reduction in sprouting response 12-48h following the

intraperitoneal injection (figure 3.6J-O). Enhanced neural inflammation in TGFβ1 null mice is also associated with reduced sprouting (Makwana et al., 2007). This also appears true in reverse, with attenuated inflammation and 50% enhanced sprouting in IL-6 null mice (Galiano et al., 2001). Finally, the reduced inflammatory response in TNFR1&2 null mice (Bohatschek et al., 2005; Liu et al., 2005) coincides with a tendency towards improved sprout outgrowth in these mutant mice shown in the current study.

Induced inflammation around the cell body has been shown to improve sensory axon outgrowth into the CNS (Lu and Richardson, 1991). However, these results were obtained when inflammatory stimulus was performed instead of peripheral nerve injury, unlike the current model where peripheral injury is followed by a robust inflammatory response inside the affected part of the brain (Raivich et al., 1999). Central injury frequently produces mild retrograde reaction, where additional perineuronal inflammation will elicit a stimulatory effect (Yin et al., 2006), raising the question with regard to those components of neuronal response that specifically enhance neurite outgrowth inside the injured CNS.

Endogenous Signals in Central Axonal Sprouting

Upregulation of neuronal transcription factors such as c-Jun, ATF3, or STAT-3 play an important role in the neural response to injury and the synthesis of molecules required for regeneration and repair (Herdegen and Leah, 1998; Schweizer et al., 2002; Tsujino et al., 2000). As shown in this study, neural expression of c-jun transcription factor is essential for the delayed appearance of central axonal sprouting. Although numerous regeneration-associated genes and proteins show an early onset and peak of expression following injury (e.g. ATF3, GAP43, CD44, CGRP, α7 integrin, subunit, etc) and that may enable the different stages in the initiation and execution of neurite outgrowth (Seijffers et al., 2007), there is a second or later group of molecules such as galanin, β1, noxa etc (Kloss et al., 1999; Galiano et al., 2001, Kiryu-Seo et al., 2004) with a relatively delayed expression that coincides with central sprouting and neuronal cell death. Moreover, many of these late but also early molecules are brain c-jun dependent, and as shown in the current study are actually expressed in the facial axonal sprouts, for example CD44, galanin and α7β1integrin. These

growth-cone localized molecules support axonal elongation and outgrowth in the peripheral nerve (Werner et al., 2000; Wynick et al., 2001; Jones et al., 2000; Kloss et al., 1999), and may enhance central sprouting as well as allow nascent central growth cones to withstand numerous inhibitory cues such as NOGO, MAG and OMGP that are present in the white matter (Liu et al., 2006). Although hypothetical, the neurite-outgrowth enhancing properties of galanin could also be involved in the much stronger sprouting observed in the galanin+ compared to the CGRP+ populations of axotomized facial motoneurons.

Interestingly, deletion of the α7-integrin subunit increases central sprouting, which could point to an inhibitory role of the α7β1 integrin. The apparently compensatory upregulation of β1 could suggest enhanced activity, for example via one of the other 11 currently identified β1-associating α subunits (Sixt et al., 2006). Moreover, the strong decrease in post-traumatic neuronal expression of β1 in brain jun-deficient mice could contribute to the failure in central sprouting in these mutant animals. This potential involvement of β1 family of integrins is qualified by incomplete overlap of peak β 1 levels (day 10) and sprouting (day 14) in the cut vs crush experiment, and the significant reduction of β1 levels in the recut experiment associated with enhanced sprouting (figures 3.7D, E), and could indicate the presence of additional pathways involved in the regulation of central axonal outgrowth under varying genetic and experimental conditions. Nevertheless, the hypothesis for β1 integrin family involvement will need to be tested using central neuronal deletion of the β subunit to settle this issue. Moreover, if these experiments do show positive involvement of β1, identifying the cognate α subunit(s) involved in central axonal sprouting could enhance the therapeutic understanding of the repair processes operating in the injured brain and spinal cord.

CHAPTER 4

Constitutively active neuronal Ras protects from lesion-induced neurodegeneration and enhances central axonal sprouting following facial nerve injury.

Introduction

Neurotrophins are essential for neuronal development and are required for maintaining function and plasticity in the adult nervous system (for a recent review see Reichardt, 2006). During development the role of neurotrophins is primarily to balance neuronal survival and induce neurite outgrowth (Lindsay, 1996; Tsuji et al., 2001). In addition, they also contribute to axon elongation (Kirstein and Farinas, 2002), pathfinding and guidance (Song and Poo, 1999), and the maturation and density of synaptic innervation (Causing et al., 1997). Moreover, neurotrophins have also been implicated in the prevention of dendritic atrophy and growth of injured cortical neurons (Kolb et al., 1997a,b) and exogenous neurotrophins can promote repair and recovery of function following axonal injury (Bregman et al., 2002; Murray et al., 2002). The discriminatory action of neurotrophins on particular cell populations is attained by the expression of high-affinity neurotrophin receptors of the tyrosine kinase (trk) family. Neurotrophins as well as their receptors are present, not only during development, but also during adult life (Huang and Reichardt 2003 and references therein).

The neurotrophin-trk receptor complex induces the activation of the Ras family of GTP-binding proteins resulting in a range of responses (Marshall, 1996). Particularly well characterised in this family is the small G-protein Ras which activates specific downstream signalling pathways such as the evolutionary conserved mitogen-activated protein kinase (MAPK) cascade and the phosphoinositide-3 kinase pathway (Leevers and Marshall, 1992; Rodriguez-Viciana et al., 1994), by switching between a GTP (on) and GDP (off) state (Marshall, 1996). This molecular switch regulates the phosphorylation of a number of downstream kinases resulting in the modification of enzymatic activities and gene expression at the nuclear level (Ahn, 1993). While the Ras

protein is found in most cell types such as spleen, liver and lung at low levels, it appears that it is highly localised in the brain (Furth et al., 1987; Tanaka et al., 1986) suggesting it has a role in certain specialised cellular functions. For instance, three independent laboratories reported the induction of morphological differentiation of PC12 cells following microinjection of the Ras oncogene protein (Bar-Sagi and Feramisco, 1985; Noda et al., 1985; Guerrero et al., 1986). Application of activated H-Ras to neurotrophin deprived embryonic chick dorsal root ganglion prevented neuronal degeneration and induced neurite outgrowth (Borasio et al., 1989). Moreover, the introduction of the Ras function blocking antibody Y13259 to chick dorsal root ganglion cells primed with neurotrophin, reduced neurite outgrowth and cell survival in a dose dependent manner (Borasio et al., 1993). These results point to a critical role of Ras in relaying signals from neurotrophins, suggesting that if Ras activity could be elevated or in a constant active state in post-mitotic neurons, the requirement for neurotrophins could be reduced or an additive effect on survival and neurite extension produced.

Peripheral nerve injury causes morphological and molecular changes at three different sites: at the point of axotomy, in the cell body of the injured neurons, and in the surrounding non-neuronal cells. In the injured peripheral nerve, the disconnected nerve fibres and associated myelin distal to the lesion site undergo Wallerian degeneration (Waller, 1850). In the proximal part, the tips of the injured axons transform into growth cones of sprouting axons which enter endoneural tubes in the distal nerve, grow back and reinnervate peripheral targets (Raivich and Makwana, 2007). The perikarya of injured neurons display morphological changes, referred to as chromatolysis, retrograde reaction, or cell the body response (reviewed in Lieberman, 1971).

In addition to the chromatolytic response, axonal injury leads to the activation of non-neuronal cells such as microglia and astrocytes around the cell body of the injured neuron. Microglial cells express numerous cell surface integrins (Kloss et al. 1999) which enable them to adhere to damaged neurons (Raivich et al., 1999). Moreover, these non-neuronal cells express major histocompatibility complex proteins (Streit et al., 1989; Bohatschek et al., 2004a; Liu et al., 2005) required for antigen presentation as well as interaction with T-lymphocytes recruited to the injured brain (Raivich et al., 1998). Furthermore, numerous late

microglial markers such as αX (Raivich et al., 1999) and B7.2 (Bohatschek et al., 2004b) are also expressed that coincide with a peak in neuronal cell death after facial nerve cut (Moller et al., 1996). Moreover, adjacent blood vessels increase expression of cell adhesion molecules such as ICAM-1 (Kloss et al., 1999) which may assist in leukocyte recruitment. The astrocytic response is associated with an increase in intermediate filaments such as GFAP (Latov et al., 1979) and vimentin (Dahl et al., 1981; Calvo et al., 1991). Astrocytes appear to rearrange their cytoskeleton, become hypertrophic, proliferate and migrate to the site of injury (Miller et al., 1986), enhancing the physical stability of the damaged parenchyma (Pekny et al., 1999).

Recently, Heumann and colleagues (2000) have created a transgenic mouse line expressing constitutively activated Ras (Ras+) under the neuronal synapsin I promoter. These mice, which show no brain or behavioural abnormality, have been shown to attenuate neurotoxin-induced degeneration of dopaminergic substantia nigra neurons in Ras+ mice and reduce lesion-induced degeneration of facial motoneurons after facial nerve cut. The results from these mice appear consistent with the hypothesis that constitutively active Ras reduces the requirement for neurotrophin induced rescue of lesioned neurons. Moreover, while the effects of neuronal survival have been tested, the in vivo response of neurite outgrowth in these animals has not been investigated. Since a time-course and molecular characterisation on central axonal sprouting in the facial motor nucleus (see Chapter 3) provides a reference model to investigate the physiological effects of various gene modifications, the present aim was to test the effects of activated Va12H-Ras, which is expressed selectively in neurons under the promoter of the synapsin I gene (syn-Ras mice), on central sprouting, speed of axonal regeneration, neuronal cell death and the post-traumatic neural inflammatory response using the facial nerve injury model.

Materials and Methods

Animals, surgical procedures and tissue treatment

Constitutively active Ras mouse transgenic lines were created as previously described (Heumann et al., 2000). Briefly, the 5' nontranslated regions of the

human Ha-Ras (Capon et al., 1983) and the rat Synapsin I (Sauerwald et al., 1990) genes were fused. The 3' flanking region of the Ha-Ras gene, including its polyadenylation signal, was removed and substituted with a fragment containing an internal ribosome entry site (IRES)/LacZ.

For genomic screening, 0.5cm of tail from 21 day old mice was taken and incubated 56°C overnight in proteinase K lysis buffer (100ug/ml, Promega, UK). Genomic DNA was extracted using the Genomic Wizard DNA extraction Kit (Promega, UK) as per manufacturer's instructions. Briefly, the lysate was treated with phenol chloroform and the genomic DNA was precipitated out of solution with isopropanol, washed and redissolved in 100ul of rehydration solution. Polymerase Chain Reaction (PCR) was conducted in 36 cycles of; 5 minutes at 94°C, 60 s at 94°C, 60 s at 60°C and 60 s at 72°C, followed by 10 minutes at 72°C. Primers were 5' to 3': TGACCATCCAGCTGA TCCAGAA and CTCCCATCAATGACCACCTG. The PCR products were resolved and visualized on a 1% agarose as described in Chapter 2 –Materials and Methods. Mutant Ras and wild-type littermate controls 8-10 weeks old were anesthetised using 10ul/g body weight of a 2.5% solution of 2,2,2-tribromoethanol (Avertin, Sigma, UK) dissolved in distilled water. The right facial nerve (including the retro-auricular branch) was cut or crushed at its exit from the stylomastoid foramen. Animals were sacrificed after survival time of 4-30 days with an overdose of Euthatal, perfusion-fixed with 200 ml phosphate-buffered saline (PBS: 10 mM Na_2HPO_4, 0.85% NaCl, pH 7.4) as described in Chapter 2 – Materials and Methods. This was followed by 200 ml of 4% paraformaldehyde in PBS (PFA/PBS), then by a 2 hour immersion of the brainstem in 1% PFA/PBS at 4° C on a rotator (8 rpm), an overnight rotating immersion in a phosphate-buffered sucrose solution (PB: 10 mM Na_2HPO_4, pH 7.4, 4°C; 30% sucrose) and frozen on dry ice.

Regeneration, functional recovery and retrograde tracing

To determine the speed of facial axonal regeneration, the facial nerve was crushed with a fine jeweller's forceps for 30 seconds 1 mm distal to the stylomastoid foramen. The animals were sacrificed after 96 hours with an overdose of Euthatal. Following a brief, 5 min perfusion with PBS, and 5 min

with 4% PFA/PBS, the facial nerve was fixed by a slow, 60 min perfusion with 1% PFA/PBS, then immediately dissected for a length of 15-20 mm and frozen on dry ice. Nerves were cut longitudinally and the regenerating axons visualized by immunostaining for galanin or for CGRP. Every fifth section was used per antibody, with an interval of 50 µm, and the distance between the most distal labeled growth cone and the crush site measured using light microscopic grid scaling. The average distance for each animal was calculated from 4-5 tissue sections.

Functional recovery in the whisker hair movement model was assessed after facial nerve cut. Whisker movement was determined during the 28 day post-operative period beginning at day 07 and scored on a 3 point scale (0 - no movement to 3 - completely normal movement) by a blinded observer (Raivich et al., 2004).

To assess whisker pad reinnervation, GelFoam (Johnson and Johnson UK) was soaked in 15µl of 4% Fluorogold, dissolved in distilled water. This was applied to the whiskerpad bilaterally 28 days post axotomy (see Chapter 2 – Materials and Methods).

Light microscopic bright-field immunohistochemistry

Twenty-micrometre thick brain stem sections were cut at the level of the facial motor nucleus at -15°C, collected on gelatine-coated slides and stored at -80°C before use. All tissue was processed in exactly the same way with regard to perfusion, fixation, cryoprotection and cutting protocols. Tissue belonging to different experiments were processed at different time points. However, all tissue sections belonging to the same experiment were stained together for the same period of time to prevent differences in the number of counted cells or differences in staining intensity. Standard light microscopic immunohistochemistry was performed as described in Chapter 2 Materials and Methods. Absence of primary antibody led to the disappearance of specific immunolabelling. The visualisation of CD3-immunoreactivity with diaminobenzidine/H_2O_2 was performed with Co/Ni enhancement (0.02% CoCl2 and 0.025% $NiCl_2$ in PB).

Quantification of central axonal sprouting

Axonal growth cones in and around the facial motor nuclei at day 14 (Kloss et al., 1999; Werner et al., 2001) were detected using immunofluorescence against CGRP or galanin, the neuropeptides expressed in axotomised facial motor neurons, followed by biotinylated goat anti-rabbit secondary antibody (1:100) then with Texas-red Stretavidin (1:1000; Jackson Laboratories, UK). Previous studies using retrograde labelling with Mini-Ruby confirmed that these growth cones were derived from the axotomised motoneurons (Werner et al., 2000; see also Chapter 3). Quantification of growth cones was performed as described in Chapter 2 – Materials and Methods

Neuronal cell counts

Motoneuron cell counts were determined in the axotomised facial nucleus and on the contralateral side 30 days after a right facial nerve cut as described in Chapter 2 – Materials and Methods.

Statistical analysis

Statistical analysis for axonal regeneration distance, neuronal cell counts, leucocyte influx into the injured nerve and microglial staining intensity (RISC) was performed using a standard two-tailed Student's t-test.

Results

Axonal regeneration in the crushed facial nerve.

Axonal regeneration in the facial nerve was examined 96h after crush injury as previously described (Werner et al., 2000; see also Materials and Methods). The axonal growth front of the regenerating CGRP-or galanin-positive motoneurites was detected in longitudinally cut, fixed 10um thin facial nerve sections using immunoreactivity for the axonally transported neuropeptides CGRP and galanin and distance to the site of the crush determined with a microscope eye piece graticule. Five tissue sections, spaced 50µm apart were used to determine the mean regeneration distance for each neuropeptide and animal (n=5 animals per group). Normal wild-type mice littermate controls

showed a regeneration distance of 5.21+/-0.35mm for the CGRP and 5.41+/-0.14mm for the galanin immunoreactive axons at day 4. Compared with wild-type littermates no difference was observed in Ras+ mutants where the growth front was 5.04+/-0.39mm in CGRP and 5.69+/-0.41mm in galanin immunostained axons; n=5 animals per group; p=0.65 for galanin and p=0.73 for CGRP (figure 4.1A).

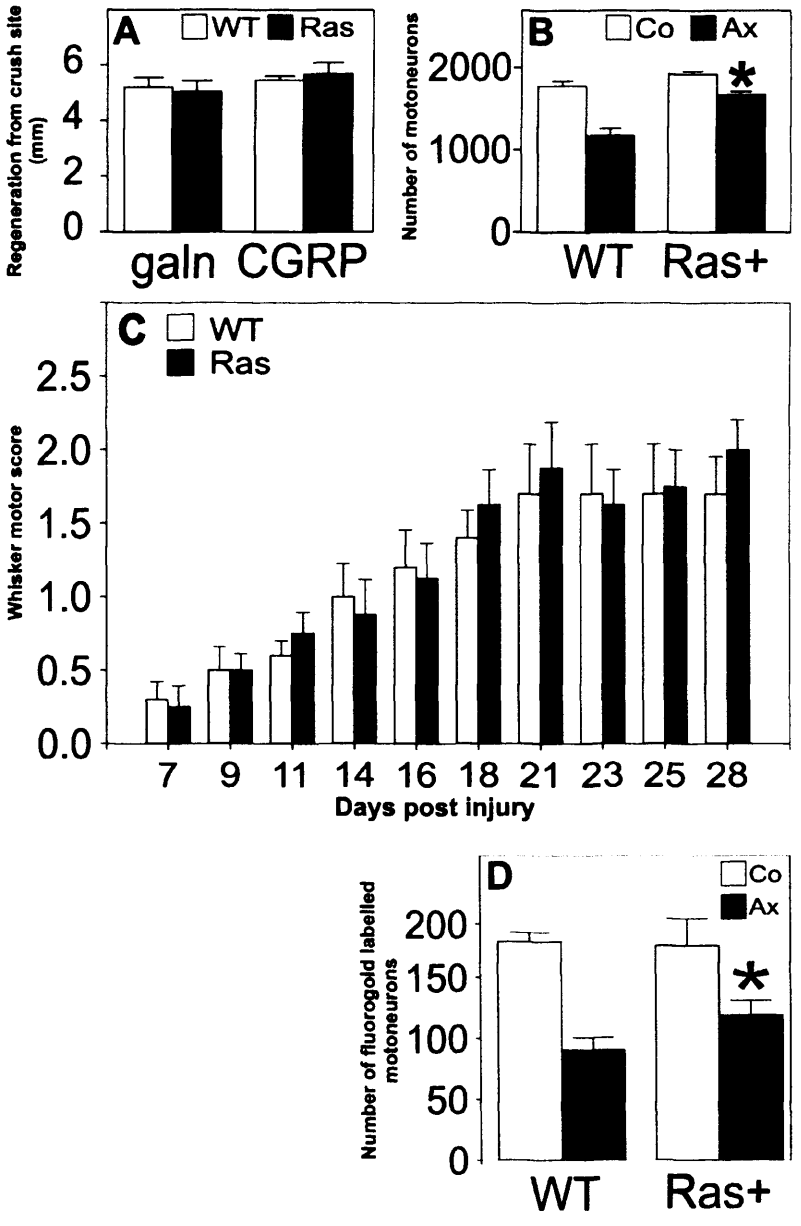

Figure 4.1. Ras and axonal regeneration, functional recovery, target reinnervation and neuronal cell death. A: No effect on the regeneration distance of CGRP- and galanin-immunoreactive motor axon populations 4 days after facial nerve crush (Error bars indicate mean +/-standard error of mean/SEM, n=5 animals per group). B: Changes in neuronal cell number in the axotomised

and contralateral facial motor nucleus, 30 days after facial nerve cut (n=8 per group; *p<0.05 in unpaired Student's t-test). C: Functional recovery of whisker hair movement after facial nerve cut (n=5 per group). D: Quantification of retrograde labelling of facial motoneurons with fluorogold 28 days after facial nerve cut. The overall ratio of labelled neurons in the operated/unoperated side is shown (n=5 per group). *p<0.05 in unpaired Student's t-test.

Neuronal survival

Facial axotomy leads to a delayed form of neuronal cell death, with a peak at day 14 (Moller et al., 1996; Raivich et al., 1998). To determine the effect on neuronal cell death, neuronal survival was examined at 30 days using Nissl-stained 25µm-thin sections (figure 4.1B). All neuronal profiles were counted through the whole facial motor nucleus on the operated and controls sides and the number corrected using the Abercrombie correction coefficient (Abercrombie, 1946) as described in the Materials and Methods. This corrected number of motoneurons on the unoperated side in WT littermates was 2012+/-57 (n=8, mean+/-SEM) is in line with previously published data on the facial nucleus of mice (Sendtner, 1997; Raivich et al., 2002). Compared to the unoperated side, facial axotomy led to a 44% loss of motoneurons in the WT mice (1325+/-98 on the axotomised side) next to just 11% in the Ras+ mutants 30 days after injury, with 2039+/-91 motoneurons versus 2288+/-78 on the axotomised side and contralateral sides respectively, (n=8 animals). This 33% reduction in neuronal cell death in Ras+ animals compared with WT controls was statistically significant (p<0.05 in Student's t-test).

Whisker motor recovery and target reinnervation.

Whisker vibrissae movement is a good indicator of motor recovery following facial nerve cut (Gilad et al., 1996; Raivich et al., 2004). To assess recovery of whisker motor function in Ras+ mice following facial nerve cut, whisker movement was scored on a scale of 0.0 (no movement) to 3.0 (normal movement as on the uninjured side) as described in Raivich et al. (2004) starting at day 7 up to day 27. There was no statistical difference in whisker recovery between wild-type and Ras+ groups (figure 4.1C) with recovery score at 2.0+/-0.2 and 1.7+/-0.3 respectively; p=0.19 at day 27 (n=5 wild-type and n=5 Ras+ animals).

To establish the extent of target reinnervation following facial nerve cut, the retrograde tracer fluorogold was applied to the whisker pad 28 days post-axotomy and the fluorogold labelled motoneurons in the facial nucleus were analysed at day 30. Target reinnervation in the Ras+ animals, although moderate, was statistically higher than WT (figure 4.1D). The total fluorogold labelled motoneuron count was 179+/-7.5 vs 90+/-10.4 for uninjured vs injured in wild-type and 176+/-22 vs 119+/-11.7 for uninjured vs injured in Ras+. The ratio of uninjured versus injured was 50.1% vs 69.8% for wild-type and Ras+ respectively ($p<0.05$, Student's t-test).

Neuronal and non-neuronal inflammatory response to axotomy

Axotomised neurons undergo characteristic metabolic and structural changes known as chromatolysis associated with the regrowth of the cut axon into the periphery (Lieberman, 1971). In the facial nucleus, chromatolytic changes can be determined by alterations in the levels of the neuropeptides CGRP and galanin; increased levels of which have previously been associated with an enhanced regenerative response (Wynick et al., 2001). Figure 4.2 shows the quantitation of the intensity of immunoreactivity of galanin and CGRP in Ras+ mutants at day 14 showed no difference in levels of these peptides. Similarly, increased levels of β1 integrin has been associated with enhanced sprouting and regeneration (Chapter 3; Kloss et al., 1999; Werner et al., 2000). However, no difference was observed between mutant and control groups (figure 4.2).

Nerve transection does not only trigger changes in the neuron but also results in activation of resident non-neuronal cells (Raivich et al., 1999; Schwaiger et al., 1998). Microglia in particular undergo a number of changes in response to neuronal stimuli that can be graded into a series of distinct steps: resting microglia (Stage 0), state of alert (Stage 1), homing and adhesion (Stage 2), phagocytosis in the presence of neuronal cell death (Stage 3a) and bystander activation of surrounding non-phagocytic microglia (Stage 3b) (Raivich et al., 1999). These stages of activation are characterized by high levels of specific antigens which can be quantified using immunoreactivity for the appropriate activation marker. Early microglial activation, or the 'State of Alert' (Stage 1) is characterized by the induction of intracellular adhesion molecules including

ICAM-1, and integrin subunits including αMβ2 (Raivich et al., 1999, Kloss et al., 1999).

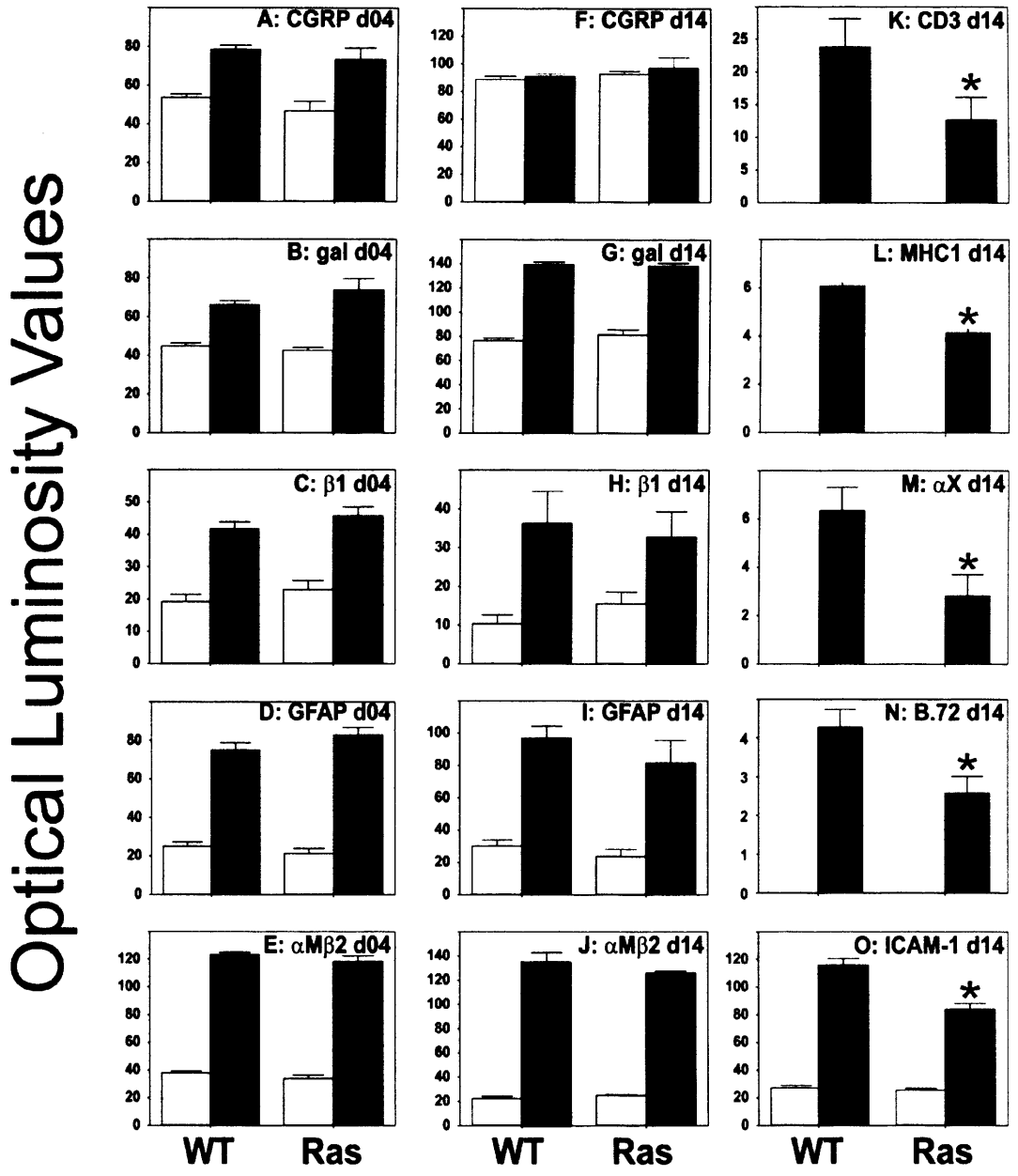

Figure 4.2. Quantitation of neuronal and non-neuronal response to axotomy at day 4 and 14. Facial motor nucleus immunoreactivity in A-J and O was quantified using the MEAN+SD algorithm (Möller et al., Glia, 1996); K shows the number of immunoreactive postive T-cells and L, M and N shows the number of immunoreactive nodules. *p<5% using student t-test. Neuronal expression of Ras causes a significant reduction in MHC1+ (L), aX+ (M) and B.72+ (N) nodules; ICAM-1 (O) immunoreactivity and influx of CD3+T cells (K) at day 14. However, it does not affect the levels of neuronal peptides such as CGRP (A, F), or galanin (B, G). Glial activation of astrocytes (D, I) and microglia (E, J) at day 4 and 14 remained unchanged compared to WT animals. Filled bars: axotomised nucleus, empty bars: uninjured nucleus. *p<0.05 in unpaired Student's t-test.

Following initial activation, the microglia enter the homing phase (Stage 2), characterized by homing and adhesion of microglia to damages structures such as lesioned neurons or degenerating nerve terminals, and a burst of proliferation. There is downregulation of the initial alert phase markers, and upregulation of β1 integrin subunits, accompanied by an increase in immunoreactivity for MHC1 and the costimulatory factor B7.2 (Raivich et al., 1999, Kloss et al., 1999; Bohatschek et al., 2004b). The presence of neuronal cell death leads to further transformation of the microglia into phagocytic cells, which form nodules consisting of 3-20 microglial phagocytes, and display very high immunoreactivity for MHC1, B7.2, and the αX integrin subunit.

In Ras+ mice, early and late microglial activation as measured by the increase in immunoreactivity for the αMβ2 integrin subunit at day 04 and 14 was unchanged compared with wild-type controls (figures 4.2E, 2J).

Since neuronal cell death leads to the removal of neural debris by phagocytic microglia forming glial nodules (Moller et al., 1996; Torvik and Skjorten, 1971), we examined the presence of these phagocytic nodules in the axotomised facial motor nucleus at day 14 using MHC1, αXβ2 integrin and B7.2 by means of a manual count of microglial nodules at x20 magnification in two sections, approximately 200μm apart, throughout the extent of the facial nucleus. Figure 2L and 2M and 2N show all three markers were significantly reduced in Ras+ mutants with αXβ2 immunoreactive nodules down by 60% and B7.2 by 40% and MHC1 by 31% compared with littermate controls ($p<0.05$, Student's t-test). Interestingly, Ras+ significantly decreased levels of ICAM-1, by 34% compared with controls (figure 4.2O) which may be due to a reduction in bystander activation (Raivich et al., 1999).

Injury to the facial nerve also causes local astrocytes to become reactive and undergo hypertrophy. Like microglial activation, the astrocyte response to injury depends on the severity of the trauma (Raivich et al., 1999). These astrocytes, which normally express low levels of the GFAP, rapidly increase GFAP synthesis. In many cases GFAP levels remain elevated for several months post lesion (Moran and Graeber, 2004). As a result, astrocytic activation after injury

can be measured by GFAP immunoreactivity. Here, astroglial activation did not change at both day 04 and 14 (figures 4.2D, 4.2I)

Facial axotomy leads to two different phases of T-lymphocyte entry into the injured facial nucleus. The first is an elevated plateau, 1-4 days after injury; the second, a much stronger increase with a peak at day 14 (Raivich et al., 1998b). Infiltrating T-cells were detected using immunoreactivity for CD3 using 5 sections in the nucleus (120µm apart) at day 14. As shown in figure 4.2K, increased levels of Ras resulted in a 50% reduction in the number of CD3 positive cells (12.7+/-3.5) compared with WT littermates (24.9+/-3.7), $p<0.05$ in Student's t-test.

Constitutively active Ras enhances central axonal sprouting following facial nerve axotomy

Since activation of Ras by neurotrophins has been implicated in axonal growth, we next assessed the effect of Ras+ on central axonal sprouting in the facial nucleus following facial nerve cut. Previous studies characterising central sprouting in the facial nucleus have shown that they peak at day 14 following facial nerve cut and were immunoreactive for the neuropeptides galanin and CGRP (see Chapter 3). In addition, sprouting neurites were positive for vesicular acetylcholine transporter, and became retrogradely labelled following application of Mini-Ruby applied on the proximal stump of the cut facial nerve, in line with their origin as central sprouts of axotomised facial motoneurons (Chapter 3; Kloss et al., 1999; Werner et al., 2001; Chapter 3).

Transection of the facial nerve led to the transient appearance of neurite growth cones in the axotomised facial nucleus, which became particularly numerous in the surrounding white matter 14 days after injury (figure 4.3). Growth cones exhibited high levels of immunoreactivity for the motoneuron markers CGRP and galanin, these sprouts were absent on the contralateral uninjured side.

Quantification of the sprouting neurites revealed that while galanin immunoreactive growth cones were already more numerous under normal conditions (9.90+/-1.41 ppt in WT mice), this stronger response to axotomy was further enhanced by 30% (14.1+/-0.94 ppt) in Ras+ mice ($p<0.05$, Student's t-test; figure 4.3). CGRP+ immunoreactive growth cones, which normally show a

lower propensity to sprout (Chapter 3), showed a 50% increase of growth cones in Ras+ mutants (3.17+/-0.48 ppt) compared with littermate controls (1.58+/-0.32 ppt; $p<0.05$, Student's t-test).

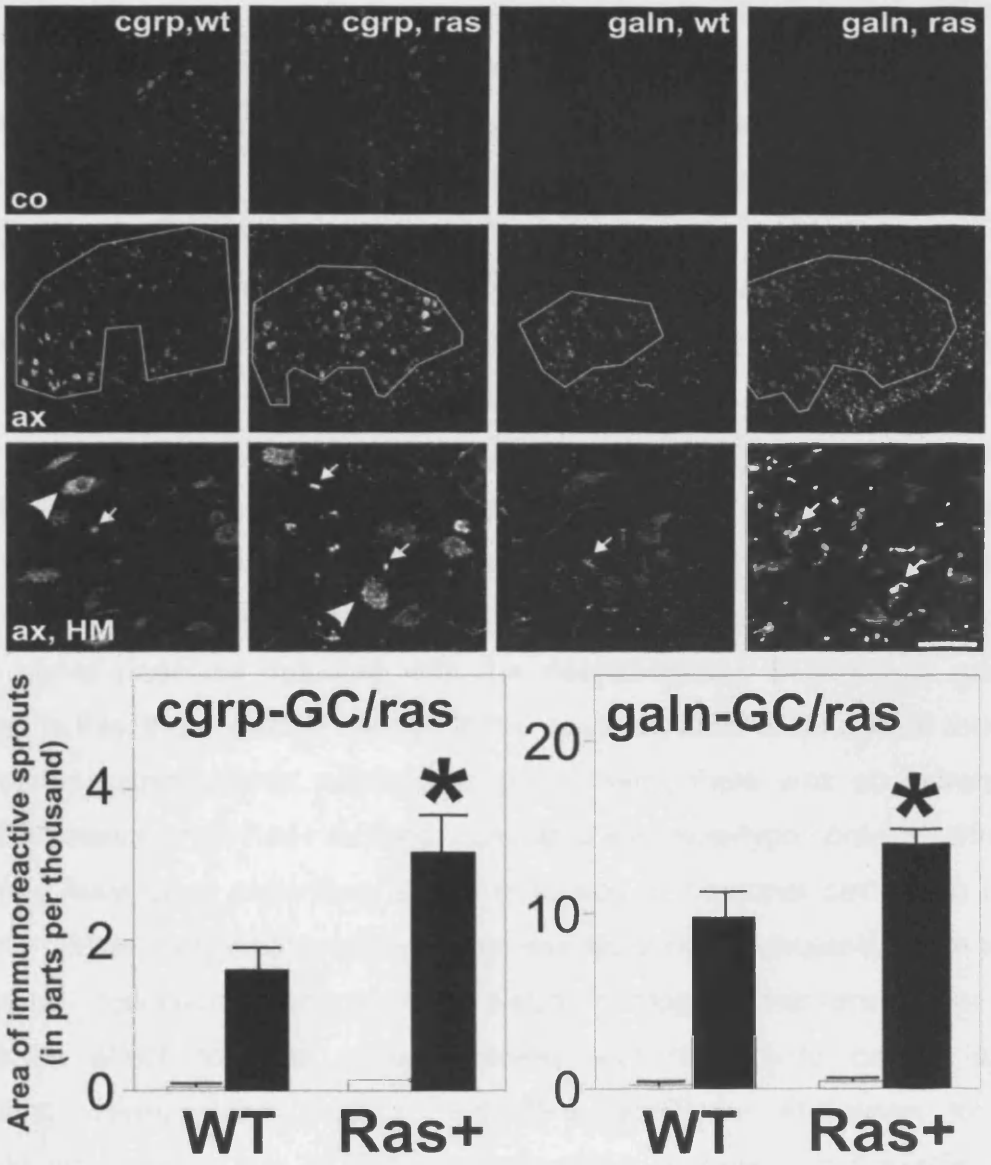

Figure 4.3. Neuronal expression of constitutively active Ras (Ras+) enhances central axonal sprouting (arrows) from the axotomised facial motor nucleus, 14 days after facial nerve cut (ax), compared with wild type animals (WT). The upper 3 rows show the immunofluorescence, the graphs show the quantitative morphology. Top: the Ras+-inducing effect is present in both CGRP (left columns) and galanin (galn, right 2 columns) motoneuron subpopulations, though galanin+ sprouts are more numerous. At high magnification inside facial the nucleus (ax, HM) the immunoreactive motoneuron cell bodies are indicated by arrowheads, the smaller sprouts by arrows. Co: contralateral side. Most neuropeptide immunoreactive sprouts are found in the white matter surrounding the facial nucleus (broken lines on the axotomised side), particularly in the corticobulbar tracts, ventral to the nucleus in the lower part of the figure. Bar scale: 250um in the upper and middle row, 62.5um in the bottom row. Bottom:

total area of neuropeptide immunoreactive sprouts (in parts per thousand) n= 7 wild type and 7 Ras+ transgenic mice. Filled bars: axotomised, empty bars: contralateral side, *p<0.05 in Student's t-test.

Discussion

Generation of axonal sprouts following injury plays a key role in establishing synaptic contacts and facilitating recovery of function. As established in Chapter 3, the facial nucleus model provides a unique paradigm to study the physiological effects of specific transgenics on peripheral and central axonal outgrowth as well as neuronal cell death and changes in resident non-neuronal cells. Numerous in vitro and in vivo studies have demonstrated a positive effect of the small GTPase Ras on axonal regrowth and neuronal survival (Bar-Sagi and Feramisco, 1985; Noda et al., 1985; Guerrero et al., 1986; Borasio et al., 1989; Borasio et al., 1993). Here, using a transgenic model, it was shown that constitutive activation of Ras under the synapsin I promoter (Heumann et al., 2000) resulted in a strong reduction in neuronal cell death following facial nerve cut. Surprisingly, no effect was seen in peripheral nerve outgrowth following facial nerve crush as detected with the neuropeptides CGRP and galanin. Parallel to this, there was no change in the speed or level of functional recovery determined using whisker movement. Interestingly, there was an increase in target reinnervation in Ras+ mutants compared with wild-type controls, although this may have been secondary to the reduction in neuronal cell death in the mutants. While early inflammatory responses were not attenuated, there was a consistent reduction amongst late stage microglial markers. The most prominent effect however, was observed with respect to central axonal sprouting. Here, Ras+ mutants exhibited significant increases in both populations, galanin and CGRP-immunoreactive sprouts, but the effect was particularly striking in the CGRP population which normally has a low propensity to sprout (see Chapter 3).

Ras+ and neuronal survival

Activation of Ras is required for normal neuronal differentiation and also promotes survival of many neuronal subpopulations. The data shown here demonstrates increased neuronal survival of facial motoneurons following nerve

cut. It has been shown previously in cultures of embryonic neurons that mitogen independent survival can be achieved by intracellular application of activated Ras in chick dorsal root ganglia neurons, superior cervical ganglion neurons and in spinal motoneurons (Borasio et al., 1989; Nobes et al., 1996; Weng et al., 1996; Mazzoni et al., 1999). The most recent study looking at the effects of Ras+ on facial motoneurons by Heumann et al. (2000) showed that they were able to attenuate neurotoxin-induced degeneration of dopaminergic substantia nigra neurons in Ras+ mice. They also showed that degeneration of facial motoneurons after facial nerve cut was completely prevented. In contrast, although our results showed a strong reduction in neuronal cell death in Ras+ mice, it does not completely prevent it. This discrepancy in neuronal survival data between Heumann et al. (2000) in facial motoneurons and the neuronal survival shown in this study can be explained by differences in methodology of stereological counting. Whilst Heumann and colleagues counted nucleated neurons in every third section of the facial nucleus 24 days following facial cut, we counted every cell body throughout the entire extent of the facial nucleus at day 30 post-axotomy, and then applied the Abercrombie correction (see Materials and Methods) to correct for cell body size. Nevertheless, the independent replication of a substantial rescue of motoneurons in this study supports the findings produced by Heumann and colleagues (2000).

Active Ras associates with multiple downstream targets to exert its biological effects (White et al., 1995; 1996), including Raf-1 kinase, the catalytic subunit of phosphatidylinositol 3-kinase (PI3K), and Ral guanine nucleotide dissociation stimulator (RalGDS) (Marshall, 1996). All three pathways have been shown to be activated following neurotrophin stimulation (Kolch, 2000), and notably activity via the Raf-1 and MEK kinase (Reichardt, 2006) as well as PI3K (Biggs et al., 1999; Namikawa et al., 2000) has been instrumental in inducing survival responses. Moreover, increased survival of axotomised motoneurons has been reported by the overexpression of Bcl-2 in transgenic mice (Martinou et al., 1994) and also in Bax knockout mice (Deckwerth et al., 1996). However, given the lack of changes in Bcl-2 and Bax expression as well as the absence of a change in PI3K expression in Ras+ mutants (Heumann et al. 2000) it may be that an unidentified downstream target of Ras other than the Bcl-2 family of proteins that may be involved in the Ras-induced rescue seen here.

One could argue that active Ras might rescue all neurons from axotomy induced death. However, Ras induced survival may depend on the mode of neuronal cell loss. Both apoptotic (Rossiter et al., 1996) and non-apoptotic (Subramaniam and Unsicker, 2006) death have been reported for facial motoneurons, although recently, this has been complicated somewhat by age and strain differences (Ferri et al., 1998; Hottinger et al., 2000; Serpe et al., 2000), and constitutive activation of Ras may block one of those survival pathways. The complexities of Ras signalling are further revealed by studies with three mutant forms of V-Ras in sympathetic neurons which appear to inhibit distinctive forms of apoptotic signalling (Xue et al., 2000). The mechanism by which the 11% of neurons in Ras+ mutants die following axotomy, in this study, remains unresolved. Interestingly, studies by Jones et al. (2005) show that certain subpopulations of neurons in the facial nucleus are consistently vulnerable to axotomy induced death; to which an inflammatory component and lack of trophic factors have been the major instigators (Serpe et al., 2005).
The limited response observed in early (αMβ2, ICAM-1) microglial activation and the decrease in αX, MHC1 and B7.2 positive microglial nodules as well as a decline in T-cell recruitment and at day 14 in the facial nucleus are probably changes secondary to the reduction in neuronal cell death.

Effects of Ras+ on peripheral regeneration and central sprouting

Numerous factors acting in concert may contribute to the Ras+ mediated central sprouting observed in the current study. Late microglial activation causes synaptic stripping (Raivich et al., 1999). Thus a reduction in B7.2, MHC1 and alpahX may have contributed to the enhanced sprouting observed in Ras+ mutants. While these effects, as well as the reduction in lymphocyte influx lie secondary to the decrease in neuronal cell death, the ultimate effect is induced by the sustained activation of Ras. The decrease in inflammatory response and concomitant increase in central sprouting is in line with previous studies (Chapter 3) where administration of LPS enhanced the inflammatory response and concomitantly decreased central sprouting.

Activation Ras did not alter the expression CGRP or galanin by axotomising facial nerve. Hence the effect of Ras+ on neuronal survival and central sprouting were not mediated by CGRP or galanin regulation. Therefore, neuronal levels of these neuropeptides, whilst being important for some growth associated responses (Galiano et al., 2001), are not essential for the enhanced central sprouting response observed in the Ras+ mutants. Both galanin and CGRP and have been implicated in peripheral nerve outgrowth (Wynick et al., 2001) and the lack of a difference observed in these molecules between Ras+ and controls may explain the absence of a Ras+ induced effect on peripheral nerve regeneration and functional recovery. Moreover the disassociation between central sprouting and peripheral outgrowth has been shown previously (Chapter 3; Chapter 5; Zhong et al., 1999; Werner et al., 2000; Galiano et al., 2001; Raivich et al., 2004). Surprisingly, Ras overexpression did not alter β1 integrin levels suggesting that this regeneration associated molecule may be upregulated as a compensatory mechanism in the absence of other regeneration mediators. For example, α7 null mice show enhanced levels β1 compensating for the reduction in peripheral nerve growth, presumably due to a lack of the α7 integrin subunit (Werner et al., 2000).

Neurotrophic factors regulate the survival and differentiation of numerous neuronal populations through Trk receptors. In the CNS, NT-3 has been implicated in axonal growth (Ma et al., 2002; Patel et al., 2003). Trk receptor-mediated axon extension and target reinnervation induced by neurotrophins involves the activation of their downstream effectors, Ras, PI3K/Akt and MEK/ERK (Atwal et al., 2000; Huang and Reichardt, 2001; Markus et al., 2002). The mice used in this study do not show increased activation of PI3K as a result of their constitutive expression of activated Ras (Heumann et al., 2000). In embryonic sensory neurons neurite extension is blocked by MEK inhibitors (Atwal et al., 2000) and specific activation of Ras-Raf-MEK-ERK cascade in Bax null mice selectively induces axonal elongation (Markus et al., 2002). These results support the evidence that Ras effectors such as ERK are likely responsible for the increased neurite outgrowth observed in the facial nucleus following axotomy.

Indeed the obvious molecular mechanism to explain the increase in fibre sprouting would be via an increase in phosphorylated ERK1/2 proteins downstream of Ras activation. Certainly, Heumann et al. (2000) has previously reported that p-ERK1 does significantly increase in Ras+ mutants. Moreover, ablation of the neurofibromin gene *Nf1* resulting in disinhibition of Ras (Zhu et al., 2002) also increases p-ERK levels and therefore the enhanced neurite effects that were observed may indeed depend on the effects of increased p-ERK levels. However, MEK, the upstream activator of ERK has been shown to play a dual role in neurite outgrowth and neuronal survival. Indeed, Chapter 5 provides some evidence of this in that partially inhibiting the activity of MEK resulted in enhanced neurite outgrowth and neuronal survival. This is discussed more fully in Chapter 5 and Chapter 8.

The mechanism by which Ras+ coordinates the assembly of microtubules for axonal sprouting and elongation remain to be elucidated. Certainly, transcription factors which are upregulated following injury such as c-jun, ATF-3, CREB and STATs may be involved downstream of ERK activation (Sheu et al., 2000; Pearson et al., 2003). Alternatively, other effector molecules could be involved such as calcineurin/NFAT which is activated by Ras signalling and is involved in axonal elongation in sensory neurons (Graef et al., 2003).

Ras activation in vivo has been noted in previous studies where sensory fibres show enhanced sprouting following rhizotomy of the dorsal root (Zhu et al., 2002; Romero et al., 2007). Romero and colleagues (2007) produced constitutive activation of Ras by ablating the neurofibromin (Nf1) gene, which normally inhibits the activity of Ras. They showed enhanced functional recovery following dorsal root injury, mediated by sprouting of spared fibres in the dorsal root and proposed that increased p-ERK signalling contributed to the enhanced sprouting. While the study by Romero et al. (2007) supports the observations shown in the facial nucleus in the current study, some caution is required since (1) these are two very different models in different areas of the CNS; (2) Romero and colleagues show abnormality in the growth and development of the Nf1 null mutants, whereas mutants in the current study have normal development; and (3) NF1 null mutants also show enhanced astrogliosis without injury in various areas of the brain including the cortex and brainstem indicating

an inherent inflammatory component in these mice which as previous chapters of this thesis have shown, could be inhibitory to axonal sprouting (Chapter 3 and Chapter 6).

The dichotomy between an absence of a significant peripheral response versus an enhanced central reaction seen in the Ras+ mutants suggests that Ras exerts its effects mainly in the CNS. Moreover, given the survival response of motoneurons in this model and other models (Heumann et al., 2000) with this particular mutation; and since the sprouting response is moderately robust, it may be particularly pertinent to assess whether the enhanced synaptic plasticity in these mutants can contribute to functional recovery in more severe forms of central injury like those that occur following spinal cord trauma. This forms the focus of Chapter 7.

CHAPTER 5

MEK Promotes Neuronal Cell Death and Inhibits Central Axonal Sprouting Following Peripheral Facial Motor Nerve Injury

Introduction

Sprouting and regeneration of axons is critical for the repair of the adult nervous system. However, the intracellular signals involved in the control of axonal sprouting and elongation in the adult organism are only just beginning to be elucidated, largely through the study of neurotrophic factors. The neurotrophins and other families of neurotrophic factors have been recognised to play a crucial role in neuronal survival, differentiation, synaptic plasticity and neurite outgrowth (for recent review see Reichardt, 2006; Zhou and Snider, 2006). The extracellular signal-regulated kinase (ERK) cascade appears to play an important role in neuronal survival and in mediating synaptic plasticity in response to neurotrophin stimulation.

In vitro, the effects of neurotrophins and similar growth factors on axonal sprouting are mediated through intracellular signalling cascades of which the Ras/Raf/MEK/ERK (Ihara et al., 1997; Kuo et al., 1997) and the PI3K/Akt pathway (Kita et al., 1998; Atwal et al., 2000) are crucial. In addition to these established intracellular mechanisms, other mediators such as Ral-GDS acting on small Ras-like GTPases like ral or rap1 (Lu et al., 2000) are also involved. Some components of the PI3K cascade transduce through MEK, highlighting the complex crosstalk between these two pathways (Schmid et al., 2000). However, there are also strong, MEK-independent and complementary mechanisms such as the Rac-JNK pathway (Kita et al., 1998). Inhibition of Ras and MEK have been shown to block neurite outgrowth in embryonic primary neurons (Borasio et al., 1989; Atwal et al., 2000) as well as in other cell line models of neuronal differentiation such as PC12 cells, immortalised rat hippocampal neurons (H19-7) and NIH-3T3 and PC6 cells (Ihara et al., 1997; Kuo et al., 1997; Shi and Andres, 2005). Inhibition of MEK has also been shown to prevent the neurite-outgrowth promoting effects of BDNF on cerebellar

granule cells cultered in the presence of the inhibitory myelin-associated glyocoprotein (MAG) (Gao et al., 2003). Recent studies have identified phospholipase D2 (PLD2) (Watanabe et al., 2004a; Watanabe et al., 2004b) and Nesca (MacDonald et al., 2004), a nuclear envelope adaptor, as critical downstream targets of MEK mediating neurite outgrowth.

However, inhibiting MEK in cultured sensory neurons produced varied effects on neurite sprouting and outgrowth, depending on the type of neurotrophic factor applied. For instance, inhibiting MEK had no effect in the absence of neurotrophins (Liu and Snider, 2001), blocked the effects of NGF, IGF, NT4 and GDNF (Sjogreen et al., 2000; Kimpinski and Mearow, 2001; Wiklund et al., 2002), but enhanced the neurite outgrowth-inducing action of NT3 and neurturin (Wiklund et al., 2002; Althini et al., 2004). Inhibition of MEK also blocked NGF-mediated dendritic growth in sympathetic neurons (Kim et al., 2004). These mixed data question whether results obtained in vitro are the best method for elucidating the effects of MEK in physiological conditions.

Since the failure of central neurons to sprout and regenerate axons successfully is the primary cause of inability to repair following brain or spinal cord injuries, there is an urgent need for in vivo models to assess MEK function. Previous in vivo studies have shown that axonal injury causes a strong and persistent upregulation in the expression and activity of MEK in facial (Kitahara et al., 1994) and hypoglossal (Kiryu et al., 1995) motoneurons. In addition, sciatic nerve axotomy caused an increase in ERK in DRG neurons which could be blocked pharmacologically with the MEK inhibitor UO126 (Obata et al., 2003). Furthermore, pharmacological inhibition of MEK has been shown to enhance axonal outgrowth from retinal ganglion cells into a peripheral nerve transplant (Park et al., 2004), suggesting that in vivo inhibition of MEK may have a pro-regenerative effect.

To determine the function of neuronal MEK and subsequent ERK activity, a new line of transgenic mice was generated wherein dominant-negative MEK1, the upstream activator of ERK1/2, was expressed using the pan-neuronal T-α1 tubulin promoter (Gloster et al., 1994; Bamji and Miller, 1996). The dominant-negative MEK contained a mutation in the ATP-binding domain (K97M) of

human MEK1, rendering it kinase inactive (Mansour et al., 1995). In the current study we have used these mice to explore the effects of MEK inhibition on neuronal cell death, peripheral regeneration, inflammatory response and central axonal sprouting in the facial nucleus following transection of the facial motor nerve and thus building on the themes presented in the preceding chapters.

Materials and Methods

Generation of Tα1:MEKdn transgenic mice

A 1.1-kb Tα1 -tubulin promoter element that confers neuron-specific and pan-neuronal transgene expression (described in detail by Gloster et al., (1994); Bamji and Miller, 1996) was used to drive the expression of a haemagglutinin-11 (HA)-tagged dominant negative (dn) form of MEK bearing a K97M mutation (Mansour et al., 1994).

This mutation is within the ATP binding site, yielding a kinase inactive mutant. The mutant MEK competes with endogenous MEK1 and MEK2 for binding to the activating kinases Raf-1 and B-Raf but cannot itself phosphorylate and activate ERK1 and ERK2. Transgenic mice were acquired from the laboratory of Freda Miller and David Kaplan, Toronto, Canada

Genotyping

Polymerase chain reaction (PCR) analysis of tail DNA was used to confirm the identity of the mice used for this study. DNA was isolated from the mice by phenol chloroform extraction using the DNA Wizard Extraction kit (Promega, UK). Primers were used to amplify the 484bp T-α HA-DN-MEK which were were sense 5'-CAC-CCACCCCCGTTTTCTTTCTTC and antisense 5'-TTCTTCTTCGGCTGCGGGTAGG. The PCR reaction was performed under the following conditions: 5 minutes at 95°C followed by 32 cycles of 30 sec at 94°C, 20 sec at 64°C and 40 sec at 74°C with a final 10 minutes at 72°C. The PCR products were resolved and visualized on a 1% agarose.

Surgical Procedures

Facial nerve axotomy, retrograde tracing and whisker motor assessment

Mutant MEK1dn and wild-type littermate controls 8-10 weeks old were anesthetised using 10ul/g body weight of a 2.5% solution of 2,2,2-tribromoethanol (Avertin, Sigma, UK) dissolved in distilled water. The right facial nerve (including the retro-auricular branch) was cut or crushed at its exit from the stylomastoid foramen. Animals were sacrificed after survival time of 4-30 days with an overdose of Euthatal, perfusion-fixed with 200 ml phosphate-buffered saline (PBS: 10 mM Na_2HPO_4, 0.85% NaCl, pH 7.4) as described in Chapter 2 – Materials and Methods. This was followed by 200 ml of 4% paraformaldehyde in PBS (PFA/PBS), then by a 2 hour immersion of the brainstem in 1% PFA/PBS at 4° C on a rotator (8 rpm), an overnight rotating immersion in a phosphate-buffered sucrose solution (PB: 10 mM Na_2HPO_4, pH 7.4, 4°C; 30% sucrose) and frozen on dry ice.

To assess whisker pad reinnervation, GelFoam (Johnson and Johnson UK) was soaked in 15ul of 4% Fluorogold, dissolved in distilled water. This was applied to the whiskerpad bilaterally 28 days post axotomy. Whisker assessment was performed every other day beginning at day 7 post axotomy until day 27. Whisker movement was scored on a scale of 0.0 (no movement) to 3.0 (normal movement as on the unoperated side) in 0.5 increments (Raivich et al., 2004).

Light microscopic bright-field immunohistochemistry

Twenty-micrometre thick brain stem sections were cut at the level of the facial motor nucleus at -15°C, collected on gelatine-coated slides and stored at -80°C before use. All tissue was processed in exactly the same way with regard to perfusion, fixation, cryoprotection and cutting protocols. Tissue belonging to different experiments were processed at different time points. However, all tissue sections belonging to the same experiment were stained together for the same period of time to prevent differences in the number of counted cells or differences in staining intensity. Standard immunohistochemistry was performed as described in Chapter 2 – Materials and Methods. Absence of primary antibody led to the disappearance of specific immunolabelling. The visualisation of CD3-immunoreactivity with diaminobenzidine/H_2O_2 was performed with Co/Ni

enhancement (0.02% CoCl2 and 0.025% NiCl2 in PB). For HA.11 detection, 40um thin free-floating sections were incubated in 5% goat serum followed by 1:800 polyclonal rabbit anti-HA.11 (Covance, UK) with 0.3% triton-X and 5% goat serum at room temperature overnight, washed in PB incubated with biotinylated goat anti-rabbit secondary antibody, followed by incubation with ABC reagent visualisation with diaminobenzidine/H2O2, mounted on gelatine coated slides, washed in xylene and then mounted with Depex.

Double immunofluorescence

Axonal growth cones in and around the facial motor nuclei were quantified using immunofluorescence against CGRP or galanin, the neuropeptides expressed in axotomized facial motoneurons. A summary of primary, secondary and tertiary antibodies used to characterize the facial sprouts using double labelling with antibodies HA.11 with αMβ2, GFAP or CD3 14 days after facial nerve cut are listed in table 2. Fixed sections were preincubated as in bright field immunohistochemistry. Both primary antibodies were applied overnight at 4°C, washed, incubated with two appropriate secondary antibodies, biotin-conjugated donkey anti-rabbit Ig and FITC-conjugated goat anti-rat Ig (1:100; Alexafluor), washed again and then incubated with a tertiary FITC-conjugated donkey anti-goat antibody (1:100; Alexafluor) and Texas-red Streptavidin (1:1,000; Jackson Laboratories).

Digital micrographs of FITC and Texas red fuorescence was taken using a Leica TCS confocal laser microscope with a 10X objective for quantification and a 25x objective for illustrations, 1024 X 1024 pixel format as described in previous studies (Raivich et al., 1998; Kloss et al., 1999). Consecutive equidistant levels within 30um were recorded and condensed onto a single bitmap using the MaxIntense algorithm.

Regeneration rate in the facial nerve

The facial nerve was crushed with fine jewellers forceps for 30s 1mm distal to the stylomastoid foramen and the animals killed after 96h as described by Werner et al. (2000). Following a brief 5-minute perfusion with PBS and 10-minutes with 4% PFA/PBS, the facial nerve was fixed by a slow 60-minute

perfusion with 1% PFA/PBS, then immediately dissected for a length of 15-20mm and frozen in OCT (Tissue-Tek, UK) on dry ice. Nerves were cut longitudinally and the regenerating axons visualised by immunostaining for galanin and calcitonin gene-related peptide (CGRP). Every fifth section was used per antibody, with an interval of 50µm, and the distance between the most distal labelled growth cone and the crush site were measured using light-microscopic grid scaling. The average distance for each animal was calculated from four or five tissue sections.

Detection and quantification of central axonal sprouting

Axonal growth cones in and around the facial motor nuclei at day 14 (Kloss et al., 1999; Werner et al., 2000; 2001) were detected using immunofluorescence against CGRP or galanin, the neuropeptides expressed in axotomised facial motor neurons, followed by biotinylated goat anti-rabbit secondary antibody (1:100) then with Texas-red Streptavidin (1:1000; Jackson Laboratories, UK). Previous studies using retrograde labelling with Mini-Ruby confirmed that these growth cones were derived from the axotomised motoneurons (Werner et al., 2000; see also Chapter 3). Growth cones were quantified as described in Chapter 2 Materials and Methods.

Neuronal cell counts

Motoneuron cell counts were determined in the axotomised facial nucleus and on the contralateral side 30 days after a right facial nerve cut as described in Chapter 2 – Materials and Methods.

Statistical analysis

Statistical analysis for axonal regeneration distance, neuronal cell counts, whisker motor assessment, leucocyte influx into the injured nerve and microglial staining intensity (RISC) was performed using a standard two-tailed Student's t-test.

Results

Expression of the T-α:DN-MEK construct in facial motor neurons.

Transgenic mice (MEK1dn) were generated as previously described (Shalin et al., 2004; Majdan et al., 1997). Genotyping of offspring was performed using PCR analysis with specific primers as described in Materials and Methods in this Chapter. The 484 base-pair product was observed only with DNA prepared from transgenic animals and not from wild-type littermate controls. To establish whether the transgene was present in the facial nucleus, immunohistochemistry was performed on sections of the brainstem of mice containing facial motoneurons with antibodies to the haemaglutinin-11 tag (HA) tag (figure 5.1A-D). HA immunoreactivity was present in neurons of the facial motor nucleus both intact and following axotomy. In addition, to confirm that transgene expression was localised to neurons and not resident non-neuronal cells, double labelling was performed for the HA-tag together with αMβ2 integrin for microglia (figure 5.1E), GFAP for astrocytes (figure 5.1F) and CD3 for lymphocytes (figure 5.1G). Microglia, astrocytes and CD3 positive lymphocytes (green) were never colocalised with HA-tag immunoreactivity (red), confirming that the transgene is expressed exclusively in neurons. Since previous reports concerning these mutants have shown that levels of p-ERK activity in the cerebral cortex were reduced by 60% compared with control mice (Shalin et al., 2004), levels of p-ERK both in the cortex and in the facial nucleus were investigated. Figure 5.1H shows that compared with wild-type littermates, levels of p-ERK in cerebral cortex and in the facial nucleus of MEK1dn mutants was decreased by 60% and 30% respectively.

Peripheral axonal regeneration, whisker motor recovery, target reinnervation and neuronal survival

Since previous studies have shown that MEK may be involved in peripheral nerve regeneration, we examined the speed of axonal outgrowth using galanin and CGRP neuropeptide markers in the crushed facial nerve 96h after injury. The axonal growth fronts of the regenerating CGRP- or galanin-immunoreactive

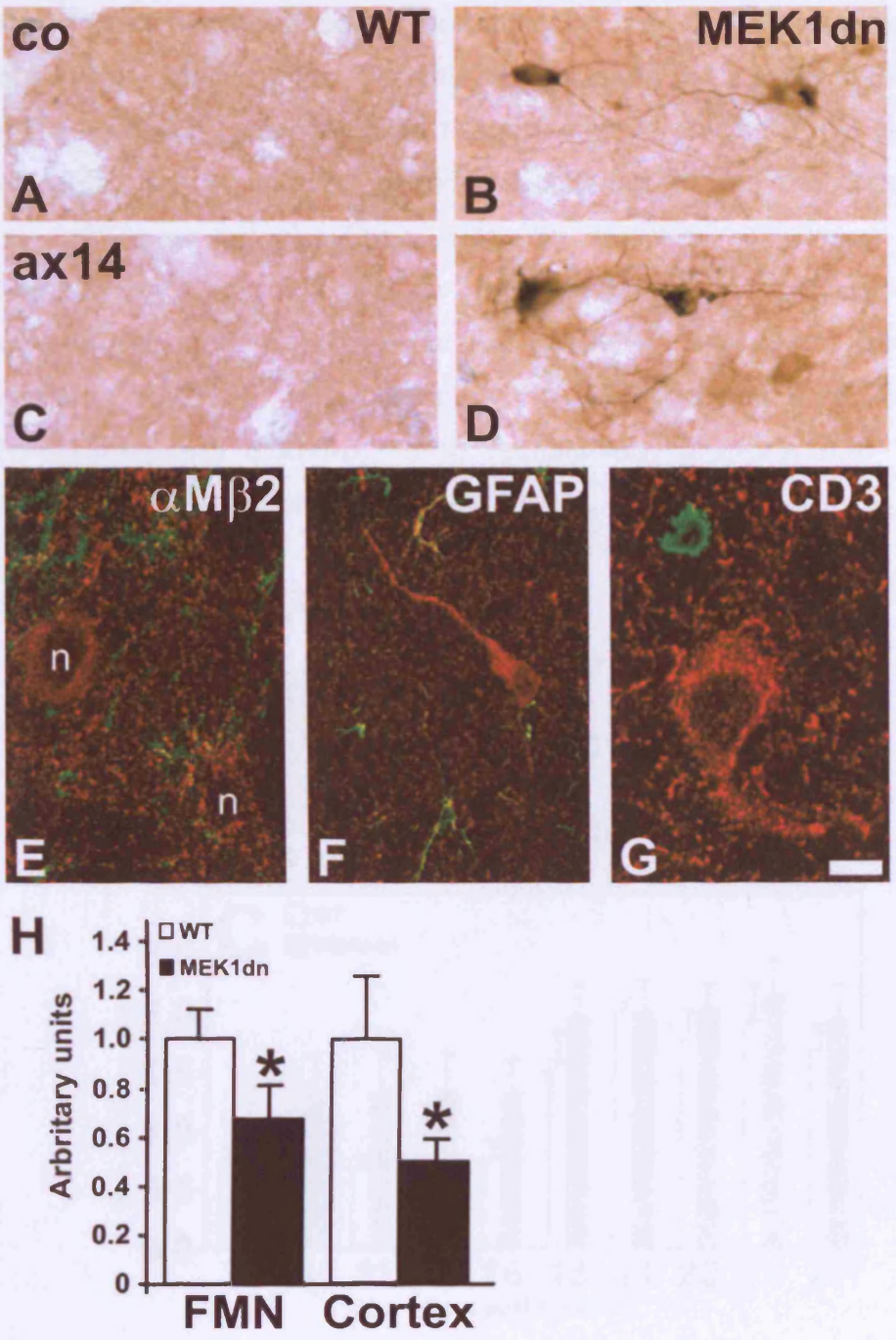

Figure 5.1. Detection of the haemagglutinin-11 (HA.11) tag of the MEK1dn construct in transgenic animals (MEKdn). Absence of HA11 immunostaining in WT mice (A, C) B,D note the constitutive presence of the HA11-immunoreactivity on motoneurons in the uninjured (co) as well as in the axotomized facial motor nuclei, 14 days after axotomy (ax14). Control, wild type animals (WT) show no HA11-immunoreactivity. Absence of HA.11 immunoreactivity in microglia (E), astrocytes (F) and lymphocytes (G) (green) versus HA.11 immunoreactivity present in the neuron (red). (H) Effects of neuronal expression of MEK1dn on facial and cortical levels of phosphorylated ERK1/2, Quantitative changes in wild type (wt) and MEK1dn. Scale bar = 25um in A-D; 10um in E; 5um in F; 20um in G. *$p<0.05$ in Student's t-test.

growth cones were detected in longitudinally cut, fixed 10µm facial nerve sections. The distance from the site of the crush was determined using a calibrated eye piece graticule. Five tissue sections, spaced 50µm apart, were used to determine the mean regeneration distance for each neuropeptide and animal (n=5 per group). There was no statistical difference in mean regeneration distance indicated by galanin neuropeptide immunoreactivity between wild-type and MEK1dn mutants (5.13+/-0.13mm and 5.44+/-0.21mm respectively) or CGRP immunoreactivity in wild-type and MEK1dn mutants (5.02+/-0.20mm and 5.53+/-0.19mm) respectively. p=27.2% and 10.5% for galanin and CGRP respectively (figure 5.2A).

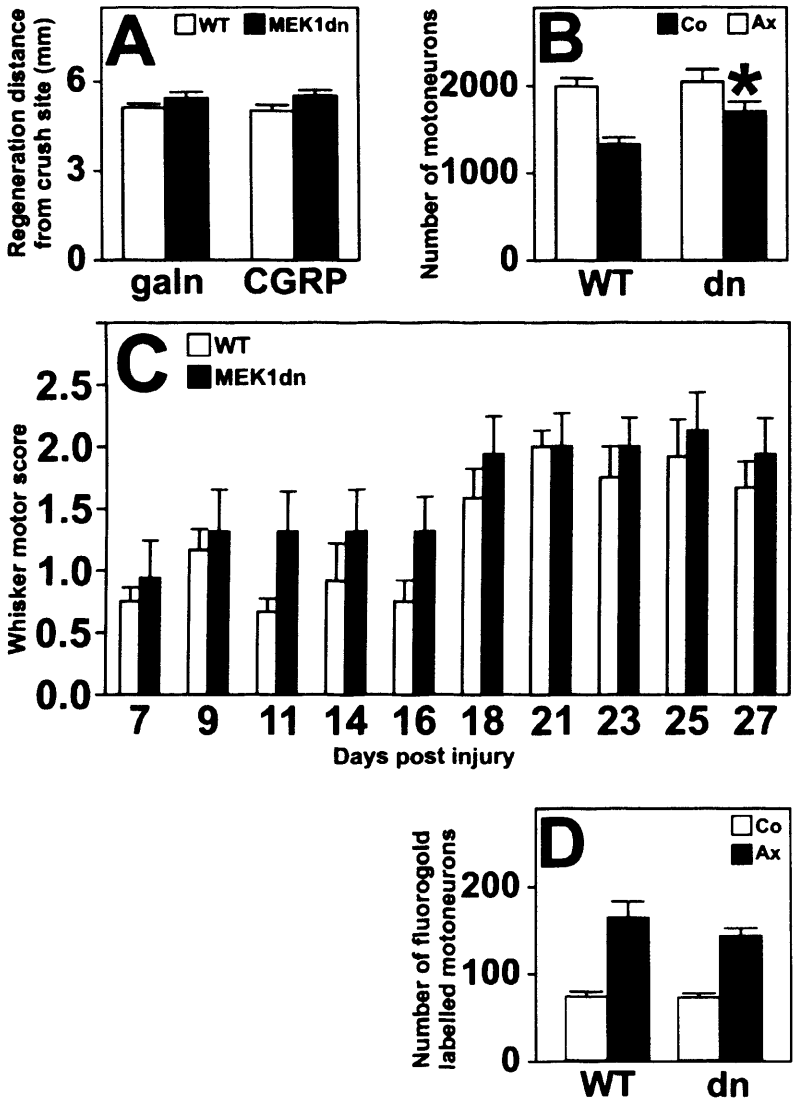

Figure 5.2. A: Inactivation of MEK in neurons using overexpression of MEK1dn reduces neuronal cell death 30 days after facial axotomy in MEK1dn animals compared with wild type (WT) controls (empty bars - contralateral, filled bars - axotomised side, *p<0.01 in Student's t-test, n=8 WT and n=8 MEK1dn mice).

B: Neuronal inactivation of MEK does not affect the maximal distance of axonal regeneration, 4 days after facial nerve crush in either one of the 2 facial motoneurite populations that are immunoreactive for CGRP or galanin (galn). Empty bars - WT, filled –MEK1dn, n= 7 wild-type and 7 MEK1dn animals). **C:** Time course of whisker hair motor performance shows that neuronal inactivation of MEK does not affect the speed of target reinnervation. Functional recovery was measured 7 days following nerve cut on a scale of 0 (no movement) to 3 (normal strong movement as on the unoperated side). n=7 for WT and n=6 for MEK1dn groups. Empty bars - WT, filled bars – MEK1dn. Multiway ANOVA revealed no significant difference between the two groups. **D:** Quantification of retrograde labelling of facial motor neurons (FMN) with fluorogold (FG) performed 30 days following facial nerve cut. Numbers of facial motor neurons is shown for WT and MEK1dn animals. Filled bars - control, empty bars - axotomised. Student's t-test indicated no overall difference in the ratio of motor neurons between WT and MEK1dn mutants.

Facial axotomy leads to a delayed form of neuronal cell death, with a peak at day 14 (Moller et al., 1996; Raivich et al., 2002). A substantial number of neurons die, probably due to failed target reinnervation and subsequent lack of trophic support (Sendtner et al., 1996). To establish whether a reduction in levels of MEK activation affected cell death, neuronal survival in the facial nucleus was examined 30 days post axotomy using Nissl stained sections (figure 5.2B). All neuronal profiles were counted through the entire extent of the facial nucleus on both the control and operated side and corrected for neuronal cell size using the Abercrombie correction coefficient (Abercrombie, 1946). Axotomy led to a loss of 37% of neurons in wild-type mice (2102+/-57 and 1325+/-98 were present on the control and axotomised sides respectively). In the mutant animals there was a dramatic reduction in the extent of neuronal cell death, with only 22% of cells dying (2148+/-21 were present on the intact side compared with 1668+/-143 cells on the axotomised side). ($p<0.05$ in Student's t-test; n=8 animals per group; figure 5.2B).

Whisker vibrissae movement is a good indicator of motor recovery following facial nerve cut and regeneration (Gilad et al., 1996; Raivich et al., 2004). To assess recovery of whisker motor function in MEK1dn mice following facial nerve cut, whisker movement was scored on a scale of 0.0 (no movement) to 3.0 (normal movement as on the uninjured side) as described in Raivich et al. (2004) starting at day 7 up to day 27. There was no statistically significant difference in motor recovery between wild-type and MEK1dn animals. At day 27

wild-type mice scored 1.8+/-0.3 and MEK1dn mice scored 1.7+/-0.2 ($p=0.42$; n=8 wild-type and n=6 MEK1dn animals; figure 5.2C).

To establish the extent of target reinnervation following facial nerve cut, the retrograde tracer fluorogold was applied to the whisker pad 28 days post-axotomy and the fluorogold labelled motoneurons in the facial nucleus were analysed at day 30. There was no difference in target reinnervation between wild-type and MEK1dn groups (figure 5.2D). The total fluorogold labelled motoneuron count was 161+/-18 vs 72+/-6 for uninjured vs injured in wild-type and 140+/-9 vs 71+/-5 for uninjured vs injured in MEK1dn. The ratio of uninjured versus injured was 46.4% vs 51.6% for wild-tye and MEK1dn respectively.

Central axonal sprouting

Since the effects of MEK on neurite outgrowth in vitro and in vivo varies in different experimental models the effects of a reduction in MEK activation on central axonal sprouting was then investigated The right facial nerve was cut and the facial nucleus examined for sprouting neurites 14 days following axotomy since previous studies (Galiano et al., 2001; Werner et al., 2000) and the experiments described in Chapter 3 suggest that the numbers of sprouting neurites peak at day 14. As expected, transection of the facial nerve led to the appearance of neurite growth cones in the axotomised facial nucleus and particularly in the surrounding white matter (figure 5.3). On inspection, it was obvious that sprouting of both CGRP+ and galanin+ growth cones was increased in the mutants. Quantification of the growth cone response revealed that both populations of neuropeptide positive growth cones were substantially increased by the expression of MEK1dn (figure 5.3). Compared with wild-type littermates, galanin immunoreactive growth cones almost 2.2-fold more abundant in the mutants (5044+/-832 and 11161+/-740 for wild-type and MEK1dn respectively). Although galanin positive growth cones were more numerous, the increase in the numbers of CGRP+ growth cones in the mutants was even greater. There was an almost 7-fold increase in CGRP-immunoreactive growth cones compared with wild-types (883+/-68 and 6615+/-746 for wild-type and MEK1dn respectively; $p<0.05$ in Student's t-test; n=6 animals per group).

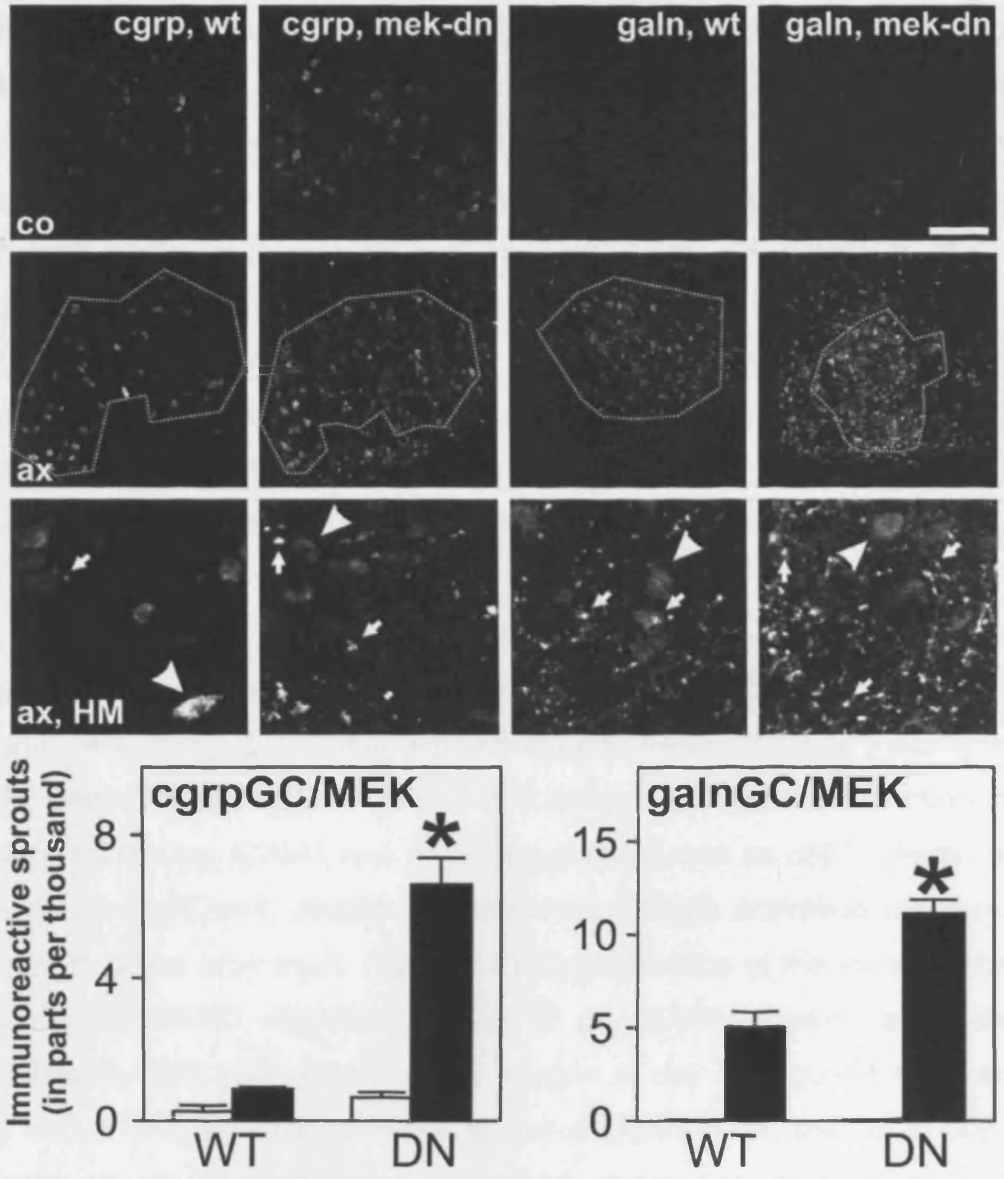

Figure 5.3. Neuronal expression of MEK1dn enhances central axonal sprouting (arrows) from the axotomised facial motor nucleus, 14 days after facial nerve cut (ax), compared with wild type animals (WT). The upper 3 rows show the immunofluorescence, the graphs show the quantitative morphology. Top: the MEK1dn-inducing effect is present in both CGRP (left columns) and galanin (galn, right 2 columns) motoneuron subpopulations, though galanin+ sprouts are more numerous. At high magnification inside facial the nucleus (ax, HM) the immunoreactive motoneuron cell bodies are indicated by arrowheads, the smaller sprouts by arrows. Co: contralateral side. Most neuropeptide immunoreactive sprouts are found in the white matter surrounding the facial nucleus (broken lines on the axotomised side), particularly in the corticobulbar tracts, ventral to the nucleus in the lower part of the figure. Bar scale: 250um in the upper and middle row, 62.5um in the bottom row. Bottom: total area of neuropeptide immunoreactive sprouts (in parts per thousand) n=7 wild type and 7 MEK1dn transgenic mice. Filled bars: axotomised, empty bars: contralateral side, *$p<0.05$ in Student's t-test.

The post-traumatic neuronal cell body and neuroinflammatory responses

Following neuronal injury, morphological changes known as chromatolysis occur in the cell body of the injured neuron, as it switches from a 'transmitting' mode to a 'growth' mode. The chromatolytic response is accompanied by changes in immunoreactivity for the neuronal peptides CGRP and galanin, which both show large increases after nerve injury (Dumoulin et al., 1991; Burazin and Gundlach, 1998; Wynick et al., 2001; Jones et al., 2000). At day 4 after injury there was no difference in galanin or CGRP expression in axotomised motoneurons of mutant animals acompared with wild-type mice (figures 5.5G, 5.5J). At day 14, there was a slight but not statistically significant increase of both neuropeptides in the mutants compared with controls (figures 5.5H, 5.5K)

Peripheral axotomy results in changes not only in neurons but also in non-neuronal cells of neuroepithelial (astrocytes) and haematopoietic (microglia and T cells) origin (Raivich et al., 1999). MEK deficiency caused a reduction in cell adhesion molecules ICAM1 and αMβ2 integrins as well as α6β1 integrin which serve as early (ICAM1, αMβ2) and midphase (α6β1) activation markers that normally increase after injury (figure 5.5). Quantification of the immunolabelling using the MEAN-SD algorithm (Moller et al., 1996), showed a significant, approximately 30% reduction in αMβ2 integrin at day 14 (figure 5.4H-K and 5. 5.5B) with a smaller 20% decrease at day 4 (figure 5.5A; $p<0.05$ in unpaired Student's t-test). The decrease in ICAM-1 expression in MEK1dn animals (figure 5.5I), was not statistically significant. There was a substantial, almost 50% decrease at in α6β1 integrin at day 4 (figure 5.4E-H and 5.5C; $p<0.05$ in unpaired Student's t-test) compared with littermate controls.

The late phagocytosis-associated microglial marker (αXβ2) was examined 14 days after facial axotomy, a time point normally coinciding with a peak of neuronal cell death (Möller et al., 1996). Quantification of αXβ2-immunoreactive nodules showed a reduction in MEK1dn mice, which was not statistically significant compared with littermate controls (figure 5.5L). Astroglial response was unaffected by inhibition of MEK at day 4 or day 14 (figures 5.4A-D and 5.5G, 5.5H).

The inhibition of MEK affected leukocyte influx at both day 4 and 14. While the reduction in CD3+ cells at these time points was not statistically significant, the decrease was approximately 50% at each time point (figure 5.5D, 5.5E).

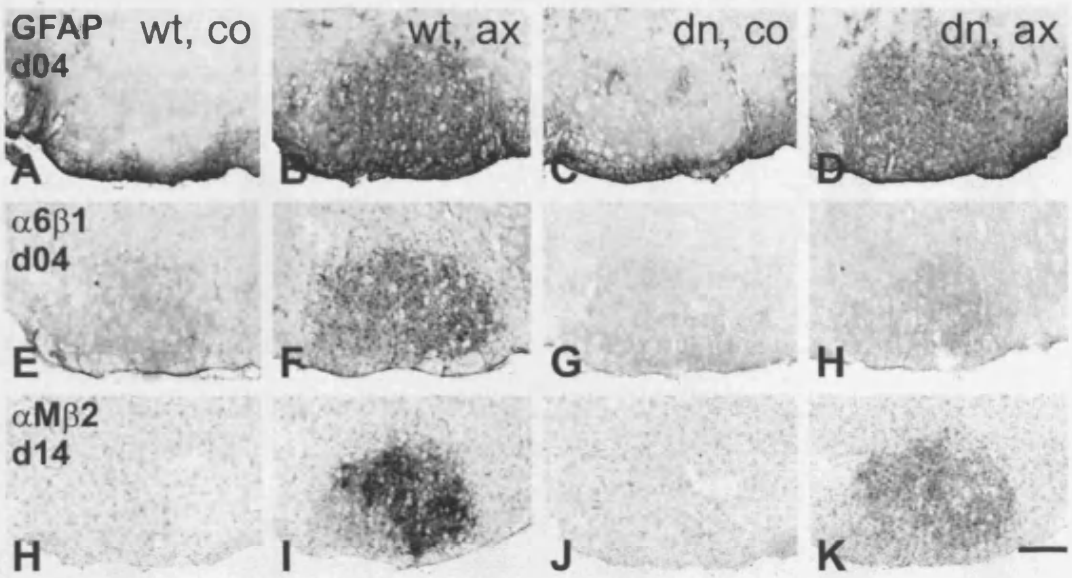

Figure 5.4. Neuronal MEK inhibition affects the glial response. Top row: astrocyte GFAP-immunoreactivity shows normal upregulation after axotomy (day 4), but no change due to MEK1dn. Middle and bottom row: Microglial activation detected with antibodies against α6β1 integrin (day 4) and αMβ2 integrin (day 14). In both cases, microglial activation is severely reduced in animals lacking neuronal MEK activity. Scale bar: 200um

Discussion

The data concerning the role MEK in neuronal survival and axonal regrowth in vitro is confusing. Moreover, the little in vivo evidence for a regeneration-pointing role of MEK is opposed by studies which show a regeneration-inhibitory role for this ubiquitous intermediate messenger. The aim of this study was to establish a definitive role of MEK in peripheral axonal regeneration and central axonal sprouting using the facial nerve axotomy model. By means of a dominant-negative MEK construct under the control of the T-α-tubulin promoter we first showed that the HA-tagged MEK1dn construct was localised within motoneurons of the facial nucleus and confirmed the absence of the construct in other non-neuronal cells of the nervous system including microglia, astrocytes and lymphocytes.

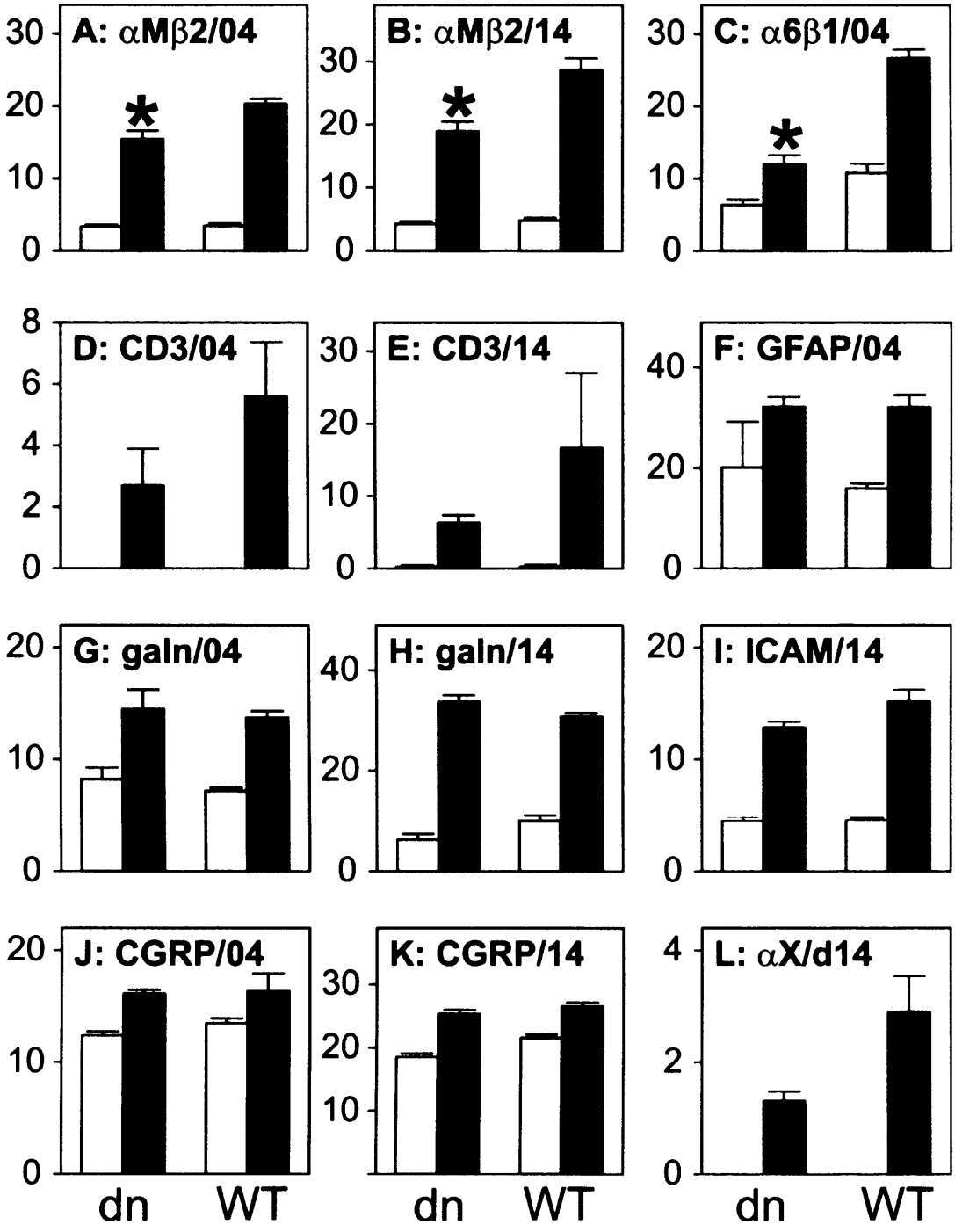

Figure 5.5. Quantitation of neuronal and non-neuronal response to axotomy at day 4 and 14. Facial motor nucleus immunoreactivity in A-C and F-K was quantified using the MEAN+SD algorithm as described in Materials and Methods. D, E and L show the numbers of lymphocytes or microglial nodules respectively. Neuronal expression of MEK1dn causes a significant reduction in microglial activation markers αMβ2 integrin (B) and α6β1 integrin (C), and also, a decreased influx of the CD3+ T-cells (D, E). However, it does not affect the induction of neuronal peptides or GFAP immunoreactivity. *$p<0.05$ using Student's t-test.

Furthermore, it was shown that resting levels of p-ERK activity, the downstream messenger of MEK1, in the facial nucleus were reduced by approximately 30% in the mutants confirming a reduction in the activity of MEK. Furthermore, peripheral facial nerve injury resulted in a 37% reduction in neuronal cell death of facial motoneurons after injury in MEK1dn animals compared with wild-type sibling controls. Inhibition of MEK also caused a clear reduction in early and late microglial activation and T-cell recruitment, which appeared secondary to neuronal cell death. Interestingly, mutant animals also revealed a striking dichotomy in the central and peripheral pattern of axonal outgrowth having normal speed of regeneration in the facial nerve, but a substantial increase in the central sprouting of motor nerve fibres in the facial nucleus. Both populations of fibres, galanin- as well as CGRP-immunoreactive ones were affected, but the increase was particularly striking in the CGRP-immunoreactive fibres, that normally show very little sprouting. Hence, a key role of MEK in controlling neuronal cell death, inflammation and central axonal sprouting in vivo was demonstrated.

Levels of the downstream messenger p-ERK were measured in both cerebral cortex and the facial nucleus. Cortical p-ERK levels in the mutants was decreased by 60% which is in line with previously reported data in these animals (Shalin et al., 2004). The 30% reduction in levels of p-ERK in the facial nucleus of MEK1dn mutants is indeed modest, but this decline was presumably enough to produce a robust response in terms of better neuronal survival, decreased post-traumatic inflammation and increased central axonal sprouting. Earlier attempts at creating knockout lines in the Ras/Raf/MEK/ERK pathway have resulted in embryonic or early postnatal lethality (Kolch, 2005). Indeed the partially inactivated mutants used in this study show normal development and growth, suggesting that residual levels of ERK1/2 may be enough to sustain development and growth (Shalin et al., 2004). Interestingly, recent reports using U0126, the pharmacological inhibitor of MEK, shows that incomplete inhibition of MEK has a neuroprotective and pro-regenerative effect on retinal ganglion cells (Luo et al., 2007), suggesting that partially removing the action of MEK provides the most benefit to axonal regrowth and neuronal survival.

Effects of MEK on neuronal survival

Neuronal survival following axonal injury is essential for the nerve to initiate and execute a regenerative program. The results presented here show that inhibition of MEK in vivo produces a robust enhancement in survival of facial motoneurons following facial nerve cut. In support of this, some in vitro reports also sustain the notion that inhibition of MEK is pro-survival and pro-regenerative. For example, a degenerative effect of MEK in cortical cultures treated with NT-4 were subsequently rescued with the addition the MEK inhibitors U0126 or PD98059 (Lobner and Liot, 2004). Moreover, substance P induced activation of MAPK in rat striatal cultures resulted in non-apoptotic programmed cell death (Castro-Obregon et al., 2004); inhibition of ERK with the inhibitor PD98059 prevented Zn^2+ induced death of PC12 cells (Seo et al., 2001); and ERK has been shown as an important executor of neuronal damage in cultured cerebellar granule cells following potassium withdrawal (Subramaniam et al., 2004).

However, there are several reports suggesting that activation of MEK, and subsequent downstream products, promote neuronal survival in vitro. For example, PACAP-38 induced the activation of ERK to rescue cerebellar granule cells from apoptosis (Journot et al., 1998) and activation of Gab1 stimulates NGF-independent survival of PC12 cells via the MEK pathway (Korhonen et al., 1999).

In vivo studies looking at the role of MEK in neuronal survival have been executed using the pharmacological inhibitors U0126 and PD98059. One study (Klocker et al., 2000) reported that BDNF induced activation of ERK produced neuroprotection of rat retinal ganglion cells. On the other hand Park et al. (2004) showed that MEK antagonist PD98059 reduced p-ERK activity and enhanced survival of retinal ganglion cells. Nevertheless one should bear in mind that while extremely useful, these inhibitors are not entirely specific for MEK1/2.

The strong decrease in microglial αMβ2 integrin at both early and late stages following facial nerve axotomy suggests that dampening the broader inflammatory response may have contributed to the neuronal survival observed here. The appearance of αXβ2 integrin and B7.2 positive immunoreactive microglial nodules has previously been correlated with the extent of neuronal cell death (Raivich et al., 2002). Whilst substantial reductions in these two

specific markers were evident in the MEK1dn mutants, they were not statistically significant because of the high interanimal variability. Since the MEK1dn construct is not expressed in microglia or CD3+ infiltrating cells the reduction in microglial homing and activation suggests that MEK related signals from the neuron dampen the microglial response and the impairment of microglial activation and T-cell recruitment is secondary to a function of MEK in neurons.

Elucidating a mechanism for the way in which the lack of MEK promotes cell survival is difficult. ERK has been shown to phosphorylate synapsin I, a major phosphoprotein found in synaptic nerve terminals (Jovanovic et al., 1996; Matsubara et al., 1996). Synapsin I maintains synaptic vesicles and phosphorylation of this protein may lead to the release of excitotoxic amino acids such as glutamate (Alessandrini et al., 1999). Thus MEK1dn may exert its effect by inhibiting the release of excitotoxic amino acids and preventing cell death; which, incidentally is a desirable hypothesis since it has recently been suggested that ERK is a predominant inducer of a non-apoptotic mode of neuronal cell death (Subramaniam and Unsicker, 2006).

The activation of regulatory transcription factors such as c-fos by MEK is plausible. c-fos has been shown to be associated with regulation of excitability and neuronal survival and was shown to up-regulated in the cortex of mice following administration of PD98059 (Zhang et al., 2002). Overall, the data presented here provide the first evidence of enhanced neuronal survival in mutants with a genetic, not pharmacological reduction in MEK function, establishing a mechanism for how this occurs remains to be elucidated.

MEK1dn enhances central sprouting but does not affect peripheral outgrowth, whisker motor recovery or target reinnervation

The central sprouting response shown here is similar to previous studies which sprouting in the facial nucleus following peripheral facial nerve cut (Werner et al., 2000, Galiano et al., 2001). Moreover, the detailed time-course and molecular characterisation of the sprouting response in the facial nucleus in Chapter 3 of this thesis shows that sprouting neurites in the facial nucleus peak at day 14, and are influenced by neuroinflammatory signals. The massive

increase in central sprouting in mutants with reduced levels of MEK could be due to a fall in the inflammatory or cytokine mediated response. Selectively blocking MEK with pharmacological inhibitors such as U0126 or PD98059 have been shown to prevent the synthesis and release of cytokines such as interleukin-6 (Dukic-Stefanovic et al., 2003), IL-8 (Vitiello et al., 2004) or TNFα both in vitro (Wang et al., 2004) and in vivo (van der Bruggen et al., 1999). Secondary to cytokine activity, inflammation in the CNS results in the activation of microglia. The 30% lower levels of activity of αMβ2 integrin positive microglia in MEK1dn mice may have contributed to the enhanced neurite response. Indeed, as investigated in Chapter 3, enhanced inflammation induced with LPS does have a detrimental effect on sprouting in the facial nucleus. In addition, enhanced neural inflammation in TGFβ null mice is associated with a decrease in the sprouting response (Makwana et al., 2007; Chapter 6). Similarly, attenuated inflammation and enhanced sprouting have been reported in IL-6 deficient mice (Galiano et al., 2001).

Studies in various mutants where neuronal cell death in the facial nucleus was altered failed to show a linear correlation with central sprouting (Chapter 3). However, while the additional 22% survival observed in these mutants may not account for the 2.2-fold better sprouting effect that was seen, it may have contributed to it.

The absence of a correlation between central axonal sprouting and peripheral regeneration observed in these mutants is not uncommon. For example, both IL-6 null (Galiano et al., 2001) and α7 null (Chapter 3) mice show enhanced sprouting in the facial nucleus and c-jun deficient animals show reduced brain sprouting (Chapter 3); all three groups of mutant mice show a significant reduction in the speed of peripheral outgrowth (Zhong et al., 1999; Werner et al., 2000; Galiano et al., 2001; Raivich et al., 2004). The absence of an effect of MEK1dn on peripheral outgrowth, functional whisker motor score and target reinnervation strengthens the argument that that intracellular signalling promoting central and peripheral neurite outgrowth may occur largely through independent mechanisms.

One of the limitations of the current study is that it does not distinguish which of the two neuronal targets of MEK, (ERK1 or ERK2) are involved in the robust

central sprouting response that is observed. Indeed, the fact that MEK1 has two targets is the most likely explanation as to why so many studies on MEK function have such diverse conclusions. One approach to clarify this issue is to use isoform specific knock-out mouse lines. Indeed two groups have generated ERK1-selective KO mice (Selcher et al., 2001; Mazzucchelli et al., 2002) and ERK2-selective KO mice are currently under preliminary investigation in this laboratory. Certainly, global ERK1 or ERK2 KO mice would provide evidence of which isoform was involved; however, motoneuron specific excision, for instance using a cre-LoxP system under a synapsin promoter would be far more desirable and would provide more conclusive evidence. Resolution of whether it is ERK1 or ERK2 which contributes to the sprouting response that we observe in the facial nucleus remains to be seen. Nevertheless, the enhanced sprouting observed in the facial nucleus in this study is promising and warrants further investigation in a model where central sprouting might be a crucial mechanism to regain lost motor and or sensory control following central nervous system injury. With this in mind, these studies were extended into the spinal cord and is the focus of Chapter 7 of this thesis.

Overall, these data point to a critical role of MEK in promoting post-traumatic neuronal cell death, in neuroimmune surveillance and in the inhibition of central axonal sprouting.

CHAPTER 6

Endogenous TGFβ1 suppresses inflammation and promotes survival in the adult CNS

Introduction

Neuroglial activation is a hallmark of central nervous system (CNS) injury, accompanying almost all neuropathologies and experimental brain lesions (Bignami, 1984; Graeber and Kreutzberg, 1988; Perry and Gordon, 1988). Upon injury, activated microglia rapidly proliferate (Raivich et al., 1994), migrate to the affected site and adhere to the injured neurons (Kalla et al, 2001), displacing the neurite terminals in a process known as synaptic stripping (Blinzinger and Kreutzberg, 1968; Trapp et al., 2007). Following synaptic stripping, the microglia gradually migrate into the nearby parenchyma, where they appear to downregulate their cellular markers and decrease in number (Jones et al., 1997). Parallel to the microglial activation, reactive astrocytes show a rapid increase in signaling receptors, neurotrophins, growth factors and extracellular matrix proteins, all of which play an important regulatory role in the repair and regeneration process (Eddleston and Mucke, 1993). Although several key molecules like MCSF and IL-6 have been identified for their role in the activation of microglia and astrocytes after neural injury (Raivich et al., 1994; Klein et al., 1997; Kalla et al., 2001; Galiano et al., 2001), little is known about the endogenous signals involved in the downregulation of these glial cells after injury, as well as for their persistently downregulated state in the uninjured CNS. One candidate molecule here is the immunosuppressive cytokine, Transforming Growth Factor β 1 (TGFβ1).

TGFβ1 is a potent, pleiotrophic cytokine, involved in several biological processes affecting growth and differentiation (Massague, 1990; Roberts and Sporn, 1991; Bommireddy and Doetschman, 2004). In the CNS, TGFβ1 has been shown to promote the survival of embryonic, neonatal adult neurons (Martinou et al. 1990, Oppenheim et al., 1993; Boche et al., 2003; Schober et al., 2007), assist in neurite outgrowth (Abe et al. 1996; Ishihara et al. 1994), protect against experimental allergic encephalomyelitis (Johns and Sriram, 1993; Racke et al. 1991; Santambrogio et al. 1993) and inhibit microglial and astrocyte proliferation (Lindholm et al. 1992; Vergeli et al. 1995). Studies using

ramified microglia grown on an astrocyte monolayer also demonstrated the strong inhibitory effect of TGFβ1 on microglial proliferation (Jones et al., 1998), agreeing with reports *in vivo* which suggest that TGFβ1 is responsible for the downregulation of the microglial response following injury (Kiefer et al. 1993b; Morgan et al. 1993).

Intraventricular infusion of TGFβ1 has been shown to potentiate aspects of glial scar formation following a cortical stab injury (Logan et al., 1994). Antibodies against TGFβ1 and TGFβ2 have been shown to decrease glial scar formation in injured nigrostriatal tract (Moon and Fawcett, 2001). Although TGFβ1 levels are strongly and rapidly upregulated after different forms of injury like cortical incision, entorhinal lesion, ischemia, experimental allergic neuritis (EAN) or peripheral axotomy (Nichols et al., 1991; Klempt et al., 1992; Kiefer et al., 1993a,b; Logan et al., 1994), TGFβ1 is also present in moderately high levels even in the normal, uninjured adult brain (Lindholm et al., 1992), and could thus be involved in mediating the persistent downregulation of microglia and astrocytes in the absence of injury. To elucidate the function of endogenous TGFβ1 in the CNS, we examined the effects of TGFβ1-deficiency on the unlesioned adult brain, and then extended these studies to an experimental model of CNS trauma and functional repair in the axotomized mouse facial motor nucleus.

Materials and Methods

Animals

Wildtype (TGFβ1+/+) and homozygous TGFβ1-deficient (TGFβ1-/-) adult mice (2 months old) were obtained from the laboratory of T Doetschman and maintained on the RAG2 null immunodeficient background to prevent lethal postnatal autoimmune inflammatory disease in the absence of TGFβ1 (Shull et al., 1992; Diebold et al., 1995). The animals were bred on a mixed 129S6 x CF-1 strain to avoid the severe embryonic lethality we and others observed in the TGFβ1 null phenotype, preventing analysis in the adult mice (Kallapur et al., 1999; Brionne et al., 2003). Both control +/+ mice and the -/- littermates were generated as the F1 generation of crossing TGFβ1+/- animals. For genomic

screening, a short piece from the tail of 2 week old mice was incubated at 56°C overnight in proteinase K lysis buffer (100ug/ml, Boehringer Mannheim). The lysate was treated with phenol-choloroform and the genomic DNA was precipitated out of solution with isopropanol, washed and redissolved in 200 ul of bi-distilled water. Polymerase Chain Reaction (PCR) was then used to detect the neomycin cassette (Diebold et al., 1995), using 0.5 µl genomic DNA template from the reverse transcription reaction, 1X PCR buffer (Eurobio, Raunheim, Germany), 3.0 mM MgCl2, 200 µM dNTPs (Pharmacia, Freiburg, Germany), 1.0 units taq polymerase (Eurobio) and 10 pmol of the sense primer: (TGFβS1) 5'-GAG AAG AAC TGC TGT GTG CG-3' and 10 pmol of the antisense primer: (TGFβAS1) 5'-GTG TCC AGG CTC CAA ATA TAG G-3'. A second PCR specific to the neomycin insert was performed to confirm the genotyping of the first PCR using the sense primer (NeoS1) 5'-GCC GAG AAA GTA TCC ATC AT-3' and the antisense primer: (TGFβAS1). PCR was performed on a Biometra Thermoblock and was initiated with a hot start using an initial denaturing temperature of 94°C for 5 minutes, and in the subsequent cycles for 45 seconds, an annealing temperature of 56°C for 50 seconds and an extension temperature of 72°C for 1 minute for a total of 35 cycles, with a final extension for 10 minutes at 72°C and then cooling to 4°C. PCR products were analyzed using 1.5 % agarose gels, stained with ethidium bromide and photographed.

Surgical Procedures and Tissue Treatment

The right facial nerve was cut or crushed under 2,2,2-tribromoethanol (Avertin) anesthesia at the level of the stylomastoid foramen. The animals were sacrificed in ether or Euthatal after 0-28 days. For PCR, the brainstem was removed immediately following sacrifice and frozen on dry ice. For light microscopy, animals were perfused with 200 ml of phosphate-buffered saline (PBS: 10 mM Na_2HPO_4, 0.85% NaCl, pH 7.4) as described in Chapter 2 – Materials and Methods. This was followed by 200 ml of 4% paraformaldehyde in PBS (PFA/PBS), then by a 2 hour immersion of the brainstem in 1% PFA/PBS at 4° C on a rotator (8 rpm), an overnight rotating immersion in a phosphate-buffered sucrose solution (PB: 10 mM Na_2HPO_4, pH 7.4, 4°C; 30% sucrose) and freezing on dry ice.

Regeneration, functional recovery and central axonal sprouting

To determine the speed of facial axonal regeneration, the facial nerve was crushed with a fine jeweller's forceps for 30 seconds 1 mm distal to the stylomastoid foramen. The animals were sacrificed after 96 hours as described by Werner et al (2000). Following a brief, 5 min perfusion with PBS, and 5 min with 4% PFA/PBS, the facial nerve was fixed by a slow, 60 min perfusion with 1% PFA/PBS, then immediately dissected for a length of 15-20 mm and frozen on dry ice. Nerves were cut longitudinally and the regenerating axons visualized by immunostaining for galanin or for calcitonin gene-related peptide (CGRP). Every fifth section was used per antibody, with an interval of 50 µm, and the distance between the most distal labeled growth cone and the crush site measured using light microscopic grid scaling. The average distance for each animal was calculated from 4-5 tissue sections.

Functional recovery in the whisker hair movement model was assessed after facial nerve cut. Whisker movement was determined during the 28 day post-operative period and scored on a 3 point scale (0 - no movement to 3 - completely normal movement) by blinded observers (Raivich et al., 2004).

Axonal growth cones in and around the facial motor nuclei at day 14 (Kloss et al., 1999; Werner et al., 1999) were detected using standard immunohistochemistry against galanin, the neuropeptide-positive population that normally shows strong sprouting in this axotomy model, with a peak at 2 weeks after injury. Previous studies using retrograde labeling with Mini-Ruby confirmed that these growth cones were derived from axotomized motoneurons (Werner et al., 1999). Quantification of growth cones was performed by blinded observers on 2 sections per facial nucleus, with an interval of 350 µm between each section.

Light Microscopic Immunohistochemistry (LM-IHC).

Standard light microscopic immunohistochemistry was performed as described in Chapter 2 Materials and Methods. The antibody specificity controls for the TGFβ RII antibody were performed by incubating the antibody with the TGFβ

RII control peptide (sc-400-p; Santa Cruz) for one hour at room temperature before applying the mixture on the tissue sections.

Immunofluorescence Double-Labeling, Confocal Microscopy and Quantification

For immunofluorescence double-labeling, the sections were simultaneously incubated with two primary antibodies - a monoclonal rodent antibody from rat or hamster, and a polyclonal antibody from rabbit overnight, as for immunohistochemistry (see above and Table 2). The sections were then incubated with two secondary antibodies, FITC-conjugated goat anti-rat Ig and biotin-conjugated donkey anti-rabbit Ig for 1h at room temperature and then incubated with a tertiary FITC-conjugated donkey anti-goat antibody and Texas Red-Avidin (Dianova) for 2 hours. After final washing, the sections were covered with VectaShield (Vector) and stored in the dark at 4°C for further use.

To record the immunofluorescence double-labeling, digital micrographs (1024 x 1024 pixels, 8 bit gray scale) of FITC and TexasRed fluorescence were taken with a 10 x objective (pinhole 30) in a Leica TCS 4D confocal laser microscope and represent areas of 1 mm x 1 mm. The immunofluorescence was detected using low ArKr laser power (0.3 V). Ten consecutive, equidistant levels were taken per section (total vertical span 30 µm), condensed to a 1 Mbyte TIFF.file for each fluorescence wavelength using the MaxIntens condensation algorithm (which picks the maximum intensity value for each pixel from the 10 available levels) and stored on a magneto-optical disk. To extract spontaneous autofluorescence from the total fluorescence recorded in the FITC- and TexasRed (TR)-channels, an additional cyanin 5 (Cy5) bitmap was recorded using maximal laser power (3.0V), an excitation wavelength of 647 nm and maximal detector voltage with a LP665 filter, and then treated the same way as the FITC and Texas Red bitmaps.

For further processing the three corresponding bitmaps per facial nucleus (FITC, Texas Red, Cy5) were transferred to OPTIMAS 6 and corrected images were obtained by subtracting the autofluorescence from the FITC and TexasRed images. Then linear extraction coefficients for the FITC-bitmap were determined by delineating highly autofluorescent structures in the Cy5-bitmap with a threshold of Mean+5*SD, these profiles were transferred to the FITC-

bitmap, and a quotient calculated, with the difference between the mean Optical Luminosity Value (OLV; grayscale 0-255) of the pixels delineated by these profiles and the overall mean OLV in the FITC bitmap in the numerator, and the difference between the corresponding means of the Cy5-bitmap in the denominator. The corrected FITC images were obtained by subtracting from the OLV of each pixel in the original FITC bitmap the product of the OLV of the corresponding pixel in the Cy5-bitmap and the linear extraction coefficient for FITC. Corrected Texas Red-images were obtained accordingly and then used for quantification.

To quantify the microglial immunoreactivity for the early (αMβ2 integrin, ICAM1), midphase (α6β1) and phagocytic (αXβ2, B7.2) markers, the digital micrographs were processed using the Relative Intensity of Staining Coefficient (RISC) algorithm as described in Werner et al. (1998). Cellular profiles were delineated in the Texas Red-image of IBA1-immunoreactivity using a Mean + 1.5 * SD threshold. The profiles were transferred to the bitmap of the counterpart fluorescence for the antibodies listed above and the Relative Intensity of Staining Coefficient for microglia in the facial nucleus (RISCmicr) was determined according to the following formula:

RISCmicr = log (1+(OLVmicr-OLVfac)/OLVout),

with OLVmicr the mean Optical Luminosity Value (OLV) for the microglial profiles in the facial nucleus, OLVfac the OLV for the whole facial nucleus and OLVout for the tissue outside the facial nucleus. This mean RISC was calculated for the axotomized and for the contralateral, unoperated facial motor nucleus within each animal group (n = 3-7) and the statistical significance between the TGFβ1+/+ and TGFβ1-/- mice was tested at a 5% level using an unpaired Student's t-test.

Quantification of Cell Numbers

Neurons.

The brain tissue was postfixed for 2 days in 4% buffered paraformaldehyde, cut in a cryostat at -15°C, and the 25µm frontal tissue sections collected throughout both facial nuclei (axotomized and contralateral) and stained with Toluidine blue

(Nissl). Neuronal cell counts were corrected for neuronal cell body size using the Abercrombie correction (see Chapter 2 – Materials and Methods).

Proliferating Cells.

To quantitate cell proliferation (2 and 3 days after axotomy), the animals were injected with 200 µCi of [^{3}H]-thymidine (NEN) 2 hours before sacrifice, perfusion fixed and cut as previously described (Raivich et al., 1994). The sections were treated with an ascending alcohol dilution series (70%, 90%, 95%, 100% ethanol, 100% isopropanol) and xylene, rehydrated with a descending alcohol dilution series to water and allowed to dry overnight, dipped in NTB2 photoemulsion (diluted with equal volume distilled water), exposed for 3 weeks at 4°C, developed with D-19 developer (Eastman Kodak) for 2 minutes, rinsed in water for 1 minute, fixed in tetanal fixative (Eastman Kodak) for 4 minutes, rinsed in water and then allowed to dry. The labeled cells were counted for the whole facial motor nucleus (6 sections per animal, n=7).

Microglia and Astrocytes.

The facial motor nucleus sections (two 20µm sections per animal, spaced 360um apart; n = 4-8) were segmented into 6 subsections of a 0.032 mm^2 size; cell counts of GFAP-positive astrocytes or nucleated αMβ2-positive microglia within each subsection were converted to cells/mm^2. Cell counts were made individually for the operated as well as the unoperated side. To determine whether microglia was the only cell type undergoing proliferation (Graeber et al. 1988), immunohistochemistry using αMβ2 or GFAP antibodies was performed on tissue sections from animals injected with [^{3}H]-thymidine, followed by treatment with alcohol, drying and autoradiography, as described in the preceding paragraph.

In situ hybridization (ISH) for TGFβ1 , TGFβ Receptor Type 1 (R1) and type 2 (R2) mRNAs

In situ hybridization was performed by Dr Heike Heuer.

Probe synthesis

A cDNA fragment corresponding to nts 298-1233 of mouse TGFβ1 (GenBank accession code NM_011577), nts 1539-2651 of mouse TGFβ Receptor Type 1 (R1) (GenBank accession code NM_009370) and nts 2447-3244 of mouse TGFβ Receptor type 2 (R2) (GenBank accession code D32072) were generated by PCR and subcloned into the pGEM-T easy vector (Promega). [^{35}S]-labeled riboprobes in sense and antisense direction were produced by in vitro transcription as described previously (Heuer et al., 2000). After synthesis, the probes were subjected to mild alkaline hydrolysis to generate fragments of about 250 nucleotides.

Combined Immunohistochemistry (IHC) and in situ hybridization (ISH): For colocalization experiments, cryosections were first stained with the monoclonal antibody against the microglial marker αMβ2 integrin followed by incubation with a biotinylated secondary antibody and ABC complex (Vector laboratories) as described above. To prevent RNA degradation, all incubation steps were carried out in the presence of 10U/ml RNase Inhibitor (Ambion). Following the peroxidase staining reaction with DAB/H_2O_2, the respective transcripts were localized by ISH as described by Friedrichsen et al. (2005). Briefly, the sections were fixed again with 4% paraformaldehyde solution (FA) in phosphate buffered saline (PBS) for 1 hour at room temperature (RT) and treated with 0.4% Triton in PBS followed by an acetylation step. After dehydration, sections were covered with hybridization mix containing radioactive cRNA probes diluted in hybridization buffer (50% formamide, 10% dextran sulfate, 0.6M NaCl, 10mM Tris/HCl pH 7.4, 1x Denhardt's solution, 100µg/ml sonicated salmon-sperm DNA, 1mM Na_2EDTA and 10 mM dithiothreitol) to a final concentration of $5x10^4$ cpm/µl. After incubation at 58°C for 16 hours, coverslips were removed in 2x standard saline citrate (SSC; 0.3M NaCl, 0.03M sodium citrate, pH 7.0). The sections were then treated with RNase A (20µg/ml) and RNase T1 (1U/ml) at 37°C for 30 min. Successive washes followed at RT in 1x, 0.5x and 0.2x SSC for 20 min each and in 0.2x SSC at 70° for 1h. The tissue was dehydrated and exposed to X-ray film (BioMax MR, Kodak) for 68 hours. For microscopic analysis, sections were dipped in Kodak NTB2 nuclear emulsion and stored at 4°C for 2 weeks. Autoradiograms were developed, stained with cresyl violet and

viewed under dark- and bright-field illuminations using an Olympus AX microscope.

Results

TGFβ1 deficiency causes gliosis throughout the adult brain

To determine the effects of TGF β1 deletion on the adult CNS, wild type (TGFβ1+/+) and homozygous deficient (TGFβ1-/-) litter mates were generated as F1 generation crossing of the TGFβ1 +/- parent animals. To prevent lethal autoimmune inflammation normally occurring 2-3 weeks after birth (Diebold et al., 1995, Bommireddy and Doetschman al., 2004), all animals were maintained on the RAG2 null immunodeficient, background (Engle et al., 1999). In spite of this background, homozygous deletion of TGFβ1 caused pronounced, consistent and very similar gliotic changes throughout the CNS, affecting astrocytes, microglia and perivascular macrophages.

Astrocytes.

TGFβ1-deficiency mediated changes were already apparent at low magnification using astrocyte immunoreactivity (IR) for glial fibrillary acidic protein or GFAP-IR (compare figures 6.1A, E for TGFβ1+/+ and figures 6.1B,F for TGFβ1-/-, respectively). In the TGFβ1+/+ control animals, GFAP-IR is confined to the stellar astrocytes in the white matter, around meninges, ventricles and large blood vessels (figure 6.1A, E) and a few grey matter regions such as hippocampus (figure 6.1A) and cerebellum (not shown). Protoplasmic astrocytes in most grey matter regions displayed very little to no GFAP-IR, as shown for example at higher magnification for the spinal nucleus of the trigeminal nerve (SNTN) in the brainstem in figure 6.1I. In contrast, the TGFβ1-/- mice showed a general increase in GFAP-IR, in the deep and superficial layers of the dorsal cerebral cortex, throughout the ventral cortex, basal ganglia, reticular thalamic nucleus (figure 6.1B) and most parts of the brain stem (figure 6.1F). Figure 6.1J shows the extensive fibrillary as well as diffuse GFAP-IR in the TGFβ1-/- SCID SNTN at higher magnification.

Similar results were observed for the cell adhesion molecule CD44 (figure 6.1M, N), which is almost completely absent from most grey matter regions of the

normal, TGFβ1 +/+ animals. In the TGFβ1-/- mice, CD44-IR was present throughout, labeling protoplasmic astrocytes as well as ameboid, microglia-like cells. Follow-up experiments using double-labeling immunofluorescence for CD44 and a standard microglial marker ionized calcium binding adaptor protein-1 (IBA1, Imai et al. 1996) confirmed the presence of CD44 on a large fraction of IBA1-positive microglia in the TGFβ1-/- but not TGFβ1+/+ mice (figure 6.2G,H), as well as in the GFAP-positive, velate astrocytes (figure 6.2K,L).

Microglia, macrophages and blood vessels.

Absence of TGFβ1 visibly affected perivascular macrophages and parenchymal microglia, but not the blood vessels. Compared to the TGFβ1+/+ mouse brains, those from TGFβ1-/- littermates showed a 2-3 fold expansion in the number of the perivascular macrophages with a strong immunoreactivity for the major histocompatibility complex class 2 (MHC2) antigen (figure 6.1Q,R), a typical marker of this perivascular cell type in normal brain (Liu et al., 2006). In contrast, TGFβ1-/- parenchymal microglia displayed a clear reduction in microglial cell number, size and staining for the αMβ2 integrin, a typical and constitutively expressed microglial cell marker (Perry et al., 1988; Raivich et al., 1994), compared to their TGFβ1+/+ littermates (figure 6.1C, D, G, H, K, L, O, P, S, T, W, X). Mutant microglia showed a consistent loss of arborisation, with shorter and stubbier processes lacking tertiary and quaternary branches. These morphological changes were observed throughout the brain, but somewhat more accentuated in the brainstem regions.

Since inflammatory brain changes can also affect blood brain vessels, with upregulation of endothelial cell adhesion molecules such as the intercellular adhesion molecule 1 (ICAM1), and alter transmigration of leukocytes and blood brain barrier function (Bohatschek et al., 2001), we also investigated these parameters. However, deletion of TGFβ1 was not associated with increased staining for blood vessel ICAM1 (figure 6.1U, V). There was no accumulation of endogenous peroxidise-positive granulocytes in brain tissue; intravascular injection of endogenous peroxidase revealed an intact blood brain barrier (data not shown).

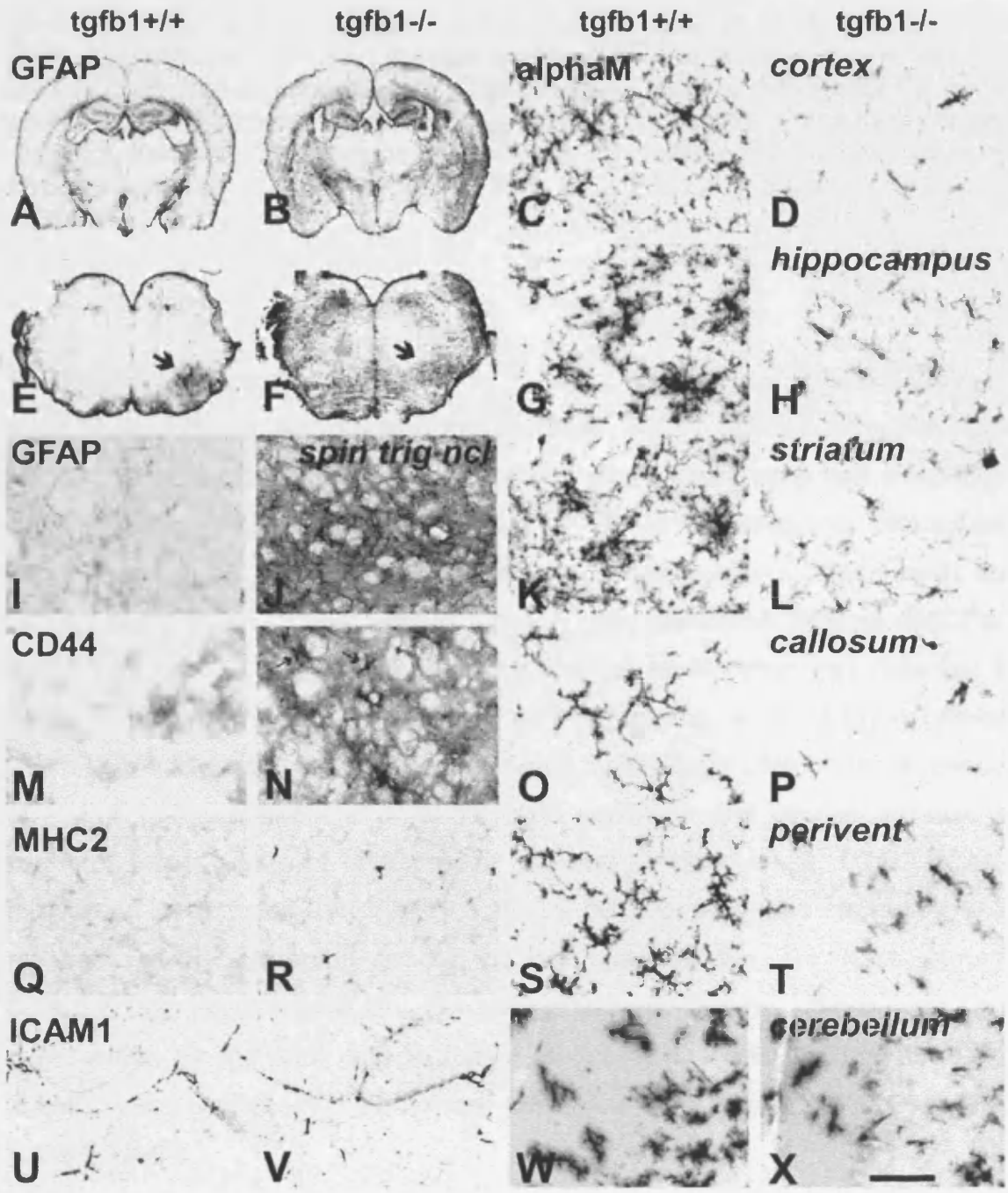

Figure 6.1. Absence of TGFβ1 (TGFβ1-/-) causes strong glial changes throughout the adult brain, affecting astrocytes, microglia and perivascular macrophages. **A, B, E, F, I, J:** Massive increase in astroglial GFAP-IR in the TGFβ1-/- mice, in low power magnification of forebrain (A,B) and brainstem (E, F), with intense labeling of the deep and superficial cortex, basal ganglia and reticular thalamic nucleus and in most parts of the brainstem. The arrows in E and F point to the facial nucleus 3 days after axotomy setting a contrast to the surrounding area in the TGFβ1+/+ animal but almost merging with background in TGFβ1-/- mouse. I and J show the typical distribution of GFAP-IR at higher magnification in the spinal nucleus of the trigeminal nerve, with strong labeling of astrocyte fibrils, as well as in diffuse areas associated with protoplasmic astrocytes in the TGFβ1-/- animal. **M, N, Q, R U, V:** Absence of TGFβ1 is associated with strong CD44 labeling of partly deramified microglia (arrows) and diffuse labeling of protoplasmic astrocyte grey matter areas (M,N) and increased number of MHC2+ perivascular macrophages (Q,R) but no change in

the ICAM1 labeling of the vascular endothelium (U,V). **C, D, G, H, K, L, O, P, S, T, W, X:** Absence of TGFβ1 causes strong reduction in the highly elaborate branching of ramified microglia and αMβ2-immunoreactivity throughout the adult forebrain and brainstem areas, including cortex, hippocampus, striatum, corpus callosum, brainstem periventricular areas and cerebellum. Bar size (X): 2mm in A&B, 1mm in E&F, 150μm in I,J,M,N,Q&R, 200μm in U&V, 50μm in the right 2 columns.

To determine the specific phenotype of microglial changes in the TGFβ1-/- mice, as a next step we explored the effects of TGFβ1 deficiency on potential markers of microglial activation including cell proliferation, early and midphase injury response (α6β1 and αMβ2 integrins, ICAM1), phagocytic phenotype (αXβ2 integrin, B7.2, MHC1) and additional inflammatory markers such as CD44 (Jones et al., 2000). Double labeling with antibodies against αMβ2 or IBA1, were used to identify microglial profiles; cell proliferation was detected 2 hours after intraperitoneal injection with [^{3}H]-thymidine, a blood brain barrier permeable nucleotide incorporated into newly synthesized DNA. In the absence of TGFβ1 (-/-), a subpopulation of microglia proliferate and strongly express a panel of phagocytic and inflammatory markers (MHC1, αXβ2, B7.2, CD44) throughout the affected CNS (figure 6.2B,D,F,H&J, respectively). None of these responses were observed in the normal brain of the +/+ mice (figure 6.2A,C,E,G,I). In contrast to the phagocytic phenotype, there was no upregulation for the early and midphase activation markers α6β1, αMβ2 and ICAM1 in the control, -/- brain without additional injury (figure 6.6C, G and K; figure 6.7A-C).

Ultrastructural changes: axonal dystrophy, focal demyelination and microglial phagocytosis.

Since presence of neural debris and other phagocytosable material is known to cause ramified microglia to lose terminal branches and transform into ameboid phagocytes (Bohatschek et al., 2001), the phagocytic phenotype of microglia in the TGFβ1-/- mouse brain could be due to a neurodegenerative process producing cellular debris.

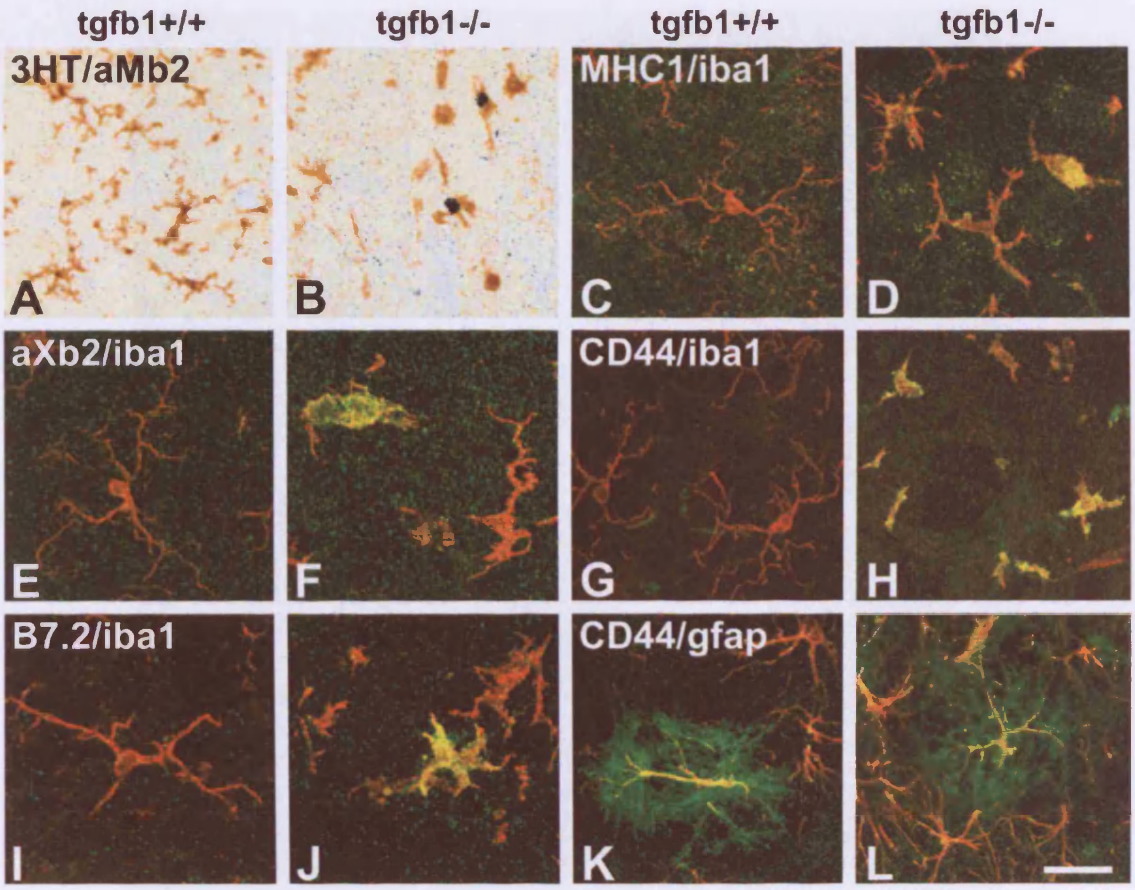

Figure 6.2. A-J: In the absence of TGFβ1 (tgfβ1-/-), microglia proliferate (compare B to A) and express a panel of late activation markers - MHC1 (C, D), αXβ2 (E, F), B7.2 (I, J) - throughout the affected CNS, a response not observed in the uninjured, normal brain (tgfβ1+/+). **A, B:** Microglial proliferation in the cerebellar peduncle, double labeling using autoradiography for tritiated thymidine and immunoreactivity for αMβ2 integrin (^{3}HT/αMβ2). **C-J:** Double immunofluorescence, with IBA1 in red. A subpopulation of activated microglia showed strong immunoreactivity for MHC1 (normal facial motor nucleus), αXβ2 (periventricular brainstem), B7.2 (cerebellar peduncle) and CD44 (spinal nucleus of the trigeminal nerve) in green. Note the changes in microglial morphology, with elaborate microglial branching in sections from TGFβ1+/+ animals. In the TGF β1-/- mice, this branching is almost completely lost in MHC1+, αXβ2+ and B7.2+ microglia, and but also strongly reduced in the those that did not stain for these phagocytosis associated markers. **K, L:** TGFβ1 deficiency had a stimulatory effect on the CD44/GFAP+ velate astrocytes in the CNS white matter, but some double positive astrocytes were also present in the normal, TGFβ1+/+ mice GFAP staining in red, CD44 staining in green. Scale bar size: 75μm in A&B, 25μm in C-L.

To explore whether this is the case, we examined ultrastructural changes in the brainstem facial motor nucleus and adjacent ventrobasal white matter in the TGFβ1-/- and TGFβ1+/+ mice using transmission electron microscopy. Compared to the +/+ littermates that appeared to be completely normal

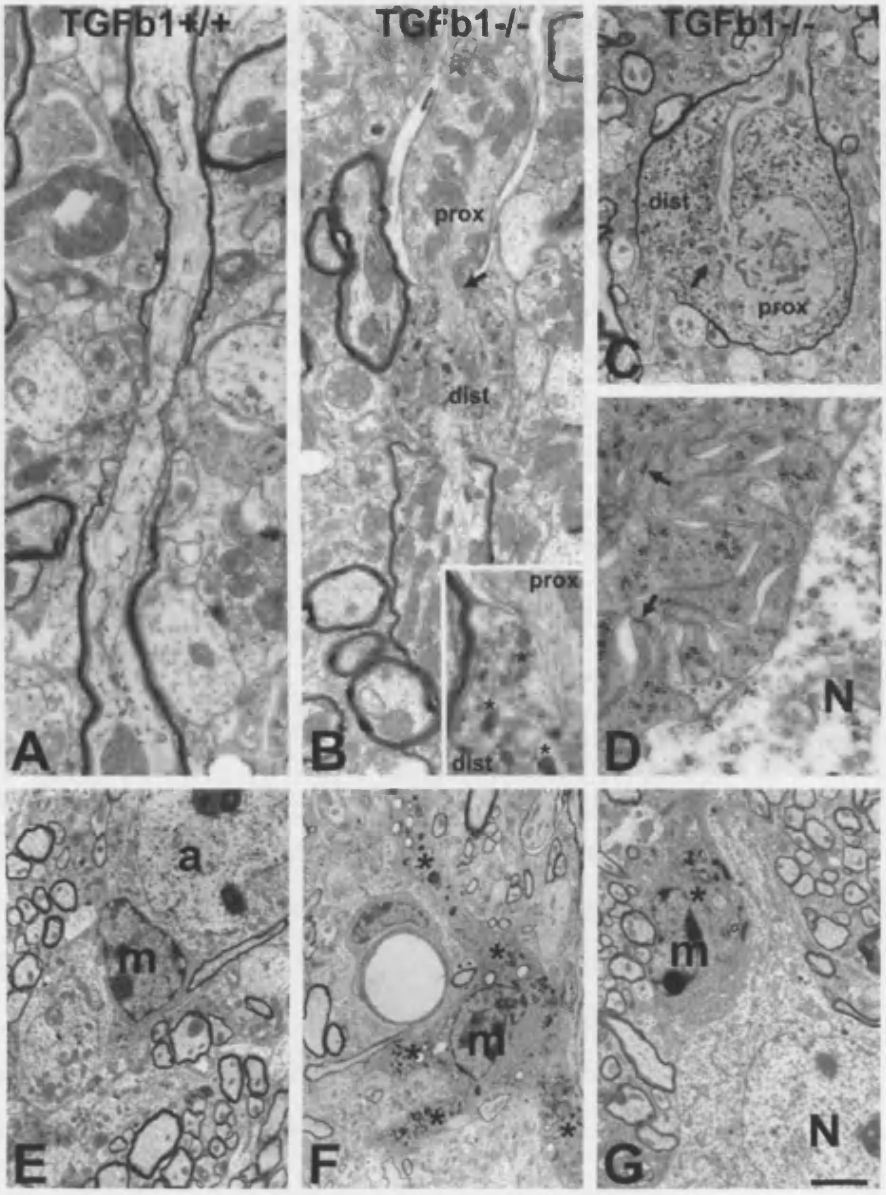

Figure 6.3. Ultrastructural changes in the brain of TGFβ1-deficient, -/- mice. **A, E:** Normal axons, microglia (m) and astrocytes (a) in the control, TGFβ1+/+ animals. **B, C:** TGFβ1-/- mice show frequent disturbances in axonal transport. These disturbances lead to the local bulging of axons to accommodate the anterogradely and retrogradely transported material, particularly mitochondria, in the proximal (prox) and distal parts of the axon, respectively. Affected axons sometimes become partly demyelinated (proximal segment). As shown in **B insert**, microtubular structure at the site of interruption (arrows) is frequently disorganized and displaced. Retrogradely transported material accumulating in the distal part also contains large and round breakdown organelles (asterisks) that may represent mitochondrial fragments. **D, F, G:** The microglia in TGFβ1-/- mice consistently show areas with numerous, moderate size phagocytic inclusions (asterisks and F insert), that extend into swollen proximal processes (F). They also exhibit an abnormal attachment to neighboring neurons (N), and at higher magnification, many membranous ruffles with frequent, homophilic focal adhesions (D). a – astrocyte nucleus. Scale bar size (G): A,B – 0.8μm; B insert – 0.3μm; C – 1.5μm; D – 0.4μm, E,F,G - 2.5μm.

(figure 6.3A), the TGFβ1-/- mice showed occasional disturbances in axonal transport, with local bulging of axons to accommodate the anterogradely and retrogradely transported material, particularly mitochondria (figure 6.3B, C). Neurofilament structure at the site of interruption was frequently disorganised. The retrogradely transported material also contained large and round structures that may represent mitochondrial fragments. As shown in figure 6.3B, affected axons sometimes also became demyelinated in a focal fashion, with some parts of the axon losing, and some others maintaining the myelinated state.

Axonal dystrophy and demyelination was accompanied by morphological changes in parenchymal microglia. Compared with TGFβ1+/+ microglia that exhibited a typical slender perikaryal cytoplasm (figure 6.3E), microglia from TGFβ1-/- mice consistently revealed numerous but moderately sized phagocytic inclusions, cell body engorgement and a swelling of proximal processes (figure 6.3F). In the facial nucleus, they also showed abnormal attachment to neighboring neurons with full apposition of their cell body to the neuronal surface (figure 6.3G), a process called synaptic stripping that is normally only observed following neuronal injury (Blinzinger and Kreutzberg, 1968; Kalla et al., 2001; Trapp et al., 2007). At higher magnification, these TGFβ1-/- adhering microglia also displayed numerous membranous ruffles with frequent, homophilic focal adhesions (figure 6.3D).

TGFβ1-Deficiency in the Injured Nervous System

Neuronal response to facial axotomy.

TGFβ1-mediated effects on adult neuronal response to injury - axonal regeneration, central sprouting and neuronal cell death - were assessed using the well characterized facial axotomy model. Axonal regeneration was examined in the crushed facial nerve 96 hours after injury as described in Werner et al (2000). The axonal growth front of the regenerating, CGRP- or galanin-positive motoneurites was detected in longitudinally cut, fixed, 10 um thin facial nerve sections using IR for the axonally transported neuropeptides CGRP and galanin and distance to the site of the crush determined with a microscope grid. As shown in figure 6.4A, there was no statistically significant


G

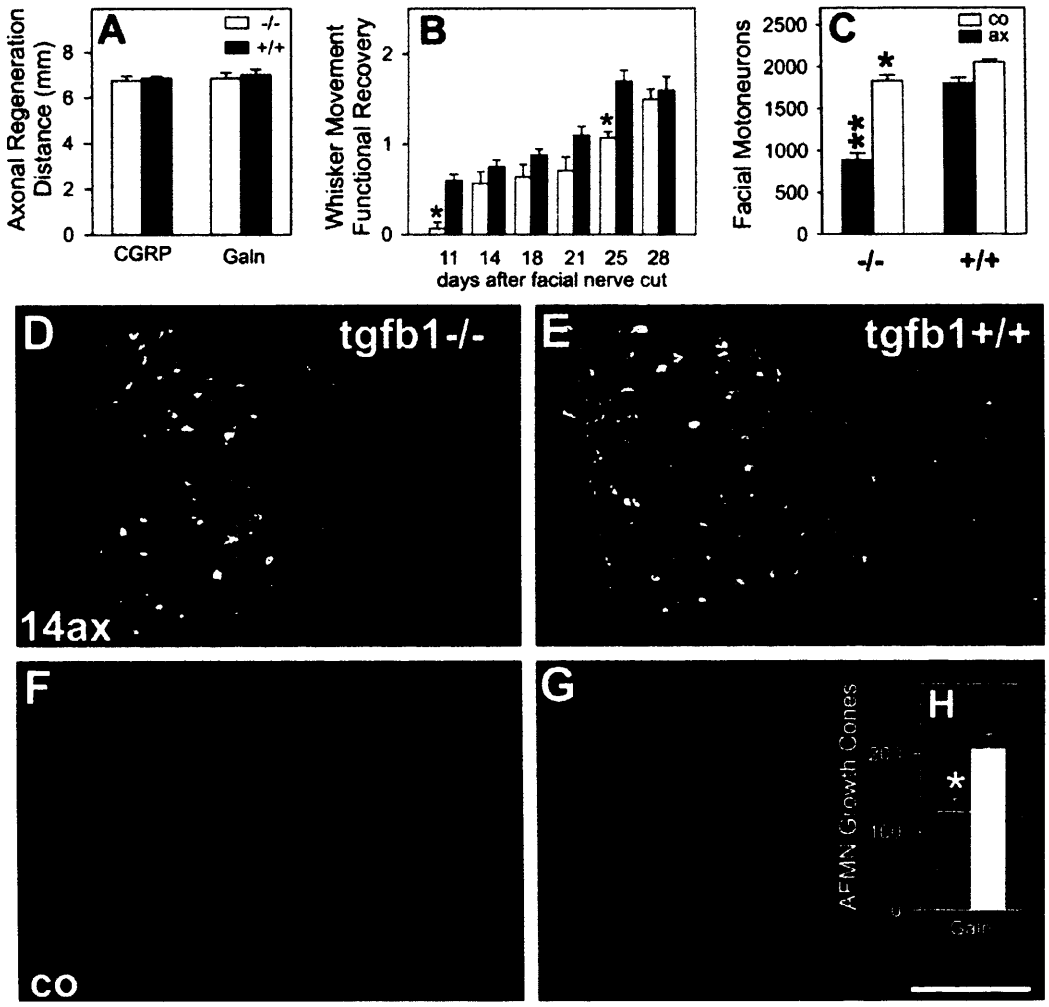

Figure 6.4. TGFβ1 and axonal regeneration, sprouting, functional recovery and neuronal cell death after facial axotomy. **A:** No effect on the regeneration distance of CGRP- and galanin-immunoreactive motor axon populations (A), 4 days after facial nerve crush (Mean +/- standard error of mean/SEM, n = 6 animals per group). **B:** Functional recovery of whisker hair movement after facial nerve cut (n = 10+/+ and 7-/- animals). *p<0.05 in unpaired Student t-test (uSTT) between +/+ and -/- groups. **C:** Changes in neuronal cell number in the axotomized and contralateral facial motor nucleus, 30 days after a left facial nerve cut. Absence of TGFβ1 enhances neuronal cell disappearance after axotomy, from 13% of the injured neurons in the +/+ to more than 52% in the -/- animals. Note the more than 10% smaller, neuronal cell number on the unoperated, contralateral side in the TGFβ1-deficient mice. n = 9+/+ and 6-/- mice, *p<0.02 in uSTT between the same side in +/+ and -/- mice, **p<0.01, uSTT for the difference in the ratio of operated/unoperated side in +/+ to -/- animals. **D-H:** Central sprouting of galanin-immunoreactive axons in TGFβ1-/- (D, F) and +/+ facial nuclei (E, G), 14 days after facial nerve cut (14ax); co – contralateral side (C, D); the insert in G (H) shows the quantification of the growth cones per tissue section, (n = 3 animals per group). Under normal conditions, facial axotomy causes an induction of neuronal galanin immunoreactivity and a proliferation of galanin-immunoreactive axonal sprouts, particularly in the white matter marked by double arrows just ventral to the facial motor nucleus, peaking 14 days after facial nerve cut (14ax). This axonal sprouting is strongly curtailed in the TGFβ1-/- mice (*p<0.05, uSTT). Scale Bar – 250μm.

difference between the TGFβ1-/- and TGFβ1+/+ animals 4 days after crush (n=6 animals per group, mean+/- standard error of mean/SEM). Wildtype, +/+ mice showed a regeneration distance of 6.9 +/- 0.1 mm for the CGRP- and 7.0 +/- 0.2 mm or the galanin-positive axons at day 4; homozygous, TGFβ1-/- mice showed a 1-2% smaller regeneration distance.

Absence of effect on speed of regeneration was mirrored by typical biochemical changes in axotomized motoneurons that did not differentiate between TGFβ1+/+ and -/- littermates, for example the induction of neuropeptides such as galanin and cell adhesion molecules such as CD44 (Raivich et al., 2004). Galanin-IR was strongly upregulated after axotomy in normal TGFβ1+/+ mice, with a peak 7 days after injury. Here, the absence of TGFβ1 did not lead to a significant difference in the expression of this neuropeptide at any of the 4 time points studied (d2, d3, d7 and d14, data not shown). Absence of TGFβ1 also did not affect CD44, with more or less identical, strong increase in neuronal CD44-IR in the wild-type and TGFβ1-deficient animals in the axotomized facial nucleus (data not shown).

To next assess the more long term functional recovery after facial nerve cut, the overall movement of whisker hair, a key target of facial innervation, was scored on a scale of 0 (no movement) to 3 (strong, normal movement). Functional recovery was somewhat slower in the TGFβ1-/- ($F_{1,113}$=33.46 in muti-way ANOVA, $p<0.01$) but the delay was moderate, with almost complete recovery by day 28 (figure 6.4B).

TGFβ1-deficiency also interfered with central axonal sprouting (figure 6.4D-H). Facial axotomy normally leads to enhanced axonal sprouting, with a maximum at day 14 (Galiano et al., 2001; Werner et al., 2000, figure 6.4D, E), which is absent on the contralateral side (figure 6.4F, G). Control, TGFβ1+/+ animals showed the prominent sprouting of the galanin-positive axons (figure 6.4D); the TGFβ1-/- mice revealed a 40% reduction in total number of axonal growth cones (figure 6.4H), with a complete disappearance of these structures in the basal stripe of central white matter ventral to the facial motor nucleus (figure 6.4E).

A substantial number of neurons die after nerve transection, probably due to failed target reinnervation and subsequent lack of trophic support (Sendtner et al., 1996). To assess whether TGFβ1 plays a role in axotomy-induced neuronal cell death, all motoneurons in the facial motor nucleus were counted using 25μm cresyl violet-stained serial brain sections, and corrected for cell size using Abercrombie correction. One month after facial nerve transection, axotomy had caused a loss of 13% in the injured facial motor nucleus of control mice, 1674+/-69 compared to 1936+/-22 on the unoperated side (n= 9). In TGFβ1-/- mice, neuronal loss by axotomy was increased by approx. 4-fold, to 53%, with 822+/-77 neurons on the axotomized and 1737+/-64 on the unoperated side, $p<0.01\%$ in unpaired Student's t-test (figure 6.4C). As in previous studies (Galiano et al., 2001; Raivich et al., 2002), neuronal cell size increased by an average of 3-5% from 22 to 23 um on the axotomized side, but without a statistically significant difference between the TGFβ1-/- and TGFβ1+/+ groups. However, the TGFβ1-/- animals did show a significant, 10% reduction in facial motoneuron number on the uninjured side compared with the +/+ controls ($p<0.02$), pointing to an underlying trophic role of TGFβ1 in the normal adult brain as well as after peripheral axonal injury.

Defective activation of glial cells in the absence of TGFβ1.

Nerve transection does not only trigger changes in affected neurons, but also results in reactive changes in adjacent astrocytes and rapid activation and proliferation of microglia. Both sets of responses were affected in TGFβ1-/- mice, but in opposite directions.

Cell proliferation.

Microglial proliferation, normally peaks 2-3 days after peripheral nerve injury (Raivich et al. 1994). Compared to their TGFβ1 +/+ littermates, TGFβ1-/- mice showed a 70%-75% reduction in the rate of [^{3}H]-thymidine labeled proliferating cells at both time points, ($p<0.05$, n = 7 per group; Student's t-test, figure 6.5A). Double-labeling using [^{3}H]-thymidine autoradiography for proliferation and antibodies against standard microglial and astrocyte markers – αMβ2 integrin

and GFAP, respectively, confirmed all proliferating cells as αMβ2-positive microglia in control as well as the TGFβ1-/- mice, with no staining on the GFAP-positive astrocytes (figure 6.5C, D, G and H). Total counts of microglia 7 days after peripheral nerve transection revealed similar results (figure 6.5B), with a 4-fold increase in the total number of microglia in the affected facial motor nucleus compared to the unoperated facial motor nucleus in the +/+ animals, and just a 1.8-fold increase in the -/- mice ($p<0.05$ compared to the TGFβ1+/+; n=4; unpaired Student's t-test).

Early microglial activation.

TGFβ1-deficiency caused a drastic reduction in cell adhesion molecules ICAM1 and αMβ2 and α6β1 integrin which serve as early (ICAM1, αMβ2) and midphase (α6β1) activation markers that normally increase after injury (figure 6.6A-L; figure 6.7A-C). In all 3 cases, quantification of the double-labeling immunofluorescence with the microglial marker IBA1 using the RISC algorithm (Werner et al., 1998), showed a significant, approximately 70-90% smaller increase in immunoreactivity following injury ($p<0.01$, unpaired Student's t-test), as well as a somewhat lower level of expression on the control, uninjured side ($p<0.05$).

Phagocytic phenotype.

Late phagocytosis-associated microglial markers (αXβ2, B7.2, IBA1) were tested 14 days after facial axotomy, a time point normally coinciding with a maximum in neuronal cell death (Möller et al., 1996). Here, quantitative immunofluorescence showed a highly significant increase in the uninjured facial motor nucleus of TGFβ1-/- mice (figures 6.6M-T, 6.7D-F, $p<0.01$). These animals also showed surprisingly little additional increase on the operated side at 14 days after facial nerve cut, in contrast to the prominent increase observed for these markers in the +/+ mice.

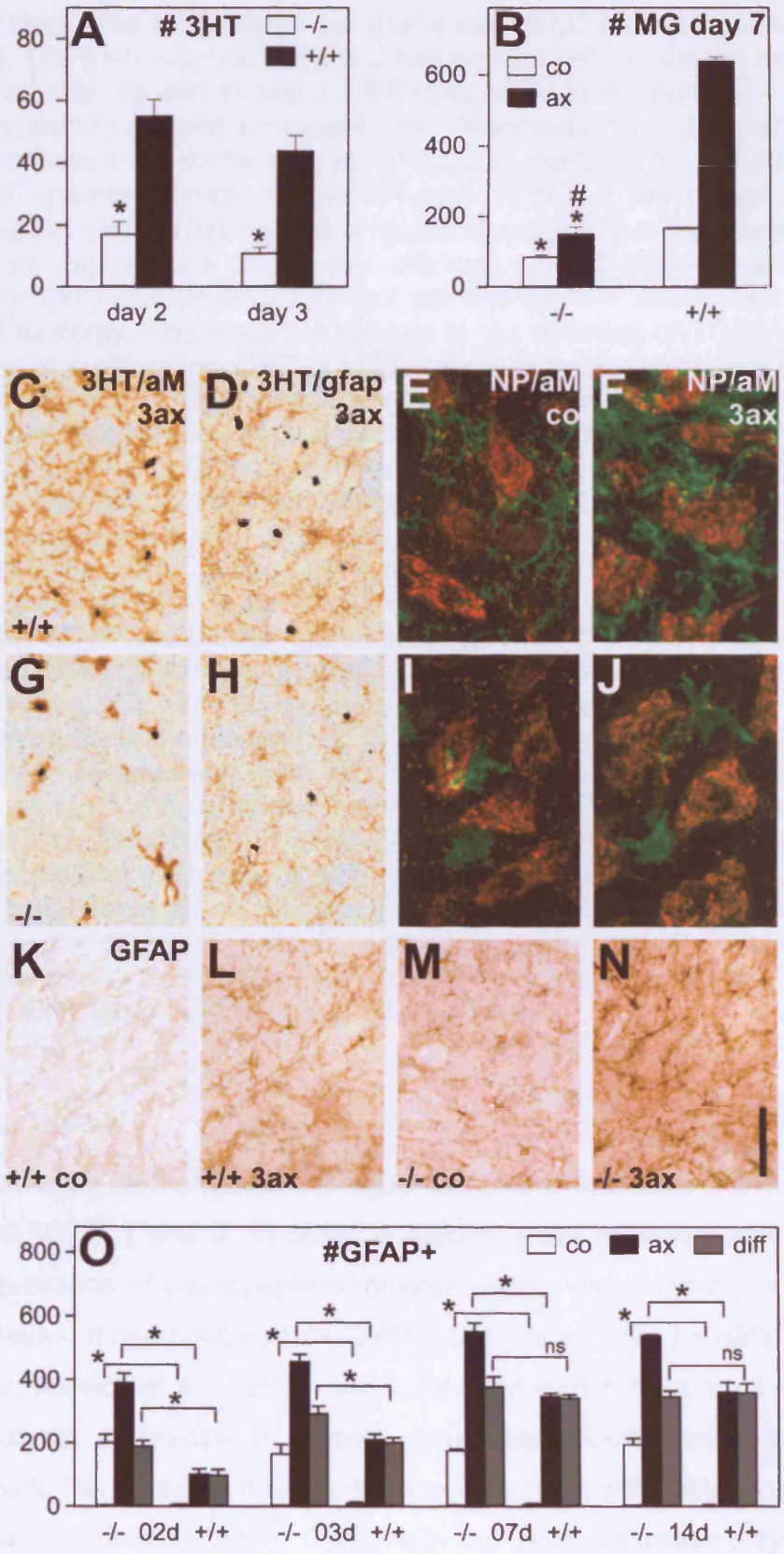

Figure 6.5. Cell proliferation, microglial response and astrogliosis following facial nerve injury. **A:** Cell proliferation in the facial motor nucleus, 2 and 3 days after nerve cut, shows a 70%-75% reduction in the rate of [^{3}H]-thymidine labeled proliferating cells per tissue section in TGFβ1-/- mice, (*$p<0.05$, n = 7 per group; uSTT). **B:** Microglial cell number in the facial motor nuclei of +/+ and

-/- mice, 7 days after facial nerve cut (nucleated αMβ2-immunoreactive profiles per 1mm^2). TGFβ1-/- animals show a 2-fold smaller cell number of microglia on the uninjured side, as well as just a 1.8-fold increase in cell number 7 days after injury, compared to a 4-fold increase in the +/+ animals (*$p<0.05$ in uSTT for the difference between the same side in +/+ and -/-, #$p<0.05$ for the difference in the ratio of operated/control side in +/+ and -/-, n = 4 per group). **C,D,G,H:** Double-labeling using [^{3}H]-thymidine autoradiography for proliferation and a standard microglial and astrocyte markers, αMβ2-integrin and GFAP, respectively. Only αMβ2+ microglia but not the GFAP+ astrocytes proliferate after facial axotomy. This does not change in the absence of TGFβ1, although the number of proliferating (3HT+) αMβ2-immunoreactive microglia is smaller. **E,F,I,J:** Absence of TGFβ1 affects microglial adhesion to motoneurons. Both populations of neuropeptide-immunoreactive motoneurons were detected with a mixture of CGRP and Galanin antibodies. In the +/+ mice, αMβ2 microglia (green) only adhere to the neuropeptide-immunoreactive neurons (red) with their processes but not with their cell bodies before axotomy (co, E). After axotomy (3 days after facial nerve cut, 3ax), cell body adhesion is also observed (F). TGFβ1-/- mice show microglial cell body adhesion on the uninjured (I), as well as on the injured side (J). **K-O:** Astrocyte response in the injured brain. **K-N:** GFAP-immunohistochemistry 3 days after transection of the right facial nerve. **K, L:** TGFβ1+/+. Increased GFAP-immunoreactivity on stellar, fibrillary astrocytes in the axotomized facial motor nucleus (L, 3ax), compared to the uninjured, contralateral side (K, co). **M,N:** Massive astrogliosis in the TGFβ1-/- animal, with a further increase in GFAP-immunoreactivity after axotomy (N). **O:** Quantification of GFPA-IR cell profiles per tissue section, for the axotomized and contralateral side, and the inter-side difference (diff), 2-14 days after facial nerve cut. At all time points, there was a significant increase for each side in the TGFβ1-/- animals, early time points (day 2, 3) also show a stronger increase in these mice (*$p<0.05$ uSTT, ns – not significant). Scale Bar (in N): C,D, G,H: 94µm; E,F,I,J: 30µm; K-N: 200µm

Neuronal adhesion.

TGFβ1-deficiency also affected microglial adhesion to motoneurons as shown in figures 6.5E, F, I and J. In order to identify most neuronal profiles, the 2 largest populations of neuropeptide-immunoreactive motoneurons in the facial motor nucleus – those positive for CGRP and those positive for galanin (Moore et al., 1992; Raivich et al., 1995) - were detected with a mixture of anti-CGRP and anti-galanin antibodies. In normal mice, αMβ2-positive microglia (green) only adhere to the neuropeptide-positive neurons (red) with their processes but not with their cell bodies (figure 6.5E), with cell body adhesion only observed after axotomy (figure 6.5F). However, it is also present in uninjured facial motor nuclei in the TGFβ1-/- mice (compare figure 6.5I and J).

Astrocytes.

In addition to the strong reactive gliosis observed in the uninjured brain shown in figure 6.1, transection of the facial nerve in the TGFβ1-/- mice resulted in a more pronounced astrogliosis compared to that observed in the normal, TGFβ1+/+ littermates (Figure 6.5K-O). Strong increase in the number of GFAP-positive stellar astrocytes was already observed in the contralateral, unoperated facial motor nucleus ($p<0.05$; n=4-8; Student's t-test) (figure 6.5O), and a similar increase was also seen on the operated side. At early time points – day 2 and day 3, one could also see a moderate but significantly higher ***difference*** in the number of GFAP+ astrocytes between the control and operated sides in the TGFβ1-/- mice, compared to their +/+ littermates, pointing to an additional, excessive astrogliotic response to injury in the absence of TGFβ1.

Regulation and cellular localization of TGFβ1, and TGFβ receptors type 1 and 2 mRNA.

To further determine possible sites of TGFβ1 synthesis and action, we explored the regulation and localization of the mRNA encoding TGFβ1 and its 2 composite receptor types R1 and R2 using high stringency in situ hybridization with [^{35}S]-labeled cRNA antisense probes, as shown in figure 6.8. Facial axotomy caused a gradual upregulation in the case of TGFβ1 mRNA, peaking at day 4 (figure 6.8B,F,J and N); in the case of TGFβ R1 this was more rapid, with high levels of expression between day 1 and 14 (figure 6.8C,G,K and O). TGFβ R2 mRNA only showed constitutive expression (figure 6.8P). Substituting sense for antisense cRNA caused disappearance of specific labeling as demonstrated for TGFβ R1 in figure 6.8D.

Since microglia in normal as well as injured brain where particularly strongly affected in the normal and injured brain, we combined the in situ hybridization protocol with the immunohistochemistry for the αMβ2 integrin as microglial cell marker (figure 6.8A,E,I,M), to determine the cellular localization for TGFβ1, TGFβ receptor type 1 (R2) and receptor type 2 (R2). In the unoperated facial motor nuclei as well as throughout the brainstem, the strongly labeled clusters

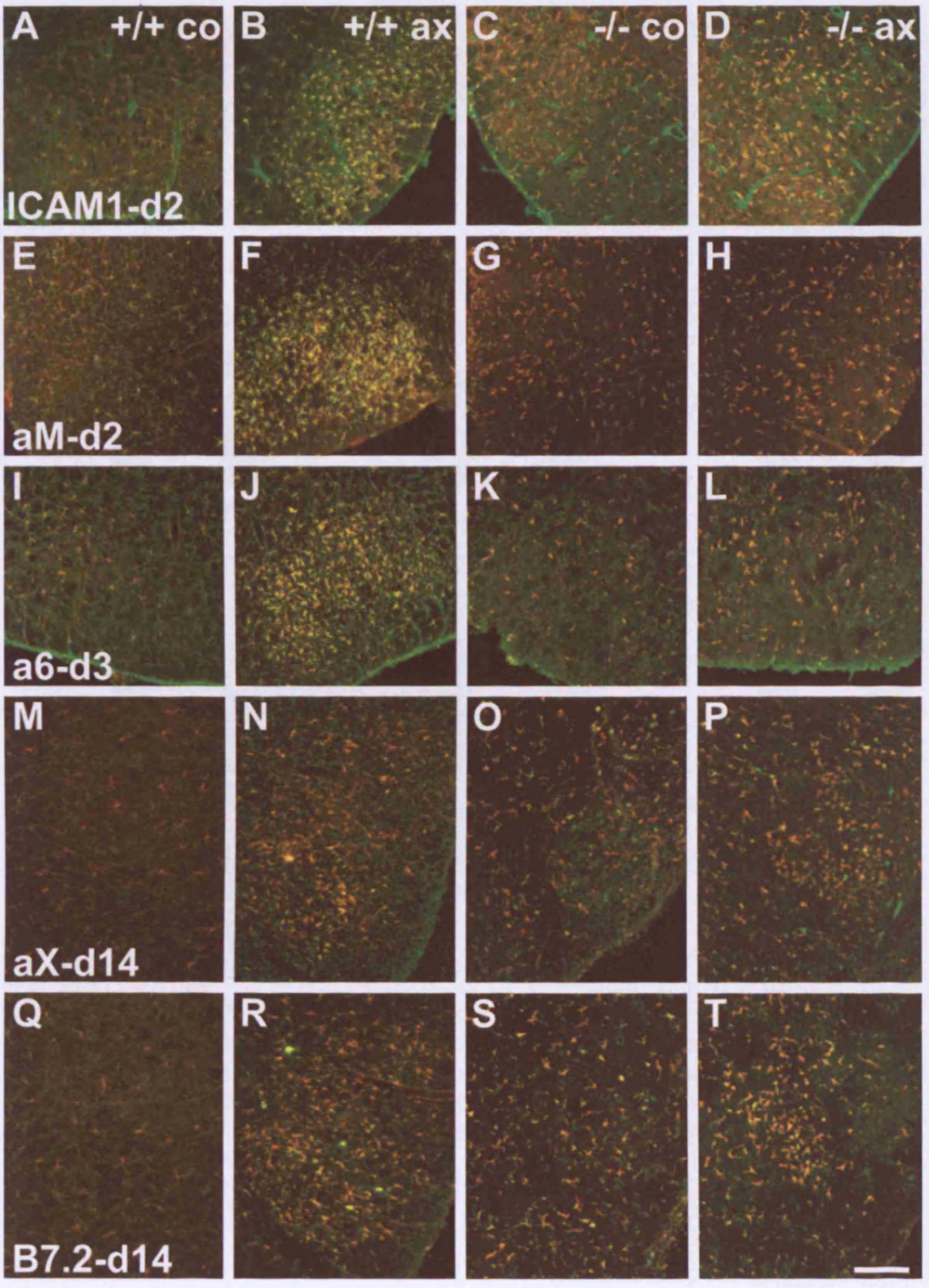

Figure 6.6. TGFβ1-/- deficiency causes a split response in the regulation of early and midphase (ICAM1 and αMβ2 integrin, and α6β1, respectively), and the phagocytic (αXβ2 and B7.2) markers on microglia after facial axotomy (ax) and on the contralateral side (co). Double immunofluorescence with microglial IBA1 counterstaining in red and other label in green. In the first group (A-L), absence of TGFβ1 interferes with the upregulation of ICAM1 (A-D), αMβ2 integrin (E-H), and α6β1 (I-L), normally observed at day 2 and day 3 in the TGF β1+/+ mice. In the second group (M-T), small αXβ2 (M-P) and B7.2 (Q-T)

immunoreactive microglia are already present in the contralateral facial motor nuclei in the TGFβ1-/- mice; their numbers are barely affected by facial axotomy. In control, TGF β1+/+ animals, facial axotomy normally leads to the appearance of large, αXβ2 and B7.2 immunoreactive microglial nodules, peaking at day 14, that remove dead neuronal debris. Scale bar: A-L, 250μm; M-T 330μm

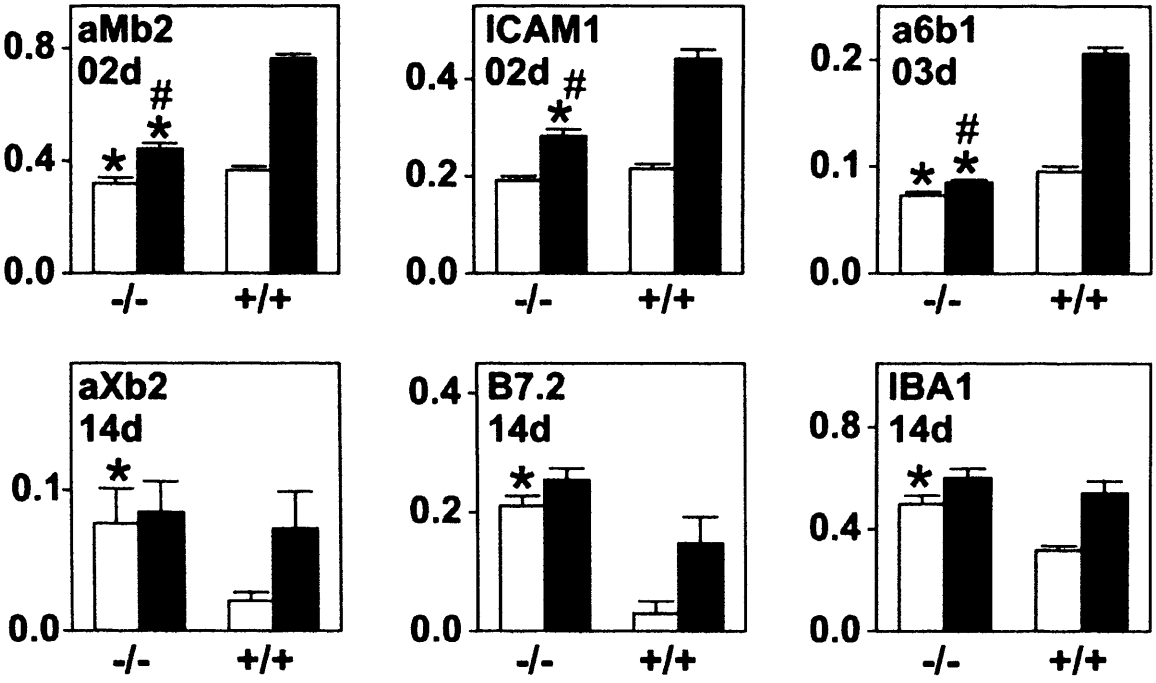

Figure 6.7. Quantitative immunofluorescence for early and late microglial activation markers in the axotomised and contralateral facial motor nucleus (empty bars: unoperated side, filled bars: axotomised side) for αMβ2 integrin (A, day 2), ICAM1 (B, day 2), α6β1 (C, day 3), αXβ2 (D, day 14), B7.2 (E, day 14) and IBA1 (F, day 14) using RISC algorithm. *p<0.05 in uSTT for +/+ vs -/- comparisons for the contralateral vs contralateral or axotomotized vs axotomized side; #p<0.05 for the comparison of the difference between the 2 sides in +/+ vs -/- animals. The TGFβ1-/- mice show a generally lower level of early markers ICAM1, αMβ2 and α6β1 on the unoperated side; a much smaller increase of ICAM1, αMβ2 and α6β1 after injury, as well as high levels of αXβ2, B7.2 and IBA1 on the uninjured side.

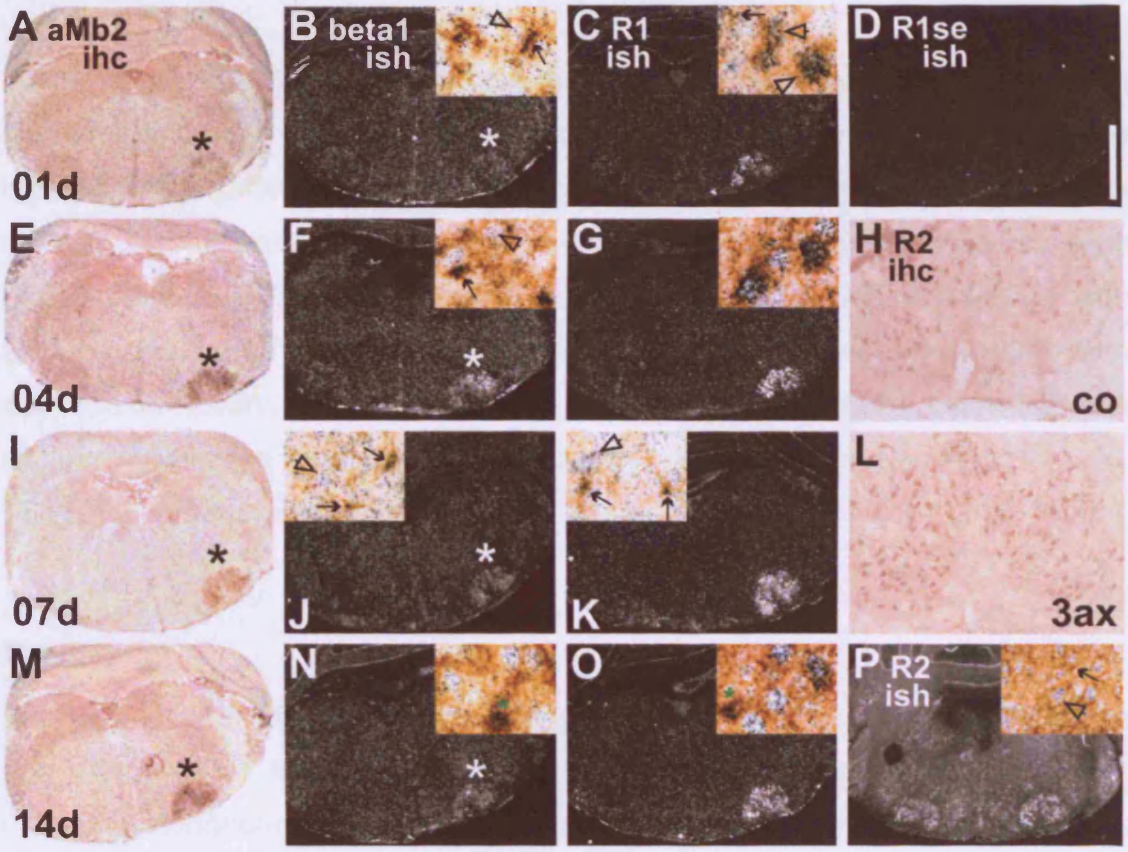

Figure 6.8. Regulation and localization of TGFβ1 (β1, B,F,J,N), TGFβ R1 (C,G,K,O) and R2 mRNA (P) and TGFβ R2 protein-IR (H,L) using in situ hybridization with [^{35}S]-labeled cRNA antisense probes (ish) and immunohistochemical (ihc) techniques. Facial axotomy caused pronounced upregulation of TGFβ1 and R1 mRNAs on microglia and neurons, but did not affect the strong constitutive, primarily neuronal expression of R2 mRNA and protein-IR. A-D: 1 day, H&L: 3 days, E-G: 4 days, I-K: 7 days and M-P: 14 days after axotomy. The level of non-specific in situ hybridization labeling with a sense probe for R1 is shown in D. The high magnification inserts show colocalisation with neurons (open arrows), αMβ2-positive microglia (simple arrows), and phagocytic microglial clusters (thick arrows) using combined staining for αMβ2 integrin and in situ hybridization. Inserts on the right (all except J&K) show the situation on the axotomised, inserts on the left (J&K) the uninjured, contralateral side. The left (A,E,I,M) and second left (B,F,J,N) columns show low-magnification, brightfield and darkfield illuminated micrographs of combined αMβ2/TGFβ1mRNA-double staining; in each case, the axotomised side (right) is marked by asterisks. Scale bar: A-P (except H&L): 1.2mm, H&L: 200µm, all inserts: 70µm

of TGFβ1 and TGFβ R1 mRNA expression were specifically localized to the cell bodies of the αMβ2-positive microglial cells, with more moderate, diffuse labeling on adjacent larger neuronal profiles (figure 6.8J,K).

Facial axotomy caused strong upregulation of mRNA encoding TGFβ1 on activated microglia (figure 6.8B,F), and TGFβ R1 on injured neurons (figure 6.8C,J). At the peak of neuronal cell death at day 14 (Möller et al., 1996), both mRNAs are particularly strongly expressed the phagocytic microglial clusters (figure 6.8N,O). Although moderate levels of TGFβ2 mRNA expression was also observed on the αMβ2-positive microglial profiles, strong expression was confined to neurons and did not change following facial axotomy (figure 6.8P). A similar, constitutive and primarily neuronal localization was also observed for TGFβ R2 immunoreactivity (figure 6.8H, L).

Discussion

The high level of TGFβ1 in normal adult brain is in contrast to other cytokines and suggests an important neural function for this constitutively expressed molecule. (Lindholm et al., 1992; Kiefer et al., 1995; Raivich et al., 1999). As shown in the current study, endogenous TGFβ1 is expressed by parenchymal microglial cells and exerts a trophic and anti-inflammatory effect in the adult CNS. Moreover, these effects were present not only after additional injury, but also without prior physical damage. TGFβ1-/- animals showed a strong neuroinflammatory response throughout the brain, excessive astrogliosis and proliferating microglia assuming a phagocytic, deramified and abnormally activated phenotype. Ultrastructurally, these changes were accompanied by local disruptions in axonal transport and focal demyelination, providing a mechanism to generate neural debris and maintain microglial phagocytes and astrocyte reactivity throughout the CNS. The significant reduction in the number of normal facial motoneurons in the uninjured facial motor nucleus, underlines the importance of constitutively expressed TGFβ1 in preventing neuronal loss in the adult.

These neurodegenerative changes present under normal conditions were enhanced following additional injury. After facial axotomy, absence of TGFβ1 caused a 4-fold increase in neuronal cell death in the injured facial motor nucleus, reduced central axonal sprouting and delayed functional recovery. It further exacerbated astroglial reaction and interfered with the normal response of microglia, reducing proliferation and causing absence of early activation

markers while maintaining a strong phagocytic phenotype. Proliferating microglia displaying normal injury-mediated responses play a significant, trophic role in a variety of disease and injury models (Schroeter et al., 2006; Streit, 2006; Lalancette-Hebert et al., 2007); interference with this function may greatly enhance the rate of loss amongst injured neurons exposed to cell stress and already near the threshold of programmed cell death.

TGFβ1 and neuronal survival

TGFβ1 belongs to a closely related family of anti-inflammatory growth factors TGFβ1, 2 and 3 that share same receptors – TGFβ receptor type 1 and type 2 (Feng and Derynck, 2005), and exhibit common neurotrophic activities (Unsicker and Strelau, 2000). In this study, the absence of TGFβ1 alone was sufficient to strongly increase adult neuronal cell death following axonal injury, indicating that it is not completely compensated by the cytokines TGFβ2 or 3. The presence of focal axonal dystrophy in the central white matter around facial motor nucleus in TGFβ-/- mice also shows that axonal injury already occurs without additional external damage. This suggests a similar mechanism causing the reduction in motoneuron number in the "normal" brain, the broad neuroinflammatory changes observed across the CNS, and massively reduced survival following axonal injury.

Such a mechanism could also be responsible for the decreased central axonal sprouting and functional recovery observed in the TGFβ1-/- mice, but indirect changes should not be excluded. For example, absence of TGFβ1 strongly enhances the astroglial and extracellular matrix responses that correlate inversely with central axonal sprouting (Logan et al., 1994; Galiano et al., 2001). Interestingly, absence of TGFβ1 increased astrogliosis which is in contrast to previous reports where treatment with TGFβ1 and TGFβ2 antbodies reduced astrogliosis (Moon and Fawcett, 2001). Nevertheless, in both cases axon regeneration was not increased. Inhibition of TGFβ signaling interferes with Schwann cell proliferation and cell death (D'Antonio et al., 2006), which could affect the speed of functional recovery following peripheral injury. Such indirect effects would also agree with the absence of TGFβ1 effect on motoneurite outgrowth on explanted central white matter (Ho et al., 2000), the lack of TGFβ1-deletion effect on the regenerative growth elongation rate of the CGRP

and galanin-immunoreactive motor axons (figure 6.4A), as well as the lack of differences in neuronal biochemical changes in +/+ and -/- mice at early time points after facial axotomy.

Glial effects

TGFβ action is initiated by the binding of the active form of TGFβ to TGFβ receptor II (R2) followed by the phosphorylation of TGFβ receptor I (R1), causing phosphorylation of Smad proteins, their translocation to the nucleus and transcriptional activation of target genes (Feng and Derynck, 2005). In the current study, the mRNAs encoding all 3 components appear present on neurons and microglia. However, there are differences in the expression level in the normal, uninjured brain, with high transcript levels for TGFβ1 and TGFβ R1 on the microglia, and TGFβ R2 mRNA and protein in the neurons. TGFβ1 and TGFβ R1 are strongly upregulated, in a coordinated fashion, in both neurons and microglia during the early phase of glial and neuronal response, 1-4 days after facial axotomy. At later stages, their levels generally decline on both microglia and neurons, but leaving persisting strong expression on the phagocytic microglial clusters labeled with the thick arrows in figure 6.8N and O. On a cellular level, the apparently coordinated presence of the cytokine as well as both receptor components would permit both autocrine stimulation and a bidirectional, neuron to microglia and microglia to neuron exchange of signals. Nevertheless, the peak period of expression in the first week after injury, the absence of TGFβ1-deficiency mediated changes on early axonal regeneration and neuronal markers, and the strong effects on astrocyte, but particularly on the early microglial activation could suggest that these glial cells are the primary target of the TGFβ1 action.

Activation of microglia normally proceeds in stages (Kloss et al., 1999; Raivich et al., 1999; Boucsein et al., 2000), encompassing initial state of alert with the induction of early activation markers (αMβ2, ICAM1), followed by homing onto damaged cellular structures, expression of α5β1 and α6β1 brisk proliferation causing 4-6 fold increase in increasing microglial cell number (Raivich et al., 1994; Klein et al., 1997). Neural cell debris transforms microglia into phagocytes that remove this debris and express a third set of additional markers typical of CNS phagocytes, associated with antigen presentation such as major

histocompatibility complex type 1 (MHC1), and costimulatory factors B7.2 and αXβ2 integrin (Kloss et al., 1999; Bohatschek et al., 2004a,b), and engage with incoming T-cells (Raivich et al., 1999). Nevertheless, although high levels of MHC1, B7.2 and αXβ2 are phagocyte-selective, they are just additional markers. In fact, normal microglial phagocytes also express particularly high levels of molecules turned on earlier, including αMβ2, α5β1, α6β1 and ICAM1 (Werner et al., 1998; Kloss et al., 1999).

In the current study, absence of TGFβ1 interfered with microglial changes in the first and second phase, causing a strong reduction in the axotomy-mediated induction of αMβ2 and ICAM1 adhesion molecules, proliferation and an almost complete inhibition of the α6β1 increase. The reduction in proliferation is surprising in view of previous in vitro data demonstrating enhanced microglial proliferation following neutralization of endogenous TGFβ1 (Jones et al., 1998). The reasons for the currently observed reduction are unclear. These could be due to a partial exhaustion of proliferative capacity due to the persistent, previous proliferation in the TGFβ1-/- brain, or to inhibitory effects of TGFβ1-deficiency on the production of putative microglial mitogens by axotomised neurons. Interestingly, absence of TGFβ1 did not interfere with the process of phagocytosis. In fact, the selective phagocytic markers were already expressed "normally" throughout the brain of the TGFβ1-deficient animals, as well as in uninjured facial motor nucleus. Both in vitro and in vivo, phagocytosis of increasing amounts of neural debris results in a step by step loss of microglial branching (Möller et al., 1996; Bohatschek et al., 2001). In fact, the current reduction in ramification observed throughout the brain in the TGFβ1-/- animals is in agreement with a moderate production of cell debris throughout the brain due to the inflammatory and neurodegenerative process initiated by the complete absence of TGFβ1.

Surprisingly, there is an apparent lack of upregulation in activation markers such as ICAM1 and α6β1, as well as the low levels of αMβ2, on phagocytic cells throughout the brain in the uninjured TGFβ1-deficient animals, similar to that observed in the injured facial motor nuclei. For example, the absence of α6β1 and ICAM1 and related cell surface components could contribute to the abnormal autoadhesion observed with the TGFβ1-/- microglia in figure 6.3D and G. Beyond this, one attractive hypothesis is that these, and many similar early-induced microglial molecules that are maintained during phagocytosis, are

required to protect damaged neural tissue, or to counteract the damaging effects of molecules first produced by microglial phagocytes. Thus, phagocytic microglia are also mainly responsible for the synthesis of potentially neurotoxic molecules including TNFα, Fas, nitric oxide and glutamate-like substances, associated with axonal dystrophy, focal demyelination and neuronal cell loss (Merrill and Zimmerman, 1991; Raivich et al., 2002; Stagi et al., 2005, Taylor et al., 2005; Domercq et al., 2007). This microglia-first notion may be supported by the fact that, in the absence of additional damage, neuron-selective expression of inactivated TGFβ R2 does not seem to be associated with pronounced neurodegeneration or glial response in the 4-10 month young adult mice, despite the strong effects in blocking TGFβ-mediated neuroprotection in cell culture (Tesseur et al., 2006).

Nevertheless, as all 3 main cell types affected in the TGFβ1-/- mice – neurons, astrocytes and microglia – they could also contribute to the neurodegenerative changes in these mutant mice. Thus, a direct elucidation of the cause and effect scenario using cell-type specific inactivation of TGFβ-mediated effects will considerably enhance the understanding into the neural effects of this crucial anti-inflammatory and neuroprotective cytokine.

Chapter 7

Constitutively active Ras and dominant-negative MEK1 enhances corticospinal and rubrospinal tract sprouting and improves functional recovery in mice with a C4 dorsal and dorsolateral hemisection

Introduction

Regeneration of axons seldom occurs following spinal cord injury. It is possible to attribute this to a number of causes: glial scarring; myelin inhibition; cell death; a lack of growth factor support; or, a favourable environment for axonal regeneration (for reviews see Fawcett and Asher, 1999; Yiu and He, 2006; Fouad et al., 2001a; Beattie et al., 2000). Regeneration of axons can occur after a conditioning lesion of a peripheral nerve or can grow into a peripheral nerve transplant where a number of intrinsically favourable properties of Schwann cells, such as neurotrophins, allow a more regenerative environment. Neurotrophic factors are essential nervous system proteins that modulate neuronal survival, axonal growth, synaptic plasticity and neurotransmission. Much evidence over the last few years has shown that neurotrophins are essential for re-growth following spinal cord injury.

There have been reports of several neurotrophic factors including NT3 and BDNF (Kobayashi et al., 1997; Giehl and Tetzlaff, 1996; Liu et al., 2002; Lu et al., 2001; Novikova et al., 2002) and GDNF (Bradbury et al., 1998; Baumgartner and Shine, 1998; Blesch and Tuszynski, 2001), which, when delivered in a variety of different ways, including continuous intrathecal infusion or with transduction with viral vectors, can prevent the atrophy and cell death of many neuronal subpopulations (Baumgartner and Shine 1997).

The populations of neurons where neurotrophins have had some effect in eliciting collateral and regenerative sprouting include both ascending sensory (Bradbury et al., 1999; Oudega and Hagg, 1999) as well as descending spinal tracts including the corticospinal (Zhou et al., 2003) and rubrospinal (Ruitenberg et al., 2003) systems. While several of the above studies talk about

neuroprotection, they also provide evidence of neuronal regeneration at the injury site or even increased regrowth of axons following cell transplants (Weidner et al., 1999; Tuszynski et al., 2002; Jin et al., 2002) or into a more hospitable environment such as a peripheral nerve graft (Grill et al., 1997; Hiebert et al., 2002; Kobayashi et al., 1997; Blits et al., 2000; Novokova et al., 2002); it is increasingly clear that application of various neurotrophic factors to induce long tract regeneration through a lesion site is indeed limited. For example, Bradbury et al. (1999) failed to see ascending sensory fibre growth after dorsal column crush, but observed a few axons cross the lesion site following treatment with NT3. Furthermore, Blits and colleagues (2003), while showing extensive sprouting up to the glial scar, failed to demonstrate regeneration across the lesion site. In some cases, growth of a very small number of fibres following the application of neurotrophins or neurotrophin modified transplanted cells does occur (Grill et al., 1997; Oudega and Hagg, 1999; Tuszynski et al., 2003; Jin et al., 2002; Schnell et al., 1994). The consistent failure of long-tract regeneration, even in the most comprehensive of studies highlights the need to concentrate on other forms of axonal regrowth such as axonal sprouting. Moreover, it may be that the reported improvement in behavioural performance seen with application of neurotrophic factors is due to sprouting both in damaged and neighbouring undamaged neuronal systems. For example, Jefferey and Fitzgerald (2001) reported sprouting of undamaged corticospinal tract with concomitant ablation of the rubrospinal tract and subsequent application of NT3. Certainly, spontaneous sprouting following partial spinal cord injury has been shown to form new, viable intraspinal circuits which contribute to functional recovery (Bareyre et al., 2004; Raineteau and Schwab, 2001; Li and Raisman, 1995). However, sprouting of injured axons into neighbouring intact axons occurs more frequently following administration of neurotrophins (Zhou et al., 2003; Zhou and Shine, 2003). The extents to which these sprouts make aberrant connections remains, as yet, unexplored and require extensive investigation.

While many previous studies, like those discussed above, focus on the exogenous application of neurotrophins, another, but related direction is to look at intracellular signalling molecules. The Ras-Raf-MEK-MAP kinase pathway is consistently activated following neurotrophin application. Previous chapters in

this thesis explored the effect of two intracellular effectors Ras and MEK which are activated following neurotrophin binding to Trk receptors. In particular Chapter 4 demonstrated that mice which express constitutively active Ha-Ras (Ras+) selectively in neurons using the neuronal promoter for the synapsin I gene, display a 65% reduction in neuronal cell death in the axotomized facial nucleus. Compared with their wild-type (WT) siblings, these mutant, neuronal Ras+ mice showed enhanced central sprouting in the axotomised facial nucleus. A similar reduction in cell death and excess sprouting was also observed in mice which express a dominant negative, kinase inactive version of MEK1 (MEK1dn) using the T-α1-tubulin neuronal promoter (Chapter 5).

Although axonal regeneration is extremely limited in the mammalian adult CNS, partial lesions of the spinal cord can be followed by spontaneous and often substantial, functional improvements (Schwab and Bartholdi, 1996; Rossignol et al., 1999; Dietz et al., 1998). Although the mechanism for this is not understood, one of the reasons this may occur is through axonal sprouting. Spontaneous sprouting following spinal lesion has been demonstrated previously (Lawrence et al., 1968; Pettersson et al., 1997; Weidner et al., 2001; Fouad et al., 2001b; Raineteau and Schwab, 2001). Murray and Goldberger, (1974) suggested that for spontaneous sprouting to improve functional recovery following spinal cord injury, transected fibres must contact spared intraspinal neuronal tracts that bridge the lesion as well as going on to form synaptic contacts on the original target cells of the transected motor or sensory tract. This plastic reorganisation was recently demonstrated to improve functional recovery in mice following spinal cord lesion (Bareyre et al., 2004).

Axonal sprouting elicited in the facial nucleus by both Ras+ and MEK1dn prompted the need for further investigation into a more vigorous form of CNS injury like that following spinal cord injury. The aim in this Chapter was to explore the effects of Ras+, MEK1dn and the combination of both mutations on the sprouting and regeneration as well as functional recovery in the injured corticospinal and rubrospinal tract following a unilateral hemisection of the dorsal and dorsolateral columns in the spinal cord; with the question, whether these mutations will increase axonal sprouting in the spinal cord and whether there would be subsequent improvement in functional recovery following injury.

Materials and Methods

Animals

Adult male and female mouse littermates 8-10 weeks old were produced by crossing constitutively active Ras (Heumann et al., 2000 and Chapter 4) with dominant negative-negative MEK1dn (Mansour et al., 1994 and Chapter 5) to create a double mutant (DM) mouse with both transgenes were crossed with C57Bl/6 wild-types, the litters of which contained all 4 groups of animals – wild-type (WT), constitutively active Ras (Ras+), dominant-negative MEK1 (MEK1dn) and Ras+ x MEK1dn double mutants (DM).

Facial nerve axotomy and assessment of neuronal cell death.

Eight week old WT, and DM mice, (n=8 per group) had a right facial nerve axotomy. 30 days later, mice were perfused-fixed and neuronal survival was assessed as described in Chapter 2, Materials and Methods.

Non-integrating lentiviral vector encoding EGFP

Virus was created, and kindly donated by Dr Ahad Rahim. Briefly, D64V non-integrating lentiviral vectors were produced using a 3 plasmid transfection system. Plasmids encoding for the viral genome, viral envelope and D64V mutant integrase were used to transfect 293T human fetal kidney cells using polyethyleneimine (PEI). The plasmids were added to serum free OptiMEM (Invitrogen) and complexed with PEI. The cell medium was replaced with the complex. Following a 4 hour period of transfection the medium was replaced on the cells and left to incubate for 48 hours. The supernatant was collected and filtered through a 0.22μm filter unit in order to remove cellular debris before being aliquoted into ultracentrifugation tubes. The tubes were spun at 23000 rpm for a period of two hours at a temperature of 4°C. The supernatant was carefully poured away and the pellet was thoroughly re-suspended in OptiMEM. The virus was then frozen immediately and stored at a temperature of -80°C.

Experiment 1: Surgery (supra-dorsal spinal cord hemisection)

Animals were anaesthetised using isoflurane (5% induction and 2.5% maintenance; 1L/min oxygen). The hair on the scalp was shaved and swabbed with 70% ethanol followed by iodine (Betadine) solution. A sagittal incision made at the midline over the cervical spinal cord. A second incision was made at the superficial muscle layers followed by blunt separation of the deep layers from the midline. The C6/7 spinal process was located and the C6 and C7 lamina were exposed. The C6 lamina was cut at the midline and a bilateral laminectomy was performed. The spinal cord was exposed by folding back the dura. A unilateral dorsal hemisection was made using microscissors to a depth of the central canal. This incorporated the main portion of the CST, the dorsolateral CST was spared. The superficial muscle layers of the back were then sutured using 6-0 Prolene sutures and the skin wound closed with wound clips. Immediately after spinal cord surgery, the CST projection on the same side was labelled with biotinylated dextran amine (see below). Mice were placed in a warm chamber (37°C) to recover; given 0.5ml of warmed sub-cutaneous saline and 10mg/g body weight of buprenorphine analgesia. Manual bladder expression was performed twice daily for 2 days post-operatively, after which, it was not deemed necessary as bladder function appeared normal.

Experiment 2: Surgery (Supra-dorsal and dorsolateral spinal cord hemisection)

Animals were anaesthetised using isoflurane (5% induction and 2.5% maintenance; 1L/min oxygen). The hair on the scalp was shaved and swabbed with 70% ethanol followed by iodine (Betadine) solution. Wild-type, Ras+, MEK1dn and DM mice (n=4 per group) underwent a sagittal incision made at the midline over the cervical spinal cord. A second incision was made at the superficial muscle layers followed by blunt separation of the deep layers from the midline. The C4 lamina was cut at the midline and a bilateral laminectomy was performed. The spinal cord was exposed by folding back the dura. A unilateral dorsal hemisection was made using microscissors to a depth of the central canal to incorporate the dorsal columns, and dorsolateral white matter.

This incorporated the main CST tract, as well as the dorsolateral CST and the rubrospinal tract. The superficial muscle layers of the back were then sutured using 6-0 Prolene sutures and the skin wound closed with wound clips. The skin and superficial muscles were exposed in sham animals (n=2) but neither a laminectomy or spinal injury was performed. Following surgery, mice were placed in a warm chamber (37°C) to recover; given 0.5ml of warmed sub-cutaneous saline and 10mg/g body weight of buprenorphine analgesia. Manual bladder expression was performed twice daily for 4 days post-operatively, after which, it was not deemed necessary as bladder function appeared normal. Mice survived for 42 days post surgery and tracer injections were performed at day 28.

BDA tracing of CST projections

CST projections were traced by injecting tetramethylrhodamine and biotin conjugated dextran amine, 10,000MW, lysine fixable (mini-ruby-BDA, Molecular Probes, Invitrogen, UK) (BDA) into the sensorimotor cortex at 28 days post-injury. All mice received injections into the cortex contralateral to the spinal cord lesion to assess the extent of regrowth on the ipsilateral side to the lesion. BDA injections were performed as previously described (Inman and Steward, 2003). Briefly, animals were anaesthetised using isoflurane (5% induction and 2.5% maintenance; 1L/min oxygen). The hair on the scalp was shaved and swabbed with 70% ethanol followed by iodine (Betadine) solution. The animal was placed in a sterotaxic frame (Stoetling, USA). The skin overlying the skull was cut at the midline and small holes were drilled in the skull overlying the sensorimotor cortex. A 10ul Hamilton syringe (World Precision Instruments, USA) fitted with a fine needle was used to inject 0.5ul of BDA at a total of 3 sites. Injection coordinates were 1.0mm lateral to the midline at 0.5mm anterior and 0.5mm posterior and 1.0mm posterior to bregma at a depth of 0.5mm from the cortical surface. After completing the injections, the scalp was clipped with wound clips and the mice were placed in a warm chamber (37°C) to recover; given 0.5ml of warmed sub-cutaneous saline and 10mg/g body weight of buprenorphine analgesia.

EFGP tracing of RST projection

Labelling of the rubrospinal tract was carried out by stereotaxic injection into the right red nucleus (coordinates -3.5mm caudal, 1.5mm to bregma and 3.75mm deep) of 3µl of a replication-deficient human immunodeficiency virus (HIV) vector encoding EGFP 28 days following spinal cord injury. Injections were performed at 150nl per minute over 20 minutes. The viral vector injected in this way only infected midbrain neurons, so that only rubrospinal axons were labelled with EGFP. This viral vector was used since BDA injection into the red nucleus often produces some corticospinal labelling in addition to rubrospinal labelling.

Tissue preparation

Mice survived for 21 days following surgery and BDA injections in experiment 1. In experiment 2 where, mice received both BDA (for CST) and EGFP (for RST) at day 28, mice were then sacrificed 14 days following injections. Animals were killed with an overdose of Euthatal (200 mg/ml sodium pentobarbital) perfused transcardially with cold phosphate-buffered saline (PBS) followed by cold 4% paraformaldehyde in PBS (PBS/PFA) as described in Chapter 2 – Materials and Methods. The brain and spinal cord were carefully dissected and post-fixed in 1% PBS/PFA for 2 hours on a rotator (8rpm) followed by overnight immersion in 30% phosphate-buffered sucrose. The C1-C2 portion was cut away from the main part of the spinal cord and both segments were embedded in Tissue-Tek separately. The brain and spinal cord were frozen on dry ice and stored at -80oC until further use.

BDA processing

The spinal cord was cut longitudinally. In experiment 1 and 2, the resulting serial 40µm horizontal sections were first stored on dry ice, with every third section processed as described by Herzog and Brosamle (1997). Briefly, sections rehydrated in distilled water, spread and dried on gelatine coated slides and fixed for 5 minutes in 4% formaldehyde in 0.1M PB. Following this, they were washed 0.05M Tris-buffered saline + 0.5% Triton-X100 (TBST) prior to a 15 minute incubation in 0.3% hydrogen peroxide (made in TBST) followed

by 2 washes in TBST. Sections were incubated in ABC complex (1:100) made in TBST, overnight at 4°C. Sections were then incubated in DAB (0.05%) with NiCl2 (1%) and CoSO4 (1%) made in 0.05M TB with hydrogen peroxide (0.0332%) until the chromagen was visible. Sections were then taken through a series of graded alcohols before being coverslipped in Depex. In experiment 2, sections were rehydrated, spread, dried and fixed in 4% formaldehyde in 0.1M PB followed by a wash in 0.1M PB and then covered using Vectashield fluorescence mounting medium (Vector Laboratories) and the coverslip sealed with nail varnish.

Quantification

For experiments 1 and 2, both BDA-labelled and EGFP labelled sprouting fibres in the spinal cord, crossing a line on a microscope graticule grid every 0.5mm from 4 mm above (rostral) to 4 mm below (caudal) the lesion site were counted across the entire depth of the spinal cord. They were recorded separately for 6 individual compartments ipsilateral and contralateral to the lesion site – the corticospinal tract (CST), the spinal cord grey matter (GM) and the lateral white matter (LWM). The middle of the lesion site was taken as point zero. Experiment 1 counts were performed using light microscopy on a Nikon Eclipse 9200. Experiment 2 counts were performed on a fluorescence microscope on a Nikon Eclipse 9200 using the 450-490 filter for green (EGFP) and 510-560 filter for red (mini-ruby-BDA).

In figure 7.2A and 7.7A, the numbers of counted BDA-labelled fibres caudal to the lesion were magnified by a factor of 10 to enhance their visibility compared to values above the lesion site. Similarly, in figure 7.7B, the EGFP labelled fibres are magnified by a factor of 3 to enhance their visibility compared to values above the lesion site. To adjust for the steep gradient below the lesion with a declining number of BDA-labelled fibres in caudal direction (figure 7.2A, 7.7A, 7.7B), the number of axons crossing each gridline was multiplied with the distance from the lesion, and summed up for each compartment. The overall, caudal sprouting index was calculated by summing up the indices for all 6 compartments. A multi-way analysis of variance (MANOVA) for MEK1dn and Ras+ was used to identify differences between the four groups. Primary data was normalised against the total number of CST axons in cross section and

then using a log(x+1) function and incorporated into the following sprouting index:

$$= 6+ \sum_{i=1}^{6} \log\ (0.1+ \sum_{j=1}^{8} n_{ij}{}^{*}\ j\ (\text{In } 0.5\text{mm})/ \sum_{i=1}^{8} j\ (\text{in } 0.5\text{mm}))$$

With nij= number of CST sprouts in CST tract (i= 1,4), grey matter (i=2,5), and lateral white matter (i=3,6) on the ipsilateral (1-3), and contralateral side (4-6), and j the distance below the lesion site (in 0.5mm).

Pearson's Correlation coefficient was used to determine the relationship between the extent of rostral and caudal sprouting determined by the following indices for ipsilateral white matter (LWM):

$$2+\log\left(0.01+2^{*}\ \frac{\text{LWM}}{\Sigma(\text{CST+GM})}\right)$$

where CST - corticospinal tract; GM - grey matter; LWM - lateral white matter.

Behavioural testing

WT, Ras, MEK1dn and DM mice (4 animals in each of the 4 groups) were examined for the rearing and grid walk tests and were based on modified experiments by Starkey et al. (2005)

Grid walk

The grid test assesses the ability of the mouse to accurately place the fore and hind paws during spontaneous exploration of an elevated grid. Mice were placed on a wire grid (330mm^2 with 15mm x15mm grid squares) and allowed to freely explore for 3 minutes. Baseline scores were taken 2 days prior to injury following which mice were videotaped and a blind experimenter scored the percentage foot slips in each paw from the first 50 footsteps at days 2, 7, 14, 21 and 28 days post injury.

Rearing

The rearing test examines forelimb use for weight bearing during vertical exploration of a cylinder. Animals were placed in a clear cylinder (90mm in diameter and 300mm in height) for 5 minutes and recorded on a Sony digital camera (DCR-HC46, Sony, UK). A mirror was placed behind the cylinder so that paws could be viewed at all times. Animals required no pre-training but were placed in the cylinder twice prior to surgery for habituation and baseline scores were obtained 2 days prior to surgery. Following C4 unilateral hemisection, mice were scored, by a blind experimenter, for independent use of the left or right forepaw or simultaneous use of both paws at day 2, 7, 14, 21 and 28 days post injury. The left involvement in rearing (LIR) was calculated using the index 3*LP+2*BP+1*RP-1, where LP, BP and RP are the percentage use of the left paw, both paws and right paw respectively.

RESULTS

Combined Ras+ and MEK1dn (DM) mice show increased neuronal survival

Since both Ras+ and MEK1dn mice showed enhanced neuronal survival following facial axotomy (Chapters 4 and 5 respectively), neuronal survival was examined 30 days post axotomy in Nissl stained sections. All neuronal profiles were counted through the entire extent of the facial nucleus on both the control and operated side and corrected for neuronal cell size using the Abercrombie coefficient (Abercrombie, 1946). Compared to the unoperated side, axotomy led to a loss of 37% of neurons in the WT (2102+/-57 and 1325+/-98 on the control and axotomised sides respectively) mice. In the mutant group there was a dramatic reduction in neuronal cell death. Here the loss was 12% compared with the unoperated side (2148+/-21 vs 1668+/-143 on the control and axotomised sides respectively; $p<0.05$ in Student's t-test; n=8 animals per group; figure 7.1A).

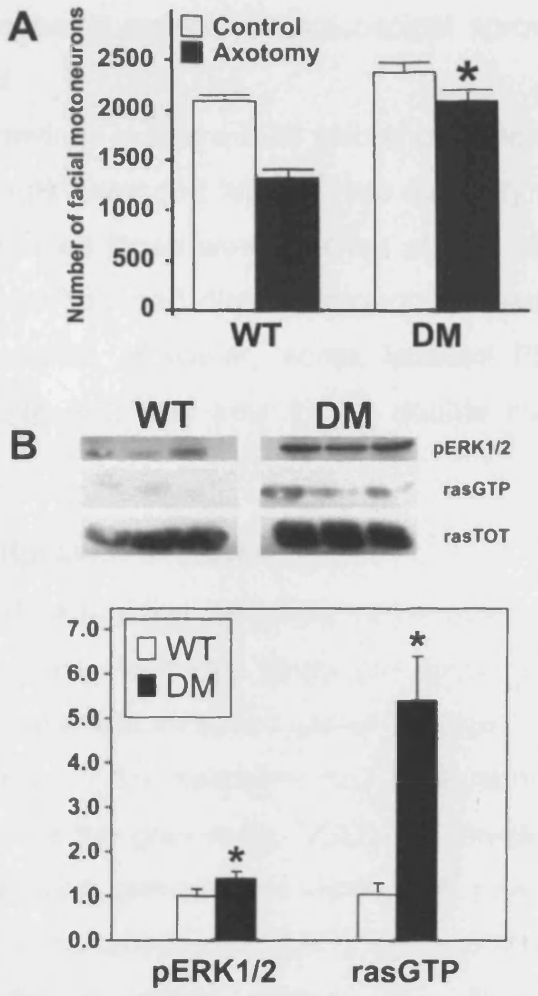

Figure 7.1. **(A)** Combined expression of constitutively active Ras and dominant negative MEK1 (DM) reduces neuronal cell death 30 days after facial axotomy in DM animals compared with wild type (WT) controls (empty bars - contralateral, filled bars - axotomised side, *p<0.05 in Student's t-test, n=8 WT and n=8 DM mice). **(B)** Effects of neuronal expression of MEK1dn on cortical levels of phosphorylated ERK1/2, total (rasTOT) and active form of ras (rasGTP). Top: Pulldown/WesternBlot assays, Bottom: Quantitative changes in wild type (WT) and ras/MEK1dn double mutants (DM). In each of three cases (pERK, rasGTP) Anova, followed by Tukey post-hoc tests showed significant difference between double mutants to wild type animals (*p<0.05).

Experiment 1: Supra-dorsal spinal cord hemisection

In a first experiment to investigate the sprouting response in the corticospinal tract following injury, a unilateral dorsal hemisection at C6, sparing the dorsolateral component, followed by anterograde labelling with BDA was performed. After a 21 day survival period the spinal cords were sectioned and stained for BDA. Compared with their wild type (WT) littermates, mutants with the overexpression of neuronal Ras, MEK1dn or of both (in the double mutants

- Ras x MEK1dn), revealed extensive corticospinal sprouting into the caudal part of the spinal cord.

The camera lucida drawings in figure 7.2B also show extensive sprouting above the lesion where sprouts extended laterally into the grey matter and the white matter tracts. BDA-labelled fibres were blocked at and, slightly retracted from, the lesion site and none crossed directly through the lesion scar in wild-type, Ras or MEK1dn mutants. However, some labelled fibres were observed crossing the lesion site and glial scar in the double mutant animals (figure 7.2C).

Improved neurite outgrowth in mutant mice

The total number of BDA-labelled sprouting axons crossing the 0.5mm optical gridlines from 4 mm above to 4 mm below the lesion site was quantified as described in Materials and Methods, and shown in figure 7.2A. Above the lesion site, all 6 compartments – the ipsilateral and contralateral corticospinal tract (iCST, cCST), as well as the grey matter (GM) and lateral white matter (LWM) contained the BDA-labelled, corticospinal axons, with a particularly high number in iCST and iGM. Both compartments (iCST, iGM) showed very little variation (+/-20%) between the 4 animal groups (WT, Ras+, MEK1dn, double mutants/DM). However, despite the strong interanimal variability, there was a tendency towards 2-3 fold higher numbers in the MEK1dn and double mutant groups in the other 4 compartments (iLWM, cCST, cGM, cLWM) which normally only contained few fibres (1-10% of iCST).

These differences were considerably more consistent below the corticospinal tract lesion site. In the WT group, only one out of 7 animals (1/7) showed BDA-labelled axons below the lesion site, restricted to the ipsilateral grey and white matter (figures 7.2A). The Ras+ animals showed a moderate increase (2/5), with a consistent improvement in the MEK1dn (4/6) and double mutant animals (5/6). The latter two groups also exhibited more widespread sprouting throughout the 6 compartments below the lesion site, pointing to an inherent increase in the ability to sprout. These changes were confirmed by the overall caudal sprouting index (figure 7.2C), which showed, using multi-way ANOVA, a moderate tendency to higher values for Ras+, and a highly significant increase for MEK1dn ($p<0.02$).

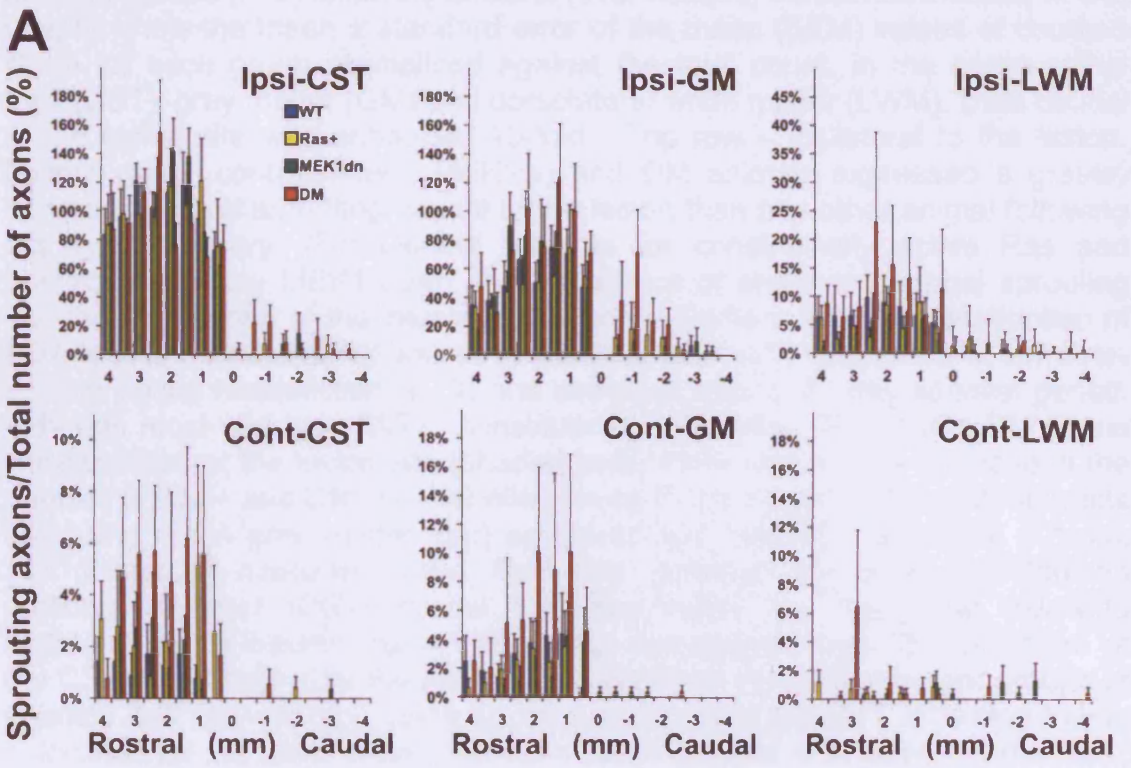
A
Sprouting axons/Total number of axons (%)
Ipsi-CST
Ipsi-GM
Ipsi-LWM
WT
Ras+
MEK1dn
DM
Cont-CST
Cont-GM
Cont-LWM
Rostral (mm) Caudal

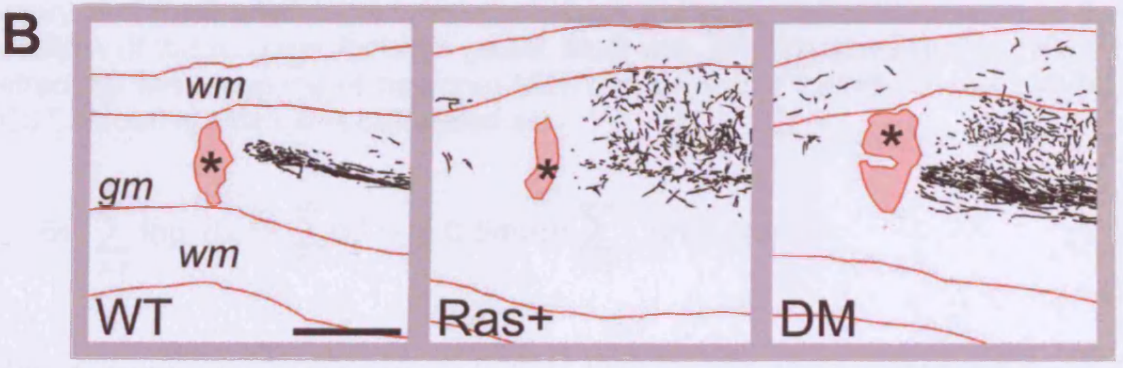
B
wm
gm
wm
WT
Ras+
DM

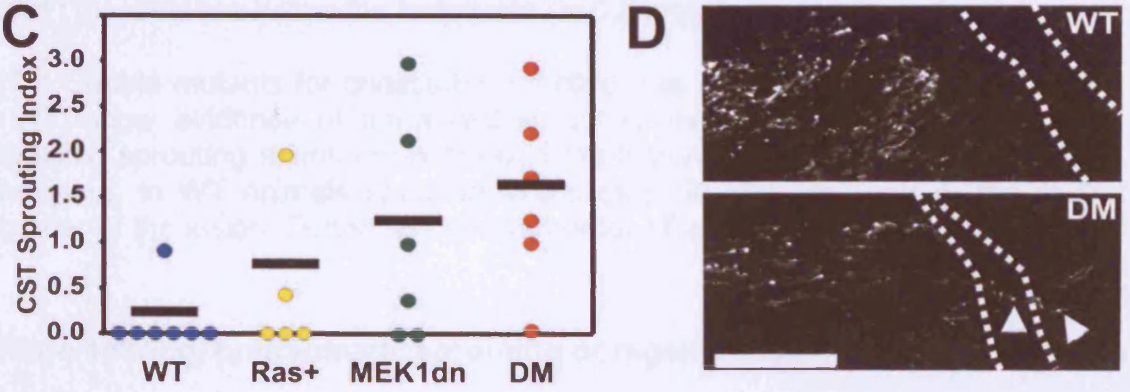
C
CST Sprouting Index
WT
Ras+
MEK1dn
DM
D
WT
DM

Figure 7.2. (A): Quantification of biotinylated dextran amine (BDA)-labelled collateral sprouts in the spinal cord of WT (n=7), Ras+ (n=5), MEK1dn (n=6) and DM groups (n=6) following unilteral (over-midline) dorsal hemisection at C6. Graphs show the mean ± standard error of the mean (SEM) values of counted fibres for each group normalised against the total count, in the corticospinal tract (CST), grey matter (GM) and dorsolateral white matter (LWM). Data caudal to the lesion site was enhanced 10-fold. Top row – ipsilateral to the lesion, bottom row – contralateral. MEK1dn and DM animals expressed a greater degree of central sprouting caudal to the lesion than any other animal following this type of injury. **(B):** Double mutants for constitutively active Ras and dominant negative MEK1 (DM) show evidence of enhanced axonal sprouting into the caudal part of the injured spinal cord. Camera lucida reconstruction of BDA-labelled corticospinal axons in animals that were subjected to an over-midline dorsal hemisection at C6 and analysed after a 21 day survival period. Although most wild-type (WT), constitutively active Ras (Ras+) and DM axons were blocked at the lesion site (shaded area) there was a clear increase in the number of Ras+ and DM BDA-labelled axons in the adjacent dorsolateral tracts (wm) and in the grey matter (gm) compared with the WT. Bar scale = 1mm. **(C):** Effect of neuronal active Ras and dominant negative MEK1dn on corticospinal tract (CST) axonal sprouting below the injury site following unilateral dorsal column injury sparing the dorsolateral tract. Quantification of the CST sprouting below the injury site in the three litter-mate mutant groups of animals and the wild-type controls. The values show the CST sprouting index, calculated on the basis of the number of BDA-labelled CST axons in the CST, grey matter and lateral white matter on the ipsilateral and contralateral site, at 0.5mm-4mm below the lesion site with linear weighting for the distance from the injury site. Each point represents one animal, the thick horizontal lines show the position of the average for each group. Multi-way ANOVA showed a significant effect for the presence of neuronal MEK1dn, with an $F_{1,21}=6.75$ and $p<0.02$. CST sprouting index was calculated as:

$$= 6+ \sum_{i=1}^{6} \log \left(0.1+ \sum_{j=1}^{8} n_{ij} * j \,(\text{ln } 0.5\text{mm})/ \sum_{i=1}^{8} j \;(\text{in } 0.5\text{mm})\right)$$

With nij= number of CST sprouts in CST tract (i= 1,4), grey matter (i=2,5), and lateral white matter (i=3,6) on the ipsilateral (1-3), and contralateral side (4-6), and j the distance below the lesion site (in 0.5mm).

(D): Double mutants for constitutively active Ras and dominant negative MEK1 (DM) show evidence of enhanced sprouting through the lesion site. BDA-labelled sprouting axons cross through the lesion site in DM animals (arrows), however, in WT animals spouting axons stop 50-100 um short of the rostral border of the lesion. Dotted line shows border of lesion site. Scale bar = 0.1mm

Fibre sparing, pretraumatic sprouting or regeneration?

In a second stage, to gain insight whether these changes are due to fibre sparing, pre-traumatic sprouting, or to a post-traumatic response, the individual

components of this sprouting response were explored. The data shown in figure 7.2A show a consistent decline in the number of BDA-labelled axons with increasing distance below the lesion site, in the 3 most axon-abundant compartments iCST, iGM and iLWM. Similar steep gradient was also noted in previous studies on spinal cord regeneration (Schwab et al., 1993; Liebscher et al., 2005), arguing against spared fibres and pointing to de novo sprouting blocked by local inhibitory molecules in grey and white matter.

Since the data shown in figure 7.2A showed enhanced number of BDA-labelled axons in the ipsilateral white matter, and in the contralateral 3 compartments, the statistical correlation between the ipsilateral and contralateral sprouting indices above the lesion site (see materials and methods), and the caudal sprouting index was assessed. Very little correlation was observed between the ipsilateral and caudal sprouting (r^2 = 0.17, not statistically significant), with many WT and mutant animals showing a high ipsilateral index, but no sprouting below (figure 7.3A). Examination of a correlation between alternative pathways above the lesion (i.e. compartments above the lesion excluding the ipsilateral CST) with caudal sprouting below the lesion again showed very little, statistically insignificant correlation (r^2=0.28).

Experiment 2: Supra-dorsal and dorsolateral spinal cord hemisection

The sprouting observed in the spinal cord following C6 lesion demonstrated that both Ras, MEK1dn or a combination of both, enhance regrowth of injured axons. To test whether the sprouting effect had an effect on functional outcome the initial experiment to accommodate three reliable testers of functional recovery was modified. Here, the effects of both CST and RST together were tested by inflicting a more severe lesion whereby the dorsal and dorsolateral columns were cut at C4 followed by labelling of the CST and RST. The injury at C4 enabled the use of rearing and gridwalk analysis on the injured forepaw. A simple dorsal column lesion test is not appropriate here since studies (Jefferey and Fitzgerald, 2001; Raineteau et al., 2001) have shown that the intact dorsolateral CST and rubrospinal tract would sprout fibres toward the main CST and may affect physiological outcome.

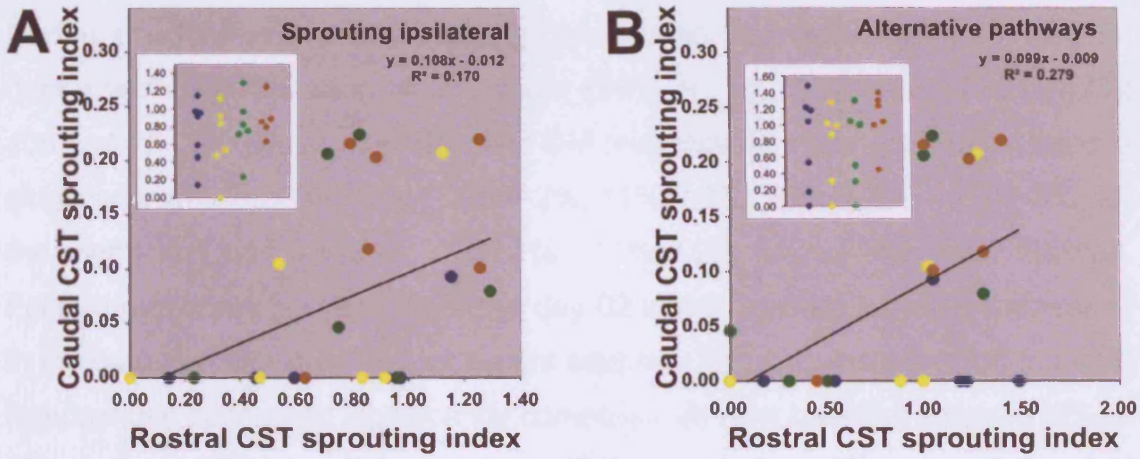

Figure 7.3. (A) Comparison of the sprouting into ipsilateral white matter (Y-axis) and the CST sprouting index (X-axis) demonstrated only a small positive correlation of $r^2 = 0.17$. Ipsilateral white matter sprouting index was calculated as:

$$2+\log\left(0.01+2^{*}\frac{LWM}{\Sigma(CST+GM)}\right)$$

where CST - corticospinal tract; GM - grey matter; LWM - lateral white matter.

(B) Comaparison of the alternative pathways contributing to the caudal sprouting. Fibre sprouting in all compartments above the lesion except the ipsilateral corticospinal tract were compared with the caudal sprouting response. Comparison showed a small positive correlation of $r^2 = 0.28$.
Inserts show the relative sprouting distribution in all compartments rostral to the injury on the ipsilateral side (A); and, all compartments rostral to the injury excluding axonal counts in the the ipsilateral CST (B).

To investigate the sprouting response in the corticospinal tract following injury, a unilateral (left) dorsal hemisection was performed at C4 and the mice were assessed for functional recovery using the rearing and gridwalk tests for 28 days at days 2, 7, 14, 21 and 28 followed by anterograde labelling with BDA. After a 42 day survival period the spinal cords were sectioned and stained for BDA.

Improved rearing and gridwalk in mutant mice

During pre-surgery baseline testing, mice used both paws (figure 7.4A, D) during vertical exploration of a cylinder (98% +/- 1%; 96%+/- 4%; 98%+/-2%; 106%+/-4%; WT, Ras+, MEK1dn and DM respectively; mean+/-SEM). Use of a single paw was less frequent (12%+/-2%; 11%+/-3%; 13%+/-2%; 10%+/-3%) for the right and (10%+/-2%; 7%+/-1%; 11%+/-2%; 16%+/-4%) for the left. Following injury mice were tested at day 02 which showed a marked alteration in the pattern of forepaw use for weight support. The percentage of left (injured) forepaw use decreased significantly compared with the baseline score to (0%+/-0%; mean+/-SEM) in all four groups (figure 7.4B, C). The use of the right (uninjured) forepaw increased significantly compared to baseline values to (100%+/-0%; 100%+/-0%; 95%+/-3%; 98%+/-2%.mean +/-SEM) in all four groups (figure 7.4E), presumably to compensate for the loss of function in the left paw.

To establish whether differences existed within groups, we calculated the percentage use of the left paw in rearing as well as the use of the left paw when both paws were being used. Both paws together combined with the use of the left paw alone, calculated using the LIR index (see methods) gave us a total score for the recovery of the injured side. Here, both Ras and MEK1dn groups did significantly better than WT littermates at day 14 (35.0%+/-9.0%; 45.0%+/-7.0% versus 9.0%+/-5.0%; mean+/-SEM; **$p<0.03$). Interestingly, the DM group performed better at a later stage, with a significant improvement at day 28 (50.0%+/-9.0% mean +/-SEM; **$p<0.03$) compared with the WT (13.0%+/-5.0%; mean +/- SEM) and the Ras (25.0%+/-3.0%; mean +/- SEM) littermates (figure 7.4F).

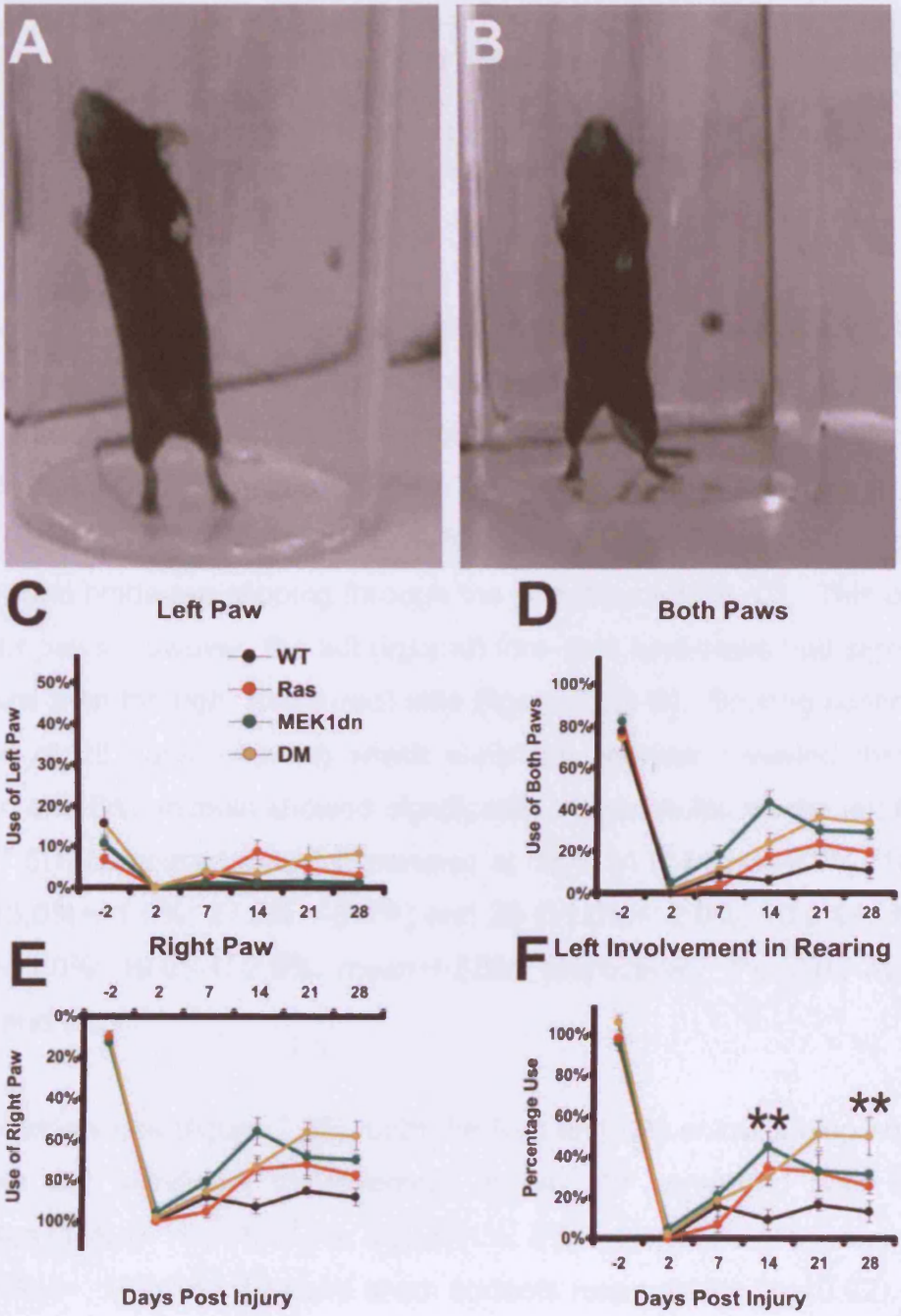

Figure 7.4. Mice expressing active Ras, MEK1dn or the combination of the 2 mutations (DM) show improved rearing following C4 unilateral dorsal hemisection compared with WT littermates. WT (n=4), Ras (n=4), MEK1dn (n=4) and DM (n=4) mice were examined for forelimb use during spontaneous vertical exploration of a cylinder for 28 days at days 2, 7, 14, 21 and 28 following C4 injury. (A) shows a control (uninjured) mouse using both paws for weight support during rearing. (B) shows use of the right (uninjured) paw for weight support during rearing. (C-E) shows quantification of forepaw use for the left (C), both (D) and right (E) following C4 injury. (F) shows an index for the use of the left paw in rearing (LIR Index) compared with right paw and both paw use. The Index was calculated as LIR = 3*C+2*D+1*E - 1.
Baseline data (day -02) show that mice use both forepaws approximately 80% of the time in all four mutant groups and use individual forepaws less frequently

(C-E). Following injury, mice used the right (uninjured) paw more than the left (injured) paw (C and E). Both Ras and MEK1dn groups did significantly better than WT littermates (one-way ANOVA followed by posthoc Tukey) at day 14 (**p<3%). Interestingly, the DM group performed better at a later stage, with a significant improvement at day 28 compared with the WT and the Ras littermates. All data are mean+/- SEM

The grid walking test assesses the ability of the mouse to accurately place the injured forepaw or hindpaw during spontaneous exploration of an elevated grid. Prior to surgery and during baseline scoring, mice accurately placed all paws on the grid during exploration (figure 7.5A). Following C4 injury, mice in all four groups (WT, Ras+, MEK1dn and DM) failed to grasp the rungs of the grid with left fore- and hindpaws slipping through the grid (figure 7.5B, C). This occurred in all four paws, however, the left (injured) fore- and hind-paws had significantly more slips than the right (uninjured) side (figure 7.5D-G). Scoring continued for a period of 28 days following which statistical analysis revealed that Ras+, MEK1dn and DM animals showed significantly less footslips on the left forepaw (figure 7.5D) compared to WT littermates at days 14 (14.0%+/-2.0%; 10.0%+/-1.0%; 13.0%+/-1.0%; 27.0%+/-3.0%) and 28 (11.0%+/-2.0%; 10.0%+/-1.0%+/-; 12.0%+/-1.0%; 19.0%+/-2.0%; mean+/-SEM, respectively. **p<0.02 overall, at day 14 and 28.

In left hindpaw use (figure 7.5F), both the Ras and DM animals also showed a moderate but significant improvement at day 28 compared with the WT littermates (14%+/-1%; 9%+/-2%; 12%+/-1%; 8%+/-1%; 1%+/-1%; mean+/-SEM for WT, Ras+, MEK1dn, DM and sham controls respectively. **p<0.02). On the uninjured side, no significant difference was observed between any of the 4 groups for the right forepaw (figure 7.5E) or the right hindpaw (figure 7.5G).

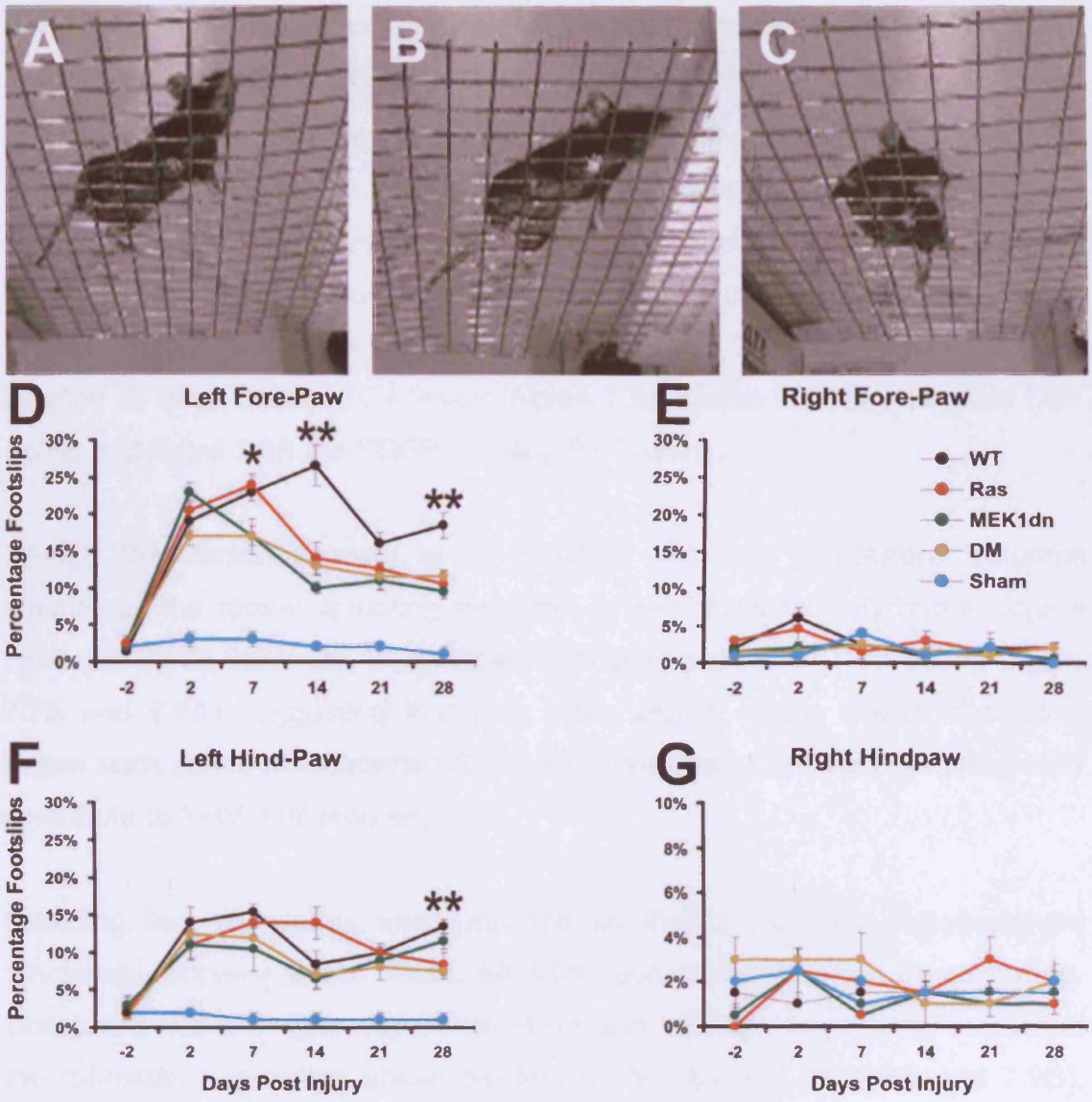

Figure 7.5. Mice expressing Ras, MEK1dn and the double mutants (DM) for both Ras and MEK1dn perform significantly less footslips than WT littermates following unilateral C4 dorsal hemisection cutting through the dorsal funiculus (containing CST), dorsal horn AND the dorsolateral tract. WT, Ras, MEK1dn and DM mice (4 animals in each of the 4 groups) were examined for paw placement following spontaneous exploration of an elevated grid. (A) shows a control mouse a accurately placing its paws on an elevated grid. Following C4 unilateral dorsal hemisection, mice fail to grasp the rungs of the grid with the left (lesioned) forepaw (B) or hindpaw (C). Statistical analysis (one-way ANOVA followed by post-hoc Tukey) revealed that Ras, MEK1dn and DM animals show significantly less footslips on the left forepaw (D) compared to WT littermates (**p<2% overall, and at day 14 and 28. *p<5% For DM or MEK1dn vs WT also at day 7). In left hindpaw use (F), both the Ras and DM animals also showed a moderate but significant improvement at day 28 compared with the WT littermates (**p<2%). On the uninjured side, no significant difference was observed between any of the 4 groups for the right forepaw (E) or the right hindpaw (G). All data are mean+/- SEM

Sprouting and neurite outgrowth in the CST and RST following dorsal column and dorsolateral lesion to the spinal cord

Previous data from experiment 1, in which the dorsal columns were injured and where the dorsolateral columns were spared, revealed extensive corticospinal sprouting in mutants expressing MEK1dn into the caudal part of the spinal cord (figure 7.2A) as well as numerous fibres being able to cross the lesion scar in the MEK1dn x Ras double mutants (figure 7.2D). The CST and RST were labelled 28 days following C4 lesion. Figure 7.6A shows the BDA- labelled CST axons and figure 7.6B the EGFP-labelled RST axons.

Injuring the dorsal columns at C4 together with the dorsolateral columns maintained the rostral sprouting response in the ipsilateral grey matter (figure 7.9A and 7.8C), however, it significantly reduced caudal CST sprouting (figure 7.7A and 7.8A) suggesting that this, more severe injury, blocks alternative routes such as the dorsolateral CST in which the main CST tract sprouting may contribute to functional recovery.

Labelling the rubrospinal tract provided an insight into how the improved functional recovery in the Ras+, MEK1dn and DM mice may be occurring. Compared with wild-type mice, both Ras+ and MEK1dn moderately increased the rubrospinal sprouting above the lesion site (figure 7.7B, 7.8D and 7.9B), however, the combined mutation in the DM animals showed more grey matter sprouting than wild-type animals or the individual Ras+ and MEK1dn mutant mice (figure 7.7B, 7.8B, 7.9B), although this was not statistically significant. Moreover, all three mutant groups showed caudal sprouting of EGFP-labelled fibres and, while the effects in Ras+ mutants were moderate compared with the wild-type, the presence of MEK1dn appeared to enhance caudal sprouting of EGFP-labelled fibres (figure 7.8B)

Interestingly, in the DM mice, some rubrospinal fibres were also observed extending from the rostral side into the lesion, although they did not cross the lesion site (figure 7.10).

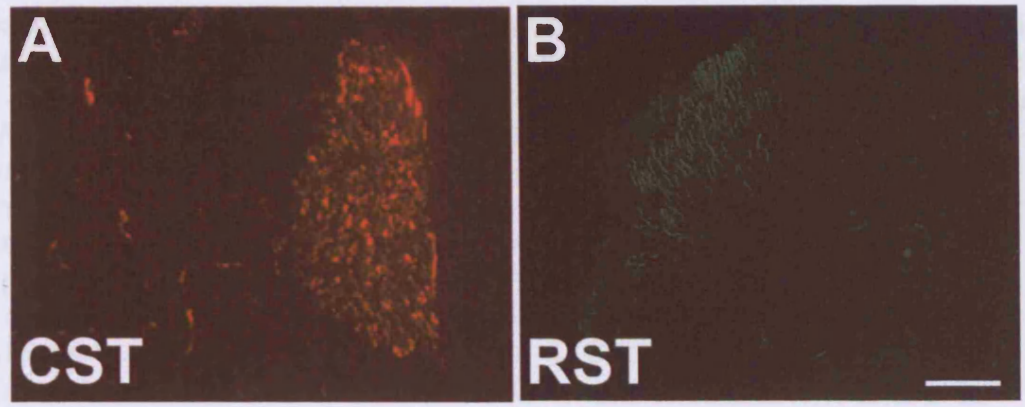

Figure 7.6. Transverse section of spinal cord at C4 showing labelling of the corticospinal tract with BDA-conjugated mini-ruby (A); and rubrospinal tract labelled with a replication deficient human immunodeficiency virus encoding enhanced green fluorescent protein (B). Scale bar: 60um in A and 80um in B

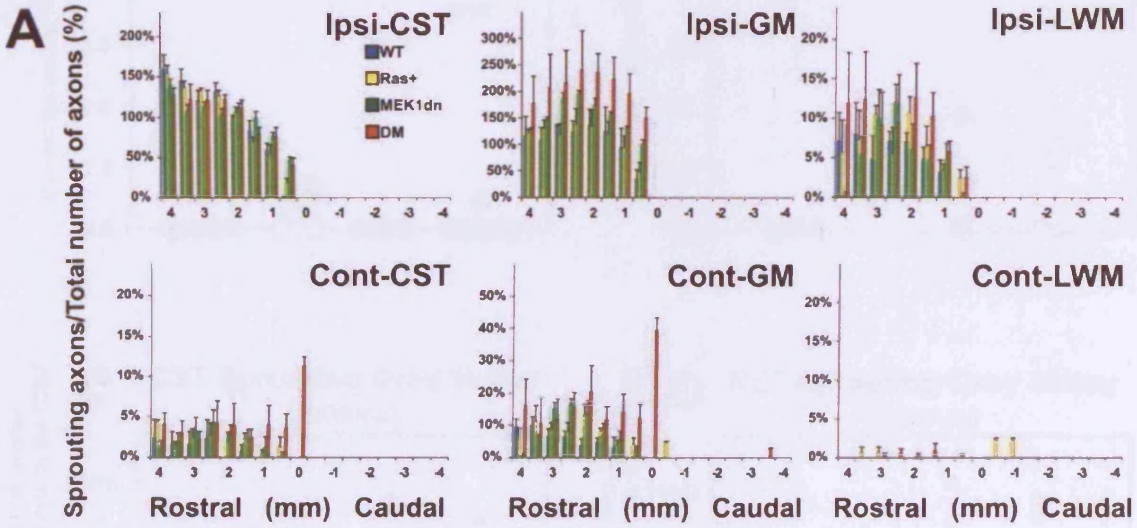

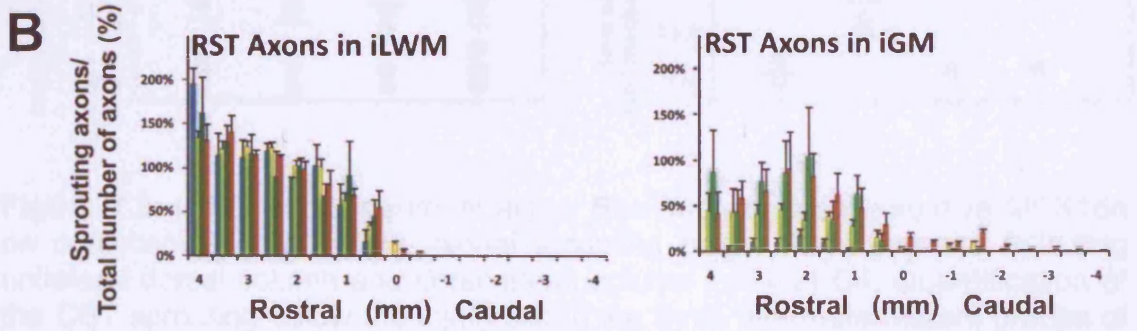

Figure 7.7. (A) Quantification of biotinylated dextran amine (BDA)-labelled collateral sprouts in the spinal cord of WT (n=8), Ras+ (n=8), MEK1dn (n=8) and DM groups (n=7) following unilteral (over-midline) dorsal and dorsolateral

hemisection at C4. Graphs show the mean ± standard error of the mean (SEM) values of counted fibres for each group normalised against the total count, in the corticospinal tract (CST), grey matter (GM) and dorsolateral white matter (LWM). Data caudal to the lesion site was enhanced 10-fold. Top row – ipsilateral to the lesion, bottom row – contralateral. Extending the dorsal hemisection to include the dorsolateral tract abolishes caudal sprouting almost entirely. (B) Quantification of EFGP-labelled rubrospinal axons in the ipsilateral lateral white matter (LWM) and in the ipsilateal grey matter (iGM). Graphs show the mean ± standard error of the mean (SEM) values of counted fibres for each group normalised against the total count.). Data caudal to the lesion site was enhanced 3-fold. Sprouting of rubrospinal axons is observed in the ipsilateral grey matter, caudal to the lesion and appears to be prominent in DM mice.

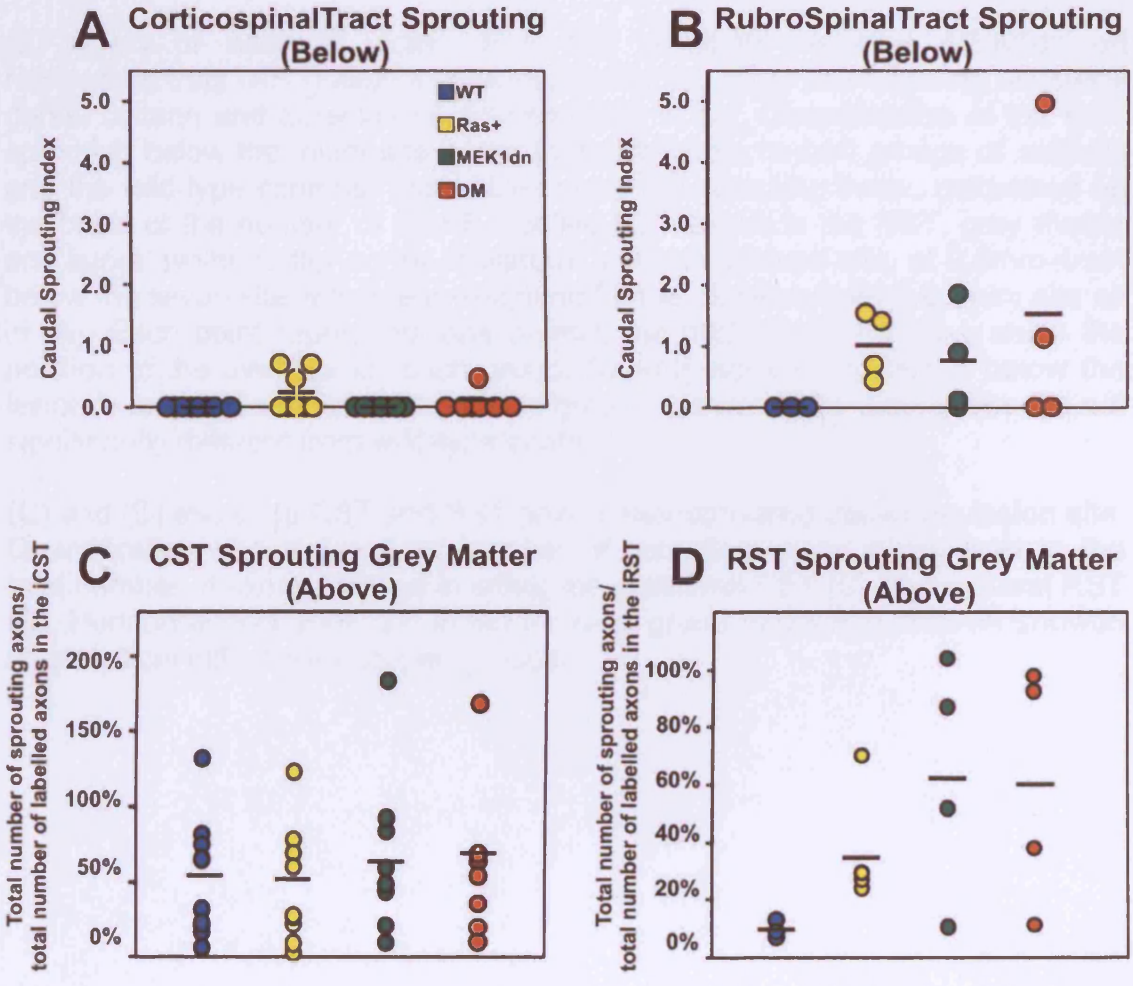

Figure 7.8. (A) Effect of neuronal active Ras and dominant negative MEK1dn on corticospinal tract (CST) axonal sprouting below the injury site following unilateral dorsal column and dorsolateral column injury at C4. Quantification of the CST sprouting below the injury site in the three littermate mutant groups of animals and the wild-type controls. The values show the CST sprouting index, calculated on the basis of the number of BDA-labelled CST axons in the CST, grey matter and lateral white matter on the ipsilateral and contralateral site, at 0.5mm-4mm below the lesion site with linear weighting for the distance from the injury site. Each point represents one animal; the thick horizontal lines show the

position of the average for each group. Combined transection of the CST at the dorsal funiculus as well as the dorsal horn and dorsolateral tract, abolishes almost all the CST sprouting below the injury site
CST sprouting index was calculated as:

$$= 6+ \sum_{i=1}^{6} \log \left(0.1+ \sum_{j=1}^{8} n_{ij} * j \,(\text{ln } 0.5\text{mm})/ \sum_{i=1}^{8} j \;(\text{in } 0.5\text{mm})\right)$$

With nij= number of CST sprouts in CST tract (i= 1,4), grey matter (i=2,5), and lateral white matter (i=3,6) on the ipsilateral (1-3), and contralateral side (4-6), and j the distance below the lesion site (in 0.5mm).

(B) Effect of neuronal active Ras and dominant negative MEK1dn on rubrospinal tract (RST) axonal sprouting below the injury site following unilateral dorsal column and dorsolateral column injury at C4. Quantification of the RST sprouting below the injury site in the three littermate mutant groups of animals and the wild-type controls. The values show the sprouting index, calculated on the basis of the number of EGFP-labelled RST axons in the RST, grey matter and lateral white matter on the ipsilateral and contralateral site, at 0.5mm-4mm below the lesion site with linear weighting for the distance from the injury site as in (A). Each point represents one animal; the thick horizontal lines show the position of the average for each group. Rubrospinal tract sprouting below the lesion is enhanced in the three mutant groups, however, the differences are not significantly different from wild-type controls.

(C) and (D) show the CST and RST grey matter sprouting above the lesion site. Quantification shows that total number of sprouting axons normalised to the total number of axons labelled in either the ipsilateral CST (C) or ipsilateral RST (D). Horizontal bars show the mean for each group. Multi-way ANOVA showed no statistical difference between groups.

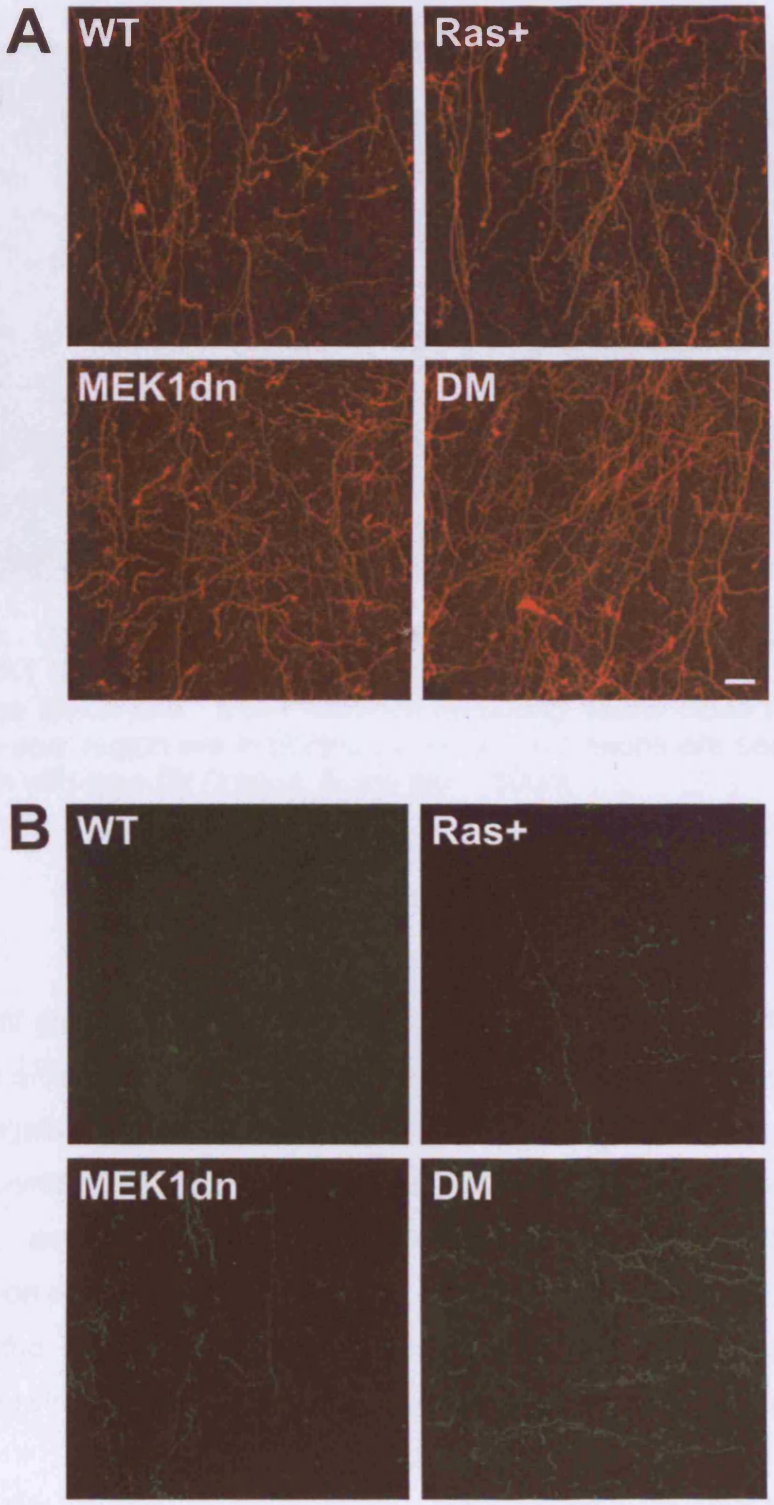

Figure 7.9. BDA-labelled CST axons (A) and EGFP labelled rubrospinal axons (B) for wild-type (WT), constitutively active Ras (Ras+), dominant-negative MEK1 (MEK1dn) and Ras+ with MEK1dn combined mutation (DM). Photomicrographs show the density of sprouting in the ipsilateral grey matter 2.0mm rostral to the lesion. Sprouting of CST axons into the grey matter is similar across all 4 mutant groups. Sprouting of rubrospinal axons into the ipsilateral grey matter appears greater in the Ras, MEK1dn and DM groups compared with wild-type (WT). Scale bar = 40um

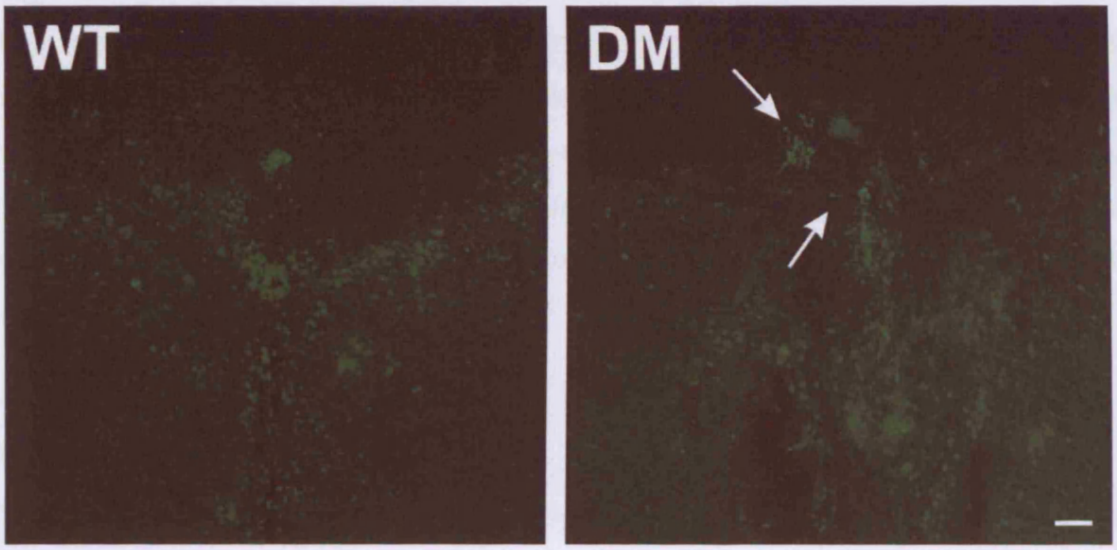

Figure 7.10. Double mutants for constitutively active Ras and dominant negative MEK1 (DM) show evidence of enhanced rubrospinal sprouting close to and within the lesion site. EGFP-labelled sprouting axons close to and in the centre of the scar region are indicated by arrows. No axons are seen within the scar region in wild-type (WT) mice. Scale bar = 50um

Discussion

In this current study three mutants were used to determine the effects of Ras, MEK1 and a combination of Ras and MEK1 in a model of spinal cord injury. A dominant negative form of MEK (MEK1dn) was used to down regulate MEK1 activity. Constitutively active Ha-Ras (Ras+) was expressed in neurons to amplify Ras activity through overexpression; and a combination of Ras overexpression and MEK1dn expression, creating a double mutant, provided an insight into the effects of the interaction of these two molecules on axonal sprouting following spinal cord injury and neuronal survival in the facial nucleus.

The data in this Chapter show that neuronal expression of MEK1dn, to some extent in combination with constitutively active Ras, strongly enhances CST sprouting below the injury site following dorsal column axotomy at C6. Following a more extensive lesion to include the dorsolateral tracts, there is an almost complete disappearance of CST sprouting. There was enhanced sprouting of rubrospinal axons both above and below the lesions in all three mutants and particularly in the presence of MEK1dn, although this was not statistically

significant. The major finding was that MEK1dn, alone, or in combination with Ras enhances functional repair (rearing, gridwalk) after C4 unilateral dorsal hemisection suggesting that local sprouting of non-ipsilateral CST fibres or the ipsilateral rubrospinal tract as primary sources for functional recovery. Indeed the increased caudal sprouting of rubrospinal axons seen in all three mutant groups suggests this is at least one route through which fore- and hind-limb recovery may be occurring.

Neuronal survival

The survival of motoneurons is mainly dependent on target derived trophic signals such as neurotrophins (reviewed in Oppenheim, 1991), and neurotrophins signal largely through the Ras pathway (Segal, 2003). One might therefore infer that motoneurons with constitutively active Ras would not be affected if the retrograde trophic support from the periphery were cut off. This certainly does seem to be the case since cell death amongst Ras+ mice was 11% compared with almost 30% in wild-type controls.

However, during the course of this study, it became evident that the Ras-Raf-MEK-ERK pathway may not be the only pathway through which cell survival was being promoted. This is because those mutants with the MEK1dn mutation also had significant, almost comparable levels of neuronal survival to those mice with the Ras+ mutation. In an attempt to address this issue, both Ras+ and MEK1dn mutants were crossed to form a double mutant (DM), in which neuronal cell death of facial motoneurons was analysed. The survival effect on the motoneurons in the DM animals was comparable to that of Ras+ or MEK1dn mutants and significantly higher from the wild-type littermates.

There are at least two hypotheses to account for this contrasting observation. Firstly, that the effects are mediated through a different pathway other than Ras-Raf-MEK-ERK such as RalGDS, since, there is strong evidence for the activation of RalGDS by Ras (Reichardt, 2006). Moreover since MEK normally creates a feedback loop for the inactivation of Ras via the protein son of sevenless (SOS), if MEK is inactivated, this feedback loop may become overloaded and thus the accumulating levels of Ras may travel via a different

route. This may occur to a greater extent in the double mutants since MEK1dn would result in further accumulation of Ras (figure 7.11). While the 3.5-fold increase in cortical Ras levels in the DM mice (figure 7.1B) lends weight to this hypothesis, levels of RalGDS would need to be assessed to confirm it. Secondly, since numerous previous studies have suggested that MEK, and its downstream signals, may have a dual role in neuronal survival; partially blocking the actions of MEK with the MEK1dn transcript may allow survival signals through but block the cell death signals. This is supported by the evidence in this thesis, since neurons are rescued with partially inactivated MEK1 (Chapter 5). However, it does not account for the Ras+ mediated neuronal survival.

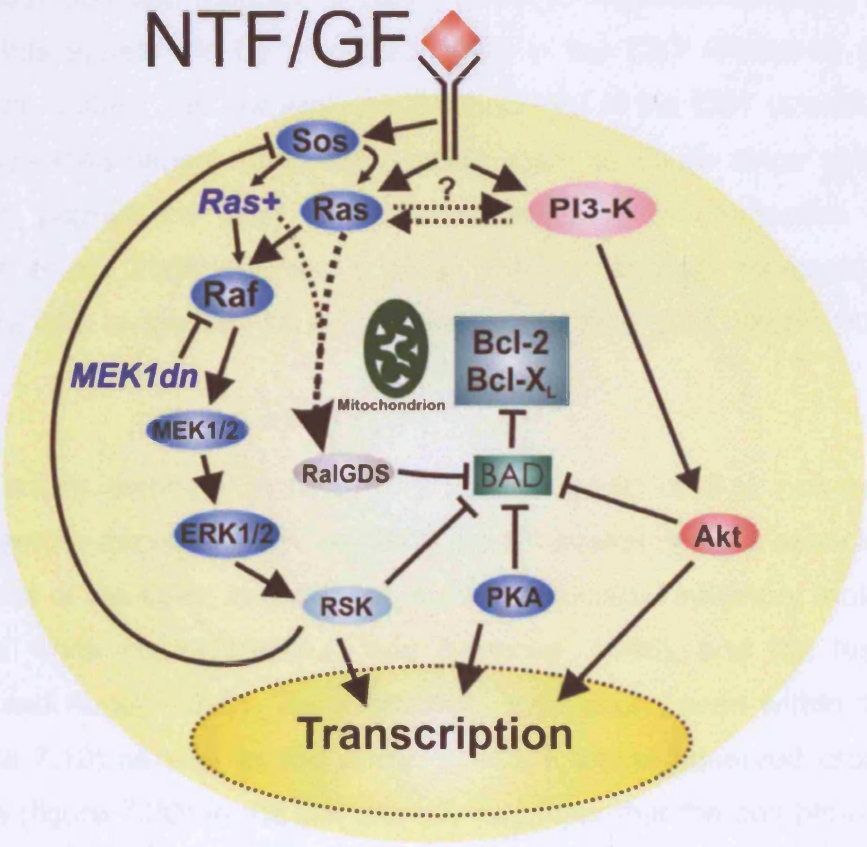

Figure 7.11 A schematic summary of the activation of the Ras-Raf-MEK1/2, ERK1/2, RSK and son of sevenless (Sos) as part of a growth factor (GF) or neurotrophin (NTF) mediated response, causing changes in nuclear transcription, based on in vitro data. In the current study, constitutively active, viral Ha-Ras (Ras+) was expressed in neuronal cells using the synapsin I promoter. A 1.1-kb Tα1 -tubulin promoter element that confers neuron-specific and pan-neuronal transgene expression was also used to drive the expression of an haemagglutinin-11 (HA)-tagged DN form of MEK1 bearing a K97M mutation. This mutation is within the ATP-binding site, yielding a kinase-inactive

mutant. The mutant MEK competes with endogenous MEK1 and MEK2 for binding to the activating kinases Raf-1 and B-Raf but cannot in itself phosphorylate and activate ERK1 and ERK2. In mice where both Ras+ and MEK1dn are expressed (double mutants, DM), it is hypothesised that Ras may induce its anti-apoptotic effect through activation of Ral-GDS (dotted line) since increased neuronal Ras levels do not augment the levels of PI3-kinase and Akt in vivo (hence the ? Mark).

Ras+ and MEK1dn mediated axonal sprouting and functional recovery in the injured spinal cord

In the days following lesion to the spinal cord, most cut axons will sprout neurites (Li and Raisman, 1994). However, unless there has been pharmacological or genetic intervention, no sprouts grow back to their synaptic targets. Both CST and rubrospinal axons undergo retraction following axotomy, although this appears to be more prominent in the CST (Pallini et al., 1988; Fabes et al., 2006). The low regenerative potential of the CST is unlikely to be due to increased sensitivity to components such as Nogo since sprouting of both axon populations after injury is enhanced by neutralisation of Nogo (Brosamle et al., 2000; Raineteau et al., 2001), although rubrospinal axons have more of a propensity to sprout and regrow than CST axons (Kim et al., 2004)

Several factors combine to make the injured spinal cord a non-permissive environment for axonal growth including growth-inhibitory cues associated with components of the CNS, in particular, myelin-associated inhibitory molecules of the spinal white matter (Schwab and Bartholdi, 1996), and the lesion scar (Fawcett and Asher, 1999). The rubrospinal tract axons seen within the lesion site (figure 7.10) as well as the numerous CST axons observed crossing the lesion site (figure 7.2D) in the DM animals suggests that the combination these two mutations can help overcome the inhibitory components of the lesion scar. This intrinsic ability of CNS axons to grow has been noted in axons that have received a prior conditioning injury (Neumann and Woolf, 1999). Thus, it may be that the constitutive presence of these mutations mimics an elevated cell body response. Analysis of the presence of elevated levels of various regeneration mediators such as c-jun and GAP-43 in the cell bodies of these mutants would add weight to this hypothesis.

The axonal sprouting observed in the spinal cord in individual mutants is in line with what has been observed in the facial nucleus in Chapter 4 for Ras+ and Chapter 5 for MEK1dn. For example Ras+ mutants show a moderate increase in sprouting axons in the facial nucleus compared with wild-type littermates. Mechanistically this has been attributed to an increase in ERK activation (Heumann et al., 2000; Markus et al., 2002; Romero et al., 2007). Whilst the results for MEK as a pro-regenerative mediator have been mixed and inconclusive in vitro, the results both in Chapter 5 and in this chapter in the spinal cord demonstrate that MEK has a predominantly negative role in axon regrowth and that, at least partial inhibition of this intracellular mediator is beneficial to neurite outgrowth and sprouting.

However, the mechanism by which axonal sprouting occurs in DM mice is somewhat complex. On the one hand, constitutively active Ras is driving the Ras-Raf-MEK-ERK pathway; however, on the other hand, the same pathway is being partially inhibited by the dominant-negative MEK1 construct. What is perplexing is how the combination of signals produces the increased sprouting response observed in these mice. The explanation for this axonal sprouting could be paralleled to the explanation offered for the effects on neuronal survival. Thus, that Ras+ may mediate its effects via alternative downstream mediators such as RalGDS. Alternatively, the partial blocking of MEK with the dominant-negative construct 'filters' through the 'positive' signals for axonal regrowth but inhibits the 'negative' signals that reduce neurite outgrowth. These hypothetical mechanisms may not be mutually exclusive, but work in tandem to produce an effect. The exact mechanism into how these downstream effectors interact to produce such a robust response remains to be elucidated and will require an extensive amount of work, which unfortunately is beyond the scope of this thesis.

The results obtained in experiment 1 where the dorsal columns were cut and the dorsolateral columns spared showed that the sprouting quantified below the lesion did not seem to correlate with sprouting fibres above the lesion both in the ipsilateral dorsolateral white matter or fibre sprouts contralateral to the lesion, suggesting that caudal fibre sprouts were independent of intact

undamaged fibres above the lesion. The correlation using the ipsilateral dorsolateral white matter with caudal sprouting is particularly useful since previous reports have shown that caudal sprouting following dorsal hemisection in which the dorsolateral white matter tract had not been damaged may be due to the intact dorsolateral corticospinal tract (Steward et al., 2004). However, these data do not show any correlation between labelled dorsolateral tract fibres and caudal fibre sprouts.

One of the mechanisms by which functional recovery may have been attained in the Ras+, MEK1dn and DM mice is through sprouting onto intact spinal interneurons. In the mammalian nervous system, recent studies have shown that intact spinal interneurons that circumvent a spinal lesion are capable of receiving new inputs from cut axons and of forming new contacts with neurons beyond the lesion (Bareyre et al., 2004; Vavrek et al., 2006). Certainly, plasticity of spinal interneurons has been shown to play a role in central pattern generation (Rossignol, 2006) highlighting the adaptive roles of spinal interneurons following spinal cord injury. Moreover, the survival effects of Ras+ and MEK1dn in the facial nucleus may have been extended to spinal interneurons allowing many neurons around the injury site to survive whilst in the wild-type these may have died. This is speculative however, and an analysis of the contribution of spinal interneurons would need to be done to account for this.

In establishing a critical analysis of this work, there are a number of key issues which arise, one of which is the issue of aberrant sprouting. Several studies have noted that not all sprouting is beneficial. For instance aberrant sprouting has been reported following spinal cord injury since Barritt and colleagues (2006) report extensive sprouting of primary afferents following SCI and chondroitinase ABC treatment. Such sprouting of primary afferents can give rise to neuropathic pain (Hofstetter et al., 2005) which would undoubtedly be a highly undesirable side effect of treatment. Moreover, axonal sprouting onto spinal interneurons following spinal cord injury has also been shown to play a role in autonomic dysreflexia (Schramm, 2006) highlighting the maladaptive response of both cut and intact spinal axons and interneurons following spinal cord injury.

Directing anatomical plasticity to make functionally viable connections has many hurdles which are beginning to be overcome (Angelov et al., 2005, Galtrey et al., 2007; Smith et al., 2007). Mechanistically axons may sprout extensively initially and then maintain viable connections, while pruning back inappropriate connections over time; indeed, evidence for this hypothesis has been shown in at least one study (Bareyre et al., 2004). Moreover, Smith et al. (2007) go on to argue that if during this 'plastic hyperactivity', connections can be defined using physiotherapy which complements pharmacological therapy; it may push anatomical circuits to maintain the correct connections.

One way of gauging whether functional recovery was due to regeneration or sprouting would be to re-injure the CST and/or RST in those animals where functional recovery was good. This would provide an indication of whether it was those tracts that contributed to the observed improvement in functional recovery.

Neuronal overexpression of dominant negative MEK1 and associated inhibition of endogenous MEK1 activity strongly enhances the sprouting of corticospinal tract axons into the distal part of the injured spinal cord following a mild spinal injury. Although, the combined effect of MEK1dn and Ras overexpression does not increase average distal regeneration, fibres from double mutant animals were now observed to cross lesion scars, and displayed a more spread out, overall sprouting. Thus, the combined effect appeared to enable the fibres to be able to better overcome the hostile environment of the lesion scar, in addition to that of the central white matter. The almost complete disappearance of CST sprouting following the more extensive dorsal hemisection is probably due to the scarring of alternative sprouting routes through dorsal horn and dorsolateral tract. The data also show that neuronal expression of dominant negative MEK1, to some extent in combination with constitutively active Ras, strongly enhances functional repair (rearing, gridwalk) after C4 dorsal hemisection, and, that this may be mediated through the rostral and caudal sprouting of rubrospinal axons.

CHAPTER 8

General Discussion

Generation of new axonal sprouts and the process of axonal elongation play a vital role in neural regeneration and repair. The facial nerve axotomy model is a well-established, prototypical experimental paradigm for the systematic study of nerve regeneration and degeneration, providing insights into molecular signals that determine axonal regeneration and neuronal cell death. Interestingly, this model of peripheral injury induces a delayed appearance of galanin+ and calcitonin gene-related peptide+ (CGRP) neuropeptide-immunoreactive growth cones in the facial nucleus which peak at 14 days following axotomy and surprisingly, increase in number if recut within this time window. Furthermore, application of the retrograde tracer mini-ruby to the distal portion of the cut nerve demonstrates the motoneuron origin of these sprouting neurites.

To gain an insight into the molecular mechanisms inducing the sprouting response we examined how neuronal cell death and the inflammatory response, following axonal injury in various transgenic mice affected central sprouting and peripheral regeneration of axons. Deletion of the α7 integrin, which has previously demonstrated a moderate reduction in peripheral nerve regeneration (Werner et al., 2000), showed enhanced central sprouting in the facial nucleus. The absence of neuronal c-jun in neurons has previously been shown to block peripheral axonal regeneration in the facial nerve, abolish regeneration-associated neuronal proteins and neuronal cell death (Raivich et al., 2004). In this study, however, the absence of neuronal c-jun completely eliminated central axonal sprouting in the facial nucleus. Absence of TNFR1&2 which has been reported to reduce neuronal cell death in and inflammation in the facial nucleus (Raivich et al., 2002), showed a tendency toward enhanced central sprouting. TGFβ1 deletion which showed an elevated inflammatory response and a 4-fold increase in neuronal cell death resulted in substantially reduced central sprouting. Similarly, enhanced neural inflammation following systemic injection of E.coli lipopolysaccharide (LPS) also reduced central sprouting.

Finally, neuronally expressed constitutively active Ras (Ras+), dominant-negative MEK1 (MEK1dn) and Ras+xMEK1dn double mutant (DM) all

demonstrated reduced neuronal cell death as well as substantially enhanced central sprouting, particularly in the MEK1dn mutant, suggesting that the sprouting response in these mutants may be beneficial for improving regeneration in the CNS.

Sprouting and regeneration studies in Ras+ and MEK1dn mutants were therefore extended to the injured corticospinal tract (CST) and rubrospinal tract. These mutants showed extensive collateral sprouting of corticospinal tract (CST) axons, in the grey and white matter on the ipsilateral side in Ras+, MEK1dn and DM animals compared with wild-type (WT) controls when the injury spared the dorsolateral CST. EGFP labelled rubrospinal axons showed increased sprouting below the site of injury following a C4 injury in Ras+, MEK1dn and DM mice but this was not statistically significant compared with wild-type controls. To determine functional recovery following left spinal lesion, rearing and grid-walk tests were used to assess both forelimb and hindlimb function on one side over a period of 28 days following a unilateral left dorsal hemisection (DH) at C4. Ras+, MEK1dn and DM groups performed significantly better in left forepaw use during rearing and showed significantly less footslips on the left side than WT at day 28.

Neuronal cell death

The means by which motoneurons in facial nucleus die has been an area of intense research and there is some debate as to whether it is mediated through an apoptotic or non-apoptotic mechanism. The majority of evidence suggests that apoptosis is completely absent from adult facial nuclei, even if massive cell death is induced by peripheral nerve avulsion or the application of neurotoxins (Moran and Graeber, 2004). There is evidence of terminal deoxynucleotidyl transferase-mediated dUTP nick end labelling (TUNEL); however, this is in neonatal mice (de Bilbao and Dubois-Dauphin, 1996). Interestingly, while DNA fragmentation, indicated by TUNEL labelling indicates increased neuronal vulnerability, it does not suggest that the cell is undergoing apoptosis (Stadelmann et al., 1998; Graeber and Moran, 2002). The results shown in this thesis can only speculate as to the precise method of cell death since TUNEL was not assessed.

There a few methodological considerations which should also be addressed. A recent study in the C57/BL6 mouse demonstrated (11 weeks after lesion) that only about 20-30% of the motoneuron loss in the facial motor nucleus is likely due to death and at least as much is due to atrophy which renders the neurons undetectable by standard methods used such as cresyl violet staining (McPhail et al. 2004). This was shown by re-axotomy which surprisingly rescued a large portion of the undetectable cells. However, there is a methodological disparity between the way in which neuronal counts were done in the McPhail study and the way neuronal counts were done for this thesis. In the McPhail et al. (2004) study, neuronal number was assessed by counting nucleated neurons in every other section, whereas in this study all neurons (regardless of whether it had a nucleolus) in every section were counted. McPhail and colleagues also showed a 60% loss of motoneurons following axotomy whereas in this study there is at most a 40% loss of motoneurons in wild-type C57black6 mice, which agrees with several previous studies (Raivich et al., 2002; Sendtner et al., 1997). The method of counting all neurons within the facial nucleus regardless of soma size is viable since one can apply the Abercrombie coefficient at the end to correct for cell body size. Moreover, because the facial motor nucleus is anatomically separated from other neuronal types and few if any interneurons are found in the facial motor nucleus (Moran and Graeber, 2004), the neuronal counts probably include all normal and possible atrophied motoneurons. Although one cannot entirely rule out the possibility that a subset of small atrophied motoneurons were excluded from the facial motoneurons counts, one could consider it unlikely that the reduction in motoneurons counts in both Ras+ and MEK1dn mice can be attributed to motoneurons atrophy, because we were able to recognize and include small motoneurons in our cell counts.

Axonal sprouting and regeneration

Three forms of axonal growth can occur in the adult nervous system following injury: collateral sprouting, which is a form of plasticity of intact axons typically growing or extending processes into denervated regions; regenerative growth, which is the growth of particular axons that have been damaged which then extend into and beyond an injury site to re-establish synaptic connections; and

finally, regenerative sprouting which involves short distance growth of axons rostral to a site of injury, but injured axons generally do not grow beyond the lesion (Woolf, 2003). The data that forms part of this thesis, particularly that in the spinal cord, represents a mixture of regenerative sprouting of injured axons and collateral sprouting of neighbouring intact axons. In fact, it is likely that a combination of these two forms of axonal plasticity may have contributed to the functional recovery observed in the mutants following spinal injury. Moreover, since the formation of spontaneous intraspinal circuits appears to contribute to functional recovery (Bareyre et al., 2004) the enhanced axonal plasticity of Ras+, MEK1dn and DM mice will undoubtedly have contributed to the increase in formation of these circuits thus contributing to functional recovery. Whether this recovery was due to regrowth in the corticospinal or rubrospinal tracts remains inconclusive. Demonstrating restoration of function of a particular tract requires not only a behavioural analysis, but also ultrastructural analysis at the level of the synapse as well as electrophysiological evidence of connectivity. The latter two pieces of evidence were not provided with respect to this study due to time constraints.

The lack of a relationship between peripheral nerve outgrowth and central axonal sprouting is consistent with previous observations where peripheral nerve outgrowth did not correlate with neurites in the facial nucleus (Galiano et al., 2001; Werner et al., 2000). Whilst there appears to be an exception to this rule since in the current study, (Chapter 6 and Makwana et al., 2007) for TGFβ null mice, both peripheral nerve outgrowth and central sprouting were abrogated; the EM observations in the peripheral nerve in TGFβ1 null mice provided conclusive evidence that the lack of regenerative growth in the peripheral facial nerve following injury was due to local disruptions in axonal transport and focal demyelination as well as a lack of clearance of axonal debris. Whereas centrally, in the facial nucleus of TGFβ1 null mice, the lack of sprouting was due to the neurodegenerative changes and enhanced inflammation. These differences in peripheral and central axonal outgrowth suggest that the regenerative mechanisms in the two compartments are largely controlled by independent mechanisms.

One point that warrants mention is that the increase in central axonal sprouting seen in Ras+ and MEK1dn mutants may be due to more facial motoneurons surviving. Certainly, TGFβ1 null mice have increased neuronal cell death following facial nerve axotomy and the central sprouting response is significantly impaired. However, while the change in neuronal cell number may be contributing to some of the change in sprouting neurites, the relationship between the two effects does not appear to be linear.

Sprouting in the central nervous system, like that shown in the facial nucleus and in the spinal cord following dorsal hemisection may act to enhance local connections thereby re-establishing connections back to the target. Certainly, this is evident in the results shown in Chapter 7. However, sprouting in the peripheral nervous system may not be beneficial. Reducing collateral branching with the application of antibodies against BDNF, FGF, NGF, IGF. CNTF or GDNF at the lesion site in the peripheral nerve has been shown to increase the precision of reinnervation to the target following facial nerve injury as measured with retrograde tracing (Guntinas-Lichius et al., 2005). While both Ras+ or MEK1dn mice did not show evidence of enhanced collateral sprouting at the peripheral nerve lesion site, surprisingly, there was also no significant difference in whisker motor recovery in Ras+ or MEK1dn mice despite the strong sprouting effect centrally. The reason for this is unclear but could be due to polyneuronal reinnervation of antagonistic muscles. Certainly, previous studies appear to demonstrate that a lack of motor effect where one was expected, is due to poly-reinnervation of the target muscles (Guntinas-Lichius et al., 2005). A histological assessment of the motor-end plates would need to be assessed to demonstrate this definitively.

Limitations and further study

One of the strengths of this study is the availability of different transgenic mice which have enabled investigation into how different mediators affect regenerative and collateral sprouting following nervous system trauma. The mutant mice used in this study have provided insight into molecular mechanisms that would not otherwise be possible. While transgenics are particularly helpful, there are limitations to their use since compensatory

mechanisms can affect the loss or gain of activity of a particular protein. While this is particularly true for globally altered genes, tissue-specific alterations could also be affected. The complexity of the Ras+ and MEK1dn double mutant mice in Chapter 7 of this thesis highlights the fact that alternative, perhaps compensatory pathways may contribute to the observed effects, or that overlapping functions of particular proteins makes their role difficult to define.

Combinatorial therapy for improving regenerative outgrowth following injury in the spinal cord is likely to be required for translating experimental research into clinical therapy. Boosting the intrinsic growth potential of neurons as well as allowing a permissive environment for growth should be a priority. The enzyme chondroitinase ABC (ChABC) which breaks down inhibitory sugar chain components of CSPG molecules has been shown to promote regrowth of lesioned axons in the brain and spinal cord (Bradbury et al., 2002; Moon et al., 2001; Yick et al., 2003). Combining ChABC treatment with other interventions has been shown to further enhance regenerative growth (Bradbury and McMahon, 2006); for example, preconditioning DRG neurons with inflammatory agents enhances growth across the dorsal root entry zone (Steinmetz et al., 2005); and, when combined with lithium chloride, a GSK-3β inhibitor, to improve rubrospinal tract regrowth and forelimb use after spinal hemisection (Yick et al., 2004). Combinatorial approaches where chondroitinase ABC and peripheral nerve grafts to bridge lesions have also been successful in improving functional outcome following spinal injury (Houle et al., 2006).

Since both Ras+ and MEK1dn mutant mice may enhance regenerative outgrowth by boosting the intracellular growth potential of neurons; combining studies in these mutant mice with ChABC might prove immensely beneficial for enhancing axonal outgrowth. Moreover, since recent reports have indicated that mice which express ChABC under the control of the GFAP promoter are now available (Cafferty et al., 2007); combining these mice with Ras+ or MEK1dn mutant mice may provide some strong evidence that the combination of enhancing intrinsic growth potential together with making the CNS environment more favourable for growth is the best way forward for improving regenerative outgrowth of CNS axons and therefore improving functional recovery following spinal injury.

The data contained within this thesis provide a novel viewpoint on the mechanisms of injury induced sprouting. The facial axotomy model provides a unique model to quickly assess the efficiency of genetically altered mutants for neuronal cell death, peripheral nerve regeneration and central sprouting. The enhanced central axonal sprouting observed in the facial nucleus as well as in the injured spinal cord in Ras+ and MEK1dn mutants demonstrates that the facial nucleus model could be reliably used as a pre-indicator of the ability of spinal axons to regrow.

The facial axotomy model has been used extensively and its advantages highlighted in several different studies (for review see Moran and Graeber, 2004). The ease at which neuronal cell death, neuroinflammation, and regenerative responses can be assessed provides both economical and time advantages to the researcher who can assess responses quickly. This is particularly pertinent since studies in spinal cord injury are time consuming and cumbersome and require a large number of animals, the availability of which is often limited. Knowing that the mutant is likely to produce some beneficial results is therefore advantageous.

The work has highlighted some of the literature where neurotrophins have proved successful in eliciting a regenerative response in axons. It also makes some progress in the advancement in improving axonal regeneration through the manipulation of intracellular signalling pathways, particularly in the Ras-Raf-MEK-ERK pathway. These studies, however, remain at an early stage. The variability in tract tracing techniques in the spinal cord, combined with the variability of in vivo experiments, means that a significantly high number of animals is required to firmly establish a conclusive result. So, while the trend towards increased sprouting with the presence of MEK1dn is evident, particularly in the rubrospinal tract of MEK1dn and DM mice, the small number of experimental mice no doubt hinders any firm conclusion that can be made about this transgene with respect to sprouting and regeneration in the CNS.

Conclusion

Overall, data from facial nucleus studies suggest central axonal sprouting is an injury but not a reinnervation-driven response that it is not directly connected to neuronal cell death, that excessive inflammation is detrimental, and that jun-, Ras-, and MEK1-mediated changes in regeneration-associated gene and protein expression play a vital part in shaping the growth cone response. Following spinal injury, expression of MEK1dn moderately enhanced CST sprouting below the injury site when the dorsolateral corticospinal tract was spared. Enhanced sprouting may have contributed to the functional recovery observed in Ras+, MEK1dn and DM mutant mice.

Manipulating intracellular signalling to enhance growth has significant potential, however as this thesis highlights, this avenue of research remains complex and requires much further study.

REFERENCES

Abe K, Chu PJ, Ishihara A, and Saito H (1996) Transforming growth factor-β 1 promotes re-elongation of injured axons of cultured rat hippocampal neurons. Brain Res 723:206-209

Abercrombie M (1946). Estimation of nuclear populations from microtome sections. Anat. Rec. 94 pp 239–247

Acheson A, Lindsay RM (1996). Non target-derived roles of the neurotrophins. Philos Trans R Soc Lond B Biol Sci. 351(1338):417-22.

Adams B, Sazgar M, Osehobo P, Van der Zee CE, Diamond J, Fahnestock M, Racine RJ (1997). Nerve growth factor accelerates seizure development, enhances mossy fiber sprouting, and attenuates seizure-induced decreases in neuronal density in the kindling model of epilepsy. J Neurosci. 17(14):5288-96.

Ahn NG (1993). The MAP kinase cascade. Discovery of a new signal transduction pathway. Mol Cell Biochem. 127-128:201-9.

Al Majed AA, Neumann CM, Brushart TM, Gordon T (2000) Brief electrical stimulation promotes the speed and accuracy of motor axonal regeneration. J Neurosci 20:2602-2608.

Alessandrini A, Namura S, Moskowitz MA, Bonventre JV (1999). MEK1 protein kinase inhibition protects against damage resulting from focal cerebral ischemia. Proc Natl Acad Sci U S A. 96(22):12866-9.

Al-Majed AA, Brushart TM, Gordon T (2000) Electrical stimulation accelerates and increases expression of BDNF and trkB mRNA in regenerating rat femoral motoneurons. Eur J Neurosci 12:4381-4390.

Althini S, Usoskin D, Kylberg A, Kaplan PL, Ebendal T (2004). Blocked MAP kinase activity selectively enhances neurotrophic growth responses. Mol Cell Neurosci. 25(2):345-54.

Ambron RT, Walters ET (1996) Priming events and retrograde injury signals. A new perspective on the cellular and molecular biology of nerve regeneration. Mol Neurobiol 13:61-79

Anderson PN, Campbell G, Zhang Y, Lieberman AR (1998). Cellular and molecular correlates of the regeneration of adult mammalian CNS axons into peripheral nerve grafts. Prog Brain Res. 117:211-32.

Anderson PN, Fabes J, Hunt D (2007). The role of inhibitory molecules in limiting axonal regeneration in the mammalian spinal cord in Model Organisms in Spinal Cord Regeneration. Edited by Becker CG and Becker T. Wiley Press

Angelov DN, Guntinas-Lichius O, Wewetzer K, Neiss WF, Streppel M (2005). Axonal branching and recovery of coordinated muscle activity after transection of the facial nerve in adult rats. Adv Anat Embryol Cell Biol. 180:1-130.

Angelov DN, Neiss WF, Streppel M, Andermahr J, Mader K, Stennert E (1996) Nimodipine accelerates axonal sprouting after surgical repair of rat facial nerve. J Neurosci 16:1041-8

Arenas E, Persson H (1994) Neurotrophin-3 prevents the death of adult central noradrenergic neurons in vivo. Nature 367:368-71

Atwal JK, Massie B, Miller FD, Kaplan DR (2000). The TrkB-Shc site signals neuronal survival and local axon growth via MEK and P13-kinase. Neuron 27(2):265-77.

Avellino AM, Hart D, Dailey AT, MacKinnon M, Ellegala D, Kliot M (1995). Differential macrophage responses in the peripheral and central nervous

system during wallerian degeneration of axons. Exp Neurol. 136(2):183-98.

Bamji SX, Miller FD (1996). Comparison of the expression of a T α 1:nlacZ transgene and T α 1 α-tubulin mRNA in the mature central nervous system. J Comp Neurol. 374(1):52-69.

Barallobre MJ, Pascual M, del Rio JA, Soriano E (2005) The Netrin family of guidance factors: emphasis on Netrin-1 signalling. Brain Res Brain Res Rev 49: 22-47.

Barde YA, Davies AM, Johnson JE, Lindsay RM, Thoenen H (1987). Brain derived neurotrophic factor. Prog Brain Res. 71:185-9.

Barde YA, Edgar D, Thoenen H (1982). Purification of a new neurotrophic factor from mammalian brain. EMBO J. 1(5):549-53.

Bareyre FM, Haudenschild B, Schwab ME (2002). Long-lasting sprouting and gene expression changes induced by the monoclonal antibody IN-1 in the adult spinal cord. J Neurosci. 22(16):7097-110.

Bareyre FM, Kerschensteiner M, Raineteau O, Mettenleiter TC, Weinmann O, Schwab ME (2004). The injured spinal cord spontaneously forms a new intraspinal circuit in adult rats. Nat Neurosci. 7(3):269-77.

Barnes G, Puranam RS, Luo Y, McNamara JO (2003) Temporal specific patterns of semaphorin gene expression in rat brain after kainic acid-induced status epilepticus. Hippocampus 13: 1-20.

Barrett LE, Van Bockstaele EJ, Sul JY, Takano H, Haydon PG, Eberwine JH (2006). Elk-1 associates with the mitochondrial permeability transition pore complex in neurons. Proc Natl Acad Sci U S A. 103(13):5155-60.

Barritt AW, Davies M, Marchand F, Hartley R, Grist J, Yip P, McMahon SB, Bradbury EJ (2006). Chondroitinase ABC promotes sprouting of intact and

injured spinal systems after spinal cord injury. J Neurosci. 26(42):10856-67.

Bar-Sagi D, Feramisco JR (1985). Microinjection of the ras oncogene protein into PC12 cells induces morphological differentiation. Cell. 42(3):841-8.

Baumgartner BJ, Shine HD (1997). Targeted transduction of CNS neurons with adenoviral vectors carrying neurotrophic factor genes confers neuroprotection that exceeds the transduced population. J Neurosci. 17(17):6504-11.

Baumgartner BJ, Shine HD (1998). Neuroprotection of spinal motoneurons following targeted transduction with an adenoviral vector carrying the gene for glial cell line-derived neurotrophic factor. Exp Neurol. 153(1):102-12.

Bavetta S, Hamlyn PJ, Burnstock G, Lieberman AR, Anderson PN (1999). The effects of FK506 on dorsal column axons following spinal cord injury in adult rats: neuroprotection and local regeneration. Exp Neurol. 158(2):382-93.

Beattie MS, Farooqui AA, Bresnahan JC (2000). Review of current evidence for apoptosis after spinal cord injury. J Neurotrauma. 17(10):915-25.

Beattie MS, Li Q, Bresnahan JC (2000). Cell death and plasticity after experimental spinal cord injury. Prog Brain Res. 128:9-21.

Becker CG, Lieberoth BC, Morellini F, Feldner J, Becker T, Schachner M (2004) L1.1 is involved in spinal cord regeneration in adult zebrafish. J Neurosci 24:7837-42

Behrens A, Sibilia M, David JP, Mohle-Steinlein U, Tronche F, Schutz G, Wagner EF (2002) Impaired postnatal hepatocyte proliferation and liver regeneration in mice lacking c-jun in the liver. EMBO J. 21:1782-90.

Benfey M, Bunger UR, Vidal Sanz M, Bray GM, Aguayo AJ (1985) Axonal regeneration from GABAergic neurons in the adult rat thalamus. J Neurocytol 14:279-296.

Benfey M, Bunger UR, Vidal Sanz M, Bray GM, Aguayo AJ (1985) Axonal regeneration from GABAergic neurons in the adult rat thalamus. J Neurocytol 14:279-296.

Benson MD, Romero MI, Lush ME, Lu QR, Henkemeyer M, Parada LF (2005) Ephrin-B3 is a myelin-based inhibitor of neurite outgrowth. Proc Natl Acad Sci U S A 102: 10694-10699.

Berdan RC, Easaw JC, Wang R (1993) Alterations in membrane potential after axotomy at different distances from the soma of an identified neuron and the effect of depolarisation on neurite outgrowth and calcium channel expression. J Neurophysiol 69:151–164.

Berkelaar M, Clarke DB, Wang YC, Bray GM, Aguayo AJ (1994) Axotomy results in delayed death and apoptosis of retinal ganglion cells in adult rats. J Neurosci. 14:4368-74.

Berry M (1982). Post-injury myelin-breakdown products inhibit axonal growth: an hypothesis to explain the failure of axonal regeneration in the mammalian central nervous system. Bibl Anat. (23):1-11.

Berry M, Hall S, Follows R, Rees L, Gregson N, Sievers J (1988a). Response of axons and glia at the site of anastomosis between the optic nerve and cellular or acellular sciatic nerve grafts. J Neurocytol. 17(6):727-44.

Berry M, Rees L, Hall S, Yiu P, Sievers J (1988b). Optic axons regenerate into sciatic nerve isografts only in the presence of Schwann cells. Brain Res Bull. 20(2):223-31.

Biggs WH 3rd, Meisenhelder J, Hunter T, Cavenee WK, Arden KC (1999). Protein kinase B/Akt-mediated phosphorylation promotes nuclear

exclusion of the winged helix transcription factor FKHR1. Proc Natl Acad Sci U S A. 96(13):7421-6.

Bignami A (1984) The role of astrocytes in CNS regeneration. J Neurosurg Sci 28:127-32

Bignami A, Dahl D, Nguyen BT, Crosby CJ (1981). The fate of axonal debris in Wallerian degeneration of rat optic and sciatic nerves. Electron microscopy and immunofluorescence studies with neurofilament antisera. J Neuropathol Exp Neurol. 40(5):537-50.

Bignami A, Ralston HJ 3rd (1969). The cellular reaction to Wallerian degeneration in the central nervous system of the cat. Brain Res. 13(3):444-61. No abstract available.

Bjorklund A, Stenevi U (1979) Regeneration of monoaminergic and cholinergic neurons in the mammalian central nervous system. Physiol Rev 59:62-100.

Bjorklund A, Stenevi U (1984) Intracerebral neural implants: neuronal replacement and reconstruction of damaged circuitries. Annu Rev Neurosci 7:279-308.

Blesch A, Tuszynski MH (2001). GDNF gene delivery to injured adult CNS motor neurons promotes axonal growth, expression of the trophic neuropeptide CGRP, and cellular protection. J Comp Neurol. 436(4):399-410.

Blinzinger K, Kreutzberg G (1968) Displacement of synaptic terminals from regenerating motoneurons by microglial cells. Z Zellforsch Mikrosk Anat 85:145-57.

Blits B, Dijkhuizen PA, Boer GJ, Verhaagen J (2000). Intercostal nerve implants transduced with an adenoviral vector encoding neurotrophin-3 promote

regrowth of injured rat corticospinal tract fibers and improve hindlimb function. Exp Neurol. 164(1):25-37.

Blits B, Oudega M, Boer GJ, Bartlett Bunge M, Verhaagen J (2003). Adeno-associated viral vector-mediated neurotrophin gene transfer in the injured adult rat spinal cord improves hind-limb function. Neuroscience. 118(1):271-81.

Blottner D, Wolf N, Lachmund A, Flanders KC, Unsicker K (1996) TGF-β rescues target-deprived preganglionic sympathetic neurons in the spinal cord. Eur J Neurosci. 8:202-10

Boche D, Cunningham C, Docagne F, Scott H, Perry VH (2006) TGFβ1 regulates the inflammatory response during chronic neurodegeneration. Neurobiol Dis 22:638-50

Boche D, Cunningham C, Gauldie J, Perry VH (2003) Transforming growth factor-β 1-mediated neuroprotection against excitotoxic injury in vivo. J Cereb Blood Flow Metab. 23:1174-82

Boeshore KL, Schreiber RC, Vaccariello SA, Sachs HH, Salazar R, Lee J, Ratan RR, Leahy P, Zigmond RE 2004 Novel changes in gene expression following axotomy of a sympathetic ganglion: a microarray analysis. J Neurobiol 59:216-35

Bohatschek M, Kloss CU, Hristova M, Pfeffer K, Raivich G (2004a). Microglial major histocompatibility complex glycoprotein-1 in the axotomized facial motor nucleus: regulation and role of tumor necrosis factor receptors 1 and 2. J Comp Neurol. 470(4):382-99.

Bohatschek M, Kloss CU, Pfeffer K, Bluethmann H, Raivich G (2004b). B7.2 on activated and phagocytic microglia in the facial axotomy model: regulation by interleukin-1 receptor type 1, tumor necrosis factor receptors 1 and 2 and endotoxin. J Neuroimmunol. 156(1-2):132-45.

Bohatschek M, Kloss CUA, Kalla R, Raivich G (2001) In vitro model of microglial deramification: Ramified microglia transform into amoeboid phagocytes following addition of brain cell membranes to microglia-astrocyte cocultures. J Neurosci Res, 64:508-22

Bohatschek M, Kloss CUA, Pfeffer K, Labow M, Raivich G (2004b) Cytokine regulation of microglial MHC1 in the axotomized facial motor nucleus: role of TNF receptors TNFR1 and TNFR2. J Comp Neurol 470:382-99

Bohatschek M, Werner A, Raivich G (2001) Systemic LPS injection leads to granulocyte influx into normal and injured brain: effects of ICAM-1 deficiency Exp Neurol. 172:137-52.

Bommireddy R, Doetschman T (2004) TGF-β, T-cell tolerance and anti-CD3 therapy. Trends Mol Med 10:3-9

Bomze HM, Bulsara KR, Iskandar BJ, Caroni P, Skene JH (2001) Spinal axon regeneration evoked by replacing two growth cone proteins in adult neurons. Nat Neurosci 4:38-43

Bonilla IE, Tanabe K, Strittmatter SM. 2002 Small proline-rich repeat protein 1A is expressed by axotomized neurons and promotes axonal outgrowth. J Neurosci. Feb 15;22(4):1303-15.

Borasio GD, John J, Wittinghofer A, Barde YA, Sendtner M, Heumann R (1989) ras p21 protein promotes survival and fiber outgrowth of cultured embryonic neurons. Neuron 2:1087-96

Borasio GD, Markus A, Wittinghofer A, Barde YA, Heumann R (1993). Involvement of ras p21 in neurotrophin-induced response of sensory, but not sympathetic neurons. J Cell Biol. 121(3):665-72.

Bothwell M (1995). Functional interactions of neurotrophins and neurotrophin receptors. Annu Rev Neurosci. 223-53.

Boucsein C, Kettenmann H, Nolte C (2000) Electrophysiological properties of microglial cells in normal and pathologic rat brain slices. Eur J Neurosci 12:2049-58

Boyd JG, Gordon T (2001). The neurotrophin receptors, trkB and p75, differentially regulate motor axonal regeneration. J Neurobiol. 49(4):314-25.

Boyd JG, Gordon T (2002) A dose-dependent facilitation and inhibition of peripheral nerve regeneration by brain-derived neurotrophic factor. Eur J Neurosci 15:613-26

Boyd JG, Gordon T (2003) Neurotrophic factors and their receptors in axonal regeneration and functional recovery after peripheral nerve injury. Mol Neurobiol 27:277-324

Boyd JG, Gordon T (2003a). Glial cell line-derived neurotrophic factor and brain-derived neurotrophic factor sustain the axonal regeneration of chronically axotomized motoneurons in vivo. Exp Neurol. 183(2):610-9.

Bradbury EJ, Khemani S, Von R, King, Priestley JV, McMahon SB (1999). NT-3 promotes growth of lesioned adult rat sensory axons ascending in the dorsal columns of the spinal cord. Eur J Neurosci. 11(11):3873-83.

Bradbury EJ, King VR, Simmons LJ, Priestley JV, McMahon SB (1998). NT-3, but not BDNF, prevents atrophy and death of axotomized spinal cord projection neurons. Eur J Neurosci. 10(10):3058-68.

Bradbury EJ, McMahon SB (2006). Spinal cord repair strategies: why do they work? Nat Rev Neurosci. 7(8):644-53.

Bradbury EJ, Moon LD, Popat RJ, King VR, Bennett GS, Patel PN, Fawcett JW, McMahon SB (2002). Chondroitinase ABC promotes functional recovery after spinal cord injury. Nature. 416(6881):636-40.

Bray GM, Villegas-Perez MP, Vidal-Sanz M, Carter DA, Aguayo AJ (1991). Neuronal and nonneuronal influences on retinal ganglion cell survival, axonal regrowth, and connectivity after axotomy. Ann N Y Acad Sci. 633:214-28.

Bregman BS, Coumans JV, Dai HN, Kuhn PL, Lynskey J, McAtee M, Sandhu F(2002). Transplants and neurotrophic factors increase regeneration and recovery of function after spinal cord injury. Prog Brain Res. 137:257-73.

Brionne TC, Tesseur I, Masliah E, Wyss-Coray T (2003) Loss of TGF-β 1 leads to increased neuronal cell death and microgliosis in mouse brain. Neuron 40:1133-45.

Brosamle C, Huber AB, Fiedler M, Skerra A, Schwab ME (2000). Regeneration of lesioned corticospinal tract fibers in the adult rat induced by a recombinant, humanized IN-1 antibody fragment. J Neurosci. 20(21):8061-8.

Brose K, Bland KS, Wang KH, Arnott D, Henzel W, Goodman CS, Tessier-Lavigne M, Kidd T (1999) Slit proteins bind Robo receptors and have an evolutionarily conserved role in repulsive axon guidance. Cell 96: 795-806.

Brose K, Tessier-Lavigne M (2000) Slit proteins: key regulators of axon guidance, axonal branching, and cell migration. Curr Opin Neurobiol 10: 95-102.

Brunet A, Bonni A, Zigmond MJ, Lin MZ, Juo P, Hu LS, Anderson MJ, Arden KC, Blenis J, Greenberg ME (1999). Akt promotes cell survival by phosphorylating and inhibiting a Forkhead transcription factor. Cell. 96(6):857-68.

Brushart TM, Hoffman PN, Royall RM, Murinson BB, Witzel C, Gordon T (2002) Electrical stimulation promotes motoneuron regeneration without increasing its speed or conditioning the neuron. J Neurosci 22:6631-6638.

Buhusi M, Midkiff BR, Gates AM, Richter M, Schachner M, Maness PF (2003) Close homolog of L1 is an enhancer of integrin-mediated cell migration. J Biol Chem 278:25024-31

Bundesen LQ, Scheel TA, Bregman BS, Kromer LF (2003) Ephrin-B2 and EphB2 regulation of astrocyte-meningeal fibroblast interactions in response to spinal cord lesions in adult rats. J Neurosci 23: 7789-7800.

Burazin TC, Gundlach AL (1998). Inducible galanin and GalR2 receptor system in motor neuron injury and regeneration. J Neurochem. 71(2):879-82.

Burgering BM, Coffer PJ (1995). Protein kinase B (c-Akt) in phosphatidylinositol-3-OH kinase signal transduction. Nature. 376(6541):599-602.

Bush TG, Puvanachandra N, Horner CH, Polito A, Ostenfeld T, Svendsen CN, Mucke L, Johnson MH, Sofroniew MV (1999). Leukocyte infiltration, neuronal degeneration, and neurite outgrowth after ablation of scar-forming, reactive astrocytes in adult transgenic mice. Neuron. 23(2):297-308.

Bussmann KA, Sofroniew MV (1999) Re-expression of p75NTR by adult motor neurons after axotomy is triggered by retrograde transport of a positive signal from axons regrowing through damaged or denervated peripheral nerve tissue. Neuroscience 91:273-281.

Butte MJ, Hwang PK, Mobley WC, Fletterick RJ (1998). Crystal structure of neurotrophin-3 homodimer shows distinct regions are used to bind its receptors.Biochemistry. 37(48):16846-52.

Cafferty WB, Gardiner NJ, Das P, Qiu J, McMahon SB, Thompson SW (2004). Conditioning injury-induced spinal axon regeneration fails in interleukin-6 knock-out mice. J Neurosci. 24(18):4432-43.

Cafferty WB, Kim JE, Lee JK, Strittmatter SM (2007). Response to correspondence: Kim et al., "axon regeneration in young adult mice lacking Nogo-A/B." Neuron 38, 187-199. Neuron. 54(2):195-9.

Cafferty WB, Yang SH, Duffy PJ, Li S, Strittmatter SM (2007). Functional axonal regeneration through astrocytic scar genetically modified to digest chondroitin sulfate proteoglycans. J Neurosci. 27(9):2176-85.

Cagnin A, Kassiou M, Meikle SR, Banati RB (2006) In vivo evidence for microglial activation in neurodegenerative dementia. Acta Neurol Scand Suppl 185:107-14

Cajal R y S (1928). Degeneration and Regeneration of the Nervous System, Oxford Univ. Press, London, 1928.

Calvo JL, Carbonell AL, Boya J (1991). Co-expression of glial fibrillary acidic protein and vimentin in reactive astrocytes following brain injury in rats. Brain Res. 6;566(1-2):333-6.

Cameron AA, Vansant G, Wu W, Carlo DJ, III CR. Identification of reciprocally regulated gene modules in regenerating dorsal root ganglion neurons and activated peripheral or central nervous system glia. J Cell Biochem. 2003 Apr 1;88(5):970-85.

Campbell G, Holt JKL, Shotton HR, Anderson PN, Bavetta S, Lieberman AR (1999) Spontaneous regeneration after optic nerve injury in adult rat. Neurorep 10:3955-3960.

Capon DJ, Chen EY, Levinson AD, Seeburg PH, Goeddel DV (1983). Complete nucleotide sequences of the T24 human bladder carcinoma oncogene and its normal homologue. Nature. 302(5903):33-7.

Cardone MH, Roy N, Stennicke HR, Salvesen GS, Franke TF, Stanbridge E, Frisch S, Reed JC (1998). Regulation of cell death protease caspase-9 by phosphorylation. Science. 282(5392):1318-21.

Carlstedt T, Dalsgaard CJ, Molander C (1987). Regrowth of lesioned dorsal root nerve fibers into the spinal cord of neonatal rats. Neurosci Lett. 74(1):14-8.

Caroni P (2001) Actin cytoskeleton regulation through modulation of PI(4,5)P(2) rafts. EMBO J. 20:4332-6

Caroni P, Schwab ME (1988a). Two membrane protein fractions from rat central myelin with inhibitory properties for neurite growth and fibroblast spreading. J Cell Biol. 106(4):1281-8.

Caroni P, Schwab ME (1988b). Antibody against myelin-associated inhibitor of neurite growth neutralizes nonpermissive substrate properties of CNS white matter. Neuron. 1(1):85-96.

Carulli D, Laabs T, Geller HM, Fawcett JW (2005) Chondroitin sulfate proteoglycans in neural development and regeneration. Curr Opin Neurobiol 15: 116-120.

Castellani V, Chedotal A, Schachner M, Faivre-Sarrailh C, Rougon G (2000) Analysis of the L1-deficient mouse phenotype reveals cross-talk between Sema3A and L1 signaling pathways in axonal guidance. Neuron 27: 237-249.

Castro-Obregon S, Rao RV, del Rio G, Chen SF, Poksay KS, Rabizadeh S, Vesce S, Zhang XK, Swanson RA, Bredesen DE (2004). Alternative, nonapoptotic programmed cell death: mediation by arrestin 2, ERK2, and Nur77. J Biol Chem. 279(17):17543-53.

Causing CG, Gloster A, Aloyz R, Bamji SX, Chang E, Fawcett J, Kuchel G, Miller FD (1997). Synaptic innervation density is regulated by neuron-derived BDNF. Neuron 18(2):257-67.

Campbell G, Zhang Y, Schachner M, Lieberman AR, Anderson PN (2003) Expression of regeneration-related molecules in injured and regenerating striatal and nigral neurons. J Neurocytol 32:161-83

Chaisuksunt V, Zhang Y, Anderson PN, Campbell G, Vaudano E, Schachner M, Lieberman AR (2000). Axonal regeneration from CNS neurons in the cerebellum and brainstem of adult rats: correlation with the patterns of expression and distribution of messenger RNAs for L1, CHL1, c-jun and growth-associated protein-43. Neuroscience. 100(1):87-108.

Chalazonitis A, Kalberg J, Twardzik DR, Morrison RS, Kessler JA (1992) Transforming growth factor β has neurotrophic actions on sensory neurons in vitro and is synergistic with nerve growth factor. Dev Biol. 152:121-32

Chan YM, Yick LW, Yip HK, So KF, Oppenheim RW, Wu W (2003) Inhibition of caspases promotes long-term survival and reinnervation by axotomized spinal motoneurons of denervated muscle in newborn rats. Exp Neurol 181:190-203

Chang S, Popov SV (1999). Long-range signaling within growing neurites mediated by neurotrophin-3. Proc Natl Acad Sci U S A. 96(7):4095-100.

Chen H, Chedotal A, He Z, Goodman CS, Tessier-Lavigne M (1997) Neuropilin-2, a novel member of the neuropilin family, is a high affinity receptor for the semaphorins Sema E and Sema IV but not Sema III. Neuron 19: 547-559.

Chen MS, Huber AB, van der Haar ME, Frank M, Schnell L, Spillmann AA, Christ F, Schwab ME (2000). Nogo-A is a myelin-associated neurite outgrowth inhibitor and an antigen for monoclonal antibody IN-1. Nature. 403(6768):434-9.

Chen ZL, Strickland S (2003) Laminin gamma1 is critical for Schwann cell differentiation, axon myelination, and regeneration in the peripheral nerve. J Cell Biol 163:889-99

Chisholm A, Tessier-Lavigne M (1999) Conservation and divergence of axon guidance mechanisms. Curr Opin Neurobiol 9: 603-615.

Chong MS, Woolf CJ, Turmaine M, Emson PC, Anderson PN (1996). Intrinsic versus extrinsic factors in determining the regeneration of the central processes of rat dorsal root ganglion neurons: the influence of a peripheral nerve graft. J Comp Neurol. 370(1):97-104.

Chung J, Grammer TC, Lemon KP, Kazlauskas A, Blenis J (1994). PDGF- and insulin-dependent pp70S6k activation mediated by phosphatidylinositol-3-OH kinase. Nature. 370(6484):71-5.

Chung J, Grammer TC, Lemon KP, Kazlauskas A, Blenis J (1994). PDGF- and insulin-dependent pp70S6k activation mediated by phosphatidylinositol-3-OH kinase. Nature. 370(6484):71-5.

Cohen S (1960). Purification of a nerve-growth promoting protein from the mouse salivary gland and its neuro-cytotoxic antiserum. Proc Natl Acad Sci U S A. 46(3):302-11.

Condic ML (2001). Adult neuronal regeneration induced by transgenic integrin expression. J Neurosci. 21(13):4782-8.

Cordon-Cardo C, Tapley P, Jing SQ, Nanduri V, O'Rourke E, Lamballe F, Kovary K, Klein R, Jones KR, Reichardt LF (1991) The trk tyrosine protein kinase mediates the mitogenic properties of nerve growth factor and neurotrophin-3. Cell. 66(1):173-83.

Cosgaya JM, Chan JR, Shooter EM (2002). The neurotrophin receptor p75NTR as a positive modulator of myelination. Science. 298(5596):1245-8.

Costigan M, Befort K, Karchewski L, Griffin RS, D'Urso D, Allchorne A, Sitarski J, Mannion JW, Pratt RE, Woolf CJ (2002). Replicate high-density rat genome oligonucleotide microarrays reveal hundreds of regulated genes in the dorsal root ganglion after peripheral nerve injury. BMC Neurosci. 3:16.

Covault J, Sanes JR (1985) Neural cell adhesion molecule (N-CAM) accumulates in denervated and paralyzed skeletal muscles. Proc Natl Acad Sci USA 82:4544-8

Crossman AR and Neary D (1998). Neuroanatomy. An illustrated colour text. Churchill Livingstone

Dahl D, Perides G, Bignami A (1989). Axonal regeneration in old multiple sclerosis plaques. Immunohistochemical study with monoclonal antibodies to phosphorylated and non-phosphorylated neurofilament proteins. Acta Neuropathol (Berl). 79(2):154-9.

D'Antonio M, Droggiti A, Feltri ML, Roes J, Wrabetz L, Mirsky R, Jessen KR (2006) TGFβeta type II receptor signaling controls Schwann cell death and proliferation in developing nerves. J Neurosci. 26:8417-27

Datta SR, Dudek H, Tao X, Masters S, Fu H, Gotoh Y, Greenberg ME (1997). Akt phosphorylation of BAD couples survival signals to the cell-intrinsic death machinery. Cell. 91(2):231-41.

David S, Aguayo AJ (1981). Axonal elongation into peripheral nervous system "bridges" after central nervous system injury in adult rats. Science. 214(4523):931-3.

Davies JE, Tang X, Denning JW, Archibald SJ, Davies SJ (2004) Decorin suppresses neurocan, brevican, phosphacan and NG2 expression and promotes axon growth across adult rat spinal cord injuries. Eur J Neurosci 19: 1226-1242.

Davies SJ, Field PM, Raisman G (1993). Long fibre growth by axons of embryonic mouse hippocampal neurons microtransplanted into the adult rat fimbria. Eur J Neurosci. 5(2):95-106.

Davies SJ, Field PM, Raisman G (1994). Long interfascicular axon growth from embryonic neurons transplanted into adult myelinated tracts. J Neurosci. 14(3):1596-612.

Davies SJ, Fitch MT, Memberg SP, Hall AK, Raisman G, Silver J (1997). Regeneration of adult axons in white matter tracts of the central nervous system. Nature. 390(6661):680-3.

de Bilbao F, Dubois-Dauphin M (1996). Time course of axotomy-induced apoptotic cell death in facial motoneurons of neonatal wild type and bcl-2 transgenic mice. Neuroscience. 71(4):1111-9.

de Bilbao F, Giannakopoulos P, Srinivasan A, Dubois-Dauphin M (2000) In vivo study of motoneuron death induced by nerve injury in mice deficient in the caspase 1/ interleukin-1 β-converting enzyme. Neurosci 98:573-83

De Winter F, Oudega M, Lankhorst AJ, Hamers FP, Blits B, Ruitenberg MJ, Pasterkamp RJ, Gispen WH, Verhaagen J (2002) Injury-induced class 3 semaphorin expression in the rat spinal cord. Exp Neurol 175: 61-75.

de Wit J, Verhaagen J (2003) Role of semaphorins in the adult nervous system. Prog Neurobiol 71: 249-267.

Deckert-Schluter M, Rang A, Weiner D, Huang S, Wiestler OD, Hof H, Schluter D (1996). Interferon-gamma receptor-deficiency renders mice highly susceptible to toxoplasmosis by decreased macrophage activation. Lab Invest. 75(6):827-41.

Deckwerth TL, Elliott JL, Knudson CM, Johnson EM Jr, Snider WD, Korsmeyer SJ (1996). BAX is required for neuronal death after trophic factor deprivation and during development. Neuron. 17(3):401-11.

Diamond J, Coughlin M, Macintyre L, Holmes M, Visheau B (1987). Evidence that endogenous beta nerve growth factor is responsible for the collateral

sprouting, but not the regeneration, of nociceptive axons in adult rats. Proc Natl Acad Sci U S A. 84(18):6596-600.

Diebold RJ, Eis MJ, Yin M, Ormsby I, Boivin GP, Darrow BJ, Saffitz JE, Doetschman T (1995) Early-onset multifocal inflammation in the transforming growth factor β 1-null mouse is lymphocyte mediated. Proc Natl Acad Sci USA 92:12215-9

Dietz V, Wirz M, Curt A, Colombo G (1998). Locomotor pattern in paraplegic patients: training effects and recovery of spinal cord function. Spinal Cord. 36(6):380-90.

Dobrea GM, Unnerstall JR, Rao MS (1992) The expression of CNTF message and immunoreactivity in the central and peripheral nervous system of the rat. Dev Brain Res 66:209-19

Domercq M, Sanchez-Gomez MV, Sherwin C, Etxebarria E, Fern R, Matute C (2007) System xc- and Glutamate Transporter Inhibition Mediates Microglial Toxicity to Oligodendrocytes. J Immunol. 178:6549-56

Donovan MJ, Hahn R, Tessarollo L, Hempstead BL (1996). Identification of an essential nonneuronal function of neurotrophin 3 in mammalian cardiac development. Nat Genet.14(2):210-3.

Dou CL, Levine JM (1994) Inhibition of neurite growth by the NG2 chondroitin sulfate proteoglycan. J Neurosci 14: 7616-7628.

Doyle CA, Hunt SP (1997) Reduced nuclear factor kappaB (p65) expression in rat primary sensory neurons after peripheral nerve injury. Neuroreport 8:2937-42

Dudek H, Datta SR, Franke TF, Birnbaum MJ, Yao R, Cooper GM, Segal RA, Kaplan DR, Greenberg ME (1997). Regulation of neuronal survival by the serine-threonine protein kinase Akt. Science. 275(5300):661-5.

Dukic-Stefanovic S, Gasic-Milenkovic J, Deuther-Conrad W, Munch G (2003). Signal transduction pathways in mouse microglia N-11 cells activated by advanced glycation endproducts (AGEs). J Neurochem.87(1):44-55.

Dumoulin FL, Raivich G, Streit WJ, Kreutzberg GW (1991). Differential Regulation of Calcitonin Gene-related Peptide (CGRP) in Regenerating Rat Facial Nucleus and Dorsal Root Ganglion. Eur J Neurosci. 3(4):338-342.

Dunican DJ, Doherty P (2000) The generation of localized calcium rises mediated by cell adhesion molecules and their role in neuronal growth cone motility. Mol Cell Biol Res Commun 3:255-63

Eberhart J, Swartz M, Koblar SA, Pasquale EB, Tanaka H, Krull CE (2000) Expression of EphA4, ephrin-A2 and ephrin-A5 during axon outgrowth to the hindlimb indicates potential roles in pathfinding. Dev Neurosci 22: 237-250.

Eckenstein FP, Shipley GD, Nishi R (1991) Acidic and basic fibroblast growth factors in the nervous system: distribution and differential alteration of levels after injury of central versus peripheral nerve. J Neurosci 11:412-9

Eddleston M, Mucke L (1993) Molecular profile of reactive astrocytes--implications for their role in neurologic disease. Neuroscience 54:15-36

Ekblom P, Lonai P, Talts JF (2003) Expression and biological role of laminin-1. Matrix Biol 22:35-47

Ellezam B, Dubreuil C, Winton M, Loy L, Dergham P, Selles-Navarro I, McKerracher L (2002) Inactivation of intracellular Rho to stimulate axon growth and regeneration. Prog Brain Res 137:371-80

Engle SJ, Hoying JB, Boivin GP, Ormsby I, Gartside PS, Doetschman T (1999) Transforming growth factor β1 suppresses nonmetastatic colon cancer at an early stage of tumorigenesis. Cancer Res 59:3379-86

English JM, Pearson G, Hockenberry T, Shivakumar L, White MA, Cobb MH (1999). Contribution of the ERK5/MEK5 pathway to Ras/Raf signaling and growth control. J Biol Chem. 274(44):31588-92.

Ernfors P, Ibanez CF, Ebendal T, Olson L, Persson H (1990). Molecular cloning and neurotrophic activities of a protein with structural similarities to nerve growth factor: developmental and topographical expression in the brain. Proc Natl Acad Sci U S A. 87(14):5454-8.

Ernfors P, Lee KF, Jaenisch R (1994). Mice lacking brain-derived neurotrophic factor develop with sensory deficits. Nature. 368(6467):147-50.

Erskine L, Williams SE, Brose K, Kidd T, Rachel RA, Goodman CS, Tessier-Lavigne M, Mason CA (2000) Retinal ganglion cell axon guidance in the mouse optic chiasm: expression and function of robos and slits. J Neurosci 20: 4975-4982.

Etienne-Manneville S, Hall A (2002) Rho GTPases in cell biology. Nature. 420:629-35

Fabes J, Anderson P, Yanez-Munoz RJ, Thrasher A, Brennan C, Bolsover S (2006). Accumulation of the inhibitory receptor EphA4 may prevent regeneration of corticospinal tract axons following lesion. Eur J Neurosci. 23(7):1721-30.

Faulkner JR, Herrmann JE, Woo MJ, Tansey KE, Doan NB, Sofroniew MV (2004). Reactive astrocytes protect tissue and preserve function after spinal cord injury.J Neurosci. 24(9):2143-55.

Fawcett JW, Asher RA (1999). The glial scar and central nervous system repair. Brain Res Bull. 49 (6):377-91.

Fawcett JW, Housden E, Smith-Thomas L, Meyer RL (1989). The growth of axons in three-dimensional astrocyte cultures. Dev Biol. 135(2):449-58.

Fawcett JW, Keynes RJ (1990). Peripheral nerve regeneration. Annu Rev Neurosci. 13:43-60.

Feng XH and R. Derynck R (2005) Specificity and versality in TGF-β signaling through smads. Ann Rev Cell Dev Biol 21:659–693.

Fenrich K, Gordon T (2004). Canadian Association of Neuroscience review: axonal regeneration in the peripheral and central nervous systems--current issues and advances. Can J Neurol Sci. 31(2):142-56.

Fenrich KK, Skelton N, Macdermid VE, Meehan CF, Armstrong S, Neuber-Hess MS, Rose PK (2007) Axonal regeneration and development of de novo axons from distal dendrites of adult feline commissural interneurons after a proximal axotomy. J Comp Neurol 502(6): 1079-1097

Ferri CC, Moore FA, Bisby MA (1998). Effects of facial nerve injury on mouse motoneurons lacking the p75 low-affinity neurotrophin receptor. J Neurobiol. 34(1):1-9.

Fitch MT, Doller C, Combs CK, Landreth GE, Silver J (1999). Cellular and molecular mechanisms of glial scarring and progressive cavitation: in vivo and in vitro analysis of inflammation-induced secondary injury after CNS trauma. J Neurosci. 19(19):8182-98.

Forman DS, Wood DK, DeSilva S (1979). Rate of regeneration of sensory axons in transected rat sciatic nerve repaired with epineurial sutures. J Neurol Sci. 44(1):55-9.

Foster GA, Schultzberg M, Gage FH, Bjorklund A, Hokfelt T, Nornes H, Cuello AC, Verhofstad AA, Visser TJ (1985). Transmitter expression and morphological development of embryonic medullary and mesencephalic raphe neurones after transplantation to the adult rat central nervous system. I. Grafts to the spinal cord. Exp Brain Res. 60(3):427-44.

Fouad K, Dietz V, Schwab ME (2001a). Improving axonal growth and functional recovery after experimental spinal cord injury by neutralizing myelin associated inhibitors. Brain Res Brain Res Rev. 36(2-3):204-12.

Fouad K, Pedersen V, Schwab ME, Brosamle C (2001b). Cervical sprouting of corticospinal fibers after thoracic spinal cord injury accompanies shifts in evoked motor responses. Curr Biol. 11(22):1766-70.

Fournier AE, GrandPre T, Strittmatter SM (2001). Identification of a receptor mediating Nogo-66 inhibition of axonal regeneration. Nature. 409(6818):341-6.

Fournier AE, Takizawa BT, Strittmatter SM (2003) Rho kinase inhibition enhances axonal regeneration in the injured CNS. J Neurosci. 23:1416-23

Frey D, Laux T, Xu L, Schneider C, Caroni P (2000) Shared and unique roles of CAP23 and GAP43 in actin regulation, neurite outgrowth, and anatomical plasticity. J Cell Biol 149:1443-54.

Friede RL, Bischhausen R (1980) The fine structure of stumps of transected nerve fibers in subserial sections. J Neurol Sci 44:181-203.

Friedrichsen S, Heuer H, Christ S, Cuthill D, Bauer K, Raivich G (2005) Gene expression of connective tissue growth factor in adult mouse. Growth Factors 23:43-53

Fry FJ, Cowan WM (1972). A study of retrograde cell degeneration in the lateral mammillary nucleus of the cat, with special reference to the role of axonal branching in the preservation of the cell. J Comp Neurol. 144(1):1-23.

Fujita H, Zhang B, Sato K, Tanaka J, Sakanaka M (2001) Expressions of neuropilin-1, neuropilin-2 and semaphorin 3A mRNA in the rat brain after middle cerebral artery occlusion. Brain Res 914: 1-14.

Fujitani M, Yamagishi S, Che YH, Hata K, Kubo T, Ino H, Tohyama M, Yamashita T (2004) P311 accelerates nerve regeneration of the axotomized facial nerve. J Neurochem 91:737-44

Fukaya K, Hasegawa M, Mashitani T, Kadoya T, Horie H, Hayashi Y, Fujisawa H, Tachibana O, Kida S, Yamashita J (2003) Oxidized galectin-1 stimulates the migration of Schwann cells from both proximal and distal stumps of transected nerves and promotes axonal regeneration after peripheral nerve injury. J Neuropathol Exp Neurol. 62:162-72

Funakoshi H, Frisen J, Barbany G, Timmusk T, Zachrisson O, Verge VM, Persson H (1993) Differential expression of mRNAs for neurotrophins and their receptors after axotomy of the sciatic nerve. J Cell Biol 123:455-65

Furth ME, Aldrich TH, Cordon-Cardo C (1987). Expression of ras proto-oncogene proteins in normal human tissues. Oncogene. 1(1):47-58.

Galiano M, Liu ZQ, Kalla R, Bohatschek M, Koppius A, Gschwendtner A, Xu S, Werner A, Kloss CU, Jones LL, Bluethmann H, Raivich G (2001). Interleukin-6 (IL6) and cellular response to facial nerve injury: effects on lymphocyte recruitment, early microglial activation and axonal outgrowth in IL6-deficient mice. Eur J Neurosci. 14(2):327-41.

Gallo G, Letourneau PC (1998). Axon guidance: GTPases help axons reach their targets. Curr Biol. 8(3):R80-2.

Galtrey CM, Asher RA, Nothias F, Fawcett JW (2007). Promoting plasticity in the spinal cord with chondroitinase improves functional recovery after peripheral nerve repair. Brain. 130(4):926-39.

Gao Y, Nikulina E, Mellado W, Filbin MT (2003). Neurotrophins elevate cAMP to reach a threshold required to overcome inhibition by MAG through extracellular signal-regulated kinase-dependent inhibition of phosphodiesterase. J Neurosci. 23(37):11770-7.

Geisert EE Jr, Frankfurter A (1989). The neuronal response to injury as visualized by immunostaining of class III β-tubulin in the rat. Neurosci Lett. 102(2-3):137-41.

George R, Griffin JW (1994). Delayed macrophage responses and myelin clearance during Wallerian degeneration in the central nervous system: the dorsal radiculotomy model. Exp Neurol. 129(2):225-36.

Gerendasy D (1999) Homeostatic tuning of Ca2+ signal transduction by members of the calpacitin protein family. J Neurosci Res 58:107-19

Gerhard A, Schwarz J, Myers R, Wise R, Banati RB (2005) Evolution of microglial activation in patients after ischemic stroke: a [11C](R)-PK11195 PET study. Neuroimage 24:591-5

Gibney J, Zheng JQ (2003). Cytoskeletal dynamics underlying collateral membrane protrusions induced by neurotrophins in cultured Xenopus embryonic neurons. J Neurobiol. 54(2):393-405.

Giehl KM, Tetzlaff W (1996). BDNF and NT-3, but not NGF, prevent axotomy-induced death of rat corticospinal neurons in vivo. Eur J Neurosci. 8(6):1167-75.

Gilad VH, Tetzlaff WG, Rabey JM, Gilad GM (1996) Accelerated recovery following polyamines and aminoguanidine treatment after facial nerve injury in rats. Brain Res 724:141-4

Gilbert RJ, McKeon RJ, Darr A, Calabro A, Hascall VC, Bellamkonda RV (2005) CS-4,6 is differentially upregulated in glial scar and is a potent inhibitor of neurite extension. Mol Cell Neurosci 29: 545-558.

Glass DJ, Nye SH, Hantzopoulos P, Macchi MJ, Squinto SP, Goldfarb M, Yancopoulos GD (1991). TrkB mediates BDNF/NT-3-dependent survival and proliferation in fibroblasts lacking the low affinity NGF receptor. Cell. 66(2):405-13.

Glazner GW, Lupien S, Miller JA, Ishii DN (1993). Insulin-like growth factor II increases the rate of sciatic nerve regeneration in rats. Neuroscience. 54(3):791-7.

Gloster A, Wu W, Speelman A, Weiss S, Causing C, Pozniak C, Reynolds B, Chang E, Toma JG, Miller FD (1994). The T α 1 α-tubulin promoter specifies gene expression as a function of neuronal growth and regeneration in transgenic mice. J Neurosci. 14(12):7319-30.

Goldberg JL, Barres BA (2000). The relationship between neuronal survival and regeneration. Annu Rev Neurosci. 23:579-612.

Goldberger ME, Murray M (1974) Restitution of function and collateral sprouting in the cat spinal cord: the deafferented animal. J Comp Neurol 158:37–53

Golding JP, Bird C, McMahon S, Cohen J (1999). Behaviour of DRG sensory neurites at the intact and injured adult rat dorsal root entry zone: postnatal neurites become paralysed, whilst injury improves the growth of embryonic neurites. Glia. 26(4):309-23.

Goldshmit Y, Galea MP, Wise G, Bartlett PF, Turnley AM (2004) Axonal regeneration and lack of astrocytic gliosis in EphA4-deficient mice. J Neurosci 24: 10064-10073.

Gordon-Weeks PR (2004). Microtubules and growth cone function. J Neurobiol. 58(1):70-83.

Gotz R, Koster R, Winkler C, Raulf F, Lottspeich F, Schartl M, Thoenen H (1994). Neurotrophin-6 is a new member of the nerve growth factor family.Nature. 372(6503):266-9.

Graeber MB, Bise K, Mehraein P (1993). Synaptic stripping in the human facial nucleus. Acta Neuropathol (Berl). 86(2):179-81.

Graeber MB, Kreutzberg GW (1986). Astrocytes increase in glial fibrillary acidic protein during retrograde changes of facial motor neurons. J Neurocytol. 15(3):363-73.

Graeber MB, Kreutzberg GW (1988) Delayed astrocyte reaction following facial nerve axotomy. J Neurocytol 17:209-220

Graeber MB, Moran LB (2002). Mechanisms of cell death in neurodegenerative diseases: fashion, fiction, and facts. Brain Pathol. 12(3):385-90.

Graef IA, Wang F, Charron F, Chen L, Neilson J, Tessier-Lavigne M, Crabtree GR (2003). Neurotrophins and netrins require calcineurin/NFAT signaling to stimulate outgrowth of embryonic axons. Cell. 113(5):657-70.

Grafstein B (1975). The nerve cell body response to axotomy. Exp Neurol. 48(3):32-51.

GrandPre T, Li S, Strittmatter SM (2002). Nogo-66 receptor antagonist peptide promotes axonal regeneration. Nature. 417(6888):547-51.

Grill RJ, Blesch A, Tuszynski MH (1997). Robust growth of chronically injured spinal cord axons induced by grafts of genetically modified NGF-secreting cells. Exp Neurol. 148(2):444-52.

Gschwendtner A, Liu Z, Hucho T, Bohatschek M, Kalla R, Dechant G, Raivich G (2003) Regulation, cellular localization, and function of the p75 neurotrophin receptor (p75NTR) during the regeneration of facial motoneurons. Mol Cell Neurosci 24:307-22

Guerrero I, Wong H, Pellicer A, Burstein DE (1986). Activated N-ras gene induces neuronal differentiation of PC12 rat pheochromocytoma cells. J Cell Physiol. 129(1):71-6.

Guntinas-Lichius O, Irintchev A, Streppel M, Lenzen M, Grosheva M, Wewetzer K, Neiss WF, Angelov DN (2005). Factors limiting motor recovery after

facial nerve transection in the rat: combined structural and functional analyses. Eur J Neurosci. 21(2):391-402.

Guth L, Barrett CP, Donati EJ, Deshpande SS, Albuquerque EX (1981). Histopathological reactions an axonal regeneration in the transected spinal cord of Hibernating squirrels. J Comp Neurol. 203(2):297-308.

Gutmann E, Guttmann L, Medawar PB, Young JZ (1942). The rate of regeneration of nerve. J Exp Biol. 19: 14-44

Hafner C, Schmitz G, Meyer S, Bataille F, Hau P, Langmann T, Dietmaier W, Landthaler M, Vogt T (2004) Differential gene expression of Eph receptors and ephrins in benign human tissues and cancers. Clin Chem 50: 490-499.

Hagg T (2006). Collateral sprouting as a target for improved function after spinal cord injury. J Neurotrauma. 23(3-4):281-94.

Hagg T, Baker KA, Emsley JG, Tetzlaff W (2005). Prolonged local neurotrophin-3 infusion reduces ipsilateral collateral sprouting of spared corticospinal axons in adult rats. Neuroscience. 130(4):875-87.

Hallbook F, Ibanez CF, Persson H (1991). Evolutionary studies of the nerve growth factor family reveal a novel member abundantly expressed in Xenopus ovary. Neuron. 6(5):845-58.

Ham J, Babij C, Whitfield J, Pfarr CM, Lallemand D, Yaniv M, Rubin LL (1995) A c-Jun dominant negative mutant protects sympathetic neurons against programmed cell death. Neuron 14:927-39

Hammarberg H, Piehl F, Cullheim S, Fjell J, Hokfelt T, Fried K (1996). GDNF mRNA in Schwann cells and DRG satellite cells after chronic sciatic nerve injury. Neuroreport. 7(4):857-60.

Hammarberg H, Piehl F, Risling M, Cullheim S (2000). Differential regulation of trophic factor receptor mRNAs in spinal motoneurons after sciatic nerve transection and ventral root avulsion in the rat. J Comp Neurol. 426(4):587-601.

Hanz S, Perlson E, Willis D, Zheng JQ, Massarwa R, Huerta JJ, Koltzenburg M, Kohler M, van-Minnen J, Twiss JL, Fainzilber M (2003) Axoplasmic importins enable retrograde injury signaling in lesioned nerve. Neuron 40:1095-104

Hartmann U, Maurer P (2001) Proteoglycans in the nervous system--the quest for functional roles in vivo. Matrix Biol 20: 23-35.

Heidenreich KA, Linseman DA (2004). Myocyte enhancer factor-2 transcription factors in neuronal differentiation and survival. Mol Neurobiol. 29(2):155-66.

Henkemeyer M, Orioli D, Henderson JT, Saxton TM, Roder J, Pawson T, Klein R (1996) Nuk controls pathfinding of commissural axons in the mammalian central nervous system. Cell 86: 35-46.

Henley J, Poo MM (2004) Guiding neuronal growth cones using Ca2+ signals. Trends Cell Biol14:320-30

Herdegen T, Kummer W, Fiallos CE, Leah J, Bravo R (1991) Expression of c-JUN, JUN B and JUN D proteins in rat nervous system following transection of vagus nerve and cervical sympathetic trunk. Neurosci 45:413-22.

Herdegen T, Leah JD (1998) Inducible and constitutive transcription factors in the mammalian nervous system: control of gene expression by Jun, Fos and Krox, and CREB/ATF proteins. Brain Res Brain Res Rev. 28:370-490

Herzog A, Brosamle C (1997). 'Semifree-floating' treatment: a simple and fast method to process consecutive sections for immunohistochemistry and neuronal tracing. J Neurosci Methods. 72(1):57-63.

Heuer H, Schafer MK, O'Donnell D, Walker P, Bauer K (2000) Expression of thyrotropin-releasing hormone receptor 2 (TRH-R2) in the central nervous system of rats. J Comp Neurol 428:319-36

Heumann R, Goemans C, Bartsch D, Lingenhohl K, Waldmeier PC, Hengerer B, Allegrini PR, Schellander K, Wagner EF, Arendt T, Kamdem RH, Obst-Pernberg K, Narz F, Wahle P, Berns H (2000). Transgenic activation of Ras in neurons promotes hypertrophy and protects from lesion-induced degeneration. J Cell Biol. 151(7):1537-48.

Hiebert GW, Khodarahmi K, McGraw J, Steeves JD, Tetzlaff W (2002). Brain-derived neurotrophic factor applied to the motor cortex promotes sprouting of corticospinal fibers but not regeneration into a peripheral nerve transplant. J Neurosci Res. 69(2):160-8.

Hirota H, Kiyama H, Kishimoto T, Taga T (1996). Accelerated Nerve Regeneration in Mice by upregulated expression of interleukin (IL) 6 and IL-6 receptor after trauma. J Exp Med. 183(6):2627-34.

Ho TW, Bristol LA, Coccia C, Li Y, Milbrandt J, Johnson E, Jin L, Bar-Peled O, Griffin JW, Rothstein JD (2000) TGFβeta trophic factors differentially modulate motor axon outgrowth and protection from excitotoxicity. Exp Neurol. 161:664-75.

Hofstetter CP, Holmstrom NA, Lilja JA, Schweinhardt P, Hao J, Spenger C, Wiesenfeld-Hallin Z, Kurpad SN, Frisen J, Olson L (2005). Allodynia limits the usefulness of intraspinal neural stem cell grafts; directed differentiation improves outcome. Nat Neurosci. 8(3):346-53.

Hohn A, Leibrock J, Bailey K, Barde YA (1990). Identification and characterization of a novel member of the nerve growth factor/brain-derived neurotrophic factor family. Nature. 344(6264):339-41.

Holtmaat AJ, De Winter F, de Wit J, Gorter JA, da Silva FH, Verhaagen J (2002) Semaphorins: contributors to structural stability of hippocampal networks? Prog Brain Res 138: 17-38.

Hopker VH, Shewan D, Tessier-Lavigne M, Poo M, Holt C (1999) Growth-cone attraction to netrin-1 is converted to repulsion by laminin-1. Nature 401: 69-73.

Horie H, Kadoya T (2000) Identification of oxidized galectin-1 as an initial repair regulatory factor after axotomy in peripheral nerves. Neurosci Res 38:131-7

Horvat A, Schwaiger F, Hager G, Brocker F, Streif R, Knyazev P, Ullrich A, Kreutzberg GW (2001). A novel role for protein tyrosine phosphatase shp1 in controlling glial activation in the normal and injured nervous system. J Neurosci. 21(3):865-74.

Hottinger AF, Azzouz M, Deglon N, Aebischer P, Zurn AD (2000). Complete and long-term rescue of lesioned adult motoneurons by lentiviral-mediated expression of glial cell line-derived neurotrophic factor in the facial nucleus. J Neurosci. 20(15):5587-93.

Houle JD, Tom VJ, Mayes D, Wagoner G, Phillips N, Silver J (2006). Combining an autologous peripheral nervous system "bridge" and matrix modification by chondroitinase allows robust, functional regeneration beyond a hemisection lesion of the adult rat spinal cord. J Neurosci. 26(28):7405-15.

Huang EJ, Reichardt LF (2001). Neurotrophins: roles in neuronal development and function. Annu Rev Neurosci. 24:677-736.

Huang EJ, Reichardt LF (2003). Trk receptors: roles in neuronal signal transduction. Annu Rev Biochem. 72:609-42.

Hynds DL, Snow DM (1999) Neurite outgrowth inhibition by chondroitin sulfate proteoglycan: stalling/stopping exceeds turning in human neuroblastoma growth cones. Exp Neurol 160: 244-255.

Iarikov DE, Kim BG, Dai HN, McAtee M, Kuhn PL, Bregman BS (2007). Delayed transplantation with exogenous neurotrophin administration enhances plasticity of corticofugal projections after spinal cord injury. J Neurotrauma. 24(4):690-702.

Ide C (1996). Peripheral nerve regeneration. Neurosci Res. 25(2):101-21.

Ide C, Kato S. 1990 Peripheral nerve regeneration. Neurosci Res Suppl 13:S157-64.

Ihara S, Nakajima K, Fukada T, Hibi M, Nagata S, Hirano T, Fukui Y (1997) Dual control of neurite outgrowth by STAT3 and MAP kinase in PC12 cells stimulated with interleukin-6. EMBO J 16:5345-52

Ihara S, Nakajima K, Fukada T, Hibi M, Nagata S, Hirano T, Fukui Y (1997) Dual control of neurite outgrowth by STAT3 and MAP kinase in PC12 cells stimulated with interleukin-6. EMBO J. 16(17):5345-52.

Inman DM, Steward O (2003). Ascending sensory, but not other long-tract axons, regenerate into the connective tissue matrix that forms at the site of a spinal cord injury in mice. J Comp Neurol. 462(4):431-49.

Inserra MM, Yao M, Murray R, Terris DJ (2001). Peripheral nerve regeneration in interleukin 6-deficient mice. Arch Otolaryngol Head Neck Surg. 126(9):1112-6.

Ishihara A, Saito H, Abe K (1994). Transforming growth factor-β 1 and -β 2 promote neurite sprouting and elongation of cultured rat hippocampal neurons. Brain Res 639:21-25.

Ishii DN, Glazner GW, Pu SF (1994) Role of insulin-like growth factors in peripheral nerve regeneration. Pharmacol Ther 62:125-44

Ito Y, Sakagami H, Kondo H (1996) Enhanced gene expression for phosphatidylinositol 3-kinase in the hypoglossal motoneurons following axonal crush. Mol Brain Res 37:329-32.

Ivins JK, Yurchenco PD, Lander AD (2000). Regulation of neurite outgrowth by integrin activation. J Neurosci. 20(17):6551-60.

Iwamasa H, Ohta K, Yamada T, Ushijima K, Terasaki H, Tanaka H (1999) Expression of Eph receptor tyrosine kinases and their ligands in chick embryonic motor neurons and hindlimb muscles. Dev Growth Differ 41: 685-698.

Iwata T, Namikawa K, Honma M, Mori N, Yachiku S, Kiyama H (2002) Increased expression of mRNAs for microtubule disassembly molecules during nerve regeneration. Mol Brain Res 102:105-9.

Jackson TR, Blader IJ, Hammonds-Odie LP, Burga CR, Cooke F, Hawkins PT, Wolf AG, Heldman KA, Theibert AB (1996). Initiation and maintenance of NGF-stimulated neurite outgrowth requires activation of a phosphoinositide 3-kinase. J Cell Sci. 109 (Pt 2):289-300.

Jeffery ND, Fitzgerald M (2001). Effects of red nucleus ablation and exogenous neurotrophin-3 on corticospinal axon terminal distribution in the adult rat. Neuroscience. 104(2):513-21.

Jenkins R, Hunt SP (1991) Long-term increase in the levels of c-jun mRNA and jun protein-like immunoreactivity in motor and sensory neurons following axon damage. Neurosci Lett 129:107-10

Jin Y, Fischer I, Tessler A, Houle JD (2002). Transplants of fibroblasts genetically modified to express BDNF promote axonal regeneration from

supraspinal neurons following chronic spinal cord injury. Exp Neurol. 177(1):265-75.

Johns LD, Sriram S (1993). Experimental allergic encephalomyelitis: neutralizing antibody to TGF β 1 enhances the clinical severity of the disease. J Neuroimmunol 47:1-7.

Johnson EM Jr, Gorin PD, Osborne PA, Rydel RE, Pearson J (1982). Effects of autoimmune NGF deprivation in the adult rabbit and offspring. Brain Res. 240(1):131-40.

Jones DM, Tucker BA, Rahimtula M, Mearow KM (2003). The synergistic effects of NGF and IGF-1 on neurite growth in adult sensory neurons: convergence on the PI 3-kinase signaling pathway. J Neurochem. 86(5):1116-28.

Jones KJ, Serpe CJ, Byram SC, Deboy CA, Sanders VM (2005). Role of the immune system in the maintenance of mouse facial motoneuron viability after nerve injury. Brain Behav Immun. 19(1):12-9.

Jones KR, Reichardt LF (1990). Molecular cloning of a human gene that is a member of the nerve growth factor family. Proc Natl Acad Sci U S A. 87(20):8060-4.

Jones LL, Banati RB, Graeber MB, Bonfanti L, Raivich G, Kreutzberg GW (1997) Population control of microglia: does apoptosis play a role? J Neurocytol 26:755-70

Jones LL, Kreutzberg GW, Raivich G (1998) Transforming growth factor β's 1, 2 and 3 inhibit proliferation of ramified microglia on an astrocyte monolayer. Brain Res, 795:301-306

Jones LL, Liu Z, Shen J, Werner A, Kreutzberg GW, Raivich G (2000) Regulation of the cell adhesion molecule CD44 after nerve transection and direct trauma to the mouse brain. J Comp Neurol.426:468-92.

Jones LL, Oudega M, Bunge MB, Tuszynski MH (2001). Neurotrophic factors, cellular bridges and gene therapy for spinal cord injury. J Physiol. 533(Pt 1):83-9.

Journot L, Villalba M, Bockaert J (1998). PACAP-38 protects cerebellar granule cells from apoptosis. Ann N Y Acad Sci. 865:100-10.

Jovanovic JN, Benfenati F, Siow YL, Sihra TS, Sanghera JS, Pelech SL, Greengard P, Czernik AJ (1996). Neurotrophins stimulate phosphorylation of synapsin I by MAP kinase and regulate synapsin I-actin interactions. Proc Natl Acad Sci U S A. 93(8):3679-83.

Junghans U, Koops A, Westmeyer A, Kappler J, Meyer HE, Muller HW (1995) Purification of a meningeal cell-derived chondroitin sulphate proteoglycan with neurotrophic activity for brain neurons and its identification as biglycan. Eur J Neurosci 7: 2341-2350.

Kalderon N, Fuks Z (1996). Structural recovery in lesioned adult mammalian spinal cord by x-irradiation of the lesion site. Proc Natl Acad Sci U S A. 1996 Oct 1;93(20):11179-84. Erratum in: Proc Natl Acad Sci U S A 93(25):14992.

Kalla R, Kloss CUA, Bohatschek M, Krol J, von Maltzan X, Raivich G (2003) Loss of microglial ramification in microglia-astrocyte cocultures: involvement of adenylate cyclase, calcium, phosphatase and Gi-protein systems. GLIA, 40:50-63

Kalla R, Liu Z, Xu S, Koppius A, Imai Y, Kloss CU, Kohsaka S, Gschwendtner A, Moller JC, Werner A, Raivich G (2001). Microglia and the early phase of immune surveillance in the axotomized facial motor nucleus: impaired microglial activation and lymphocyte recruitment but no effect on neuronal survival or axonal regeneration in macrophage-colony stimulating factor-deficient mice. J Comp Neurol. 436(2):182-201.

Kallapur S, Ormsby I, Doetschman T (1999) Strain dependency of TGF ß1 function during embryogenesis. Mol Reprod Dev 52: 341-349

Kanje M, Skottner A, Sjoberg J, Lundborg G (1989). Insulin-like growth factor I (IGF-I) stimulates regeneration of the rat sciatic nerve. Brain Res. 486(2):396-8.

Kantor DB, Chivatakarn O, Peer KL, Oster SF, Inatani M, Hansen MJ, Flanagan JG, Yamaguchi Y, Sretavan DW, Giger RJ, Kolodkin AL (2004) Semaphorin 5A is a bifunctional axon guidance cue regulated by heparan and chondroitin sulfate proteoglycans. Neuron 44: 961-975.

Kaplan DR, Martin-Zanca D, Parada LF (1991). Tyrosine phosphorylation and tyrosine kinase activity of the trk proto-oncogene product induced by NGF. Nature. 350(6314):158-60.

Kaplan DR, Miller FD (2000). Neurotrophin signal transduction in the nervous system. Curr Opin Neurobiol. 10(3):381-91.

Kiefer R, Gold R, Gehrmann J, Lindholm D, Wekerle H, Kreutzberg GW (1993a) Transforming growth factor β expression in reactive spinal cord microglia and meningeal infalmmatory cells during experimental allergic neuritis. J Neurosci Res 36:391-398

Kiefer R, Lindholm D, Kreutzberg GW (1993b) Interleukin-6 and transforming growth factor-ß1 mRNAs are induced in rat facial nucleus following motoneuron axotomy. Eur J Neurosci 5:775-781

Kim IJ, Drahushuk KM, Kim WY, Gonsiorek EA, Lein P, Andres DA, Higgins D (2004). Extracellular signal-regulated kinases regulate dendritic growth in rat sympathetic neurons. J Neurosci. 24(13):3304-12.

Kim JE, Li S, GrandPre T, Qiu D, Strittmatter SM (2003). Axon regeneration in young adult mice lacking Nogo-A/B. Neuron. 38(2):187-99.

Kim JE, Liu BP, Park JH, Strittmatter SM (2004). Nogo-66 receptor prevents raphespinal and rubrospinal axon regeneration and limits functional recovery from spinal cord injury. Neuron. 44(3):439-51.

Kimpinski K, Mearow K (2001). Neurite growth promotion by nerve growth factor and insulin-like growth factor-1 in cultured adult sensory neurons: role of phosphoinositide 3-kinase and mitogen activated protein kinase. J Neurosci Res. 63(6):486-99.

Kirsch M, Schneider T, Lee MY, Hofmann HD (1998). Lesion-induced changes in the expression of ciliary neurotrophic factor and its receptor in rat optic nerve. Glia. 23(3):239-48.

Kirstein M, Farinas I (2002). Sensing life: regulation of sensory neuron survival by neurotrophins. Cell Mol Life Sci. 59(11):1787-802.

Kiryu S, Morita N, Ohno K, Maeno H, Kiyama H (1995) Regulation of mRNA expression involved in Ras and PKA signal pathways during rat hypoglossal nerve regeneration. Mol Brain Res 29:147-56.

Kiryu S, Morita N, Ohno K, Maeno H, Kiyama H (1995). Regulation of mRNA expression involved in Ras and PKA signal pathways during rat hypoglossal nerve regeneration. Brain Res Mol Brain Res. 29(1):147-56.

Kiryu-Seo S, Hirayama T, Kato R, Kiyama H (2005) Noxa is a critical mediator of p53-dependent motor neuron death after nerve injury in adult mouse. J Neurosci. 25:1442-7.

Kita Y, Kimura KD, Kobayashi M, Ihara S, Kaibuchi K, Kuroda S, Ui M, Iba H, Konishi H, Kikkawa U, Nagata S, Fukui Y (1998) Microinjection of activated phosphatidylinositol-3 kinase induces process outgrowth in rat PC12 cells through the Rac-JNK signal transduction pathway.

Kitahara T, Kiryu S, Ohno K, Morita N, Kubo T, Kiyama H (1994). Up-regulation of ERK (MAP kinase) and MEK (MAP kinase kinase) transcription after rat facial nerve transection. Neurosci Res. 20(3):275-80.

Klein MA, Moller JC, Jones LL, Bluethmann H, Kreutzberg GW, Raivich G (1997). Impaired neuroglial activation in interleukin-6 deficient mice. Glia. 19(3):227-33.

Klein R, Jing SQ, Nanduri V, O'Rourke E, Barbacid M (1991). The trk proto-oncogene encodes a receptor for nerve growth factor. Cell. 65(1):189-97.

Klempt ND, Sirimanne E, Gunn AJ, Klempt M, Singh C, Williams C, Gluckman PD (1992) Hypoxia-ischaemia induces transforming growth factor-β1 mRNA in the infant rat brain. Mol Brain Res 13:93-101

Klesse LJ, Parada LF (1998). p21 ras and phosphatidylinositol-3 kinase are required for survival of wild-type and NF1 mutant sensory neurons. J Neurosci. 18(24):10420-8.

Klocker N, Kermer P, Weishaupt JH, Labes M, Ankerhold R, Bahr M (2000). Brain-derived neurotrophic factor-mediated neuroprotection of adult rat retinal ganglion cells in vivo does not exclusively depend on phosphatidyl-inositol-3'-kinase/protein kinase B signaling. J Neurosci. 20(18):6962-7.

Kloss CU, Werner A, Klein MA, Shen J, Menuz K, Probst JC, Kreutzberg GW, Raivich G (1999). Integrin family of cell adhesion molecules in the injured brain: regulation and cellular localization in the normal and regenerating mouse facial motor nucleus. J Comp Neurol. 411(1):162-78.

Knoll B, Zarbalis K, Wurst W, Drescher U (2001) A role for the EphA family in the topographic targeting of vomeronasal axons. Development 128: 895-906.

Kobayashi NR, Fan DP, Giehl KM, Bedard AM, Wiegand SJ, Tetzlaff W (1997). BDNF and NT-4/5 prevent atrophy of rat rubrospinal neurons after cervical axotomy, stimulate GAP-43 and Tα1-tubulin mRNA expression, and promote axonal regeneration. J Neurosci. 17(24):9583-95.

Kolb B, Cote S, Ribeiro-da-Silva A, Cuello AC (1997a). Nerve growth factor treatment prevents dendritic atrophy and promotes recovery of function after cortical injury.Neuroscience. 76(4):1139-51.

Kolb B, Gorny G, Cote S, Ribeiro-da-Silva A, Cuello AC (1997b). Nerve growth factor stimulates growth of cortical pyramidal neurons in young adult rats. Brain Res. 1997 751(2):289-94.

Kolch W (2000). Meaningful relationships: the regulation of the Ras/Raf/MEK/ERK pathway by protein interactions. Biochem J. 351 Pt 2:289-305.

Kolch W (2005). Coordinating ERK/MAPK signalling through scaffolds and inhibitors. Nat Rev Mol Cell Biol. 6(11):827-37.

Koliatsos VE, Clatterbuck RE, Winslow JW, Cayouette MH, Price DL (1993) Evidence that brain-derived neurotrophic factor is a trophic factor for motor neurons in vivo. Neuron 10:359-67

Koprivica V, Cho KS, Park JB, Yiu G, Atwal J, Gore B, Kim JA, Lin E, Tessier-Lavigne M, Chen DF, He Z (2005) EGFR activation mediates inhibition of axon regeneration by myelin and chondroitin sulfate proteoglycans. Science 310: 106-110.

Korhonen JM, Said FA, Wong AJ, Kaplan DR (1999). Gab1 mediates neurite outgrowth, DNA synthesis, and survival in PC12 cells. J Biol Chem. 274(52):37307-14.

Korsching S, Thoenen H (1985). Nerve growth factor supply for sensory neurons: site of origin and competition with the sympathetic nervous system. Neurosci Lett. 54(2-3):201-5.

Kost SA, Oblinger MM (1993). Immature corticospinal neurons respond to axotomy with changes in tubulin gene expression. Brain Res Bull. 30(3-4):469-75.

Kreutzberg GW, Raivich G (2000) Neurobiology of regeneration and degeneration. In The Facial Nerve (May M, Ed). Thieme, New York, 2nd edition

Krieglstein K, Richter S, Farkas L, Schuster N, Dunker N, Oppenheim RW, Unsicker K (2000) Reduction of endogenous transforming growth factors β prevents ontogenetic neuron death. NAT NEUROSCI 3:1085-1090

Kubo T, Yamashita T, Yamaguchi A, Hosokawa K, Tohyama M. Analysis of genes induced in peripheral nerve after axotomy using cDNA microarrays. J Neurochem. 2002 Sep;82(5):1129-36.

Kulbatski I, Cook DJ, Tator CH (2004) Calcium entry through L-type calcium channels is essential for neurite regeneration in cultured sympathetic neurons. J Neurotrauma. 21:357-74.

Kullander K, Croll SD, Zimmer M, Pan L, McClain J, Hughes V, Zabski S, DeChiara TM, Klein R, Yancopoulos GD, Gale NW (2001) Ephrin-B3 is the midline barrier that prevents corticospinal tract axons from recrossing, allowing for unilateral motor control. Genes Dev 15: 877-888.

Kullander K, Klein R (2002) Mechanisms and functions of Eph and ephrin signalling. Nat Rev Mol Cell Biol 3: 475-486.

Kuo WL, Chung KC, Rosner MR (1997). Differentiation of central nervous system neuronal cells by fibroblast-derived growth factor requires at least

two signalling pathways: roles for Ras and Src. Mol Cell Biol. 17(8):4633-43.

Kury P, Abankwa D, Kruse F, Greiner-Petter R, Muller HW. 2004 Gene expression profiling reveals multiple novel intrinsic and extrinsic factors associated with axonal regeneration failure. Eur J Neurosci. 19:32-42

Lai KO, Fu WY, Ip FC, Ip NY (1998). Cloning and expression of a novel neurotrophin, NT-7, from carp. Mol Cell Neurosci. 11(1-2):64-76.

Lalancette-Hebert M, Gowing G, Simard A, Weng YC, Kriz J (2007) Selective ablation of proliferating microglial cells exacerbates ischemic injury in the brain. J Neurosci 27:2596-605

Lamballe F, Klein R, Barbacid M (1991). trkC, a new member of the trk family of tyrosine protein kinases, is a receptor for neurotrophin-3. Cell. 66(5):967-79.

Large TH, Bodary SC, Clegg DO, Weskamp G, Otten U, Reichardt LF (1986). Nerve growth factor gene expression in the developing rat brain. Science. 17;234(4774):352-5.

Lassmann H, Ammerer HP, Jurecka W, Kulnig W (1978). Ultrastructural sequence of myelin degradation. II. Wallerian degeneration in the rat femoral nerve. Acta Neuropathol (Berl). 44(2):103-9.

Latov N, Nilaver G, Zimmerman EA, Johnson WG, Silverman AJ, Defendini R, Cote L (1979). Fibrillary astrocytes proliferate in response to brain injury: a study combining immunoperoxidase technique for glial fibrillary acidic protein and radioautography of tritiated thymidine. Dev Biol. 72(2):381-4.

Laux T, Fukami K, Thelen M, Golub T, Frey D, Caroni P (2000) GAP43, MARCKS, and CAP23 modulate PI(4,5)P(2) at plasmalemmal rafts, and regulate cell cortex actin dynamics through a common mechanism. J Cell Biol 149:1455-72.

Lavie Y, Dybowski J, Agranoff BW (1997). Wortmannin blocks goldfish retinal phosphatidylinositol 3-kinase and neurite outgrowth. Neurochem Res. 22(4):373-8.

Lawrence DG, Kuypers HG (1968). The functional organization of the motor system in the monkey. II. The effects of lesions of the descending brain-stem pathways. Brain. 91(1):15-36.

Le Gros Clark WE (1943). The problem of neuronal regeneration in the central nervous system: II. The insertion of peripheral nerve stumps into the brain. J Anat. 77(3):251-9.

Leevers SJ, Marshall CJ (1992). Activation of extracellular signal-regulated kinase, ERK2, by p21ras oncoprotein. EMBO J. 11(2):569-74.

Leibrock J, Lottspeich F, Hohn A, Hofer M, Hengerer B, Masiakowski P, Thoenen H, Barde YA (1989). Molecular cloning and expression of brain-derived neurotrophic factor. Nature. 341(6238):149-52.

Lemons ML, Condic ML (2007). Integrin signaling is integral to regeneration. Exp Neurol. Jun 14; [Epub ahead of print]

Levi-Montalcini R, Hamburger V (1951). Selective growth stimulating effects of mouse sarcoma on the sensory and sympathetic nervous system of the chick embryo. J Exp Zool. 116(2):321-61.

Li D, Field PM, Yoshioka N, Raisman G (1994). Axons regenerate with correct specificity in horizontal slice culture of the postnatal rat entorhino-hippocampal system. Eur J Neurosci. 6:1026-37.

Li L, Zhou XF (2001) Pericellular Griffonia simplicifolia I isolectin B4-binding ring structures in the dorsal root ganglia following peripheral nerve injury in rats. J Comp Neurol. 439:259-74

Li M, Shibata A, Li C, Braun PE, McKerracher L, Roder J, Kater SB, David S (1996) Myelin-associated glycoprotein inhibits neurite/axon growth and causes growth cone collapse. J Neurosci Res. 46:404-14.

Li Y, Raisman G (1993). Long axon growth from embryonic neurons transplanted into myelinated tracts of the adult rat spinal cord. Brain Res. 629(1):115-27.

Li Y, Raisman G (1994). Schwann cells induce sprouting in motor and sensory axons in the adult rat spinal cord. J Neurosci. 14(7):4050-63.

Li Y, Raisman G (1995). Sprouts from cut corticospinal axons persist in the presence of astrocytic scarring in long-term lesions of the adult rat spinal cord. Exp Neurol. 134:102-11.

Lieberman AR (1971). The axon reaction: a review of the principal features of perikaryal responses to axon injury. Int Rev Neurobiol. 14:49-124.

Liebl DJ, Morris CJ, Henkemeyer M, Parada LF (2003) mRNA expression of ephrins and Eph receptor tyrosine kinases in the neonatal and adult mouse central nervous system. J Neurosci Res 71: 7-22.

Liebscher T, Schnell L, Schnell D, Scholl J, Schneider R, Gullo M, Fouad K, Mir A, Rausch M, Kindler D, Hamers FP, Schwab ME (2005). Nogo-A antibody improves regeneration and locomotion of spinal cord-injured rats. Ann Neurol. 58:706-19.

Linda H, Risling M, Cullheim S (1985) 'Dendraxons' in regenerating motoneurons in the cat: do dendrites generate new axons after central axotomy? Brain Res. 358(1-2):329-33.

Lindholm D, Castren E, Kiefer R, Zafra F, Thoenen H (1992) Transforming growth factor-β 1 in the rat brain: increase after injury and inhibition of astrocyte proliferation. J Cell Biol. 117:395-400

Lindholm D, Heumann R, Meyer M, Thoenen H (1987) Interleukin-1 regulates synthesis of nerve growth factor in non-neuronal cells of rat sciatic nerve. Nature 330:658-9

Lindsay RM (1988). Nerve growth factors (NGF, BDNF) enhance axonal regeneration but are not required for survival of adult sensory neurons. J Neurosci. 8(7):2394-405.

Lindsay RM (1996). Role of neurotrophins and trk receptors in the development and maintenance of sensory neurons: an overview. Philos Trans R Soc Lond B Biol Sci. 351(1338):365-73.

Lindwall C, Dahlin L, Lundborg G, Kanje M (2004) Inhibition of c-Jun phosphorylation reduces axonal outgrowth of adult rat nodose ganglia and dorsal root ganglia sensory neurons. Mol Cell Neurosci 27:267-79

Liu BP, Cafferty WB, Budel SO, Strittmatter SM (2006). Extracellular regulators of axonal growth in the adult central nervous system. Philos Trans R Soc Lond B Biol Sci. 361:1593-610.

Liu BP, Strittmatter SM (2001) Semaphorin-mediated axonal guidance via Rho-related G proteins. Curr Opin Cell Biol 13: 619-626.

Liu CN, Chambers WW (1958). Intraspinal sprouting of dorsal root axons; development of new collaterals and preterminals following partial denervation of the spinal cord in the cat. AMA Arch Neurol Psychiatry. 79(1):46-61.

Liu HM, Yang LH, Yang YJ (1995). Schwann cell properties: 3. C-fos expression, bFGF production, phagocytosis and proliferation during Wallerian degeneration. J Neuropathol Exp Neurol. 54(4):487-96.

Liu RY, Snider WD (2001) Different signaling pathways mediate regenerative versus developmental sensory axon growth. J Neurosci 21:RC164

Liu W, Hirata K, Kawabuchi M (2005) The occurrence of nitric oxide synthase-containing axonal baskets surrounding large neurons in rat dorsal root ganglia after sciatic nerve ligation. Arch Histol Cytol 68:29-40

Liu Y, Himes BT, Murray M, Tessler A, Fischer I (2002). Grafts of BDNF-producing fibroblasts rescue axotomized rubrospinal neurons and prevent their atrophy. Exp Neurol. 178(2):150-64.

Liu ZQ, Bohatschek M, Pfeffer K, Bluethmann H, Raivich G (2005) Major histocompatibility complex (MHC2+) perivascular macrophages in the axotomized facial motor nucleus are regulated by receptors for interferon-gamma (IFNgamma) and tumor necrosis factor (TNF). Neuroscience. 131:283-92.

Liu ZQ, Bohatschek M, Pfeffer K, Bluethmann H, Raivich G (2005). Major histocompatibility complex (MHC2+) perivascular macrophages in the axotomized facial motor nucleus are regulated by receptors for interferon-gamma (IFNgamma) and tumor necrosis factor (TNF). Neuroscience. 131(2):283-92.

Liuzzi FJ, Lasek RJ (1987). Astrocytes block axonal regeneration in mammals by activating the physiological stop pathway. Science. 237(4815):642-5.

Livesey FJ, O'Brien JA, Li M, Smith AG, Murphy LJ, Hunt SP (1997) A Schwann cell mitogen accompanying regeneration of motor neurons. Nature 390:614-8

Lobner D, Liot G (2004). Role of MAPK/ERK in neurotrophin-4 potentiation of necrotic neuronal death. Neurochem Res. 29(12):2303-9.

Loewy AD, Schader RE (1977). A quantitative study of retrograde neuronal changes in Clarke's column. J Comp Neurol. 171(1):65-81.

Logan A, Berry M, Gonzalez AM, Fratschy SA, Sporn MB, Baird A (1994) Effects of transforming growth factor β1 on scar production in the injured central nervous system of the rat. Eur J Neurosci 6:355-363

Lu L, Anneren C, Reedquist KA, Bos JL, Welsh M (2000). NGF-Dependent neurite outgrowth in PC12 cells overexpressing the Src homology 2-domain protein shb requires activation of the Rap1 pathway. Exp Cell Res. 259(2):370-7.

Lu P, Blesch A, Tuszynski MH (2001). Neurotrophism without neurotropism: BDNF promotes survival but not growth of lesioned corticospinal neurons. J Comp Neurol. 436(4):456-70.

Lu X, Richardson PM (1991) Inflammation near the nerve cell body enhances axonal regeneration. J Neurosci. 11:972-8.

Ludwin SK, Bisby MA (1992). Delayed wallerian degeneration in the central nervous system of Ola mice: an ultrastructural study. J Neurol Sci. 109(2):140-7.

Lundborg G (2005). Nerve Injury and Repair. Churchill Livingstone.

Luo JM, Cen LP, Zhang XM, Chiang SW, Huang Y, Lin D, Fan YM, van Rooijen N, Lam DS, Pang CP, Cui Q (2007). PI3K/akt, JAK/STAT and MEK/ERK pathway inhibition protects retinal ganglion cells via different mechanisms after optic nerve injury. Eur J Neurosci. 26(4):828-42.

Ma L, Harada T, Harada C, Romero M, Hebert JM, McConnell SK, Parada LF (2002). Neurotrophin-3 is required for appropriate establishment of thalamocortical connections. Neuron. 36(4):623-34.

MacDonald JI, Kubu CJ, Meakin SO (2004). Nesca, a novel adapter, translocates to the nuclear envelope and regulates neurotrophin-induced neurite outgrowth. J Cell Biol. 164(6):851-62.

Madura T, Yamashita T, Kubo T, Tsuji L, Hosokawa K, Tohyama M (2004) Changes in mRNA of Slit-Robo GTPase-activating protein 2 following facial nerve transection. Mol Brain Res 123:76-80

Maisonpierre PC, Belluscio L, Friedman B, Alderson RF, Wiegand SJ, Furth ME, Lindsay RM, Yancopoulos GD (1990b). NT-3, BDNF, and NGF in the developing rat nervous system: parallel as well as reciprocal patterns of expression. Neuron. 5(4):501-9.

Maisonpierre PC, Belluscio L, Squinto S, Ip NY, Furth ME, Lindsay RM, Yancopoulos GD (1990a). Neurotrophin-3: a neurotrophic factor related to NGF and BDNF. Science. 247(4949 Pt 1):1446-51.

Makwana M, Jones LL, Cuthill D, Heuer H, Bohatschek M, Hristova M, Friedrichsen S, Ormsby I, Bueringer D, Koppius A, Bauer K, Doetschman T, Raivich G (2007). Endogenous TGF-β 1 suppresses inflammation and promotes survival in adult CNS. J Neurosci *in press*

Mamounas LA, Blue ME, Siuciak JA, Altar CA (1995). Brain-derived neurotrophic factor promotes the survival and sprouting of serotonergic axons in rat brain. J Neurosci. 15(12):7929-39.

Manitt C, Colicos MA, Thompson KM, Rousselle E, Peterson AC, Kennedy TE (2001) Widespread expression of netrin-1 by neurons and oligodendrocytes in the adult mammalian spinal cord. J Neurosci 21: 3911-3922.

Mansour SJ, Resing KA, Candi JM, Hermann AS, Gloor JW, Herskind KR, Wartmann M, Davis RJ, Ahn NG (1995). Mitogen-activated protein (MAP) kinase phosphorylation of MAP kinase kinase: determination of phosphorylation sites by mass spectrometry and site-directed mutagenesis. J Biochem (Tokyo).116(2):304-14.

Markus A, Patel TD, Snider WD (2002). Neurotrophic factors and axonal growth. Curr Opin Neurobiol. 12(5):523-31.

Markus A, Zhong J, Snider WD (2002). Raf and akt mediate distinct aspects of sensory axon growth. Neuron. 35(1):65-76.

Marshall CJ (1996). Ras effectors. Curr Opin Cell Biol. 8(2):197-204.

Martini R, Schachner M (1988). Immunoelectron microscopic localization of neural cell adhesion molecules (L1, N-CAM, and myelin-associated glycoprotein) in regenerating adult mouse sciatic nerve. J Cell Biol. 106(5):1735-46.

Martinou JC, Dubois-Dauphin M, Staple JK, Rodriguez I, Frankowski H, Missotten M, Albertini P, Talabot D, Catsicas S, Pietra C (1994). Overexpression of BCL-2 in transgenic mice protects neurons from naturally occurring cell death and experimental ischemia. Neuron. 13(4):1017-30.

Martinou JC, Le Van Thai A, Valette A, Weber MJ (1990) Transforming growth factor β one is a potent survival factor for rat embryo motoneurons in culture. Dev. Brain Res 52:175-181.

Mason MR, Lieberman AR, Grenningloh G, Anderson PN (2002) Transcriptional upregulation of SCG10 and CAP-23 is correlated with regeneration of the axons of peripheral and central neurons in vivo. Mol Cell Neurosci 20:595-615

Mason MR, Lieberman AR, Grenningloh G, Anderson PN (2002). Transcriptional upregulation of SCG10 and CAP-23 is correlated with regeneration of the axons of peripheral and central neurons in vivo. Mol Cell Neurosci. 20(4):595-615.

Massagué J (1990) The transforming growth factor-β family. Ann Rev Cell Biol 6:597-641

Matsubara M, Kusubata M, Ishiguro K, Uchida T, Titani K, Taniguchi H (1996). Site-specific phosphorylation of synapsin I by mitogen-activated protein kinase and Cdk5 and its effects on physiological functions. J Biol Chem. 271(35):21108-13.

Mattsson P, Janson AM, Aldskogius H, Svensson M (2001) Nimodipine promotes regeneration and functional recovery after intracranial facial nerve crush. J Comp Neurol 437:106-17

Mayer U, Saher G, Fassler R, Bornemann A, Echtermeyer F, von der Mark H, Miosge N, Poschl E, von der Mark K (1997) Absence of integrin α 7 causes a novel form of muscular dystrophy. Nat Genet. 117:318-23.

Mazzoni IE, Said FA, Aloyz R, Miller FD, Kaplan D (1999). Ras regulates sympathetic neuron survival by suppressing the p53-mediated cell death pathway. J Neurosci. 19(22):9716-27.

Mazzucchelli C, Vantaggiato C, Ciamei A, Fasano S, Pakhotin P, Krezel W, Welzl H, Wolfer DP, Pages G, Valverde O, Marowsky A, Porrazzo A, Orban PC, Maldonado R, Ehrengruber MU, Cestari V, Lipp HP, Chapman PF, Pouyssegur J, Brambilla R (2002). Knockout of ERK1 MAP kinase enhances synaptic plasticity in the striatum and facilitates striatal-mediated learning and memory. Neuron. 34(5):807-20.

McBride RL, Feringa ER, Smith BE (1988). The fate of prelabeled Clarke's column neurons after axotomy. Exp Neurol. 102(2):236-43.

McGraw J, McPhail LT, Oschipok LW, Horie H, Poirier F, Steeves JD, Ramer MS, Tetzlaff W (2004) Galectin-1 in regenerating motoneurons. Eur J Neurosci 20:2872-2880

McKeon RJ, Hoke A, Silver J (1995) Injury-induced proteoglycans inhibit the potential for laminin-mediated axon growth on astrocytic scars. Exp Neurol 136: 32-43.

McKerracher L, David S, Jackson DL, Kottis V, Dunn RJ, Braun PE (1994). Identification of myelin-associated glycoprotein as a major myelin-derived inhibitor of neurite growth. Neuron. 13(4):805-11.

McLachlan EM, Hu P (1998) Axonal sprouts containing calcitonin gene-related peptide and substance P form pericellular baskets around large diameter neurons after sciatic nerve transection in the rat. Neuroscience. 84:961-5

McLachlan EM, Janig W, Devor M, Michaelis M. (1993) Peripheral nerve injury triggers noradrenergic sprouting within dorsal root ganglia. Nature 363:543-6

McNamara RK, Jiang Y, Streit WJ, Lenox RH (2000) Facial motor neuron regeneration induces a unique spatial and temporal pattern of myristoylated alanine-rich C kinase substrate expression. Neuroscience 97:581-9

McPhail LT, Fernandes KJ, Chan CC, Vanderluit JL, Tetzlaff W (2004). Axonal reinjury reveals the survival and re-expression of regeneration-associated genes in chronically axotomized adult mouse motoneurons. Exp Neurol. 188(2):331-40.

McQuarrie IG, Grafstein B (1973) Axon outgrowth enhanced by a previous nerve injury. Arch Neurol 29:53-55.

McQuarrie IG, Grafstein B, Gershon MD (1977) Axonal regeneration in the rat sciatic nerve: effect of a conditioning lesion and of dbcAMP. Brain Res 132:443-453.

Meller K (1987). Early structural changes in the axoplasmic cytoskeleton after axotomy studied by cryofixation. Cell Tissue Res. 250(3):663-72.

Merline M, Kalil K (1990). Cell death of corticospinal neurons is induced by axotomy before but not after innervation of spinal targets. J Comp Neurol. 296(3):506-16.

Merrill JE, Zimmermann RP (1991) Natural and induced cytotoxicity of oligodendrocytes by microglia is inhibitable by TGFβ. Glia 4:327-331

Meyer M, Matsuoka I, Wetmore C, Olson L, Thoenen H (1992). Enhanced synthesis of brain-derived neurotrophic factor in the lesioned peripheral nerve: different mechanisms are responsible for the regulation of BDNF and NGF mRNA. J Cell Biol. 119(1):45-54.

Mi S, Lee X, Shao Z, Thill G, Ji B, Relton J, Levesque M, Allaire N, Perrin S, Sands B, Crowell T, Cate RL, McCoy JM, Pepinsky RB (2004). LINGO-1 is a component of the Nogo-66 receptor/p75 signaling complex. Nat Neurosci. 7(3):221-8.

Mikucki SA, Oblinger MM (1991). Corticospinal neurons exhibit a novel pattern of cytoskeletal gene expression after injury. J Neurosci Res. 30(1):213-25.

Mikule K, Sunpaweravong S, Gatlin JC, Pfenninger KH (2003) Eicosanoid activation of protein kinase C epsilon: involvement in growth cone repellent signaling. J Biol Chem 278: 21168-21177.

Miller RH, Abney ER, David S, Ffrench-Constant C, Lindsay R, Patel R, Stone J, Raff MC (1986). Is reactive gliosis a property of a distinct subpopulation of astrocytes? J Neurosci. 6(1):22-9.

Ming G, Song H, Berninger B, Inagaki N, Tessier-Lavigne M, Poo M (1999). Phospholipase C-gamma and phosphoinositide 3-kinase mediate cytoplasmic signaling in nerve growth cone guidance. Neuron. 23(1):139-48.

Ming GL, Wong ST, Henley J, Yuan XB, Song HJ, Spitzer NC, Poo MM (2002). Adaptation in the chemotactic guidance of nerve growth cones. Nature. 417(6887):411-8.

Miranda JD, White LA, Marcillo AE, Willson CA, Jagid J, Whittemore SR (1999) Induction of Eph B3 after spinal cord injury. Exp Neurol 156: 218-222.

Misantone LJ, Gershenbaum M, Murray M (1984). Viability of retinal ganglion cells after optic nerve crush in adult rats. J Neurocytol. 13(3):449-65.

Miyata Y, Kashihara Y, Homma S, Kuno M (1986) Effects of nerve growth factor on the survival and synaptic function of Ia sensory neurons axotomized in neonatal rats. J Neurosci 6:2012-8

Moller JC, Klein MA, Haas S, Jones LL, Kreutzberg GW, Raivich G (1996) Regulation of thrombospondin in the regenerating mouse facial motor nucleus. Glia. 17(2):121-32.

Moon LD, Asher RA, Rhodes KE, Fawcett JW (2001) Regeneration of CNS axons back to their target following treatment of adult rat brain with chondroitinase ABC. Nat Neurosci 4: 465-466.

Moon LD, Fawcett JW (2001). Reduction in CNS scar formation without concomitant increase in axon regeneration following treatment of adult rat brain with a combination of antibodies to TGFβ1 and β2. Eur J Neurosci. 14(10):1667-77.

Moore RY (1989) Cranial motor neurons contain either galanin- or calcitonin gene-related peptidelike immunoreactivity J Comp Neurol. 282:512-22.

Moran LB, Duke DC, Turkheimer FE, Banati RB, Graeber MB. 2004 Towards a transcriptome definition of microglial cells. Neurogenetics. 5:95-108

Moran LB, Graeber MB (2004) The facial nerve axotomy model. Brain Res Rev. 44:154-78

Moreau-Fauvarque C, Kumanogoh A, Camand E, Jaillard C, Barbin G, Boquet I, Love C, Jones EY, Kikutani H, Lubetzki C, Dusart I, Chedotal A (2003) The transmembrane semaphorin Sema4D/CD100, an inhibitor of axonal

growth, is expressed on oligodendrocytes and upregulated after CNS lesion. J Neurosci 23: 9229-9239.

Morgan TE, Nichols NR, Pasinetti GM, Finch CE (1993) TGF-β 1 mRNA increases in macrophage/microglial cells of the hippocampus in response to deafferentation and kainic acid-induced neurodegeneration. Exp Neurol 120:291-301.

Mori N, Morii H (2002) SCG10-related neuronal growth-associated proteins in neural development, plasticity, degeneration, and aging. J Neurosci Res 70:264-73

Morrison EE, Costanzo RM (1995). Regeneration of olfactory sensory neurons and reconnection in the aging hamster central nervous system. Neurosci Lett. 198(3):213-7.

Morrow DR, Campbell G, Lieberman AR, Anderson PN (1993). Differential regenerative growth of CNS axons into tibial and peroneal nerve grafts in the thalamus of adult rats. Exp Neurol. 120(1):60-9.

Moss A, Alvares D, Meredith-Middleton J, Robinson M, Slater R, Hunt SP, Fitzgerald M (2005) Ephrin-A4 inhibits sensory neurite outgrowth and is regulated by neonatal skin wounding. Eur J Neurosci 22: 2413-2421.

Mount MP, Lira A, Grimes D, Smith PD, Faucher S, Slack R, Anisman H, Hayley S, Park DS (2007) Involvement of interferon-gamma in microglial-mediated loss of dopaminergic neurons. J Neurosci 27:3328-37.

Munoz LM, Zayachkivsky A, Kunz RB, Hunt JM, Wang G, Scott SA (2005) Ephrin-A5 inhibits growth of embryonic sensory neurons. Dev Biol 283: 397-408.

Murakami Y, Suto F, Shimizu M, Shinoda T, Kameyama T, Fujisawa H (2001) Differential expression of plexin-A subfamily members in the mouse nervous system. Dev Dyn 220: 246-258.

Murashov AK, Ul Haq I, Hill C, Park E, Smith M, Wang X, Wang X, Goldberg DJ, Wolgemuth DJ (2001) Crosstalk between p38, Hsp25 and Akt in spinal motor neurons after sciatic nerve injury. Mol Brain Res 93:199-208

Murray M, Goldberger ME (1974) Restitution of function and collateral sprouting in the cat spinal cord: the partially hemisected animal. J Comp Neurol 158:19–36.

Murray M, Goldberger ME (1974). Restitution of function and collateral sprouting in the cat spinal cord: the partially hemisected animal. J Comp Neurol. 158(1):19-36.

Murray M, Kim D, Liu Y, Tobias C, Tessler A, Fischer I (2002). Transplantation of genetically modified cells contributes to repair and recovery from spinal injury. Brain Res Brain Res Rev. 40(1-3):292-300.

Namgung U, Choi BH, Park S, Lee JU, Seo HS, Suh BC, Kim KT (2004) Activation of cyclin-dependent kinase 5 is involved in axonal regeneration. Mol Cell Neurosci 25:422-32

Namikawa K, Honma M, Abe K, Takeda M, Mansur K, Obata T, Miwa A, Okado H, Kiyama H (2000) Akt/protein kinase B prevents injury-induced motoneuron death and accelerates axonal regeneration. J Neurosci 20:2875-86

Neumann S, Woolf CJ (1999). Regeneration of dorsal column fibers into and beyond the lesion site following adult spinal cord injury. Neuron. 23(1):83-91.

Neumann S, Woolf CJ (1999). Regeneration of dorsal column fibers into and beyond the lesion site following adult spinal cord injury. Neuron. 23(1):83-91.

Nguyen Ba-Charvet KT, Brose K, Marillat V, Kidd T, Goodman CS, Tessier-Lavigne M, Sotelo C, Chedotal A (1999) Slit2-Mediated chemorepulsion and collapse of developing forebrain axons. Neuron 22: 463-473.

Nguyen QT, Sanes JR, Lichtman JW (2002) Pre-existing pathways promote precise projection patterns. Nat Neurosci 5:861-7

Nichols NR, Laping NJ, Day JR, Finch CE (1991) Increases in transforming growth factor-β mRNA in hippocampus during response to entorhinal cortex lesions in intact and andrenectomized rats. J Neurosci Res 28:134-139

Nobes CD, Reppas JB, Markus A, Tolkovsky AM (1996). Active p21Ras is sufficient for rescue of NGF-dependent rat sympathetic neurons. Neuroscience. 70(4):1067-79.

Noda M, Ko M, Ogura A, Liu DG, Amano T, Takano T, Ikawa Y (1985). Sarcoma viruses carrying ras oncogenes induce differentiation-associated properties in a neuronal cell line. Nature. 318(6041):73-5.

Nornes H, Bjorklund A, Stenevi U (1983) Reinnervation of the denervated adult spinal cord of rats by intraspinal transplants of embryonic brain stem neurons. Cell Tissue Res 230:15-35.

Novikova LN, Novikov LN, Kellerth JO (2002). Differential effects of neurotrophins on neuronal survival and axonal regeneration after spinal cord injury in adult rats. J Comp Neurol. 452(3):255-63.

Nurse CA, Macintyre L, Diamond J (1984) Reinnervation of the rat touch dome restores the Merkel cell population reduced after denervation Neuroscience. 13:563-71.

Obata K, Yamanaka H, Dai Y, Tachibana T, Fukuoka T, Tokunaga A, Yoshikawa H, Noguchi K (2003). Differential activation of extracellular signal-regulated protein kinase in primary afferent neurons regulates

brain-derived neurotrophic factor expression after peripheral inflammation and nerve injury. J Neurosci. 23(10):4117-26.

Oble DA, Burton L, Maxwell K, Hassard T, Nathaniel EJ (2004) A comparison of thyroxine- and polyamine-mediated enhancement of rat facial nerve regeneration. Exp Neurol 189:105-11.

Obouhova G, Clowry GJ, Vrbova G (1994) Changes in retrogradely labelled neurones in the red nucleus and cortex after depletion of motoneurones by axotomy in neonatal rats. Dev Neurosci 16:34-7

Oertle T, van der Haar ME, Bandtlow CE, Robeva A, Burfeind P, Buss A, Huber AB, Simonen M, Schnell L, Brosamle C, Kaupmann K, Vallon R, Schwab ME (2003). Nogo-A inhibits neurite outgrowth and cell spreading with three discrete regions. J Neurosci. 23(13):5393-406.

Ohyama K, Kawano H, Kawamura K (1997). Localization of extracellular matrix molecules, integrins and their regulators, TGF betas, is correlated with axon pathfinding in the spinal cord of normal and Danforth's short tail mice. Brain Res Dev Brain Res. 103(2):143-54.

Okada S, Nakamura M, Mikami Y, Shimazaki T, Mihara M, Ohsugi Y, Iwamoto Y, Yoshizaki K, Kishimoto T, Toyama Y, Okano H (2004). Blockade of interleukin-6 receptor suppresses reactive astrogliosis and ameliorates functional recovery in experimental spinal cord injury. J Neurosci Res. 76(2):265-76.

Olson MF, Marais R (2000). Ras protein signalling. Semin Immunol. 12(1):63-73.

Oohashi T, Hirakawa S, Bekku Y, Rauch U, Zimmermann DR, Su WD, Ohtsuka A, Murakami T, Ninomiya Y (2002). Bral1, a brain-specific link protein, colocalizing with the versican V2 isoform at the nodes of Ranvier in developing and adult mouse central nervous systems. Mol Cell Neurosci. 19(1):43-57.

Oppenheim RW (1991). Cell death during development of the nervous system. Annu Rev Neurosci. 14:453-501.

Oppenheim RW, Prevette D, Haverkamp LJ, Houenou L, Yin QW, McManaman J (1993) Biological studies of a putative avian muscle-derived neurotrophic factor that prevents naturally occurring motoneuron death in vivo. J Neurobiol. 1993 Aug;24(8):1065-79.

Oudega M, Hagg T (1996). Nerve growth factor promotes regeneration of sensory axons into adult rat spinal cord. Exp Neurol. 140(2):218-29.

Oudega M, Hagg T (1999). Neurotrophins promote regeneration of sensory axons in the adult rat spinal cord. Brain Res. 818(2):431-8.

Oudega M, Varon S, Hagg T (1994) Regeneration of adult rat sensory axons into intraspinal nerve grafts: promoting effects of conditioning lesion and graft predegeneration. Exp Neurol 129:194-206.

Ouwens DM, de Ruiter ND, van der Zon GC, Carter AP, Schouten J, van der Burgt C, Kooistra K, Bos JL, Maassen JA, van Dam H (2002). Growth factors can activate ATF2 via a two-step mechanism: phosphorylation of Thr71 through the Ras-MEK-ERK pathway and of Thr69 through RalGDS-Src-p38. EMBO J. 21(14):3782-93.

Ozdinler PH, Macklis JD (2006). IGF-I specifically enhances axon outgrowth of corticospinal motor neurons. Nat Neurosci. 9(11):1371-81.

Pallini R, Fernandez E, Sbriccoli A (1988). Retrograde degeneration of corticospinal axons following transection of the spinal cord in rats. A quantitative study with anterogradely transported horseradish peroxidase. J Neurosurg. 68(1):124-8.

Palmada M, Kanwal S, Rutkoski NJ, Gustafson-Brown C, Johnson RS, Wisdom R, Carter BD (2002) c-jun is essential for sympathetic neuronal death

induced by NGF withdrawal but not by p75 activation. J Cell Biol 158:453-61

Park EM, Joh TH, Volpe BT, Chu CK, Song G, Cho S (2004). A neuroprotective role of extracellular signal-regulated kinase in N-acetyl-O-methyldopamine-treated hippocampal neurons after exposure to in vitro and in vivo ischemia. Neuroscience 123(1):147-54.

Pasquale EB (2005) Eph receptor signalling casts a wide net on cell behaviour. Nat Rev Mol Cell Biol 6: 462-475.

Pasterkamp RJ, Anderson PN, Verhaagen J (2001) Peripheral nerve injury fails to induce growth of lesioned ascending dorsal column axons into spinal cord scar tissue expressing the axon repellent Semaphorin3A. Eur J Neurosci 13: 457-471.

Pasterkamp RJ, De Winter F, Giger RJ, Verhaagen J (1998) Role for semaphorin III and its receptor neuropilin-1 in neuronal regeneration and scar formation? Prog Brain Res 117: 151-170.

Patel MN, McNamara JO (1995). Selective enhancement of axonal branching of cultured dentate gyrus neurons by neurotrophic factors. Neuroscience. 69(3):763-70.

Patel TD, Kramer I, Kucera J, Niederkofler V, Jessell TM, Arber S, Snider WD (2003). Peripheral NT3 signaling is required for ETS protein expression and central patterning of proprioceptive sensory afferents. Neuron. 38(3):403-16.

Pearson AG, Gray CW, Pearson JF, Greenwood JM, During MJ, Dragunow M (2003) ATF3 enhances c-Jun-mediated neurite sprouting. Mol Brain Res 120:38-45.

Pearson AG, Gray CW, Pearson JF, Greenwood JM, During MJ, Dragunow M (2003). ATF3 enhances c-Jun-mediated neurite sprouting. Brain Res Mol Brain Res. 120(1):38-45.

Pearson G, Robinson F, Beers Gibson T, Xu BE, Karandikar M, Berman K, Cobb MH (2001). Mitogen-activated protein (MAP) kinase pathways: regulation and physiological functions. Endocr Rev. 22(2):153-83.

Pekny M, Johansson CB, Eliasson C, Stakeberg J, Wallen A, Perlmann T, Lendahl U, Betsholtz C, Berthold CH, Frisen J (1999). Abnormal reaction to central nervous system injury in mice lacking glial fibrillary acidic protein and vimentin. J Cell Biol. 145(3):503-14.

Pekny M, Johansson CB, Eliasson C, Stakeberg J, Wallen A, Perlmann T, Lendahl U, Betsholtz C, Berthold CH, Frisen J (1999). Abnormal reaction to central nervous system injury in mice lacking glial fibrillary acidic protein and vimentin. J Cell Biol. 145(3):503-14.

Pekny M, Leveen P, Pekna M, Eliasson C, Berthold CH, Westermark B, Betsholtz C (1995). Mice lacking glial fibrillary acidic protein display astrocytes devoid of intermediate filaments but develop and reproduce normally. EMBO J. 14(8):1590-8.

Perry VH, Brown MC (1992). Macrophages and nerve regeneration. Curr Opin Neurobiol. 2(5):679-82.

Perry VH, Brown MC, Gordon S (1987). The macrophage response to central and peripheral nerve injury. A possible role for macrophages in regeneration. J Exp Med. 165(4):1218-23.

Perry VH, Gordon S (1988). Macrophages and microglia in the nervous system. Trends. Neurosci 11:273-277.

Perry VH, Tsao JW, Fearn S, Brown MC (1995) Radiation-induced reductions in macrophage recruitment have only slight effects on myelin degeneration in sectioned peripheral nerves of mice. Eur J Neurosci 7:271-280.

Pettersson LG, Lundberg A, Alstermark B, Isa T, Tantisira B (1997). Effect of spinal cord lesions on forelimb target-reaching and on visually guided switching of target-reaching in the cat. Neurosci Res. 29(3):241-56.

Pettmann B, Henderson CE (1998). Neuronal cell death. Neuron. 20(4):633-47.

Pezet S, McMahon SB (2006). Neurotrophins: mediators and modulators of pain. Annu Rev Neurosci. 29:507-38.

Plump AS, Erskine L, Sabatier C, Brose K, Epstein CJ, Goodman CS, Mason CA, Tessier-Lavigne M (2002) Slit1 and Slit2 cooperate to prevent premature midline crossing of retinal axons in the mouse visual system. Neuron 33: 219-232.

Popovich PG, Guan Z, McGaughy V, Fisher L, Hickey WF, Basso DM (2002). The neuropathological and behavioral consequences of intraspinal microglial/macrophage activation. J Neuropathol Exp Neurol. 61(7):623-33.

Popovich PG, Guan Z, Wei P, Huitinga I, van Rooijen N, Stokes BT (1999). Depletion of hematogenous macrophages promotes partial hindlimb recovery and neuroanatomical repair after experimental spinal cord injury. Exp Neurol. 158(2):351-65.

Poulsen KT, Armanini MP, Klein RD, Hynes MA, Phillips HS, Rosenthal A (1994) TGF β 2 and TGF β 3 are potent survival factors for midbrain dopaminergic neurons. Neuron. 13:1245-52.

Povelones M, Tran K, Thanos D, Ambron RT (1997) An NF-kappaB-like transcription factor in axoplasm is rapidly inactivated after nerve injury in Aplysia. J Neurosci 17:4915-20

Powell SK, Kleinman HK (1997) Neuronal laminins and their cellular receptors. Int J Biochem Cell Biol 29:401-14

Prendergast J, Stelzner DJ (1976). Changes in the magnocellular portion of the red nucleus following thoracic hemisection in the neonatal and adult rat. J Comp Neurol. 166(2):163-71.

Prior IA, Hancock JF (2001). Compartmentalization of Ras proteins. J Cell Sci. 114:1603-8.

Racke MK Dhib-Jalbut, S Cannella, B Albert, PS Raine, CS and McFarlinDE (1991) Prevention and treatment of chronic relapsing experimental allergic encephalomyelitis by transforming growth factor-β 1. J. Immunol 146:3012-3017.

Raineteau O, Fouad K, Bareyre FM, Schwab ME (2002). Reorganization of descending motor tracts in the rat spinal cord. Eur J Neurosci. 2002 Nov;16(9):1761-71.

Raineteau O, Fouad K, Noth P, Thallmair M, Schwab ME (2001). Functional switch between motor tracts in the presence of the mAb IN-1 in the adult rat. Proc Natl Acad Sci U S A. 98(12):6929-34.

Raineteau O, Schwab ME (2001). Plasticity of motor systems after incomplete spinal cord injury. Nat Rev Neurosci. 2(4):263-73.

Raivich and Makwana (2007).The making of successful axonal regeneration: genes, molecules and signal transduction pathways. Brain Res Rev 53(2):287-311

Raivich G (2005). Like cops on the beat: the active role of resting microglia. Trends Neurosci. 28(11):571-3.

Raivich G and Kreutzberg G (2001) Inflammatory Responses Following Nerve Injury. Marcel Dekker, Inc., New York, Basel.

Raivich G, Bohatschek M, Da Costa C, Iwata O, Galiano M, Hristova M, Nateri AS, Makwana M, Riera-Sans L, Wolfer DP, Lipp HP, Aguzzi A, Wagner EF, Behrens A (2004) The AP-1 transcription factor c-Jun is required for efficient axonal regeneration. Neuron 43(1):57-67.

Raivich G, Bohatschek M, Kloss CU, Werner A, Jones LL, Kreutzberg GW (1999) Neuroglial activation repertoire in the injured brain: graded response, molecular mechanisms and cues to physiological function. Brain Res Brain Res Rev. 30:77-105

Raivich G, Bohatschek M, Kloss CUA, Werner A, Jones LL, Kreutzberg GW (1999) Neuroglial activation in the injured brain: graded response, molecular mechanisms and cues to physiological function. Brain Res Rev, 30:77-105

Raivich G, Haas S, Werner A, Klein MA, Kloss C, Kreutzberg GW (1998b) Regulation of MCSF receptors on microglia in the normal and injured mouse central nervous system: a quantitative immunofluorescence study using confocal laser microscopy. J Comp Neurol. 395(3):342-58.

Raivich G, Haas S, Werner A, Klein MA, Kloss C, Kreutzberg GW (1998a). Regulation of MCSF receptors on microglia in the normal and injured mouse central nervous system: a quantitative immunofluorescence study using confocal laser microscopy. J Comp Neurol. 395(3):342-58.

Raivich G, Hellweg R, Kreutzberg GW (1991) NGF receptor-mediated reduction in axonal NGF uptake and retrograde transport following sciatic nerve injury and during regeneration. Neuron 7:151-64

Raivich G, Jones LL, Kloss CU, Werner A, Neumann H, Kreutzberg GW (1998b). Immune surveillance in the injured nervous system: T-lymphocytes invade the axotomized mouse facial motor nucleus and aggregate around sites of neuronal degeneration. J Neurosci. 18(15):5804-16.

Raivich G, Kreutzberg GW (1987) Expression of growth factor receptors in injured nervous tissue. I. Axotomy leads to a shift in the cellular distribution of specific beta-nerve growth factor binding in the injured and regenerating PNS. J Neurocytol 16:689-700

Raivich G, Kreutzberg GW (1993) Peripheral nerve regeneration: role of growth factors and their receptors. Int J Dev Neurosci 11:311-24

Raivich G, Liu ZQ, Kloss CU, Labow M, Bluethmann H, Bohatschek M (2002) Cytotoxic potential of proinflammatory cytokines: combined deletion of TNF receptors TNFR1 and TNFR2 prevents motoneuron cell death after facial axotomy in adult mouse. Exp Neurol. 178:86-93.

Raivich G, Moreno-Flores MT, Möller JC, Kreutzberg GW (1994) Inhibition of posttraumatic microglial proliferation in a genetic model of macrophage colony stimulating factor deficiency in mouse. Eur J Neurosci 6:1615-1618

Raivich G, Reddington M, Haas CA, Kreutzberg GW (1995) Peptides in motoneurons Prog Brain Res. 104:3-20.

Ramer MS, Priestley JV, McMahon SB (2000). Functional regeneration of sensory axons into the adult spinal cord. Nature. 403(6767):312-6.

Reichardt LF (2006) Neurotrophin-regulated signalling pathways. Philos Trans R Soc Lond B Biol Sci. 361(1473):1545-64.

Reichert F, Saada A, Rotshenker S (1994). Peripheral nerve injury induces Schwann cells to express two macrophage phenotypes: phagocytosis and the galactose-specific lectin MAC-2. J Neurosci. 14:3231-45.

Reier PJ (1979). Penetration of grafted astrocytic scars by regenerating optic nerve axons in Xenopus tadpoles. Brain Res. 23;164:61-8.

Reier PJ, Houle JD (1988). The glial scar: its bearing on axonal elongation and transplantation approaches to CNS repair. Adv Neurol. 47:87-138.

Rende M, Muir D, Ruoslahti E, Hagg T, Varon S, Manthorpe M (1992) Immunolocalization of ciliary neuronotrophic factor in adult rat sciatic nerve. Glia 5:25-32

Reuther GW, Der CJ (2000). The Ras branch of small GTPases: Ras family members don't fall far from the tree. Curr Opin Cell Biol. 12(2):157-65.

Richardson PM, Issa VM (1984). Peripheral injury enhances central regeneration of primary sensory neurones. Nature. 309(5971):791-3.

Richardson PM, Issa VM, Shemie S (1982). Regeneration and retrograde degeneration of axons in the rat optic nerve. J Neurocytol. 11(6):949-66.

Richardson PM, McGuinness UM, Aguayo AJ (1980). Axons from CNS neurons regenerate into PNS grafts. Nature. 284(5753):264-5.

Richardson PM, Riopelle RJ (1984). Uptake of nerve growth factor along peripheral and spinal axons of primary sensory neurons. J Neurosci. 4(7):1683-9.

Richardson PM, Verge VM (1986). The induction of a regenerative propensity in sensory neurons following peripheral axonal injury. J Neurocytol. 15(5):585-94.

Richardson PM, Verge VM (1987). Axonal regeneration in dorsal spinal roots is accelerated by peripheral axonal transection. Brain Res. 411(2):406-8.

Ridet JL, Malhotra SK, Privat A, Gage FH (1997). Reactive astrocytes: cellular and molecular cues to biological function.Trends Neurosci. 20(12):570-7.

Ridet JL, Pencalet P, Belcram M, Giraudeau B, Chastang C, Philippon J, Mallet J, Privat A, Schwartz L (2000). Effects of spinal cord X-irradiation on the recovery of paraplegic rats. Exp Neurol. 161(1):1-14.

Roberts AB, Sporn MB (1990) The transforming growth factor-β's. In Handbook of Experimental Pharmacology: Peptide Growth Factors and their Receptors I (Roberts AB, Sporn MB eds). Springer Verlag, Berlin/Heidelberg

Robinson KN, Manto K, Buchsbaum RJ, MacDonald JI, Meakin SO (2005). Neurotrophin-dependent tyrosine phosphorylation of Ras guanine-releasing factor 1 and associated neurite outgrowth is dependent on the HIKE domain of TrkA. J Biol Chem. 280(1):225-35.

Robinson RC, Radziejewski C, Stuart DI, Jones EY (1995). Structure of the brain-derived neurotrophic factor/neurotrophin 3 heterodimer.Biochemistry. 34(13):4139-46.

Rodriguez-Viciana P, Warne PH, Dhand R, Vanhaesebroeck B, Gout I, Fry MJ, Waterfield MD, Downward J (1994). Phosphatidylinositol-3-OH kinase as a direct target of Ras. Nature. 370(6490):527-32.

Rodriguez-Viciana P, Warne PH, Dhand R, Vanhaesebroeck B, Gout I, Fry MJ, Waterfield MD, Downward J (1994). Phosphatidylinositol-3-OH kinase as a direct target of Ras. Nature. 370(6490):527-32.

Rodriguez-Viciana P, Warne PH, Vanhaesebroeck B, Waterfield MD, Downward J (1996). Activation of phosphoinositide 3-kinase by interaction with Ras and by point mutation. EMBO J. 15(10):2442-51.

Romero MI, Lin L, Lush ME, Lei L, Parada LF, Zhu Y (2007). Deletion of Nf1 in neurons induces increased axon collateral branching after dorsal root injury. J Neurosci. 27(8):2124-34.

Romero MI, Lin L, Lush ME, Lei L, Parada LF, Zhu Y (2007). Deletion of Nf1 in neurons induces increased axon collateral branching after dorsal root injury. J Neurosci. 27(8):2124-34.

Rosenthal A, Goeddel DV, Nguyen T, Lewis M, Shih A, Laramee GR, Nikolics K, Winslow JW (1990). Primary structure and biological activity of a novel human neurotrophic factor. Neuron. 4(5):767-73.

Rossi F, Jankovski A, Sotelo C (1995). Differential regenerative response of Purkinje cell and inferior olivary axons confronted with embryonic grafts: environmental cues versus intrinsic neuronal determinants. J Comp Neurol. 359(4):663-77.

Rossignol S (2006). Plasticity of connections underlying locomotor recovery after central and/or peripheral lesions in the adult mammals. Philos Trans R Soc Lond B Biol Sci. 361(1473):1647-71.

Rossignol S, Drew T, Brustein E, Jiang W (1999). Locomotor performance and adaptation after partial or complete spinal cord lesions in the cat. Prog Brain Res. 123:349-65.

Rossiter JP, Riopelle RJ, Bisby MA (1996). Axotomy-induced apoptotic cell death of neonatal rat facial motoneurons: time course analysis and relation to NADPH-diaphorase activity. Exp Neurol. 138(1):33-44.

Ruitenberg MJ, Plant GW, Hamers FP, Wortel J, Blits B, Dijkhuizen PA, Gispen WH, Boer GJ, Verhaagen J (2003). Ex vivo adenoviral vector-mediated neurotrophin gene transfer to olfactory ensheathing glia: effects on rubrospinal tract regeneration, lesion size, and functional recovery after implantation in the injured rat spinal cord. J Neurosci. 23(18):7045-58.

Sanchez-Capelo A, Corti O, Mallet J (1999) Adenovirus-mediated over-expression of TGFβeta1 in the striatum decreases dopaminergic cell survival in embryonic nigral grafts. Neuroreport 10:2169-73.

Santambrogio L, Hochwald GM, Saxena B, Leu CH, Martz JE, Carlino JA, Ruddle NH, Palladino MA, Gold LI, Thorbecke GJ (1993) Studies on the mechanisms by which transforming growth factor-β (TGF-β) protects against allergic encephalomyelitis. Antagonism between TGF-β and tumor necrosis factor. J. Immunol 151:1116-1127

Sauerwald A, Hoesche C, Oschwald R, Kilimann MW (1990). The 5'-flanking region of the synapsin I gene. A G+C-rich, TATA- and CAAT-less, phylogenetically conserved sequence with cell type-specific promoter function. J Biol Chem. 265(25):14932-7.

Scapoli L, Ramos-Nino ME, Martinelli M, Mossman BT (2004). Src-dependent ERK5 and Src/EGFR-dependent ERK1/2 activation is required for cell proliferation by asbestos. Oncogene. 23(3):805-13.

Scherer J, Friedrich G, Schnitzer J (1995). Differentiation and maturation of rabbit retinal oligodendrocyte precursor cells in vitro. Brain Res Dev Brain Res. 89(2):214-26.

Schmalbruch H (1987) Loss of sensory neurons after sciatic nerve section in the rat. Anat Rec 219:323-9

Schmalfeldt M, Bandtlow CE, Dours-Zimmermann MT, Winterhalter KH, Zimmermann DR (2000) Brain derived versican V2 is a potent inhibitor of axonal growth. J Cell Sci 113 (Pt 5): 807-816.

Schmid RS, Pruitt WM, Maness PF (2000). A MAP kinase-signaling pathway mediates neurite outgrowth on L1 and requires Src-dependent endocytosis. J Neurosci. 2000 20(11):4177-88.

Schmitt AB, Breuer S, Liman J, Buss A, Schlangen C, Pech K, Hol EM, Brook GA, Noth J, Schwaiger FW (2003) Identification of regeneration-associated genes after central and peripheral nerve injury in the adult rat. BMC Neurosci. 4:8

Schnell L, Fearn S, Klassen H, Schwab ME, Perry VH (1999). Acute inflammatory responses to mechanical lesions in the CNS: differences between brain and spinal cord. Eur J Neurosci. 11(10):3648-58.

Schnell L, Schneider R, Kolbeck R, Barde YA, Schwab ME (1994). Neurotrophin-3 enhances sprouting of corticospinal tract during development and after adult spinal cord lesion. Nature. 367(6459):170-3.

Schnell L, Schwab ME (1990). Axonal regeneration in the rat spinal cord produced by an antibody against myelin-associated neurite growth inhibitors. Nature. 343(6255):269-72.

Schober A, Peterziel H, von Bartheld CS, Simon H, Krieglstein K, Unsicker K (2007) GDNF applied to the MPTP-lesioned nigrostriatal system requires TGF-β for its neuroprotective action. Neurobiol Dis. 25:378-91

Schramm LP (2006). Spinal sympathetic interneurons: their identification and roles after spinal cord injury. Prog Brain Res. 152:27-37.

Schreiber RC, Boeshore KL, Laube G, Veh RW, Zigmond RE (2004) Polyamines increase in sympathetic neurons and non-neuronal cells after axotomy and enhance neurite outgrowth in nerve growth factor-primed PC12 cells. Neuroscience 128:741-9

Schroeter M, Zickler P, Denhardt DT, Hartung HP, Jander S (2006) Increased thalamic neurodegeneration following ischaemic cortical stroke in osteopontin-deficient mice. Brain 129:1426-37

Schwab ME (2004). Nogo and axon regeneration. Curr Opin Neurobiol. 14(1):118-24.

Schwab ME, Bartholdi D (1996). Degeneration and regeneration of axons in the lesioned spinal cord. Physiol Rev. 76(2):319-70.

Schwab ME, Caroni P (1988). Oligodendrocytes and CNS myelin are nonpermissive substrates for neurite growth and fibroblast spreading in vitro. J Neurosci. 8(7):2381-93.

Schwab ME, Kapfhammer JP, Bandtlow CE (1993). Inhibitors of neurite growth. Annu Rev Neurosci. 16:565-95.

Schwaiger FW, Hager G, Raivich G, Kreutzberg GW (1998). Cellular activation in neuroregeneration. Prog Brain Res. 117:197-210.

Schwaiger FW, Hager G, Schmitt AB, Horvat A, Hager G, Streif R, Spitzer C, Gamal S, Breuer S, Brook GA, Nacimiento W, Kreutzberg GW (2000) Peripheral but not central axotomy induces changes in Janus kinases (JAK) and signal transducers and activators of transcription (STAT). Eur J Neurosci 12:1165-76

Schwartz M, Kohsaka S, Agranoff BW (1981) Ornithine decarboxylase activity in retinal explants of goldfish undergoing optic nerve regeneration. Brain Res 227:403-13

Schweizer U, Gunnersen J, Karch C, Wiese S, Holtmann B, Takeda K, Akira S, Sendtner M (2002) Conditional gene ablation of Stat3 reveals differential signaling requirements for survival of motoneurons during development and after nerve injury in the adult. J Cell Biol 156:287-97

Sebille A, Bondoux-Jahan M (1980) Motor function recovery after axotomy: enhancement by cyclophosphamide and spermine in rat. Exp Neurol 70:507-15

Segal RA (2003). Selectivity in neurotrophin signaling: theme and variations. Annu Rev Neurosci. 26:299-330.

Segal RA (2003). Selectivity in neurotrophin signaling: theme and variations. Annu Rev Neurosci. 26:299-330.

Segal RA, Greenberg ME (1996). Intracellular signaling pathways activated by neurotrophic factors. Annu Rev Neurosci. 19:463-89.

Seijffers R, Mills CD, Woolf CJ (1997) ATF3 increases the intrinsic growth state of DRG neurons to enhance peripheral nerve regeneration. J Neurosci. 27:7911-20.

Selcher JC, Nekrasova T, Paylor R, Landreth GE, Sweatt JD (2001). Mice lacking the ERK1 isoform of MAP kinase are unimpaired in emotional learning. Learn Mem. 8(1):11-9.

Sendtner M, Dittrich F, Hughes RA, Thoenen H (1994) Actions of CNTF and neurotrophins on degenerating motoneurons: preclinical studies and clinical implications. J Neurol Sci 124[Suppl]:77-83

Sendtner M, Gotz R, Holtmann B, Escary JL, Masu Y, Carroll P, Wolf E, Brem G, Brulet P, Thoenen H (1996) Cryptic physiological trophic support of motoneurons by LIF revealed by double gene targeting of CNTF and LIF. Curr Biol 6:686-94.

Sendtner M, Gotz R, Holtmann B, Thoenen H (1997). Endogenous ciliary neurotrophic factor is a lesion factor for axotomized motoneurons in adult mice. J Neurosci. 17(18):6999-7006.

Sendtner M, Kreutzberg GW, Thoenen H (1990) Ciliary neurotrophic factor prevents the degeneration of motor neurons after axotomy. Nature. 345:440-1

Seo SR, Chong SA, Lee SI, Sung JY, Ahn YS, Chung KC, Seo JT (2001). Zn2+-induced ERK activation mediated by reactive oxygen species causes cell death in differentiated PC12 cells. J Neurochem. 78(3):600-10.

Serpe CJ, Byram SC, Sanders VM, Jones KJ (2005). Brain-derived neurotrophic factor supports facial motoneuron survival after facial nerve transection in immunodeficient mice. Brain Behav Immun. 19(2):173-80.

Serpe CJ, Sanders VM, Jones KJ (2000). Kinetics of facial motoneuron loss following facial nerve transection in severe combined immunodeficient mice. J Neurosci Res. 15;62(2):273-8.

Shadiack AM, Sun Y, Zigmond RE (2001). Nerve growth factor antiserum induces axotomy-like changes in neuropeptide expression in intact sympathetic and sensory neurons. J Neurosci. 21(2):363-71.

Shalin SC, Zirrgiebel U, Honsa KJ, Julien JP, Miller FD, Kaplan DR, Sweatt JD (2004). Neuronal MEK is important for normal fear conditioning in mice. J Neurosci Res. 75(6):760-70.

Shao Z, Browning JL, Lee X, Scott ML, Shulga-Morskaya S, Allaire N, Thill G, Levesque M, Sah D, McCoy JM, Murray B, Jung V, Pepinsky RB, Mi S (2005). TAJ/TROY, an orphan TNF receptor family member, binds Nogo-66 receptor 1 and regulates axonal regeneration. Neuron. 45(3):353-9.

Shearer MC, Niclou SP, Brown D, Asher RA, Holtmaat AJ, Levine JM, Verhaagen J, Fawcett JW (2003). The astrocyte/meningeal cell interface is a barrier to neurite outgrowth which can be overcome by manipulation of inhibitory molecules or axonal signalling pathways. Mol Cell Neurosci. 24(4):913-25.

Sheu JY, Kulhanek DJ, Eckenstein FP (2000). Differential patterns of ERK and STAT3 phosphorylation after sciatic nerve transection in the rat. Exp Neurol. 166(2):392-402.

Shi GX, Andres DA (2005). Rit contributes to nerve growth factor-induced neuronal differentiation via activation of B-Raf-extracellular signal-regulated kinase and p38 mitogen-activated protein kinase cascades. Mol Cell Biol. 25(2):830-46.

Shull MM, Ormsby I, Kier AB, Pawlowski S, Diebold RJ, Yin M, Allen R, Sidman C, Proetzel G, Calvin D, Annunziata N, Doetschman T (1992) Targeted

disruption of the mouse transforming growth factor-ß1 gene results in multifocal inflammatory disease. Nature 359:693-699

Sievers J, Hausmann B, Unsicker K, Berry M (1987). Fibroblast growth factors promote the survival of adult rat retinal ganglion cells after transection of the optic nerve. Neurosci Lett. 76(2):157-62.

Simonen M, Pedersen V, Weinmann O, Schnell L, Buss A, Ledermann B, Christ F, Sansig G, van der Putten H, Schwab ME (2003). Systemic deletion of the myelin-associated outgrowth inhibitor Nogo-A improves regenerative and plastic responses after spinal cord injury. Neuron. 38(2):201-11.

Sivasankaran R, Pei J, Wang KC, Zhang YP, Shields CB, Xu XM, He Z (2004). PKC mediates inhibitory effects of myelin and chondroitin sulfate proteoglycans on axonal regeneration. Nat Neurosci. 7(3):261-8.

Sixt M, Bauer M, Lammermann T, Fassler R (2006) B1 integrins: zip codes and signaling relay for blood cells. Curr Opin Cell Biol. 18:482-90

Sjogreen B, Wiklund P, Ekstrom PA (2000). Mitogen activated protein kinase inhibition by PD98059 blocks nerve growth factor stimulated axonal outgrowth from adult mouse dorsal root ganglia in vitro. Neuroscience. 100(2):407-16.

Skene JH, Willard M (1981) Characteristics of growth-associated polypeptides in regenerating toad retinal ganglion cell axons. J Neurosci. 1:419-26

Smith JM, Lunga P, Story D, Harris N, Le Belle J, James MF, Pickard JD, Fawcett JW (2007). Inosine promotes recovery of skilled motor function in a model of focal brain injury. Brain. 130(4):915-25.

Snow DM, Lemmon V, Carrino DA, Caplan AI, Silver J (1990) Sulfated proteoglycans in astroglial barriers inhibit neurite outgrowth in vitro. Exp Neurol 109: 111-130.

So KF, Aguayo AJ (1985). Lengthy regrowth of cut axons from ganglion cells after peripheral nerve transplantation into the retina of adult rats. Brain Res. 328(2):349-54.

Sobel RA (2005) Ephrin A receptors and ligands in lesions and normal-appearing white matter in multiple sclerosis. Brain Pathol 15: 35-45.

Sofroniew MV, Isacson O (1988). Distribution of degeneration of cholinergic neurons in the septum following axotomy in different portions of the fimbria-fornix: a correlation between degree of cell loss and proximity of neuronal somata to the lesion. J Chem Neuroanat. 1(6):327-37.

Song H, Ming G, He Z, Lehmann M, McKerracher L, Tessier-Lavigne M, Poo M (1998) Conversion of neuronal growth cone responses from repulsion to attraction by cyclic nucleotides. Science 281: 1515-1518.

Song HJ, Poo MM (1999). Signal transduction underlying growth cone guidance by diffusible factors. Curr Opin Neurobiol. 9(3):355-63.

Song MS, Posse de Chaves EI (2004). Inhibition of rat sympathetic neuron apoptosis by ceramide. Role of p75NTR in ceramide generation. Neuropharmacology. 45(8):1130-50.

Spencer ML, Shao H, Andres DA (2002a). Induction of neurite extension and survival in pheochromocytoma cells by the Rit GTPase. J Biol Chem. 277(23):20160-8.

Spencer ML, Shao H, Tucker HM, Andres DA (2002b). Nerve growth factor-dependent activation of the small GTPase Rin. J Biol Chem. 277(20):17605-15.

Spira ME, Oren R, Dormann A, Ilouz N, Lev S (2001) Calcium, protease activation, and cytoskeleton remodeling underlie growth cone formation and neuronal regeneration. Cell Mol Neurobiol 21:591-604

Springer JE, Seeburger JL, He J, Gabrea A, Blankenhorn EP, Bergman LW (1995) cDNA sequence and differential mRNA regulation of two forms of glial cell line-derived neurotrophic factor in Schwann cells and rat skeletal muscle. Exp Neurol 131:47-52

Stadelmann C, Bruck W, Bancher C, Jellinger K, Lassmann H (1998). Alzheimer disease: DNA fragmentation indicates increased neuronal vulnerability, but not apoptosis. J Neuropathol Exp Neurol. 57(5):456-64.

Stagi M, Dittrich PS, Frank N, Iliev AI, Schwille P, Neumann H (2005) Breakdown of axonal synaptic vesicle precursor transport by microglial nitric oxide. J Neurosci 25:352-62

Starkey ML, Barritt AW, Yip PK, Davies M, Hamers FP, McMahon SB, Bradbury EJ (2005). Assessing behavioural function following a pyramidotomy lesion of the corticospinal tract in adult mice. Exp Neurol. 195(2):524-39.

Stein E, Lane AA, Cerretti DP, Schoecklmann HO, Schroff AD, Van Etten RL, Daniel TO (1998) Eph receptors discriminate specific ligand oligomers to determine alternative signaling complexes, attachment, and assembly responses. Genes Dev 12: 667-678.

Steindler DA, Settles D, Erickson HP, Laywell ED, Yoshiki A, Faissner A, Kusakabe M (1995) Tenascin knockout mice: barrels, boundary molecules, and glial scars. J Neurosci 15: 1971-1983.

Steinmetz MP, Horn KP, Tom VJ, Miller JH, Busch SA, Nair D, Silver DJ, Silver J (2005). Chronic enhancement of the intrinsic growth capacity of sensory neurons combined with the degradation of inhibitory proteoglycans allows functional regeneration of sensory axons through the dorsal root entry zone in the mammalian spinal cord. J Neurosci. 25(35):8066-76.

Stenevi U, Bjorklund A, Svendgaard NA (1976) Transplantation of central and peripheral monoamine neurons to the adult rat brain: techniques and conditions for survival. Brain Res 114:1-20.

Steup A, Ninnemann O, Savaskan NE, Nitsch R, Puschel AW, Skutella T (1999) Semaphorin D acts as a repulsive factor for entorhinal and hippocampal neurons. Eur J Neurosci 11: 729-734.

Steward O, Zheng B, Banos K, Yee KM (2007). Response to: Kim et al., "axon regeneration in young adult mice lacking Nogo-A/B." Neuron 38, 187-199. Neuron. 54(2):191-5.

Steward O, Zheng B, Ho C, Anderson K, Tessier-Lavigne M (2004). The dorsolateral corticospinal tract in mice: an alternative route for corticospinal input to caudal segments following dorsal column lesions. J Comp Neurol. 472(4):463-77.

Streit WJ (2006) Microglial senescence: does the brain's immune system have an expiration date? Trends Neurosci 29:506-10

Streit WJ, Graeber MB, Kreutzberg GW (1988). Functional plasticity of microglia: a review. Glia. 1(5):301-7.

Streit WJ, Graeber MB, Kreutzberg GW (1989). Peripheral nerve lesion produces increased levels of major histocompatibility complex antigens in the central nervous system. J Neuroimmunol. 21(2-3):117-23.

Streppel M, Azzolin N, Dohm S, Guntinas-Lichius O, Haas C, Grothe C, Wevers A, Neiss WF, Angelov DN (2002). Focal application of neutralizing antibodies to soluble neurotrophic factors reduces collateral axonal branching after peripheral nerve lesion. Eur J Neurosci. 15(8):1327-42.

Su QN, Namikawa K, Toki H, Kiyama H (1997) Differential display reveals transcriptional up-regulation of the motor molecules for both anterograde and retrograde axonal transport during nerve regeneration. Eur J Neurosci. 9:1542-7

Subramaniam S, Unsicker K (2006). Extracellular signal-regulated kinase as an inducer of non-apoptotic neuronal death. Neuroscience. 138(4):1055-65.

Subramaniam S, Zirrgiebel U, von Bohlen Und Halbach O, Strelau J, Laliberte C, Kaplan DR, Unsicker K (2004). ERK activation promotes neuronal degeneration predominantly through plasma membrane damage and independently of caspase-3. J Cell Biol. 165(3):357-69.

Sun W, Oppenheim RW (2003) Response of motoneurons to neonatal sciatic nerve axotomy in Bax-knockout mice. Mol Cell Neurosci. 24:875-86.

Sundaresan V, Mambetisaeva E, Andrews W, Annan A, Knoll B, Tear G, Bannister L (2004) Dynamic expression patterns of Robo (Robo1 and Robo2) in the developing murine central nervous system. J Comp Neurol 468: 467-481.

Suzuki Y, Nakagomi S, Namikawa K, Kiryu-Seo S, Inagaki N, Kaibuchi K, Aizawa H, Kikuchi K, Kiyama H (2003) Collapsin response mediator protein-2 accelerates axon regeneration of nerve-injured motor neurons of rat. J Neurochem 86:1042-50

Taira E, Takaha N, Taniura H, Kim CH, Miki N (1994) Molecular cloning and functional expression of gicerin, a novel cell adhesion molecule that binds to neurite outgrowth factor. Neuron 12:861-872.

Talts U, Kuhn U, Roos G, Rauch U (2000) Modulation of extracellular matrix adhesiveness by neurocan and identification of its molecular basis. Exp Cell Res 259: 378-388.

Tanabe K, Bonilla I, Winkles JA, Strittmatter SM (2003) Fibroblast growth factor-inducible-14 is induced in axotomized neurons and promotes neurite outgrowth. J Neurosci 23:9675-86

Tanaka T, Ida N, Shimoda H, Waki C, Slamon DJ, Cline MJ (1986). Organ specific expression of ras oncoproteins during growth and development of the rat. Mol Cell Biochem. 70(1):97-104.

Tang X, Davies JE, Davies SJ (2003) Changes in distribution, cell associations, and protein expression levels of NG2, neurocan, phosphacan, brevican, versican V2, and tenascin-C during acute to chronic maturation of spinal cord scar tissue. J Neurosci Res 71: 427-444.

Tanigawa N, Saito T, Ogawa K, Iida H (2005) Origin of regenerated axons in nerve bypass grafts. J Neurotrauma 22:605-12.

Taniuchi M, Clark HB, Johnson EM Jr (1986). Induction of nerve growth factor receptor in Schwann cells after axotomy. Proc Natl Acad Sci U S A. 183(11):4094-8.

Taniuchi M, Clark HB, Schweitzer JB, Johnson EM Jr (1988). Expression of nerve growth factor receptors by Schwann cells of axotomized peripheral nerves: ultrastructural location, suppression by axonal contact, and binding properties. J Neurosci. 8(2):664-81.

Taylor DL, Jones F, Kubota ES, Pocock JM (2005) Stimulation of microglial metabotropic glutamate receptor mGlu2 triggers tumor necrosis factor α-induced neurotoxicity in concert with microglial-derived Fas ligand. J Neurosci 25:2952-64

Terenghi G (1999) Peripheral nerve regeneration and neurotrophic factors. J Anat 194:1-14

Terrado J, Monnier D, Perrelet D, Vesin D, Jemelin S, Buurman WA, Mattenberger L, King B, Kato AC, Garcia I (2000) Soluble TNF receptors partially protect injured motoneurons in the postnatal CNS. Eur J Neurosci. 12:3443-7

Tessarollo L, Vogel KS, Palko ME, Reid SW, Parada LF (1994). Targeted mutation in the neurotrophin-3 gene results in loss of muscle sensory neurons. Proc Natl Acad Sci U S A. 91(25):11844-8.

Tesseur I, Zou K, Esposito L, Bard F, Berber E, Can JV, Lin AH, Crews L, Tremblay P, Mathews P, Mucke L, Masliah E, Wyss-Coray T (2006) Deficiency in neuronal TGF-β signaling promotes neurodegeneration and Alzheimer's pathology. J Clin Invest. 116:3060-9.

Tetzlaff W, Alexander SW, Miller FD, Bisby MA (1991). Response of facial and rubrospinal neurons to axotomy: changes in mRNA expression for cytoskeletal proteins and GAP-43. J Neurosci. 11(8):2528-44.

Tetzlaff W, Gilad VH, Leonard C, Bisby MA, Gilad GM (1988) Retrograde changes in transglutaminase activity after peripheral nerve injuries. Brain Res 445:142-6

Thallmair M, Metz GA, Z'Graggen WJ, Raineteau O, Kartje GL, Schwab ME (1998). Neurite growth inhibitors restrict plasticity and functional recovery following corticospinal tract lesions. Nat Neurosci. 1(2):124-31.

Thoenen H, Bandtlow C, Heumann R, Lindholm D, Meyer M, Rohrer H (1988). Nerve growth factor: cellular localization and regulation of synthesis. Cell Mol Neurobiol. 8(1):35-40.

Tom VJ, Steinmetz MP, Miller JH, Doller CM, Silver J (2004). Studies on the development and behavior of the dystrophic growth cone, the hallmark of regeneration failure, in an in vitro model of the glial scar and after spinal cord injury. J Neurosci. 24(29):6531-9.

Torvik A, Skjorten F (1971). Electron microscopic observations on nerve cell regeneration and degeneration after axon lesions. II. Changes in the glial cells. Acta Neuropathol (Berl). 17(3):265-82.

Trapp BD, Wujek JR, Criste GA, Jalabi W, Yin X, Kidd GJ, Stohlman S, Ransohoff R (2007) Evidence for synaptic stripping by cortical microglia. Glia. 55:360-8

Trojanowski JQ, Lee VM, Schlaepfer WW (1984). Neurofilament breakdown products in degenerating rat and human peripheral nerves. Ann Neurol. 1984 Sep;16(3):349-55.

Tronche F, Kellendonk C, Kretz O, Gass P, Anlag K, Orban PC, Bock R, Klein R, Schutz G. (1999) Disruption of the glucocorticoid receptor gene in the nervous system results in reduced anxiety. Nat Genet. 23 16

Tsuji M, Inanami O, Kuwabara M (2001). Induction of neurite outgrowth in PC12 cells by α -phenyl-N-tert-butylnitron through activation of protein kinase C and the Ras-extracellular signal-regulated kinase pathway. J Biol Chem. 276(35):32779-85.

Tsujino H, Kondo E, Fukuoka T, Dai Y, Tokunaga A, Miki K, Yonenobu K, Ochi T, Noguchi K (2000) Activating transcription factor 3 (ATF3) induction by axotomy in sensory and motoneurons: A novel neuronal marker of nerve injury. Mol Cell Neurosci. 15:170-82.

Tuszynski MH, Armstrong DM, Gage FH (1990). Basal forebrain cell loss following fimbria/fornix transection. Brain Res. 508(2):241-8.

Tuszynski MH, Grill R, Jones LL, Brant A, Blesch A, Low K, Lacroix S, Lu P (2003). NT-3 gene delivery elicits growth of chronically injured corticospinal axons and modestly improves functional deficits after chronic scar resection. Exp Neurol. 181(1):47-56.

Tuszynski MH, Grill R, Jones LL, McKay HM, Blesch A (2002). Spontaneous and augmented growth of axons in the primate spinal cord: effects of local injury and nerve growth factor-secreting cell grafts. J Comp Neurol. 449(1):88-101.

Tuszynski MH, Murai K, Blesch A, Grill R, Miller I (1997). Functional characterization of NGF-secreting cell grafts to the acutely injured spinal cord. Cell Transplant. 6(3):361-8.

Ughrin YM, Chen ZJ, Levine JM (2003) Multiple regions of the NG2 proteoglycan inhibit neurite growth and induce growth cone collapse. J Neurosci 23: 175-186.

Ugolini G, Raoul C, Ferri A, Haenggeli C, Yamamoto Y, Salaun D, Henderson CE, Kato AC, Pettmann B, Hueber AO (2003) Fas/tumor necrosis factor receptor death signaling is required for axotomy-induced death of motoneurons in vivo. J Neurosci 23:8526-31

Umanoff H, Edelmann W, Pellicer A, Kucherlapati R (1995). The murine N-ras gene is not essential for growth and development. Proc Natl Acad Sci U S A. 92(5):1709-13.

Unsicker K, Strelau J (2000) Functions of transforming growth factor-β isoforms in the nervous system. Cues based on localization and experimental in vitro and in vivo evidence. Eur J Biochem. 267:6972-5

Valero-Cabre A, Tsironis K, Skouras E, Navarro X, Neiss WF (2004). Peripheral and spinal motor reorganization after nerve injury and repair. J Neurotrauma. 21(1):95-108.

Vallee RB, Bloom GS (1991). Mechanisms of fast and slow axonal transport. Annu Rev Neurosci. 14:59-92.

van der Bruggen T, Nijenhuis S, van Raaij E, Verhoef J, van Asbeck BS (1999). Lipopolysaccharide-induced tumor necrosis factor α production by human monocytes involves the raf-1/MEK1-MEK2/ERK1-ERK2 pathway. Infect Immun. 67(8):3824-9.

Van der Zee CE, Fawcett J, Diamond J (1992). Antibody to NGF inhibits collateral sprouting of septohippocampal fibers following entorhinal cortex lesion in adult rats. J Comp Neurol. 326(1):91-100.

Vanhaesebroeck B, Leevers SJ, Ahmadi K, Timms J, Katso R, Driscoll PC, Woscholski R, Parker PJ, Waterfield MD (2001). Synthesis and function of 3-phosphorylated inositol lipids. Annu Rev Biochem. 70:535-602.

Varon S, Manthorpe M, Williams LR (1983) Neuronotrophic and neurite-promoting factors and their clinical potentials. Dev Neurosci. 6:73-100

Vavrek R, Girgis J, Tetzlaff W, Hiebert GW, Fouad K (2006). BDNF promotes connections of corticospinal neurons onto spared descending interneurons in spinal cord injured rats. Brain. 129(Pt 6):1534-45.

Verge VM, Richardson PM, Wiesenfeld-Hallin Z, Hokfelt T (1995) Differential influence of nerve growth factor on neuropeptide expression in vivo: a novel role in peptide suppression in adult sensory neurons. J Neurosci. 15:2081-96

Vergeli M, Mazzanti B, Ballerini C, Gran B, Amaducci L, Massacesi L (1995). Transforming growth factor-β 1 inhibits the proliferation of rat astrocytes induced by serum and growth factors. J Neurosci Res 40:127-133

Verhaagen J, van Hooff CO, Edwards PM, De Graan PN, Oestreicher AB, Schotman P, Jennekens FG, Gispen WH (1986) The kinase C substrate protein B-50 and axonal regeneration. Brain Res Bull 17:737-41.

Vitiello M, D'Isanto M, Galdiero M, Raieta K, Tortora A, Rotondo P, Peluso L, Galdiero M (2004). Interleukin-8 production by THP-1 cells stimulated by Salmonella enterica serovar Typhimurium porins is mediated by AP-1, NF-kappaB and MAPK pathways. Cytokine.;27(1):15-24.

Vogelaar CF, Hoekman MF, Gispen WH, Burbach JP (2003) Homeobox gene expression in adult dorsal root ganglia during sciatic nerve regeneration: is

regeneration a recapitulation of development? Eur J Pharmacol. 480:233-50

von Bartheld CS, Byers MR, Williams R, Bothwell M (1996). Anterograde transport of neurotrophins and axodendritic transfer in the developing visual system. Nature. 379(6568):830-3.

Wallace MC, Tator CH, Lewis AJ (1987). Chronic regenerative changes in the spinal cord after cord compression injury in rats. Surg Neurol. 27(3):209-19.

Waller A (1850). Experiments on the section of the glossopharyngeal and hypoglossal nerves of the frog, and observations of the alterations produced thereby in the structure of their primitive fibers. Phil Transact Royal Soc London 140;423-429

Wang KC, Kim JA, Sivasankaran R, Segal R, He Z (2002b). P75 interacts with the Nogo receptor as a co-receptor for Nogo, MAG and OMgp. Nature. 420(6911):74-8.

Wang KC, Koprivica V, Kim JA, Sivasankaran R, Guo Y, Neve RL, He Z (2002a). Oligodendrocyte-myelin glycoprotein is a Nogo receptor ligand that inhibits neurite outgrowth. Nature. 417(6892):941-4.

Wang KH, Brose K, Arnott D, Kidd T, Goodman CS, Henzel W, Tessier-Lavigne M (1999) Biochemical purification of a mammalian slit protein as a positive regulator of sensory axon elongation and branching. Cell 96: 771-784.

Wang ZQ, Wu DC, Huang FP, Yang GY (2004). Inhibition of MEK/ERK 1/2 pathway reduces pro-inflammatory cytokine interleukin-1 expression in focal cerebral ischemia. Brain Res. 996(1):55-66.

Watanabe H, Yamazaki M, Miyazaki H, Arikawa C, Itoh K, Sasaki T, Maehama T, Frohman MA, Kanaho Y (2004a). Phospholipase D2 functions as a downstream signaling molecule of MAP kinase pathway in L1-stimulated

neurite outgrowth of cerebellar granule neurons. J Neurochem. 89(1):142-51.

Watanabe H, Yokozeki T, Yamazaki M, Miyazaki H, Sasaki T, Maehama T, Itoh K, Frohman MA, Kanaho Y(2004b). Essential role for phospholipase D2 activation downstream of ERK MAP kinase in nerve growth factor-stimulated neurite outgrowth from PC12 cells. J Biol Chem. 279(36):37870-7.

Watson FL, Heerssen HM, Bhattacharyya A, Klesse L, Lin MZ, Segal RA (2001). Neurotrophins use the Erk5 pathway to mediate a retrograde survival response. Nat Neurosci. 4(10):981-8.

Wehrle R, Camand E, Chedotal A, Sotelo C, Dusart I (2005) Expression of netrin-1, slit-1 and slit-3 but not of slit-2 after cerebellar and spinal cord lesions. Eur J Neurosci 22: 2134-2144.

Weidner N, Blesch A, Grill RJ, Tuszynski MH (1999). Nerve growth factor-hypersecreting Schwann cell grafts augment and guide spinal cord axonal growth and remyelinate central nervous system axons in a phenotypically appropriate manner that correlates with expression of L1. J Comp Neurol. 413(4):495-506.

Weidner N, Ner A, Salimi N, Tuszynski MH (2001). Spontaneous corticospinal axonal plasticity and functional recovery after adult central nervous system injury. Proc Natl Acad Sci U S A. 98(6):3513-8.

Weng G, Markus MA, Markus A, Winkler A, Borasio GD (1996). p21ras supports the survival of chick embryonic motor neurones. Neuroreport. 7(5):1077-81.

Werner A, Galiano M, Mayer U, Kreutzberg GW & Raivich G (1999) Molecular constituents of regenerating growth cones of mouse facial motoneurons. Ann Anat 181 [Suppl], 323

Werner A, Kloss CUA, Walter J, Kreutzberg GW, Raivich G (1998) Intercellular adhesion molecule-1 (ICAM1) in the regenerating mouse facial motor nucleus. J Neurocytol, 27:219-232

Werner A, Martin S, Gutierrez-Ramos JC, Raivich G (2001). Leukocyte recruitment and neuroglial activation during facial nerve regeneration in ICAM-1-deficient mice: effects of breeding strategy. Cell Tissue Res. 305(1):25-41.

Werner A, Willem M, Jones LL, Kreutzberg GW, Mayer U, Raivich G (2000). Impaired axonal regeneration in α7 integrin-deficient mice. J Neurosci. 20(5):1822-30.

White MA, Nicolette C, Minden A, Polverino A, Van Aelst L, Karin M, Wigler MH (1995). Multiple Ras functions can contribute to mammalian cell transformation. Cell. 80(4):533-41.

White MA, Vale T, Camonis JH, Schaefer E, Wigler MH (1996). A role for the Ral guanine nucleotide dissociation stimulator in mediating Ras-induced transformation. J Biol Chem. 271(28):16439-42.

Wictorin K, Bjorklund A (1992). Axon outgrowth from grafts of human embryonic spinal cord in the lesioned adult rat spinal cord. Neuroreport. 3(12):1045-8.

Wictorin K, Brundin P, Gustavii B, Lindvall O, Bjorklund A (1990). Reformation of long axon pathways in adult rat central nervous system by human forebrain neuroblasts. Nature. 347(6293):556-8.

Widenfalk J, Lundstromer K, Jubran M, Brene S, Olson L (2001). Neurotrophic factors and receptors in the immature and adult spinal cord after mechanical injury or kainic acid. J Neurosci. 21(10):3457-75.

Wiese S, Metzger F, Holtmann B, Sendtner M (1999) The role of p75NTR in modulating neurotrophin survival effects in developing motoneurons. Eur J Neurosci. 11:1668-76

Wiklund P, Ekstrom PA, Edstrom A (2002) Mitogen-activated protein kinase inhibition reveals differences in signalling pathways activated by neurotrophin-3 and other growth-stimulating conditions of adult mouse dorsal root ganglia neurons. J Neurosci Res. 67:62-8

Willson CA, Irizarry-Ramirez M, Gaskins HE, Cruz-Orengo L, Figueroa JD, Whittemore SR, Miranda JD (2002) Upregulation of EphA receptor expression in the injured adult rat spinal cord. Cell Transplant 11: 229-239.

Witzel C, Rohde C, Brushart TM (2005) Pathway sampling by regenerating peripheral axons. J Comp Neurol. 485:183-90.

Woolf CJ (2003). No Nogo: now where to go? Neuron. 38(2):153-6.

Woolf CJ, Shortland P, Coggeshall RE (1992) Peripheral nerve injury triggers central sprouting of myelinated afferents. Nature 355:75-8

Wu W, Gloster A, Miller FD (1997). Transcriptional repression of the growth-associated T α1 α-tubulin gene by target contact. J Neurosci Res. 48(5):477-87.

Wynick D, Thompson SW, McMahon SB (2001) The role of galanin as a multi-functional neuropeptide in the nervous system Curr Opin Pharmacol. 1:73-7

Xia Z, Dickens M, Raingeaud J, Davis RJ, Greenberg ME (1995) Opposing effects of ERK and JNK-p38 MAP kinases on apoptosis. Science. 270:1326-31

Xiao D, Miller GM, Jassen A, Westmoreland SV, Pauley D, Madras BK (2006) Ephrin/Eph receptor expression in brain of adult nonhuman primates: Implications for neuroadaptation. Brain Res 1067: 67-77.

Xing J, Kornhauser JM, Xia Z, Thiele EA, Greenberg ME (1998). Nerve growth factor activates extracellular signal-regulated kinase and p38 mitogen-

activated protein kinase pathways to stimulate CREB serine 133 phosphorylation. Mol Cell Biol. 18(4):1946-55.

Xue L, Murray JH, Tolkovsky AM (2000). The Ras/phosphatidylinositol 3-kinase and Ras/ERK pathways function as independent survival modules each of which inhibits a distinct apoptotic signaling pathway in sympathetic neurons. J Biol Chem. 275(12):8817-24.

Yamada H, Fredette B, Shitara K, Hagihara K, Miura R, Ranscht B, Stallcup WB, Yamaguchi Y (1997) The brain chondroitin sulfate proteoglycan brevican associates with astrocytes ensheathing cerebellar glomeruli and inhibits neurite outgrowth from granule neurons. J Neurosci 17: 7784-7795.

Yamashita T, Higuchi H, Tohyama M (2002). The p75 receptor transduces the signal from myelin-associated glycoprotein to Rho. J Cell Biol. 157(4):565-70.

Yan Q, Elliott J, Snider WD (1992) Brain-derived neurotrophic factor rescues spinal motor neurons from axotomy-induced cell death. Nature 360:753-5

Yick LW, Cheung PT, So KF, Wu W (2003). Axonal regeneration of Clarke's neurons beyond the spinal cord injury scar after treatment with chondroitinase ABC. Exp Neurol. 182(1):160-8.

Yick LW, So KF, Cheung PT, Wu WT (2004). Lithium chloride reinforces the regeneration-promoting effect of chondroitinase ABC on rubrospinal neurons after spinal cord injury. J Neurotrauma. 21(7):932-43.

Yin Y, Henzl MT, Lorber B, Nakazawa T, Thomas TT, Jiang F, Langer R, Benowitz LI (2006). Oncomodulin is a macrophage-derived signal for axon regeneration in retinal ganglion cells. Nat Neurosci. 9(6):843-52.

Yiu G, He Z (2006). Glial inhibition of CNS axon regeneration. Nat Rev Neurosci. 7(8):617-27.

Yoo S, Nguyen MP, Fukuda M, Bittner GD, Fishman HM (2003) Plasmalemmal sealing of transected mammalian neurites is a gradual process mediated by Ca(2+)-regulated proteins. J Neurosci Res 74:541-51.

Zeman RJ, Feng Y, Peng H, Visintainer PF, Moorthy CR, Couldwell WT, Etlinger JD (2001). X-irradiation of the contusion site improves locomotor and histological outcomes in spinal cord-injured rats. Exp Neurol. 2001 Nov;172(1):228-34.

Zeng BY, Anderson PN, Campbell G, Lieberman AR (1995). Regenerative and other responses to injury in the retinal stump of the optic nerve in adult albino rats: transection of the intracranial optic nerve. J Anat. 186(3):495-508.

Z'Graggen WJ, Metz GA, Kartje GL, Thallmair M, Schwab ME (1998). Functional recovery and enhanced corticofugal plasticity after unilateral pyramidal tract lesion and blockade of myelin-associated neurite growth inhibitors in adult rats. J Neurosci. 18(12):4744-57.

Zhang Y, Roslan R, Lang D, Schachner M, Lieberman AR, Anderson PN (2000) Expression of CHL1 and L1 by neurons and glia following sciatic nerve and dorsal root injury. Mol Cell Neurosci 16:71-86.

Zhang Y, Tohyama K, Winterbottom JK, Haque NS, Schachner M, Lieberman AR, Anderson PN (2001). Correlation between putative inhibitory molecules at the dorsal root entry zone and failure of dorsal root axonal regeneration. Mol Cell Neurosci. 17(3):444-59.

Zhang Y, Winterbottom JK, Schachner M, Lieberman AR, Anderson PN (1997) Tenascin-C expression and axonal sprouting following injury to the spinal dorsal columns in the adult rat. J Neurosci Res 49: 433-450.

Zheng B, Atwal J, Ho C, Case L, He XL, Garcia KC, Steward O, Tessier-Lavigne M (2005). Genetic deletion of the Nogo receptor does not reduce

neurite inhibition in vitro or promote corticospinal tract regeneration in vivo. Proc Natl Acad Sci U S A. 102(4):1205-10.

Zheng B, Ho C, Li S, Keirstead H, Steward O, Tessier-Lavigne M (2003). Lack of enhanced spinal regeneration in Nogo-deficient mice. Neuron. 38(2):213-24.

Zheng JQ, Kelly TK, Chang B, Ryazantsev S, Rajasekaran AK, Martin KC, Twiss JL (2001) A functional role for intra-axonal protein synthesis during axonal regeneration from adult sensory neurons. J Neurosci. 21:9291-303

Zhong J, Dietzel ID, Wahle P, Kopf M, Heumann R (1999) Sensory impairments and delayed regeneration of sensory axons in interleukin-6-deficient mice. J Neurosci. 19:4305-13.

Zhong J, Dietzel ID, Wahle P, Kopf M, Heumann R (1999). Sensory impairments and delayed regeneration of sensory axons in interleukin-6-deficient mice. J Neurosci. 19(11):4305-13.

Zhou FQ, Snider WD (2006) Intracellular control of developmental and regenerative axon growth. Philos Trans R Soc Lond B Biol Sci. 361(1473):1575-92.

Zhou FQ, Walzer MA, Snider WD (2004) Turning on the machine: genetic control of axon regeneration by c-Jun. Neuron. 43:1-2

Zhou L, Baumgartner BJ, Hill-Felberg SJ, McGowen LR, Shine HD (2003). Neurotrophin-3 expressed in situ induces axonal plasticity in the adult injured spinal cord. J Neurosci. 23(4):1424-31.

Zhou L, Baumgartner BJ, Hill-Felberg SJ, McGowen LR, Shine HD (2003). Neurotrophin-3 expressed in situ induces axonal plasticity in the adult injured spinal cord. J Neurosci. 23(4):1424-31.

Zhou L, Shine HD (2003). Neurotrophic factors expressed in both cortex and spinal cord induce axonal plasticity after spinal cord injury. J Neurosci Res. 74(2):221-6.

Zhu Y, Ghosh P, Charnay P, Burns DK, Parada LF (2002). Neurofibromas in NF1: Schwann cell origin and role of tumor environment. Science. 296(5569):920-2.

Zigmond RE, Hyatt-Sachs H, Mohney RP, Schreiber RC, Shadiack AM, Sun Y, Vaccariello SA (1996). Changes in neuropeptide phenotype after axotomy of adult peripheral neurons and the role of leukemia inhibitory factor. Perspect Dev Neurobiol. 4(1):75-90.